# Duty-cycled Wake-up Schemes for Ultra-low Power Wireless Communications

Seyed Mazloum, Nafiseh

2016

*Document Version:*
Other version

# Duty-cycled Wake-up Schemes for Ultra-low Power Wireless Communications

Nafiseh Seyed Mazloum

Lund University
Lund, Sweden
2016

Department of Electrical and Information Technology
Lund University
Box 118, SE-221 00 LUND
SWEDEN

This thesis is set in Computer Modern 10pt
with the LaTeX Documentation System

Series of licentiate and doctoral theses
No. 87
ISSN 1654-790X
ISBN: 978-91-7623-842-4 (print)
ISBN: 978-91-7623-843-1 (pdf)


Printed in Sweden by *Tryckeriet i E-huset*, Lund.
May 2016.

# Popular Science Summary

Imagine that you only have a small bucket of water to use in a hot summer day, a small basket of coal to burn in a cold winter day, or a very limited number of candles to light up a room on a dark winter night. The first thing that probably comes to your mind is to use them as efficiently as possible so that they last longer. For similar reasons and with limited resources on our planet, we are using more and more efficient and intelligent solutions in our daily life. One approach that has been widely used is to automatically switch off instruments or devices after not being in use for a certain time. Many of us have experienced this feature in, for instance, newly manufactured cars having a start-stop system, escalators and auto-walks with automatic start-stop control, water taps in public places having automatic stop functions, and our electronic devices going to standby mode. An important part of the automatic stand-by solutions in the above examples is that full functionality is automatically restored whenever necessary.

In this study, our aim is to find energy efficient solutions, based on the above type of techniques, for small-size battery-powered devices used to communicate wirelessly. These devices are typically placed a short distance from each other and consist of one or more sensors and a transceiver for transmitting/receiving data to/from other devices. In medical applications, these devices can be electrodes placed on the body to measure vital signs of a patient, hearing aids for patients having impaired ears, or different small devices used on the body of a patient for distance health monitoring. In industrial and environmental applications, these devices can be sensor nodes used, for instance, on railways or bridges for fault tracking, in different parts of manufactured devices such as cars or air planes for quality control, or for monitoring natural disasters such as forest fires or floods. In homes and offices, these devices can be sensor nodes used in different parts of a building measuring temperature or checking water pipes for leakage.

In most of these applications, the devices need to be small and are possibly in out-of-reach places where batteries cannot easily be replaced. Both

these make energy resources extremely precious. The types of devices we are addressing here are often used for tracking or monitoring rare events, which means that measurement data only need to be transmitted infrequently. It therefore makes sense to use an approach similar to what was described in our previous examples, switching off the transceivers when not needed. Unlike the previous examples, however, there is no direct human intervention to bring back the system to full functionality. Considering that both the transmitter and receiver are switched off, we need an energy-efficient *autonomous* approach to establish communication between devices whenever needed. While there exist solutions targeting low-power long life-time wireless connectivity, recent technological advances in ultra low-power circuitry have opened new opportunities.

This study presents and analyzes a new approach that allows for reduction of idle state energy consumption and establishes connectivity whenever needed. In this approach all devices are equipped with an extra ultra-low power receiver, called a wake-up receiver. These wake-up receivers typically have two orders of magnitude lower power consumption than the main receiver and only switches on for short periods of time to listen for potential communication. The combination of these two allows for extreme reduction of power consumption. The wake-up receiver switches on the main receiver only if it detects a signal with a certain pattern. This signal is referred to as a wake-up beacon and it is transmitted periodically by a device that wants to establish communication. An important part of the proposed approach is to decide how often the wake-up receivers needs to listen to the channel. The balance between rare and frequent listening determines total energy consumption and where in the system energy is consumed. The time it takes to establish the connection is also influenced by this balance. A detailed energy analysis is used to optimize this approach and establish how much energy can be saved under different conditions. Optimization is done both with and without requirements on the time it takes to establish a connection. Approximations of optimal results are derived and a wake-up receiver digital baseband circuit is implemented as a proof of concept.

# Abstract

In sensor network applications with low traffic intensity, idle channel listening is one of the main sources of energy waste. The use of a dedicated low-power wake-up receiver (WRx) which utilizes duty-cycled channel listening can significantly reduce idle listening energy cost. In this thesis such a scheme is introduced and it is called DCW-MAC, an acronym for duty-cycled wake-up receiver based medium access control.

We develop the concept in several steps, starting with an investigation into the properties of these schemes under idealized conditions. This analysis show that DCW-MAC has the potential to significantly reduce energy costs, compared to two established reference schemes based only on low-power wake up receivers or duty-cycled listening. Findings motivate further investigations and more detailed analysis of energy consumption. We do this in two separate steps, first concentrating on the energy required to transmit wake-up beacons and later include all energy costs in the analysis. The more complete analysis makes it possible to optimize wake-up beacons and other DCW-MAC parameters, such as sleep and listen intervals, for minimal energy consumption. This shows how characteristics of the wake-up receiver influence how much, and if, energy can be saved and what the resulting average communication delays are. Being an analysis based on closed form expressions, rather than simulations, we can derive and verify good approximations of optimal energy consumption and resulting average delays, making it possible to quickly evaluate how a different wake-up receiver characteristic influences what is possible to achieve in different scenarios.

In addition to the direct optimizations of the DCW-MAC scheme, we also provide a proof-of-concept in 65 nm CMOS, showing that the digital base-band needed to implement DCW-MAC has negligible energy consumption compared to many low-power analog front-ends in literature. We also propose a a simple frame-work for comparing the relative merits of analog front-ends for wake-up receivers, where we use the experiences gained about DCW-MAC energy consumption to provide a simple relation between wake-up receiver/analog front-

end properties and energy consumption for wide ranges of scenario parameters. Using this tool it is possible to compare analog front-ends used in duty-cycled wake-up schemes, even if they are originally designed for different scenarios.

In all, the thesis presents a new wake-up receiver scheme for low-power wireless sensor networks and provide a comprehensive analysis of many of its important properties.

# Preface

This doctoral thesis concludes my work as a Ph.D. student at the department of Electrical and Information Technology, Lund University, and comprises two parts. The first part gives an overview of the research field and a brief summary of my contribution whereas the second part is composed of five research papers that constitute my main scientific work. The included research papers are:

[1] Nafiseh Seyed Mazloum and Ove Edfors, "DCW-MAC: An Energy Efficient Medium Access Scheme Using Duty-cycled Low-power Wake-up Receivers," in *Proc. IEEE Vehicular Technology Conference (VTC Fall))*, San Francisco, CA, United States, pp. 1–5, September 2011.

[2] Nafiseh Seyed Mazloum, Ove edfors, "Performance Analysis and Energy Optimization of Wake-up Receiver Schemes for Wireless Low-power Applications," in *IEEE Transaction on Wireless Communications*, Vol. 13, No. 12, pp. 7050-7061, 2014.

[3] Nafiseh Seyed Mazloum and Ove Edfors, "Duty-cycled Wake-up Receivers and Single-hop Wireless Sensor Network Energy Optimization" under review for publication in *IEEE Transactions on Wireless Communications*.

[4] Nafiseh Seyed Mazloum, Joachim Neves Rodrigues, Oskar Andersson, Anders Nejdel, and Ove Edfors, "Improving Practical Sensitivity of Energy Optimized Wake-up Receivers: Proof of Concept in 65nm CMOS," under review for publication in *IEEE Sensors Journal*.

[5] Nafiseh Seyed Mazloum and Ove Edfors, "Comparing Analog Front-ends for Duty-cycled Wake-up Receivers in Wireless Sensor Networks," under review for publication in *IEEE Sensors Journal*.

During my Ph.D. studies, I have also contributed to the following publications. However, these publications are not included in the thesis:

[6] Nafiseh Seyed Mazloum, Joachim Neves Rodrigues, Ove Edfors, "Sub-$V_T$ Design of a Wake-up Receiver Back-end in 65nm CMOS," in *IEEE Subthreshold Microelectronics Conference*, Waltham, Massachusetts, USA, pp. 1–3, September 2012.

[7] Henrik Sjöland, John B. Anderson, Carl Bryant, Rohit Chandra, Ove Edfors, Anders J. Johansson, Nafiseh Seyed Mazloum, Reza Meraji, Peter Nilsson, Dejan Radjen, Joachim Neves Rodrigues, S. M. Yasser Sherazi, and Viktor wall, "A Receiver Architecture for Devices in Wireless Body Area Networks," in *IEEE Journal on Emerging and Selected Topics in Circuits and Systems (JETCAS)*, vol. 2, no. 1, pp. 82–95, March 2012.

[8] Henrik Sjöland, John B. Anderson, Carl Bryant, Rohit Chandra, Ove Edfors, Anders J. Johansson, Nafiseh Seyed Mazloum, Reza Meraji, Peter Nilsson, Dejan Radjen, Joachim Neves Rodrigues, S. M. Yasser Sherazi, and Viktor wall, "Ultra Low Power Transceivers for Wireless Sensors and Body Area Networks," in *8th International Symposium on Medical Information and Communication Technology (ISMICT)*, Firenze, Italy, pp. 1–5, April 2014.

# Acknowledgements

This work would have not been possible without the help and support from many.

First of all, I would like to express my special thanks to my supervisor Ove Edfors who has supported and encouraged me through all these years. Thank you Ove for your enthusiasm in trying new methods. Having a discussion with you always gives me a lot of new insights. A very big thank you Ove for your friendship. I would like to also express my gratitude to my co-supervisors Viktor övall and Henrik Sjöland.

Thanks to Joachim Rodrigues for providing me with the opportunity to implement a part of my work in hardware and thank you to you Oskar Andersson, Anders Nejdel, and Babak Mohammadi for helping me to do the measurements.

Special thanks to my mentor Björn Ekelund for all fruitful discussions.

Thanks to former and current colleagues in the radio systems group, Peter Hammerberg, Anders J Johansson, Meifang Zhu, Fredrik Tuvesson, Fredrik Rusek, Saeedeh Moloudi, Sha Hu, Muris Sarajlic, Zachary Miers, Ghassan Dahman, Dimitrios Vlastaras, Erik Bengsston Jose Flordelis, Carl Gustafson, Joao Vieira, Xuhong Li, Zachary Miers, Linnea Larsson, Mattias Holmer, Hamid Behjat, Xiang Gao, Taimoor Abbass, and Rohit Chandra, for joyful discussions during coffee breaks and lunch times. Special thank you to my friends for their kindness and their support. Thanks to all the administrative staff for all the help with practical issues.

Last but not least to my family: thank you for your unconditional love and support!

# List of Acronyms and Abbreviations

**ACK** ACKnowledgement

**ADC** Analog to Digital Coverter

**AFE** Analog Front-End

**AMF** Addres-spreadings Matched Filter

**ASIC** Application Specific Integrated Circuit

**AWGN** Additive White Gaussian Noise

**BACK** Beacon ACKnowledgement

**BER** Bit Error Rate

**BFSK** Binary Frequency Shift keying

**BLE** Bluetooth Low Energy

**BPF** Band Pass Filter

**DACK** Data ACKnowledgement

**DARPA** Defence Advanced Research Projects Administration

**DBB** Digital Base-Band

**DC** Direct Current

**DCW** Duty-Cycled Wake-up receiver

**DN** Destination Node

**DSN** Distributed Sensor Networks

**FA** False Alarm

**FIR** Finite Impulse Response

**FSK** Frequency Shift Keying

**ID** IDentity

**IEEE** Institute of Electrical and Electronics Engineers

**ISM** Industrial, Scientific and Medical

**IoT** Internet of Things

**LPF** Low Pass Filter

**LP-SVT** Low Power Standard Threshold

**M** Miss

**MAC** Medium Access Control

**MF** Matched Filter

**NDN** None-Destination Node

**OOK** On-Off Keying

**OVSF** Orthogonal Variable Spreading Factor

**PPM** Pulse Position Modulation

**PMF** Preamble Matched Filter

**PN** Pseudo Noise

**PWM** Pulse Width Modulation

**RF** Radio Frequency

**ROC** Receiver Operating Frequency

**Rx/RX** Receiver

**SN** Source Node

**SNR** Signal to Noise Ratio

**SOSUS** SOund and SUrveillance System

**SR** Shift Register

**Sw** Switch

**Tx/TX** Transmitter

**ULV** Ultra-Low Voltage

**WACK** Wake-up beacon ACKnowledgement

**WB** Wake-up Beacon

**WBAN** Wireless Body Area Network

**WRx** Wake-up Receiver

**WSN** Wireless Sensor Network

# Contents

# Part I

# Overview of Research Field and Complementary Results

# Chapter 1

# Introduction

## 1.1 Background

As with many technologies, the history of wireless sensor networks (WSNs) originates in military applications. An early distributed sensing system though not wireless, Sound Surveillance System (SOSUS) was introduced and developed at the beginning of the cold-war (1950). The SOSUS, a system of acoustic sensors (hydrophones) on the ocean bottom in the north Atlantic, was placed at strategic locations and used to detect and track quiet Soviet submarines [1].

Modern research on sensor networks started around 1980 with the Distributed Sensor Networks (DSN) program at the Defense Advanced Research Project Agency (DARPA), an agency of the United States Department of Defense. By this time, the ARPANET (predecessor of the Internet) had been operating for a number of years. The task of the DSN program was to check the applicability of the ARPANET for a network of area-distributed sensors. The network was assumed to have a collection of spatially distributed low-cost sensing nodes that operate autonomously and exchange data independently. Such demands are still considered when developing sensor networks for modern WSNs, ranging from military surveillance, medical monitoring, emergency rescue, target tracking, to building automation.

Today, the success of Internet of Things (IoT) has led to increasing demands on WSN applications, as more devices are now capable of more intelligent communication with each other, which opens many opportunities for pervasive environments, e.g., smart homes, smart offices, smart farms, and smart public places. The devices in WSNs are typically battery powered and sources of energy are very limited due to the small size of the devices and their possible placements. Even if a part of the energy can now be supplied by potential

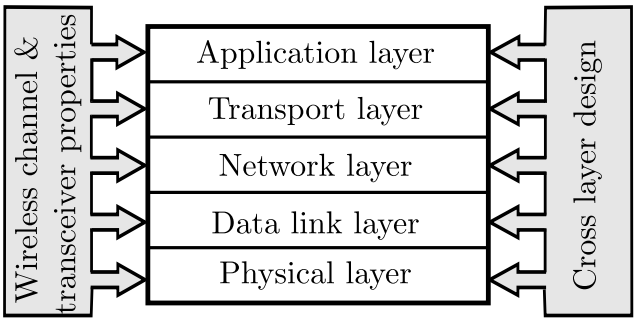


**Figure 1.1:** Protocol stack for wireless sensor networks. (Inspired by [4].)

energy harvesting techniques, the amount of energy available is, however, still very low [2]. It is, therefore, imperative that both communication protocols and circuits are carefully designed so that energy sources last the device/network life-time.

Inherited from Internet protocols, WSN communication protocols are designed according to the layered model presented in Fig. 1.1, consisting of physical, data link, network, transport, and application layers. Despite extensive success of the Internet protocol, design of a reliable and energy-efficient communication protocol based on the layered model becomes a challenging task due to the characteristics of WSN applications. Several examples of these are restrained energy resources, limited computational and memory resources, high network dynamics, and changing data traffic patterns. The unique characteristics of WSNs motivate cross-layer protocol design where strict boundaries between layers are removed and functionality of two or more layers are included in a single framework [3, 4]. In addition, the broadcast nature and non-deterministic characteristics of WSN channels and low-power design of transceiver circuitry have strong impact on higher layers and create interdependency between each layer. This motivates that properties of low-power transceivers and wireless channel conditions should be considered in the protocol design.

This research deals with co-design and co-optimization of a low-power medium access scheme (MAC), in the data link layer, responsible for communication establishment and a physical layer responsible for modulation, transmit and receive techniques. More specifically, we investigate how changes in the addressed MAC scheme parameters, transceiver design characteristics, and channel conditions relate to energy performance and delay of the target network. The importance of the analysis is that the final results of the

cross-layer optimization rely on analytical calculation rather than simulations allowing more detailed understanding of the relationships.

## 1.2 Outline

Chapter 2 presents an overview of WSN communication protocol layers serving as a background information for the readers who are not very familiar with the field. In Chapter 3 an overview of low-power medium access schemes is presented. The purpose is to provide a background to existing solutions as well as an introduction to the approach investigated in this thesis. Chapter 4 presents how the analysis and optimization of this study can be adapted to other systems with different radio designs. This also includes a more detailed description of a node functionality as well as presentation of packet structures used to establish communication between nodes. A summary of optimization problems used together with some results complementary to the ones in the included papers are presented in Chapter 5. Finally, Chapter 6 presents a summary of the included papers and highlights the contributions to the research field.

# Chapter 2

# Wireless Sensor Networks

A WSN is a network comprised of spatially distributed sensing nodes in a sensor field which exchange sensed data through wireless communication, as illustrated in Fig. 2.1. A sensor node is a device typically consisting of one or several sensors, a processor, a transceiver, and an energy source. With advances of technology and increasing demand on interconnected devices, more new WSN applications in biomedical, household, industry, and military are emerging. Low cost, small size and energy autonomy are typical main requirements in WSN design. In this chapter, we first provide an overview of network topology and data traffic, the two main factors influencing WSN design. We then give a brief overview of communication protocol layers. We finally discuss the importance of cross-layer solutions for efficient WSN design and briefly describe our approach in this direction.

## 2.1 Network Topology

The topology of a network refers to both the locations of the nodes that are available for communication and the wireless links between them. In WSNs, the topology plays an important role in minimizing power consumption and latency and in providing connectivity and quality of communication. The most common topologies deployed, as shown in Fig. 2.2, are peer-to-peer, star, cluster tree and mesh:

- In a *peer-to-peer* topology all nodes are allowed to communicate directly with each other without any need to go through a central communication unit (hub).

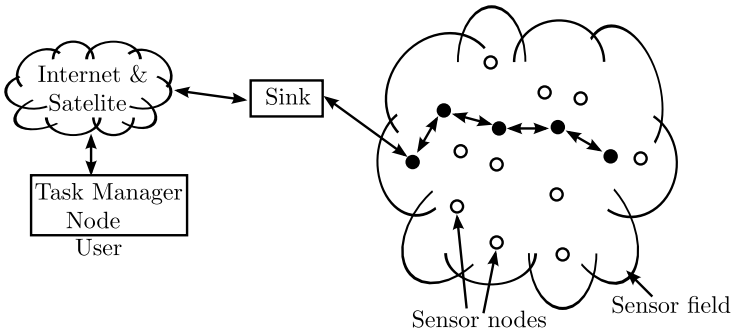


**Figure 2.1:** Sensor nodes scattered in a sensor field. (Figure originally found in [3].)

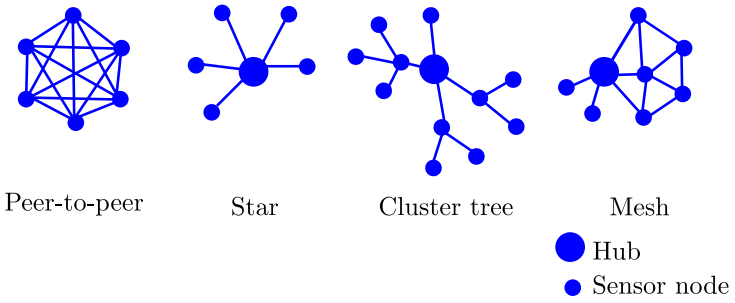


**Figure 2.2:** Network topologies in WSN design.

- In a *star* topology all nodes are connected to a central unit (hub) where all the communications need to go through.
- In a *cluster tree* topology each node is connected to a node higher in the tree and then to a hub. Data or communication from the lowest nodes needs to go through the tree to get to the hub.
- In a *mesh* topology nodes are connected to multiple nodes and communication is performed by choosing the most optimal route to the hub.

The analysis in this study addresses what we call symmetric networks with a non-hierarchical topology such as peer-to-peer or (a subset of) mesh topologies where all nodes are equal and directly connected to each other. As we show in Chapter 4, the analysis can also be adapted to more general cases.

## 2.2 Data Traffic

Data traffic dynamics in WSNs are highly application dependent. WSN applications can typically be divided to two categories: monitoring and event-detection. Monitoring applications often lead to periodic data generation and event-driven applications typically result in bursty data traffic.

When analyzing WSNs a traffic model, suitable for the application in hand, is necessary to characterize data traffic and communication patterns. For the analysis performed in this study we assume rare data packets where the traffic follow a distribution with an average packet inter-arrival time $1/\lambda$ seconds. As the results only depend on the average packet-arrival intervals, the analysis can be used for a wide range of applications. One traffic model often used is the Poisson process and we adopt terminologies from there.

## 2.3 Energy Efficient Communication Protocols

Sources of energy consumption in a typical WSN are due to three main functionalities of the nodes: sensing, processing, and communication. In this study, we focus on reducing energy consumption resulting from communication. In the following, we give an overview of different layers of the communication stack, shown in Fig. 1.1, with focus on physical and data link layers since they are central to the work presented.

### 2.3.1 Physical layer

The physical layer is responsible for data transmission over a wireless channel. More specifically the physical layer is responsible for frequency selection, carrier frequency generation, data coding, modulation, and signal detection [3]. These choices also highly influence transceiver circuitry designs as well as antenna properties. With the low cost, small size, and low power consumption requirements, an optimized physical layer design becomes a challenging task. In the following we first give an overview of the physical layer from a digital communication perspective. We then turn our attention to physical layer implementation aspects and transceiver circuitry.

The design choices will be different depending on the medium used for communications. In this study we address radio frequency-based (RF-based) wireless communications which is the most common one in WSNs[1].

[1]Other possible wireless links are infrared, body coupled communications, and acoustic or magnetic induction technique.

When designing a low-power small-size physical layer, the choice of operating frequency, transmit power, and coverage distance are key design factors. In general, the received signal power $P_s^{rx}$ of a receiver is characterized as (in dB)

$$P_s^{rx} = P_o^{tx} - L_p + G^{tx} + G^{rx}, \tag{2.1}$$

where $P_o^{tx}$ is the transmitter output power, $L_p$ the channel propagation loss at the investigated distance, $G^{tx}$, and $G^{rx}$ the transmitter and receiver antenna gains. Since size of antenna is proportional to wavelength, it makes sense to select higher operating frequencies as they allows for smaller antennas. On the other hand, the propagation loss in wireless channels depends on wavelength/frequency and distance. This means that the choice of higher operating frequencies leads to higher propagation loss. Increasing transmit power or improving receiver sensitivity can compensate for the propagation losses, both are however working against the low-power requirement. Increasing antenna gains is an alternative solution. With scattered sensor nodes omni-directional antennas are more favorable and for this reason the antenna gains are small. Therefore, for all the above practical reasons high operating frequencies result in higher propagation losses. Considering that the propagation loss is also proportional to distance, reducing the coverage distance by using a larger number of nodes and applying multi-hop networking can help to both fulfill low-power and small-size requirements [2,5,6]. Short coverage distance are also beneficial for reducing other channel effects such as fading, shadowing and diffraction.

Other important design factors are the choice of modulation and coding schemes as they directly influence transmitter efficiency, receiver complexity, as well as data transmission energy cost. Energy efficient non-coherent binary modulation techniques, such as non-coherent binary frequency shift keying (BFSK) or on-off keying (OOK), are typically considered as they also allow for low-power low-complex receiver designs [6–8]. Modulation scheme performance in terms of bit-error-rate (BER) depends on the signal-to-noise ratio (SNR). Using (2.1), SNR and modulation scheme performance are simply related to transmit output power and propagation losses (in dB)

$$\mathrm{SNR} = P_o^{tx} - L_\mathrm{p} + G^{tx} + G^{rx} - P_\mathrm{n}, \tag{2.2}$$

where $P_\mathrm{n}$ is the noise power.

For every application, a maximum BER or a minimum received signal power, typically referred to as sensitivity, is specified to achieve a certain reliability. Depending on channel conditions or characteristics of transceiver circuitry receivers may not be able to meet the requirement on BER or SNR. To maintain the BER or SNR within the limits, we either need to increase the transmit signal power, reduce data rate, or use more sophisticated schemes

such as coding. As mentioned earlier, increasing transmit power is working against a low-power requirement. Reducing data rate or introducing coding increases the active time of the transceiver or add complexity but the resulting improvement in detection performance reduces other energy costs instead. When we design the packet structure needed for establishing communication between nodes we reduce the actual data rate by applying spreading, which can be seen as a repetition code.

**Low-power circuit design** – In addition to careful selection of the modulation, operating frequency, and coverage distance, each architectural block in a transceiver needs to be designed carefully so that small-size, low-cost and low-power operation requirements in a sensor node are fulfilled.
*From an architectural perspective:* Low-power design strategies at architectural level typically lead to implementation/performance losses compared to performance predicted by theory. Depending on the chosen architecture the trade-off between performance and energy consumption can vary. We can include the performance loss, resulting from low-power design, in the link budget by changing (2.2) to

$$\mathrm{SNR} = P_o^{tx} - L_\mathrm{p} + G^{tx} + G^{rx} - P_\mathrm{n} - L_\mathrm{impl}, \tag{2.3}$$

where $L_\mathrm{impl}$ is the implementation loss. As we show later, by including this design trade-off in our design framework we study how implementation loss influences the design of the rest of the system. With this we take our first steps towards a cross-layer design.
*From an implementation and operation perspective:* To minimize size, the radio transceiver in a sensor node should be integrated into a single chip. Nanometer Complementary Metal-Oxide-Semiconductor (CMOS) technologies are typically chosen as we benefit from their versatility for mixed-signal functionalities. Their low cost in large volume production also fulfills the low-cost requirement. As technology evolves, CMOS continues to scale and provides new opportunities for saving energy in both analog and digital circuits. The analog circuit design is not directly addressed in this thesis. However, we design a digital circuit as a proof of concept in one of the papers.

### 2.3.2 Data link layer

The task of the data link layer is to provide a reliable point-to-point or point-to-multi point communication link. Multiplexing of data streams, data frame detection, medium access scheme, and error control are the main responsibilities of the data link layer [3]. Among the above tasks, we specifically discuss medium access techniques.

**Medium access scheme**

Medium access scheme is responsible for establishing the communication link between nodes and efficiently sharing the time, frequency, and energy among the nodes in the network. Since energy efficiency is the primary design requirement, it is crucial to identify the sources that cause an inefficient use of energy. The major sources of energy consumption during communication are [9]:

- *Collisions* which occur if two or more nodes decide to access the channel at the same time. With collision, nodes need to retransmit the data packet and retransmission consumes extra energy.
- *Idle listening* which refers to cases where the transceiver is listening to the channel for potential communication without receiving or transmitting data.
- *Overhearing* where a node picks up a packet that is not destined to it.
- *Control packet overhead*, while control packets assist in protecting and delivering the data packets, transmitting and receiving control packets consume power.

The radio of a node conventionally consists of a transmitter for data transmission and a receiver for both data reception and channel monitoring. With a relatively light data traffic in typical WSN applications, receiver idle channel listening becomes a dominant source of communication energy waste. One approach commonly used to reduce the cost of idle channel listening is duty-cycling where the transceiver is switched off when not used. By turning off the transceiver, nodes get disconnected from the network and it is therefore necessary to arrange simultaneous wake-ups if we want to maintain connectivity. While with the duty-cycle operation the overhearing energy cost is also reduced to a large extent, the energy cost resulting from collisions and packet overhead highly depends on the approach used to provide the connectivity of the nodes. There are three main approaches for keeping the connectivity of the nodes: *synchronous*, *asynchronous*, and *wake-up receiver* schemes. In the following, we briefly describe these methodologies and for details we refer the reader to Chapter 3.

- Synchronous schemes – all nodes wake-up and sleep periodically according to a predefined common schedule to communicate with each other.
- Asynchronous schemes – nodes wake up periodically but not based on a common synchronized schedule.

- Wake-up receiver schemes – All nodes have an ultra-low power receiver, typically referred to as a wake-up receiver (WRx), dedicated for channel listening. The ultra-low power receiver listens continuously or periodically to the channel and wakes up the main radio whenever it detects a potential communication.

WRx schemes can potentially fall into synchronous or asynchronous classification. We, however, address these schemes separately to single them out from the conventional synchronous and asynchronous schemes where node's radios only consist of a main transceiver.

Energy efficiency is the primary goal in the above schemes, but they also need to deliver reasonable performance in terms of delay and reliability. Periodic channel listening increases data transmission delay which is not favorable in many WSN applications. It is therefore of importance to design our protocol not to exceed the network tolerance ranges. On the other hand, WRx low power operation is often at a cost of lower performance compared to the main receiver. Unless compensated somehow, using a low-power low-performance WRx leads to extra errors in packet detection. As we show in this thesis, the design of control packets, used for establishing the communication, becomes an important part of the WRx schemes design.

### 2.3.3 Network layer

When nodes are not in the transmission range of a destination node (sink), detected events or sensed data needs to be delivered to the destination node through other nodes in the network, as illustrated in Fig. 2.1. The network layer determines the path for forwarding the collected/sensed data between source and destination nodes. This forwarding of data through other nodes is typically referred to as multi-hop networking. In this thesis we are targeting peer-to-peer single-hop networks and therefore do not focus on the analysis related to routing algorithms.

### 2.3.4 Transport Layer

The transport layer is responsible for reliable data delivery and quality of service in an energy efficient fashion. The nature of traffic in WSNs flowing from sensor nodes to a sink can lead to congestion, collision, and full memory capacity and thereby packet loss. Any packet loss impairs the reliability and can lead to an increase in energy consumption. The transport layer needs to provide packet loss recovery and a congestion control mechanism. Again, since we assume peer-to-peer single-hop networks, we do not include the transport layer in our analysis.

### 2.3.5 Application layer

The application layer is the highest layer and is responsible for providing necessary interface to interact with the physical world through the WSN. Algorithms related to the application layer are also beyond the scope of this thesis.

## 2.4 Discussion – Cross Layer Design

The layered architecture stack provides guidelines or strategies to design a WSN. Unique characteristics of WSNs in terms of highly employed number of nodes, dynamic topology and restricted resources, however, require removing the boundaries between layers. They also motivate inclusion of low-power radio transceiver property and wireless channel conditions in the protocol design. Cross layer solutions/integration prevents data overhead and results in a more energy efficient design.

Existing solutions addressing cross layer interaction are often designed and optimized for parameters in the upper layers without including the influence of radio design characteristics, e.g., [1, 3, 10–16]. On the other hand, there are many transceiver designs focusing on fulfilling low-power consumption requirements, e.g., [17–20]. While these designs may achieve a very high performance in terms of metrics necessary for transmitter or receiver, they are not fully optimized to minimize network energy consumption while maximizing the overall network performance. Only a few studies have addressed cross layer design of communication protocols in combination with radio design, e.g., [21, 22]. New standards, e.g., Bluetooth Low Energy (BLE), and IEEE 802.15.6, as well as classic ones, e.g., IEEE 802.15.4, addressing low-power long life-time wireless connectivity are based on cross-layer approaches. Their corresponding power saving mechanisms may, however, not always be applicable for low-power WSN applications.

In this study we take it one step further and perform a co-design of the physical layer, the characteristics of its implementation, and the medium channel access scheme. We break the node into its basic functionality to identify the most important radio parameters affecting energy consumption. We also parameterize transceiver performance characteristics and include their influence into our analysis through the link budget. We identify the relations between control packet design parameters, transceiver performance characteristics, and protocol parameters. We include all these parameters in a single framework and perform a joint analysis and optimization of the transceiver, physical layer, and medium access scheme designs. In the following chapters we detail this analysis and optimization.

# Chapter 3

# Low-power Medium Access Schemes

This chapter provides an overview of low-power channel listening schemes, namely *synchronous*, *asynchronous*, and *WRx schemes* as we characterize them in Chapter 2. For each type of scheme, we provide a summary of its overall operation, give a brief history, list some examples of existing solutions, and highlight their most important characteristics. We also give a brief description of the approach used to evaluate and compare these schemes. Before we start we introduce two naming conventions widely used. In all the schemes, the node with data available for transmission is called a source node and the intended receiver one the destination node.

## 3.1 Synchronous Schemes

In synchronous medium access schemes, nodes periodically wake up and sleep based on a common schedule to avoid idle listening energy cost. The basic principle of the communication procedure in a typical synchronous scheme is as follows. First each node goes through a setup phase, before starting regular periodic wake-up and sleep. In the setup phase, a node needs to select a schedule and exchange it with its neighbors. It also maintains a schedule table which stores the schedule of all its neighbors. To choose its schedule and establish its schedule table, a node first listens to the channel for a certain time. If the node does not receive any schedule from the neighboring nodes during this time period, it selects a random time as its own schedule and announces it to its neighbors by broadcasting a synchronization message. If the node

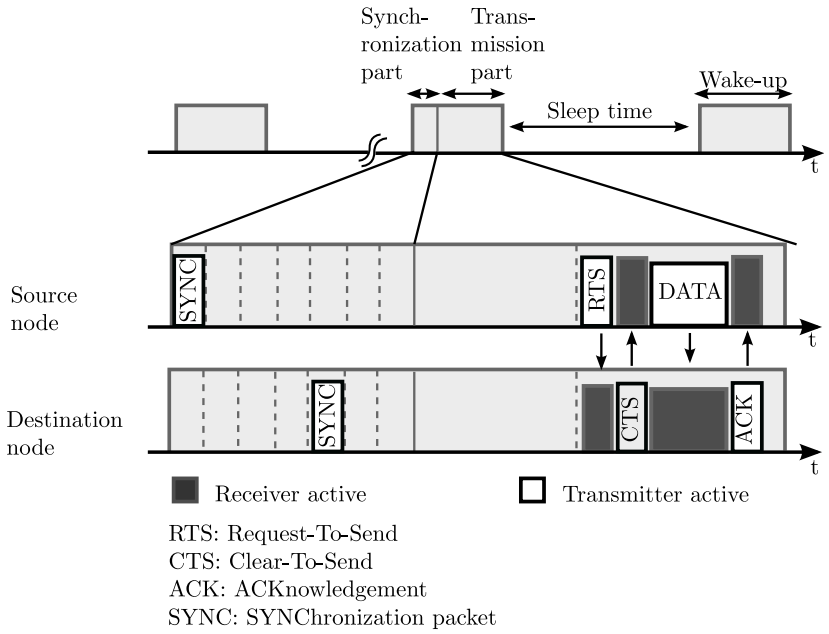


**Figure 3.1:** A simple timing diagram of a synchronous scheme.

receives a schedule from a neighboring node, it follows that schedule and also announces it to neighbor nodes. After the setup phase, nodes with the same wake-up schedule form a virtual cluster and start periodic sleep and wake up synchronously. During sleep a node turns off its radio and sets a clock that wakes it up later. At wake-up, as illustrated in Fig. 3.1, it enters two phases: the first one is synchronization and the second one data transmission. During synchronization a node updates or maintains the wake-up schedule by transmitting or receiving synchronization packets. During the transmission part, an actual data transmission occurs. A source node sets up its transmitter and transmits a request-to-send packet to the destination node. The destination node replies with a clear-to-send packet after receiving the request-to-send packet. Upon receiving the clear-to-send packet, the source node starts to transmit the data packet whose reception is acknowledged by the destination node in an acknowledgment packet.

The synchronous nature of this type of scheme accentuates the probability of collisions. To avoid collisions resulting from synchronous wake-ups, both synchronization and data transmission parts are divided into several slots. With this, nodes follow a normal contention procedure, where a randomized carrier

sense reduces the chance of collisions. Providing information regarding the duration of data transmission in the ready-to-send/clear-to-send packets is another approach which to a large extent mitigates the chance of collisions. The data transmission based on the above four-way handshake protects the data packet and also avoids collisions. To protect nodes from overhearing, control packets, i.e., ready-to-send, clear-to-send, and acknowledgment, include destination node addresses. With this, all non-destination nodes can go to sleep immediately after they hear the control packet.

#### A brief history

Sensor MAC (S-MAC) is a classical synchronous duty-cycled medium access scheme [9]. In S-MAC, nodes wake up and sleep periodically based on a common schedule with fixed wake-up intervals, independent of channel conditions and data traffic. S-MAC adaptivity to traffic is further improved by a new version of S-MAC (S-MAC with adaptive listening) [23] and timeout-MAC (T-MAC) [24] where, in both schemes, the wake-up interval is adjusted to data traffic. S-MAC with adaptive listening allows a node who overhears its neighbors to wake up at the end of data communication of the neighboring nodes. If the overhearing node is the next-hop node, its neighbor is able to immediately pass the data to it instead of waiting for its scheduled wake-up interval. Through this mechanism long latencies resulting from fixed wake-up schedules are avoided. In T-MAC, all transmissions are performed at the beginning of the data transmission phase. A node therefore needs to listen to the channel only for a short time, called the contention interval, after the synchronization phase. If no data is received during the contention interval, the node ends the wake-up and goes back to sleep. While this approach reduces the cost of periodic wake-up, it has the disadvantage of increased collisions as many nodes may intend to transmit at the same time. Moreover, the cost of idle listening during synchronization and data transmission is still substantial. SCP-MAC [25], RMAC [26], DW-MAC [13], and Z-MAC [27] are other examples of synchronous medium access schemes. These approaches propose new strategies to improve on latency or channel utilization.

### Characteristics

Synchronous medium access schemes achieve low-power operation by waking up the nodes only for a certain time period. They also simplify the communications as all nodes are awake at the same time. The drawback is, however, the complexity and overhead resulting from synchronization. In synchronous duty-cycled schemes, each node is required to enter a set up phase to estab-

lish or maintain its wake-up schedule. Therefore, there is always a constant energy consumption due to synchronization-packet exchange. Moreover, each node needs to constantly coordinate and update their wake-up schedules, which again leads to more overhead and more energy consumption. These schemes also have the disadvantage of increased end-to-end delay as a source node needs to wait until the next wake-up interval before it can initiate its data transmission. We do not include the synchronous schemes in our analysis, as they are costly in terms of energy and maintenance for our target WSN applications with low-traffic intensity.

## 3.2 Asynchronous Schemes

In asynchronous schemes, nodes wake up and sleep periodically, independent of the wake-up schedule of other nodes in the network to reduce idle listening cost. While asynchronous duty-cycled channel listening avoids costly synchronization, the challenge is how to establish communication between two nodes. Depending on which node initiates the communication, asynchronous schemes are classified as *transmitter-* or *receiver-initiated*. We start by reviewing transmitter-initiated schemes, we then move on to receiver-initiated schemes.

### 3.2.1 Transmitter-initiated schemes

All nodes in transmitter-initiated schemes wake up asynchronously for a certain interval to listen to the channel for potential communication, along the lines of what is illustrated in Fig. 3.2, and then go back to sleep if no data is detected. A source node transmits a series of short wake-up beacons (WBs) ahead of data to be able to communicate with the destination node. Each WB carries the destination node address to avoid overhearing. Whenever WB transmission and wake-up interval of the destination node coincide and the WB is detected the actual data transmission is initiated. Inter-beacon intervals are inserted so that the destination node can reply with an acknowledgment after receiving a WB. This allows the source node to immediately start the data transmission. Data reception is then acknowledged by the destination node in a data acknowledgment.

Since nodes access the channel independently in the transmitter-initiated schemes, collisions are not as critical as in the synchronous schemes. However, to avoid collisions resulting from channel access, nodes follow a random access contention procedure. Data transmission follows after the four-way handshake, as described above, to both protect the data packet and avoid collisions. To

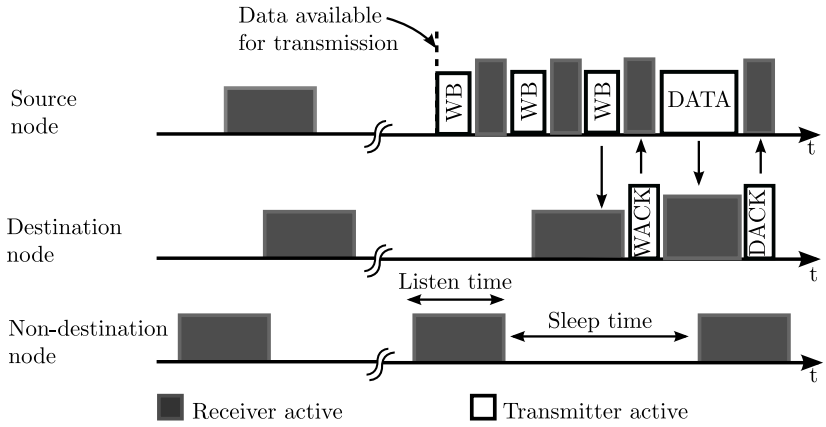


**Figure 3.2:** A simplifies timing diagram of an asynchronous transmitter-initiated scheme.

protect nodes from overhearing, control packets, i.e., WB, WB acknowledgment, and data acknowledgment, include destination node addresses.

### A brief history

Preamble sampling [28] and sparse topology and energy management (STEM) [29] are early asynchronous duty-cycled transmitter-initiated schemes. STEM separates wake-up and data transmission by using two radios on different channels. A series of short beacons which carries the destination node address are transmitted in the wake-up channel. Inter-beacon intervals are also inserted so that the destination node can reply with an acknowledgment after receiving a beacon. When the source node receives the acknowledgment, it initiates data transmission over the data channel. In preamble sampling, the source node appends a preamble, equal in length to sleep plus listen intervals, to the front of the data packet. If the destination node detects the preamble during wake-up, it stays on and continues listening to the channel until data is received. While preamble sampling allows low-power channel listening, the long wake-up preambles result in high power consumption overhead in transmission and reception. Different strategies are proposed to improve asynchronous channel listening performance. Wise-MAC [30], B-MAC [31], Wake-up frame MAC [32], and SyncWUF MAC [33] improve on preamble sampling MAC.

Wise-MAC reduces the length of the wake-up preamble by exploiting the sleep schedule information provided in the acknowledgment. In Wake-up frame and SyncWUF schemes a wake-up frame is used instead of the long preamble. The wake-up frames comprised of multiple short frames that are transmitted during an entire sleep plus listen intervals. This guarantees that the short wake-up frames can be heard by the destination node. Each short wake-up frame consists of a node destination address and information regarding start time of the data transmission. Both destination node and non-destination nodes go to sleep immediately after preamble detection. The destination node wakes up again at the data transmission time. CSMA-MPS [34], X-MAC [35] and TICER [36] are the most promising approaches in terms of low energy consumption. These schemes are based on the same principle as STEM but only one radio is used for both wake-up and data. CSMA-MPS, similar to Wise-MAC, reduces the wake-up cost by exploiting the wake-up schedule of neighboring nodes provided in the acknowledgment. X-MAC reduces the wake-up cost by adapting sleep and listen intervals to data traffic. DPS-MAC [37], C-MAC [38], and LWT-MAC [39] are some other transmitter-initiated scheme examples proposed to improve on preamble sampling scheme or X-MAC.

### 3.2.2 Receiver-initiated schemes

In a typical receiver-initiated scheme, similar to transmitter-initiated schemes, nodes asynchronously sleep and wake up. In contrast to transmitter-initiated schemes, it is the destination node that initiates packet exchanges. During wake-up, as illustrated in Fig. 3.3, nodes broadcast a WBs to announce that they are awake and then monitor the channel for a response for a certain interval. A source node switches on its receiver and listens for a WB from the destination node. Whenever WB transmission of the destination node and listen interval of the source node coincide, and the WB is detected, the source node starts data transmission. Reception of the data is then acknowledged by the destination node in a data acknowledgment.

When a node transmits a WB, it is possible that more than one node replies with a data packet and this may lead to collisions. Collisions can be reduced by introducing a random interval between hearing the WB and the start of data transmission[1]. This interval can be used in two different ways. In one approach [36], the WB is designed as the reference time synchronization point for all source nodes and a slotted scheme is adopted for the introduced interval. The source node selects one of the slots randomly to initiate data transmission. In the other approach [40] the WB includes a back-off window size. The source

[1]Note that for simplicity this extra random interval is not illustrated in Fig. 3.3.

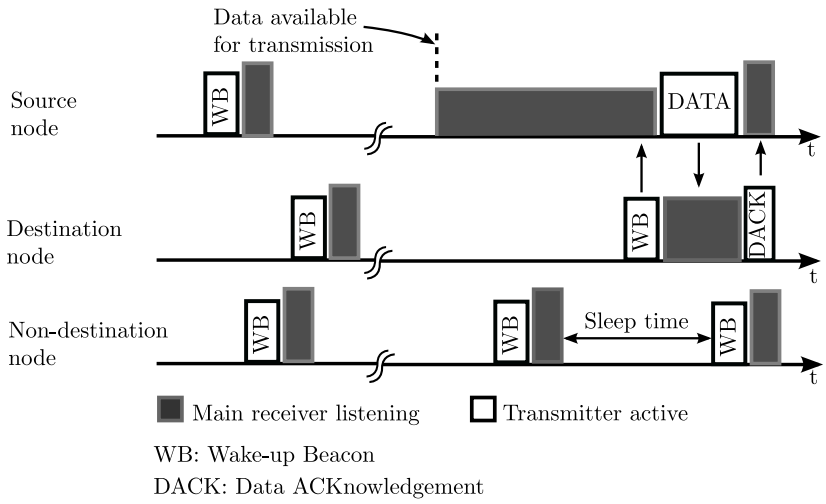


**Figure 3.3:** A simplified timing diagram of an asynchronous receiver-initiated scheme.

node performs a random back-off based on the introduced window size before data transmission. To mitigate collisions resulting from accessing the channel, similar to other schemes, nodes follow a random access contention procedure before initiating any transmission. Data transmission follows the above three way handshake to protect the data and avoid collisions.

### A brief history

Receiver initiated cycled receiver (RICER) [36] is an early duty-cycled receiver-initiated MAC scheme based on the above principles. In RICER collision avoidance is based on the time slotted approach. Receiver-initiated-MAC (RI-MAC) [40] is also based on duty-cycled receiver-initiated MAC scheme principles. In this scheme, however, WBs are used both for wake-up and acknowledgment purposes. In RI-MAC collision avoidance is based on the back-off window approach. Pseudo-random asynchronous duty-cycle MAC [41], PW-MAC [42], EM-MAC [43], and SA-RI-MAC [44] are other MAC scheme examples based on asynchronous duty-cycled receiver-initiated MAC principles. These schemes are particularly designed to improve on energy performance and channel utilization of the RI-MAC scheme. Different strategies are proposed to avoid collisions and to reduce the amount of idle listening of source nodes.

**Characteristics**

Asynchronous schemes are particularly attractive as nodes operate independently to avoid costly synchronization. The drawback, however, is that the energy consumption resulting from periodic channel listening or periodic WB broadcasting is still a substantial issue. This is especially true for applications where a maximum delay requirement is set and nodes are required to wake up more often. Another drawback is the overhead needed for establishing communication between nodes. In transmitter-initiated schemes, the overhead is related to periodic WBs need to be transmitted ahead of data by the source node. In receiver-initiated schemes, the overhead is due to long listen interval of the source node, before a source and destination node can communicate. In these schemes, cost of collisions caused by broadcasting periodic WBs also leads to extra overhead and increased energy consumption. Moreover, any increase in network size will dramatically increases collisions as more nodes need to access the channel for periodic WB broadcasting. For the above reasons we also exclude receiver-initiated MAC schemes from our analysis.

## 3.3 Wake-up Receiver (WRx) Schemes

In WRx schemes, to reduce the idle listening cost, an extra ultra-low power receiver, i.e., a WRx, is used for channel monitoring. The main receiver is mostly off and only powered on by the WRx when data is available on the channel. To save power, WRxs need to operate at a very limited power consumption – typically two orders of magnitude lower than the main receiver, e.g., in the order of $10\mu$W [5]. There are two approaches for how a WRx can be used. A WRx can be always on and continuously listen to the channel or it can utilize duty-cycling and only listen to the channel for a certain time period to achieve even lower energy consumption. In the following we give a brief description of both principles.

### 3.3.1 Always-On WRx schemes

In Always-On WRx type of schemes, as shown in Fig. 3.4, WRxs of all nodes are always on to monitor the channel for activity. A source node switches on its transmitter and initiates communication by transmitting a WB to the destination node. As WRxs continuously monitor the channel, a single WB is ideally enough to wake-up the main radio. After WRx of the destination node detects a WB the node switches on its transmitter and transmits a WB acknowledgment back to the source node where-after data transmission is initiated by the source node. The reception of the data is then acknowledged in

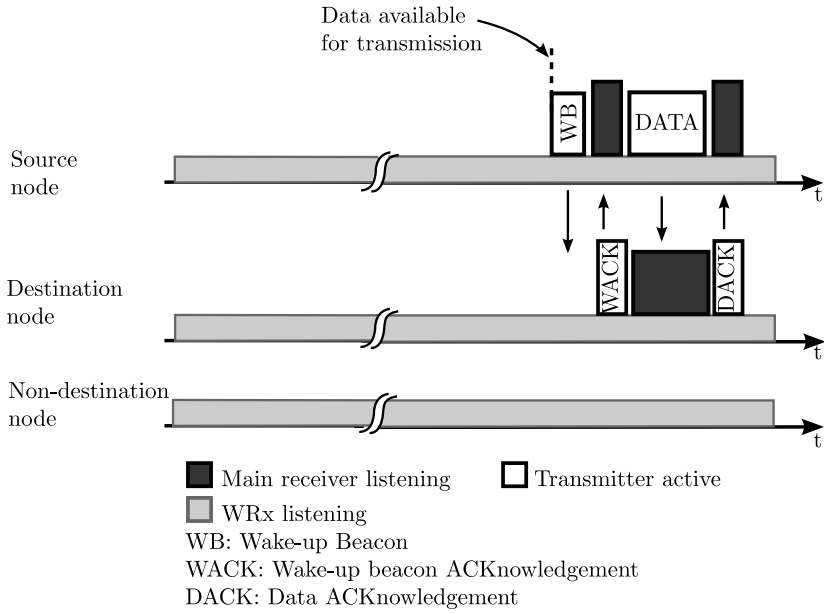


**Figure 3.4:** A simplifies timing diagram of an always-on wake-up receiver scheme.

a data acknowledgment.

### 3.3.2 Duty-cycled WRx (DCW) schemes

All nodes in DCW schemes, as shown in Fig. 3.5, turn on their WRxs periodically and asynchronously to monitor the channel for potential communication. The main receiver is switched on only when there is data to receive. Data transmission in the DCW-MAC scheme is performed based on the same principle as asynchronous transmitter-initiated MAC schemes, described in Section 3.2. The difference is that WBs, which have a major role for establishing the communication, are now detected by a separate low-power low-performance WRx. The principle of data communication in DCW-MAC schemes is as follows. When data is available for transmission, the source node switches on its transmitter to transmit periodic WB. When the listen interval of the WRx coincides with a WB transmission carrying its address, and a WB is detected, the destination node switches on its transmitter to transmit a WB acknowledgment. The source node therefore has to change to receive mode after each WB to investigate if a WB acknowledgment is available. If a WB

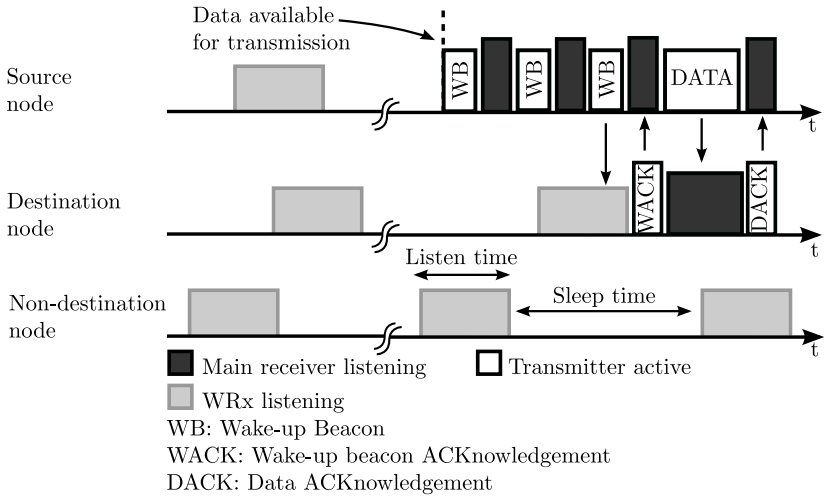


**Figure 3.5:** A simplified timing diagram of a duty-cycled wake-up receiver scheme.

acknowledgment is received, the source node initiates its data transmission, which is then acknowledged by the destination node with a data acknowledgment.

In both WRx schemes, since nodes access the channel independent of wake-up schedule of other nodes, the cost of collisions is less critical than synchronous and asynchronous receiver-initiated schemes. However, to avoid collisions nodes follow a random access contention procedure when accessing the channel. All nodes also follow a four-way handshake to protect data transmission and avoid collisions. To avoid overhearing, control packets, i.e., WB, WB acknowledgment, and data acknowledgment, include destination node addresses. Furthermore, one of the control packet, i.e., the WB, is now received by a low-power low-performance WRx and some strategies are needed to avoid performance loss in terms of WB detection.

### A brief history

The use of a low-power WRxs originally proposed in [5] where a low-power radio serves as a "small ear" that keeps listening to the channel when the main receiver is switched off. First steps towards design and analysis of DCW schemes was taken in [36]. However, as the success of the WRx schemes strongly depends on if a WRx with low power consumption and reasonable performance

can be implemented in hardware, most studies on WRx schemes focus their attention on low-power design of WRx circuitry and more specifically on its analog front-end architecture [45–66]. The prime focus of this study is design, analysis and a cross-layer optimization of DCW-MAC schemes.

#### Characteristics

Always-On WRx schemes reduce the cost of idle channel listening, since the main receiver only needs to be switched on when data is available on the channel. These schemes are particularly interesting for applications where delay is the main design requirement since, in contrast to asynchronous duty-cycled transmitter-initiated MAC schemes, only a single WB is necessary to establish the communication between nodes. With an Always-On WRx scheme, however, the average energy consumption of the network is relatively high and cannot go below the (always-on) WRx energy consumption. In asynchronous DCW-MAC schemes, on the other hand, by adding duty-cycling to low-power WRx schemes we can potentially save even more energy. The associated drawback is longer wake-up delays.

Low-power WRx design often comes at the cost of degraded performance compared to the main receiver. The performance loss resulting from the WRx low-power design together with the choice of transmission power and coverage distance, *cf* (2.3), strongly influences the WB detection performance, in terms of WB miss and false-alarm probabilities. Both error probabilities lead to extra energy cost, as we detail in Chapter 4.2. Therefore, while it first may seem appealing to go for lower and lower WRx power to save energy cost, the associated increase of WB detection errors can at the end prevent us from saving energy. It is therefore important to find a balance, which we will come back to in the following chapters.

## 3.4 Discussion – Performance Evaluation and Optimization

In the previous sections we described the main characteristics of DCW-MAC and other low-power channel listening schemes. To evaluate the respective strengths and weaknesses of the DCW-MAC scheme, we need to compare its performance with other schemes under different network settings and traffic conditions. Energy efficiency is the most important design requirement, we therefore use energy consumption as a measure for our performance comparisons. Duty-cycling adds an extra delay and there are many WSN applications

that are sensitive to long delays. Communication delay is therefore another measure we use to evaluate different schemes.

To narrow down the scope of our optimizations and comparisons with previous schemes, we make use of the fact that our proposed DCW-MAC scheme is a combination duty-cycling and low-power WRxs. Both these classes of MAC schemes have been analyzed separately for energy consumption and delay. The Always-ON schemes have been compared [67, 68] to duty-cycled schemes without low-power WRxs and duty-cycled schemes compared [30, 32–35, 37, 69] primarily against each other. Very few of these schemes have, however, been optimized in a structured way for low energy consumption [35, 38, 69–73]. We perform a systematic joint optimization of both duty-cycling and WBs for DCW-MAC, where minimal total energy consumption per data packet is the objective. The optimization takes into account both WRxs characteristics, network size, and packet arrival rates.

Throughout our work we use the transmitter initiated X-MAC and Always-On WRx MAC as points of reference, against which we make all our comparisons, since our proposed DCW-MAC can be seen as a combination of the two. This makes it possible to directly study how and when duty-cycled schemes can gain from employing low-power WRxs as well as how and when low-power wake-up schemes can gain from introducing duty cycling. As we will show, achieved gains depend largely on the characteristics of the low-power WRxs used.

Our optimization procedure is different from most other approaches in that we do not rely on system simulations. Instead, we use analytical derivations and numerical optimization. The optimization process is rather complex, but the analytical approach allows us to derive simple and accurate approximations of the optimal energy gains for wide parameter ranges. Through these approximations it possible to quickly assess how large an impact a design change has on system energy consumption and what the resulting communication delays are.

Based on the optimization results we also derive simple expressions for comparing WRxs or, more correctly, their analog front-ends, in terms of their impact on the energy cost for performing a wake-up. This leads to a relative "figure of merit" frame-work that can be used to compare different analog front-end designs [45–66] when applied in the DCW-MAC context.

In the coming chapters we discuss both how the analytical derivations of energy consumption are done and how we perform the numerical optimizations.

# Chapter 4

# System Design Considerations

In this chapter we discuss how the analysis and optimization of this study can be adapted to more general cases than what is presented in included papers. This chapter also provides detailed state-transition diagrams of our reference radio where we break the radio functionality down into basic operations. The space-state model is used to develop the energy consumption expressions in Paper III. We end the chapter by presenting possible WB structures and their corresponding WB detection techniques.

## 4.1 BER Performance Analysis

As mentioned earlier, limited power budget and low-power design of WRxs lead to an architecture with a performance typically lower than the main receiver. In Fig. 4.1(a) we show block diagrams of a source and a destination node. Each node consists of a transmitter, a receiver, and a wake-up receive, i.e., WRx, and a sleep timer. In the source node, the transmitter is used both for transmitting WBs and data. In the destination node, the WB is received by the low-power low-performance WRx, while data is received by high performance main receiver. Their different performance is indicated by different receiver noise for the two. The effect of this is also illustrated in Fig. 4.1(b) which shows the BER characteristics for the two receivers, as a function of received power. The WRx loss of performance, compared to the main receiver, needs to be taken into account in the design of the WRx scheme. For instance, when transmitting WBs, transmit power may have to be increased since the WRx is

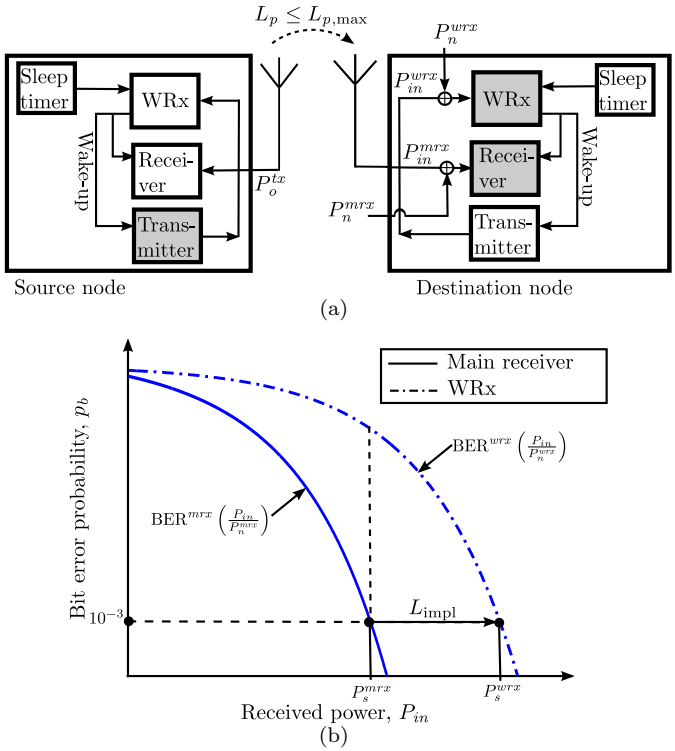


**Figure 4.1:** (a) Block diagrams of a source and a destination node. (b) Illustration of BER performance of WRx and main receiver versus received power.

the receiver. Another approach is to employ spreading, allowing WBs to carry more energy without increased transmit power. Combinations thereof are, of course, also possible. If we use different transmit power for data and WBs,

$$P_o^{tx} = \begin{cases} P_o & \text{, for data transmission} \\ P_o + \Delta P & \text{, for WB transmission} \end{cases} \tag{4.1}$$

the received power for the two cases becomes

$$P_{in}^{mrx} = P_o - L_p, \text{ and} \tag{4.2}$$

$$P_{in}^{wrx} = P_o + \Delta P - L_p. \tag{4.3}$$

Depending on the propagation loss $L_p$ and what numbers we use for $P_o$ and $\Delta P$, we can theoretically select any suitable BERs for data and WBs. To

fully compensate for the implementation loss, at the $10^{-3}$ BER where our receiver sensitivity is defined, using only an increase in transmit power we need $\Delta P = L_{\text{impl}}$[1]. Large variations in transmit power can be a viable solution in certain applications where the transmitter is designed to allow a large dynamic range.

For the type of applications where simplicity of nodes and transmitters are of importance, we need to keep $\Delta P$ small and BER of the WRx can be significantly larger than that of the main receiver. For the case when $\Delta P = 0$, we have $P_{in}^{wrx} = P_{in}^{mrx}$ and considering the performance difference in the form of $P_n^{wrx} = P_n^{mrx} + L_{\text{impl}}$, the WRx BER can be expressed in terms of main-receiver SNR as

$$p_b^{wrx} = \text{BER}^{wrx}\left(\text{SNR}^{mrx} - L_{\text{impl}}\right), \tag{4.4}$$

where

$$\text{SNR}^{mrx} = \frac{P_{in}^{mrx}}{P_n^{mrx}}. \tag{4.5}$$

For the case where the same type of modulation is used both for data and WBs, i.e., where $\text{BER}^{wrx}(\text{SNR}) = \text{BER}^{mrx}(\text{SNR}) = \text{BER}(\text{SNR})$, an implementation loss $L_{\text{impl}} > 0$ leads to a degradation

$$p_b^{wrx} = \text{BER}\left(\text{SNR}^{mrx} - L_{\text{impl}}\right) > p_b^{mrx} = \text{BER}\left(\text{SNR}^{mrx}\right), \tag{4.6}$$

since BER decreases with increasing SNR. This particular case with the same type of modulation and $\Delta P = 0$ is the focus of our study, but the entire analytical framework can be applied to the more general case with different modulation types and/or different transmit powers by substituting the expressions above.

## 4.2 State-space Model

When designing a low-power medium access scheme, a good understanding of the amount of power/energy consumed in different parts of the circuitry is necessary. From a system point of view, it is also important to understand how the functionality of different parts influence the total energy consumption. The overall operation of a single node accessing the medium using the DCW-MAC is illustrated as a state diagram in Fig. 4.2 (also in Paper III). The node only periodically switches on its low-power WRx to listen for a WB in the duty-cycling (DC) mode. Both the transmitter and the main receiver are switched off in this mode. The main receiver and the transmitter are only switched on when data packets are expected to be received, in receive (RX) mode, or data is available for transmission, in transmit (TX) mode. In this

[1]This is necessary to make $P_{in}^{mrx} = P_s^{mrx}$ and $P_{in}^{wrx} = P_s^{wrx}$.

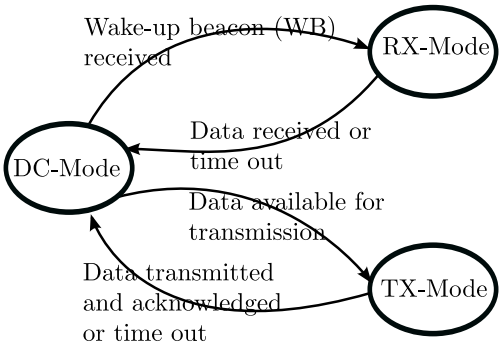


**Figure 4.2:** State-transition diagram of overall operation of a node for the DCW-MAC scheme.

section, we provide a detailed description of each macro-state by defining their internal states. We have used these detailed state-space models to develop energy consumption expressions in Paper III, but the page limitation prevented us from presenting all details. In the more detailed state-space figures presented here, the parameters $(P_{state}^{part}, T_{state}^{part})$, shown below each state represent the power consumption of, and the time interval spent in, the corresponding state. When both the *state* of operation and the active *part* are the same, we simplify notation to $P^{part}$ and $T_{state}$.

### 4.2.1 DC-Mode

As stated earlier, nodes sleep and wake up periodically in the DC-Mode. The detailed behavior of the node in this macro-state is shown in Fig. 4.3. We see three states which are cycled through during the channel listening; SLEEP, SETUP-WRX and LISTEN. The node cycles through these three states until a WB is received or data is available for transmission, in which cases the node enters the RX-Mode or TX-Mode macro-states, respectively. The SLEEP state represents the node status when both the WRx and the main radio are switched off. The energy consumption in this state is determined by the sleep/listen timer and sleep power of the radio. In the LISTEN state the low-power WRx is turned on to examine the channel for an incoming WB. When the WRx decides whether a WB is present, two types of error may occur: (i) the WRx may miss a WB transmitted to it or (ii) it may falsely detect a non-existing WB. The latter can happen both when only noise is received or, more likely, when a WB addressed to another node is present on the channel. Both WB miss and false-alarm occur with some probabilities. We denote these two fundamental

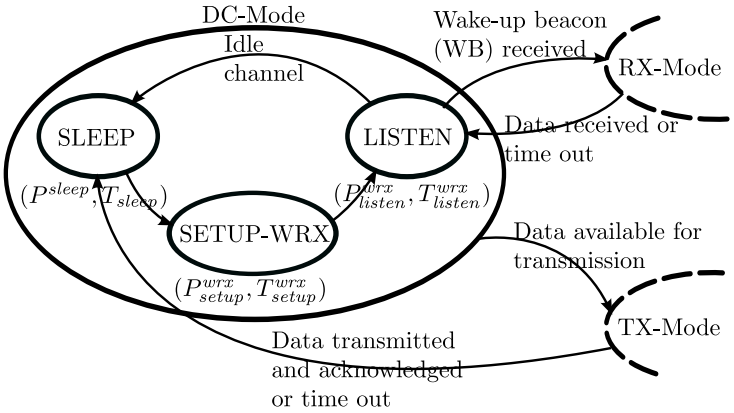


**Figure 4.3:** State-space model of a node in the DC-Mode.

error probabilities by $p_M^{wb}$ and $p_{FA}^{wb}$, respectively. A WB miss results in extra energy cost at the source node as it needs to transmit extra WBs until the WB transmission and listen intervals coincide again. We take into account this extra energy cost when calculating average consumed energy of the source node in the TX-Mode, reflected in (16) in Paper III. A falsely detected WB leads to an extra energy cost as the node enters the RX-Mode erroneously. The WRx power consumption and time spent to listen for a WB together with the extra cost resulting from erroneously detecting a WB determine the average energy consumption in the LISTEN state, reflected in (26) in Paper III.

### 4.2.2 TX-Mode

Whenever a node has data to transmit, it enters the TX-Mode, which is presented in more detail in Fig. 4.4. The number of states in TX-Mode is much larger than in the DC-Mode discussed earlier, but the behavior is relatively straight forward. We sub-divide the TX-Mode in two separate macro-states, the WTX-Mode and the DTX-Mode, which follow each other in a sequence. Energy consumption of a node in TX-Mode is the sum of energy consumption of these two macro-states, as calculated in (17) in Paper III. When data is available for transmission, the node enters the WTX-Mode, where WBs are transmitted until acknowledged by a WACK. The node then enters the DTX-Mode to transmit the data. When data is acknowledged by a DACK, or if the node anytime during this procedure reaches a timeout, the node returns to the DC-Mode. In addition to the transmission of WBs and receiving WACKs, the WTX-Mode also includes a state for setting up the transmitter (TX-SETUP)

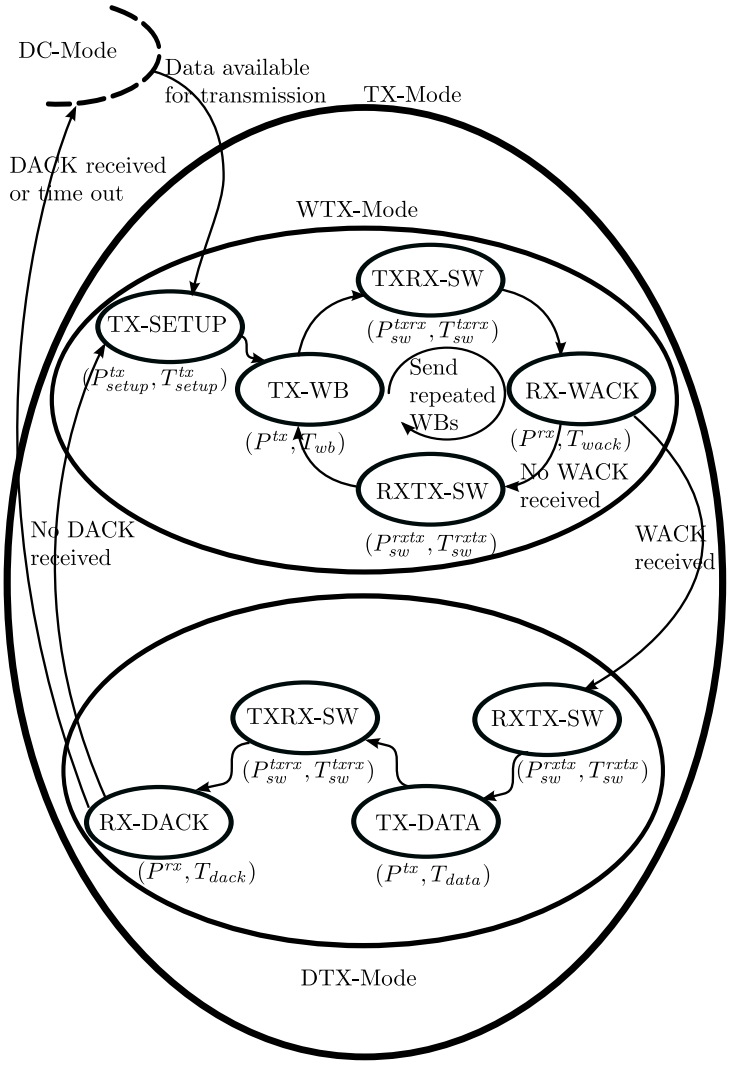


**Figure 4.4:** State-space model of a node in the TX-Mode.

and two states for switching back and forth between transmitter and receiver (TXRX-SW and RXTX-SW). States representing switching between transmitter and receiver also appear in the DTX-Mode, where they are needed before data transmission and DACK reception. Given the power consumption and

time spent in each state, there are two things that determine the average energy consumed in these states: (i) the average number of WBs we transmit per attempt to transmit a data packet and (ii) with what probability each data transmission is unsuccessful (probability of miss). In more detail (i) is determined by when the WB transmission cycle first coincides with listen period of the destination node, the probability that there is a miss in the WB/WACK exchange when they coincide, and how many extra WBs need to be transmitted before the WB transmission and listen intervals coincide again. The extra number of WBs per wake-up is proportional to the WRx sleep time. When data is finally transmitted, there is a certain probability that there is a miss in the DATA/DACK exchange and, if that occurs, the node returns to the periodic WB transmission again in the WTX-Mode, where it essentially starts all over gain. The influence of this error event is reflected in (16) in Paper III.

### 4.2.3 RX-Mode

If the WRx detects a WB with its address, the node enters the RX-Mode which is illustrated in more detail in Fig. 4.5. The RX-Mode consists of two macro-states, DRX-Mode and DARX-Mode. Energy consumption in RX-Mode is calculated by summing the energy consumption of these two macro-states, as in (23) in Paper III. Contrary to what the name RX-Mode may suggest, the first action in the RX-Mode is to enter the DRX-Mode where the transmitter is switched on to transmit the WB acknowledgment WACK. After that initial transmission, the main receiver is switched on to receive data. If data is received, the node continues to the DARX-Mode, where the data acknowledgment DACK is transmitted. After this, or if no data is received in the DRX-Mode within a given time limit, the node returns to DC-Mode. Like in the TX-Mode, as described earlier, the RX-Mode contains a number of states where the transmitter is set up (TX-SETUP) and where switching between transmission/reception is performed (TXRX-SW and RXTX-SW).

There are no internal cycles in the RX-Mode, which means that energy consumption in this mode only has two different levels depending on: (i) if the data reception works without errors or (ii) if there is a miss in the WACK/DATA exchange. In (i) all states in the RX-Mode are traversed in order, while the RX-Mode is exited after the RX-DATA state if no data is received within a certain time limit. This last error event happens with some probability and generates additional energy consumption in the duty-cycled listening of the destination node and in the TX-Mode of the source node, which has to re-initiate its transmission of the data by sending new WBs (see TX-Mode above).

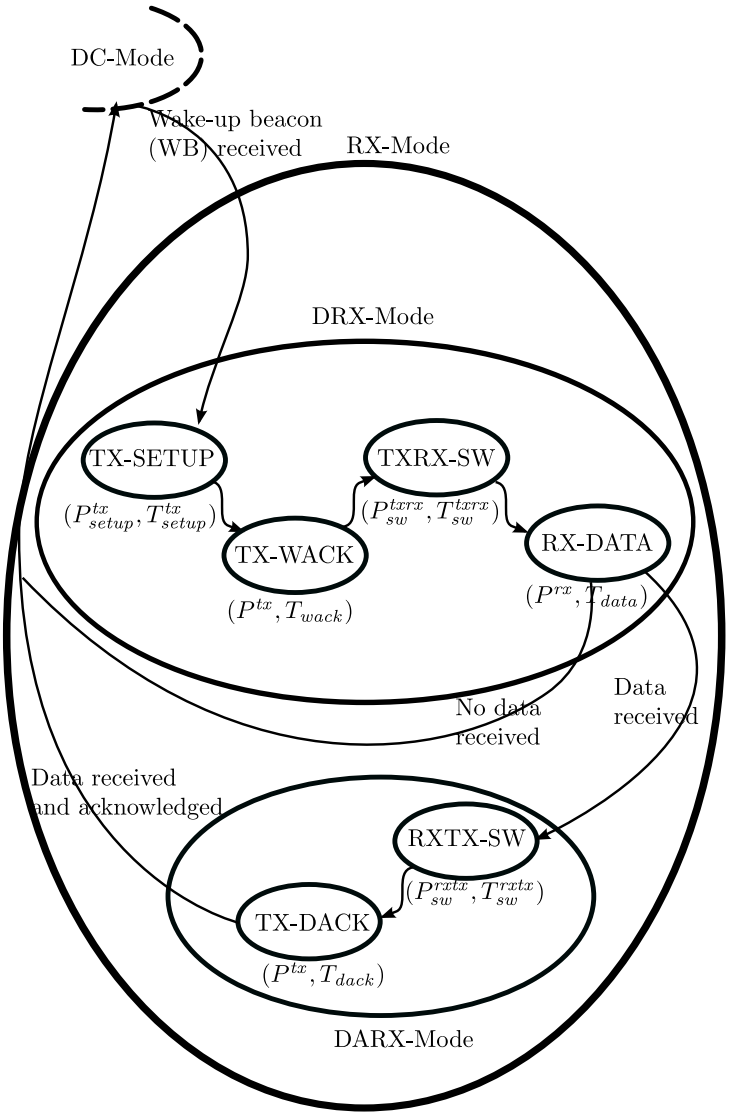


**Figure 4.5:** State-space model of a node in the RX-Mode.

## 4.3 Wake-up Beacon Detection Techniques

The WB structure is an important part of the DCW-MAC design. With asynchronous communication WBs may arrive at any time in the listen interval and

they are received by a WRx with a performance lower than the main receiver. Both the unknown arrival time of the WB and using a low-performance WRx highly influence WB detection. Any error events related to WB detection are costly and lead to longer delays, and result in higher total energy consumption. Additionally, the WB length directly determines the length of listen interval, thereby affects the number of transmitted WBs and resulting delays. It is, therefore, important to structure the WB so that

- it provides synchronization and avoids unnecessary wake-up due to overhearing,
- no complex processing is needed, and it allows small memory usage and low hardware cost both in terms of power consumption and area,
- scalability to networks of different size is provided,
- long delays can be avoided,
- it is robust to noise and interference and supports strategies to compensate for the WRx performance loss so that probabilities of WB miss and false alarm are kept low[2].

A WB in its simplest form is a signal with a certain pattern. A correlator based on analogue processing [48, 49] can be used to detect the WB signal. While this approach allows for low power operation, it makes it difficult to meet any of the above requirements. Digital processing, on the other hand, allows for more flexible WB signal processing and detection algorithms. For these reasons we focus on digital WB detectors. To start with, we assume that the WRx consists of an analog front-end and a digital processing part. During the listen interval, the WRx front-end delivers its received signal in the form of a bit-sequence to the digital base-band. The digital base-band task is to search for a WB in this bit-sequence. An alternative to this is to use an analog-to-digital converter (ADC) and perform bit detection in the digital base-band as well. While this improves accuracy and lowers BER, energy consuming ADC circuitry leads to higher total power consumption. This is due to the fact that the power consumption of ADCs increases both with sampling frequency and ADC word-length [74, 75].

In the following, we present different WB structures and give an overview of suitable digital base-band processing approaches used to detect them. We also discuss which of the above requirements that are fulfilled by each technique. In all approaches we use matched filters as the main building block, a common technique to detect known deterministic signals in noise.

[2]In this thesis, these aspects are investigated in various degrees.

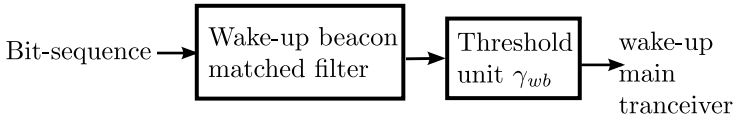


**Figure 4.6:** Digital base-band block diagram with a wake-up beacon matched filter for the wake-up beacon detection.

### Unique sequences

One type of WBs consist of node unique sequences where the uniqueness is necessary to suppress overhearing [45, 47, 51, 61, 66]. The sequences also need good correlation properties to allow time-synchronization and to lower WB miss and false-alarm probabilities. Example of such sequences are Pseudo-Noise (PN) sequences [45]. Additionally the sequences should be long enough to compensate for the WRx performance loss. This is done by selecting longer sequences or lowering the data rate.

The digital base-band used to detect this type of WBs, as shown in Fig. 4.6, consists of a WB matched filter and a decision unit. To detect the WB, the matched filter is used to search for the WB by correlating the known WB sequence with the incoming bit-sequence for all the possible arrival times of the WB. Whenever the matched filter output exceeds a certain decision threshold, the matched filter announces that a WB is detected and the main transceiver is switched on. To increase time resolution, the matched filter can be operated at oversampling. If we use oversampling to increase time resolution, we can also use matched filters in parallel, all operating at lower clock rate.

While this WB structure is simple to implement, it makes the design limited to networks of small sizes since the number of sequences with good correlation properties is limited. Moreover, long correlators are needed to detect the WBs, making the signal processing inefficient both in terms of power consumption and hardware architecture flexibility.

### Preamble plus unique sequences

The preamble plus unique sequences type WBs consist of a preamble and a node identity [50,57,63,76]. The preamble is selected to be the same for all nodes and is used both for detecting the presence of a WB and for time synchronization. The identity part is used to avoid overhearing. Both preamble and node identity need to be long enough to compensate for the WRx performance loss. Similar to unique sequences type WBs, this is done by transmitting the WBs at very low data rate or selecting long preambles and long node identity sequences. To lower WB detection error probabilities the node identities are selected from sequences

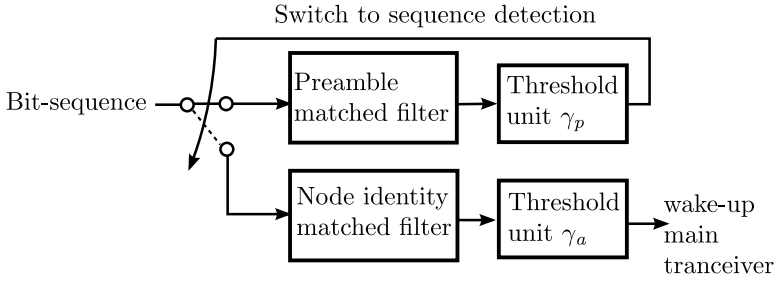


**Figure 4.7:** Digital base-band block diagram with a preamble matched filter for the preamble detection, node identity matched filter for node identity detection.

with good cross-correlation properties, e.g., Pseudo-Noise (PN) sequences or Orthogonal Variable Spreading Factor (OVSF) [76].

Fig. 4.7 illustrates the digital base-band consisting of preamble and node identity matched filters, with corresponding decision units, used to detect WBs of the above type. To detect the WB, first the preamble matched filter is used to detect the preamble needed for time-synchronization and presence of the WB. After preamble detection, the node sequence matched filter is switched on and correlates the incoming bit-sequence with the node known sequence. If the node sequence matched filter output exceeds a certain decision threshold, the WB is detected and the main transceiver is switched on. Again, to provide more time resolution, we can operate both matched filters with oversampling and exploiting parallel implementation.

By separating time-synchronization and node identity parts, this WB structure allows for shorter correlators compared to the previous approach. This makes the signal processing more efficient both in terms of power consumption and hardware architecture flexibility. However, similar to the previous approach, the design is not scalable to large network sizes since the number of unique sequences with good correlation properties is limited.

### Preamble plus spread address

In this study, we have selected a WB structure consisting of a preamble and an address part. Below we provide an overview of this structure and for details we refer to Paper II and Paper IV. Similar to the previous structure, we use the preamble for time synchronization but we use spread addresses to avoid overhearing. When deciding on the sequence, we select them differently than what

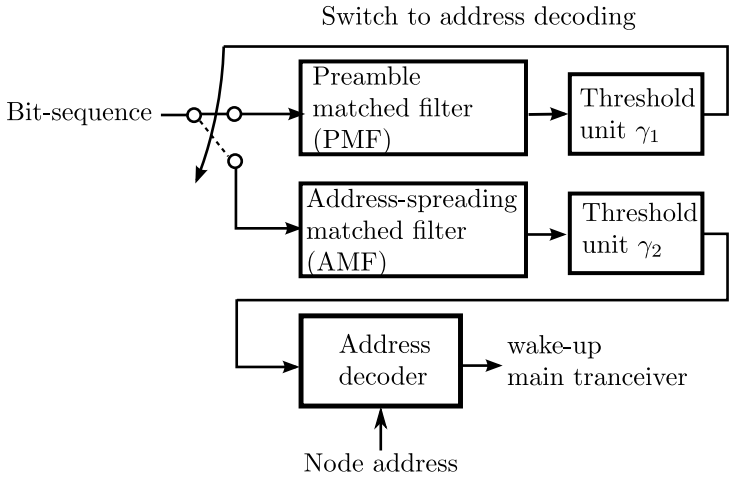


**Figure 4.8:** Digital base-band block diagram with a preamble matched filter for the preamble detection, address-spreading matched filter for address bits detection, and an address decoder.

was done for the previous structure. For accurate time synchronization and to lower WB error probabilities, we select the preamble from sequences with good auto-correlation properties and long enough to compensate for WRx performance loss. For the addresses we do not need the auto-correlation properties, since the synchronization is already taken care of by the preamble, but the WRx performance loss needs to be compensated. We do this by applying spreading to each address bit, using an arbitrary code.

Fig. 4.8 shows the block diagram of the digital baseband, consisting of preamble and address-spreading matched filters and their corresponding decision units. Last in the chain we have an address decoder. To detect the WB, first the preamble matched filter is used to look for the WB and establish its timing. After preamble detection, the address-spreading matched filter and the address decoder are switched on. The rest of the bit-sequence is then fed to the address-spreading matched filter where individual address bits are detected. At this stage the digital base-band knows the synchronization and performs the matched filter correlation only once per address bit. Finally, the detected address bits are collected by the address decoder and compared against the node address. If there is a match, the main transceiver is powered up. The preamble matched filter is the only the one we need to operate at oversampling, since it is responsible for time synchronization. After preamble detection and synchronization, the rest of the processing is performed at lower rate.

With our proposed digital base-band design, the preamble and address-spreading matched filters are identical in all nodes of a network. Only the address decoder needs to be programmed with the respective node addresses. The advantages of our WB structure, and digital base-band design, over the structures proposed in the previous sections are that the selection of WB pattern and address code is not limited to a certain code-book, and the programmable address decoder enables a large address-space scalability.

# Chapter 5

# Optimization and Performance Evaluation

This chapter gives a brief overview of the optimization strategies used in the included papers. We start with a brief introduction on mathematical and numerical optimization. We then describe the optimization problems addressed and discuss the approaches used to find optimal solutions, using mathematical programming techniques. We also present some results serving as a complement to the results in the included papers.

## 5.1 Background

Optimization is an important tool applicable in different fields, e.g., in decision science or for the analysis of physical systems in engineering. Mathematically speaking, optimization, often called *mathematical programming*, refer to minimization (or maximization) of a function, subject to constraints on its variables [77]. In its general form an optimization problem can be expressed as,

$$\underset{\omega \in \mathcal{R}}{\text{minimize}}\ J(\omega) \qquad \text{subject to} \quad \begin{cases} c_i(\omega) = 0 & i \in \varepsilon \\ c_i(\omega) \geq 0 & i \in \zeta \end{cases} \tag{5.1}$$

where

- $\omega$ is the vector of variables or unknown parameters in a permissible space $\mathcal{R}$,
- $J(\omega)$ is the objective function we want to minimize (or maximize),

- $c_i(\omega)$ are constraint functions, depending on $\omega$,
- and $\varepsilon$ and $\zeta$ are sets of indices for equality and inequality constraints.

Optimization problems can be classified according to the nature of their objective functions and constraints (linear, convex, or non-linear), the feasible set of their variables (discrete-integer or continuous), and the characteristics of the model (stochastic or deterministic). Other important distinctions are the number of variables (large or small), the smoothness of the functions (differentiable or non-differentiable), or whether there are constraints on the variables or not.

Applying the general optimization problem in (5.1) to our mathematical models leads to a continuous non-linear programming problem in Paper I, an integer non-linear programming problem in Paper II, and a mixed integer non-linear programming problem in Paper III. We solve the problem in Paper I analytically by differentiating the objective function. In Paper II we use an exhaustive or direct search method [78,79]. Combining the approaches in Paper I and Paper II, we use a two-step optimization strategy and solve the problem in Paper III. In the following, we detail the above programming problems and their corresponding optimization strategies.

## 5.2 Optimization Problem

We use energy consumption as a quantitative measure and perform a complete parameter optimization of the DCW-MAC. The ultimate goal is to find optimal parameters so that the energy consumption of the addressed network is minimized, while fulfilling some constraints and requirements.

Using the state-space model in Chapter 4, we develop an analytical framework for the energy consumed in an entire network for successful delivery of a data packet to a destination node. The analysis framework becomes a function of main transceiver and WRx hardware properties, WB and data exchange error probabilities, listen and sleep intervals, network size and traffic intensity. In this analysis, design characteristics of the WRx, in terms of power consumption and its corresponding performance, have a strong impact on the chosen duty-cycle and WB error probabilities. As discussed in the previous chapter, by adjusting WB parameters in accordance to WRx characteristics we can compensate for the WRx performance loss and also improve on WB detection performance. This in return influences WRx listen and sleep intervals, and thereby total network energy consumption. To fully characterize the energy consumption we, therefore, need to include the inter-relation between WRx and main receiver design characteristics, WB parameters, and DCW-MAC listen and sleep intervals. We do this through a simple model which relates WRx

power consumption and performance loss compared to the main receiver as two relative measure, relative power consumption $R^{wrx}$ and implementation loss $L_{\text{impl}}$. We also develop analytical expressions for WB detection performance, based on the WB structure and the detection technique described in Chapter 4.3. Through these expressions we connect WB parameters and WRx characteristics to the energy analysis framework.

When minimizing energy consumption we can only influence certain parameters in the network, while other are defined by the scenario. Parameters that are typically given are those related to hardware properties, network size, traffic density, and propagation channel. We consider a five-parameter problem where all parameters are optimized jointly to minimize energy consumption. These parameters are WRx listen $T_{listen}$ and sleep $T_{sleep}$ intervals, WB parameters, i.e., preamble length $M$ expressed in the number of bit times, address spreading factor $K$, and preamble matched filter threshold $\gamma_1$. In its general form the energy optimization problem is formulated as

$$\underset{T_{listen},T_{sleep},M,K,\gamma_1}{\text{minimize}} \; J(T_{listen},T_{sleep},M,K,\gamma_1,\Theta) \quad \text{such that} \tag{5.2}$$

$$\begin{cases} T_{listen}(M,K,\Theta) \geq T_x(M,K,\Theta), \\ T_{sleep}(M,K,\gamma_1,\Theta) \geq 0, \\ M,K \in \mathbb{N}, \\ \gamma_1 \in [0, M-1], \end{cases}$$

where $\Theta$ contains all the known parameters and $T_x \geq 0$ is the shortest possible listen time that guarantees a full WB can be heard by the WRx. Observing that the optimization problem includes two continuous non-negative real parameters, $T_{listen}$ and $T_{sleep}$, two discrete positive integer parameters, $M$ and $K$, and one discrete constrained integer parameter, $\gamma_1$, the energy optimization problem falls in the potentially very difficult category of non-linear mixed integer programming.

Optimizing parameters in networks where nodes need to, on average, respond before a certain time-limit is also of interest. This adds another constraint to the optimization problem and changes (5.2) to

$$\underset{T_{listen},T_{sleep},M,K,\gamma_1}{\text{minimize}} \; J(T_{listen},T_{sleep},M,K,\gamma_1,\Theta) \quad \text{such that} \tag{5.3}$$

$$\begin{cases} T_{listen}(M,K,\Theta) \geq T_x(M,K,\Theta) \\ T_{sleep}(M,K,\gamma_1,\Theta) \geq 0, \\ M,K \in \mathbb{N}, \\ \gamma_1 \in [0, M-1], \\ \bar{D}(T_{listen},T_{sleep},M,K,\gamma_1,\Theta) < D^{req}, \end{cases}$$

where $\bar{D}$ is the average communication delay and $D^{req}$ the average delay requirement.

## 5.3 Optimization Methods and Complementary Results

After describing the optimization problems in their general forms, we now discuss the steps we took to find optimal solutions for (5.2) and (5.3). We also present some complementary results, this to provide more insight into the results presented in the included papers.

### 5.3.1 Including only continuous parameters

We solve (5.2) in Paper I by reforming it into a simplified problem; we assume the discrete parameters $M$, $K$, and $\gamma_1$ are known and we only optimize for the continuous parameters $T_{listen}$ and $T_{sleep}$. More specifically, we assume WRx design characteristics, its power consumption and performance loss relative to the main receiver, are known and $M$, $K$, and $\gamma_1$ are selected to both compensate for the WRx performance loss and to allow for ideal WB detection performance. With these assumptions (5.2) changes to a continuous non-linear programming problem,

$$\underset{T_{listen},T_{sleep}}{\text{minimize}}\ J(T_{listen},T_{sleep},\Theta) \quad \text{such that} \quad \begin{cases} T_{listen}(\Theta) \geq T_x(\Theta), \\ T_{sleep}(\Theta) \geq 0, \end{cases} \tag{5.4}$$

where $J$ is the average energy consumed in an entire network for successful delivery of a data packet to a destination node. First we set the listen time to its smallest value $T_x$ which guarantees that a full WB can be heard. We then find optimal sleep interval by differentiating the energy consumption expression w.r.t. $T_{sleep}$ and solve $\partial E/\partial T_{sleep} = 0$. This results in two local optima, as shown in Fig. 5.1, of which one is always negative and thus not valid. Since energy consumption decreases monotonically with sleep time in the interval $[0, \widetilde{T}_{sleep}]$, where $\widetilde{T}_{sleep}$[1] is the optimal sleep interval, $\widetilde{T}_{sleep}$ corresponds to a minimum. When a restriction on average delay is required, as in (5.3), the sleep time is selected to both fulfill average delay requirement and minimize network energy consumption. With the monotonic behavior of the energy consumption, the optimal sleep interval is the largest value in the interval $[0, \widetilde{T}_{sleep}]$ that fulfills the delay requirement.

[1]Note that in the entire thesis we use *tilde* to indicate optimal parameter values.

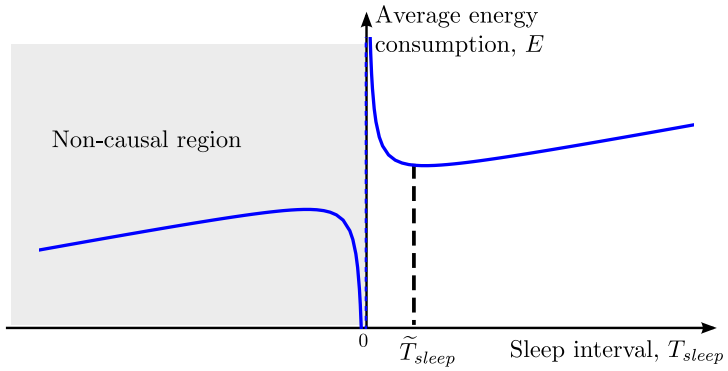


**Figure 5.1:** Illustration of average energy consumption as a function of sleep interval. The optimal sleep time is denoted by $\widetilde{T}_{sleep}$.

The energy-minimizing listen and sleep intervals are substituted back in the energy and average communication delay expressions for further evaluation of the DCW-MAC performance, as detailed in Paper I.

### 5.3.2 Including only discrete parameters

In Paper II, we consider a simplified energy analysis where we only optimize for WB transmit energy. The WB transmit energy is determined by the chosen duty-cycle of the WRx and WB detection performance through the number of WBs that need to be transmitted on average to establish communication between nodes. In this analysis we assume a constant activity factor where the listen interval is a constant fraction of an entire sleep-listen cycle. Through this, there will always be a fixed number of WBs per sleep-listen cycle, independent of WB length and thereby of WB parameters. These assumptions change (5.2) to a simpler problem as it becomes independent of the continuous parameters and only depends on WB parameters, network size, and WRx performance loss (through its bit error probability). Therefore, we only need to find the optimal discrete WB parameters, preamble length $M$ in number of bit times, address spreading factor$K$, and preamble matched filter threshold $\gamma_1$ for different WRx bit error probabilities. The optimization problem in (5.2), therefore, becomes an integer optimization problem

$$\underset{M,K,\gamma_1}{\text{minimize}}\ J(M,K,\gamma_1,\Theta) \quad \text{such that} \quad \begin{cases} M,K \in \mathbb{N}, \\ \gamma_1 \in [0, M-1], \end{cases}$$

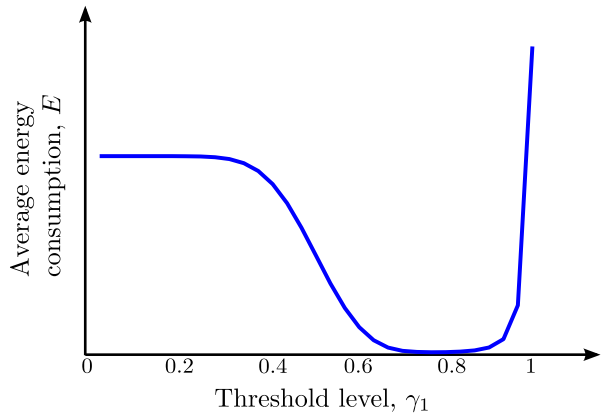


**Figure 5.2:** Illustration of energy consumption as a function of threshold level $\gamma_1 \in [0, M-1]$. Threshold is normalized to $M-1$, where $M$ is the preamble length.

where WB transmit energy $J$ is a non-linear function of $M$, $K$, and $\gamma_1$. With discrete integer parameters, we resort to a structured search over $M$, $K$, and $\gamma_1$ to find their optimal values.

For the optimal $\gamma_1$, when $M$ and $K$ are given, we can perform a tractable exhaustive/direct search by calculating the energy consumption for each of the $M$ possible values. In Fig. 5.2 we illustrate the general energy consumption behavior for different threshold levels. For lower and higher thresholds the energy cost is largely influenced by reduced WB detection probability. For low thresholds we get false alarms and for high thresholds we miss the WBs entirely, both resulting in extra energy cost at the transmitter.

For the optimal $M$ and $K$, we have not been able to fully characterize the optimization problem, since it contains highly non-linear relations. However, by studying contour plots of the energy consumption for different network sizes and system parameters, like the ones shown in Figs. 5.3(a)-(c), we conjecture that there is a single energy minimum. For short preambles and short address spreading factors, energy costs are high due to synchronization and address decoding errors. Increasing preamble length and address spreading factor reduces the energy cost related to these errors. Beyond a certain point the energy cost resulting from long preambles and address spreading outweigh these gains. These observations support our conjecture and we use a simple search, increasing $M$ and $K$ from low values. As soon as a local minimum is

found, we assume it is the global one. Figs. 5.3(a)-(c) also illustrate how optimal preamble length $\widetilde{M}$ and address spreading factor $\widetilde{K}$ changes for different network sizes at a certain bit error probability. As we observe, both $\widetilde{M}$ and $\widetilde{K}$ increase with network size. There are two different costs associated with network size. The WB transmission cost increases with $K$ being multiplied by more nodes in larger networks. Another cost that increases with network size is the one related to WB misses. If we increase the number of address bits, without changing $M$ and $K$, the probability of miss and associated transmit costs will increase. To avoid this, the optimal $M$ and $K$ increase with network size/number of address bits, despite the increased transmit energy cost per WB. In Fig. 5.3(d)[2] we show these results for the same three network sizes as Figs. 5.3(a)-(c) but for a wider range of WRx bit error probabilities. As we observe, at low BER all three trajectories follow the same behavior and are essentially linear, with $M$ roughly eight times bigger than $K$. The probability of WB miss in larger networks, with more address bits, increases faster with increasing channel BER. For this reason the $\widetilde{M}, \widetilde{K}$-trajectories diverge more and more as BER increases. Fig. 5.4 shows the optimal preamble and address spreading for the same parameter settings as in Paper II. We use these optimal values when evaluating WB transmit energy in Paper II, but do not show them explicitly there.

### 5.3.3 Including both continuous and discrete parameters

We perform a complete parameter optimization in Paper III by including both continuous and discrete parameters in the energy calculation. The optimization problems therefore follow all constraints and conditions in (5.2) and (5.3). To solve the problem we do the optimization in two steps, combining the above two optimization strategies:

- For given values on the discrete parameters, we analytically calculate optimal values for continuous parameters, i.e., $\widetilde{T}_{listen}$ and $\widetilde{T}_{sleep}$ following the same steps as in Section 5.3.1. The optimal listen interval becomes a function of $M$ and $K$ and the optimal sleep interval a function of all free parameters $M$, $K$, and $\gamma_1$.
- With expressions for optimal continuous parameters we then perform a numerical optimization, as in Section 5.3.2, using direct search over discrete parameters, i.e., $M$, $K$, and $\gamma_1$.

[2]The investigated system when creating these plots was using non-coherent on-off-keying, thereby the 'on-off keying' label in this and the following figures.

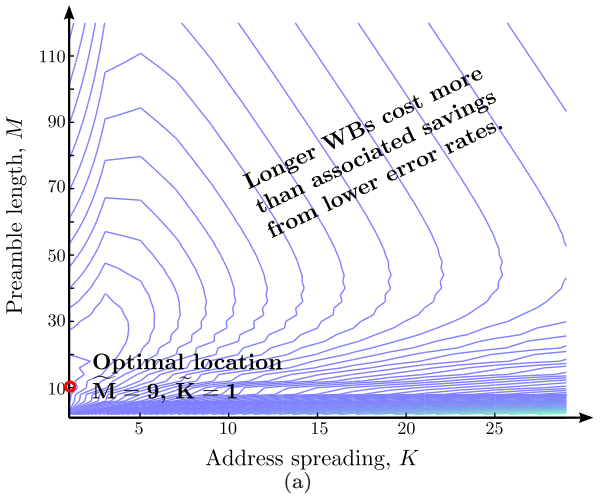


(a)

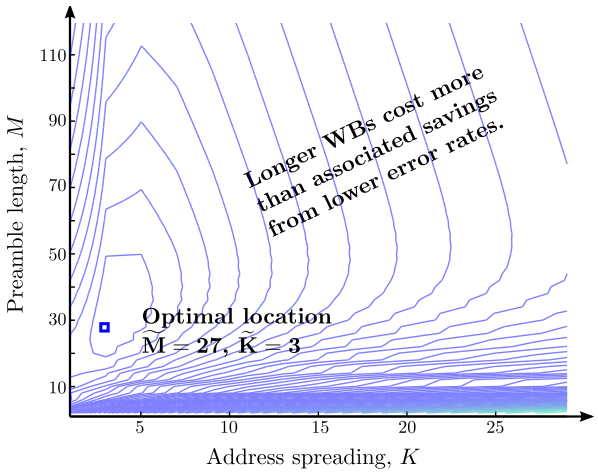


(b)

As we perform a full parameter optimization, we find the optimal parameters for a wide range of WRx design characteristics, in terms of both power consumption and its corresponding performance loss, various traffic conditions, and different network sizes. In Fig. 5.5 we show the optimal preamble and address spreading, like we did in Fig, 5.4, but now as a function WRx per-

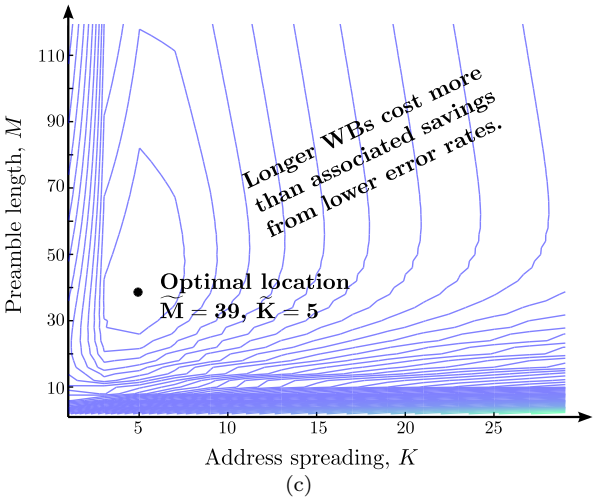


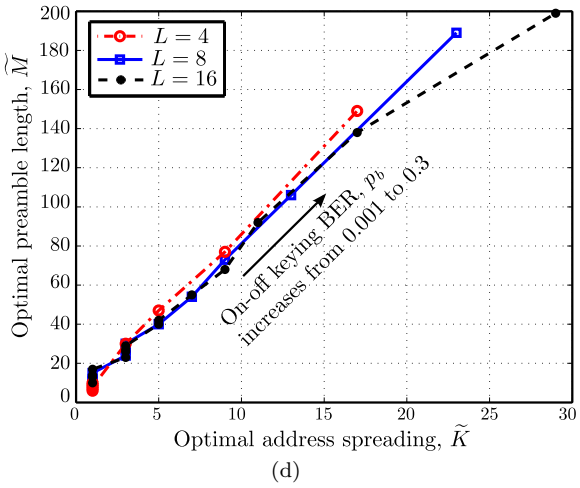


**Figure 5.3:** Illustration of energy consumption as a function of wake-up beacon (WB) parameters, preamble $M$ and address spreading $K$. Energy contours used are for bit error probability $p_b$ of $10^{-1}$ and address-space of size (a) 4-bit (b) 8-bit, and (c) 16-bit. (d) Trajectories of optimal preamble length $\widetilde{M}$ and optimal address spreading $\widetilde{K}$ for address-spaces of size 4, 8, and 16 bits and different bit error probabilities $p_b$s.

formance loss instead of BER $p_b$[3]. Since WRx listening cost is included in this optimization, the optimal values on $M$ and $K$ now also change with WRx power consumption. These variations are shown as the shaded area between the lines. For the largest address space, $L = 16$, there are no variations with WRx power consumption and only a single line is shown. The parameter setting is the same as in Paper III. While not explicitly shown in Paper III, the evaluations in there are based on these optimal values. The WB transmit part of the total energy cost tends to drive $M$ and $K$ towards higher values with WRx implementation loss, for the same reasons as discussed in Section 5.3.2. However, as more than transmit energy costs are included in the optimization, there are other mechanisms that are holding back the values on $M$ and $K$. For instance, when $M$ and $K$ grow, WBs become longer and the cost for WRx listening increases.

Finally, to give an alternate view of the optimization results shown as level curves in Fig. 6 of Paper III, we present them as surfaces in Fig. 5.6. In the three sub-figures we show how optimized DCW-MAC energy savings relative to X-MAC, energy savings relative to Always-on WRx MAC, and average delays relative to X-MAC, vary with WRx power consumption and implementation loss. Three surfaces are shown in each plot, representing a reference scenario, what happens when traffic is increased and when a delay requirement is introduced. For details about these scenarios and parameters, we refer to Paper III.

[3]The 0–9 dB range of implementation losses correspond to the same range of BERs as in Fig. 5.4, namely 0.001–0.3.

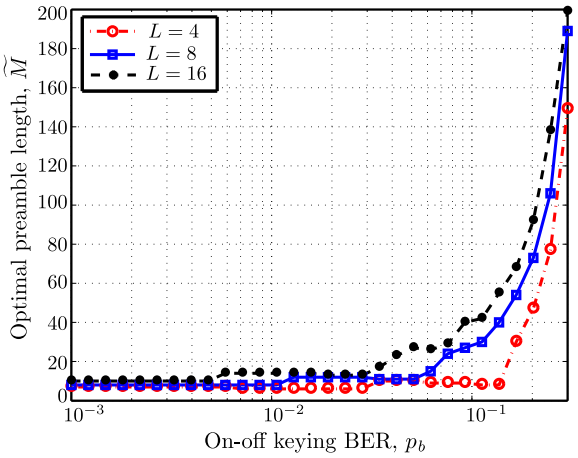


(a)

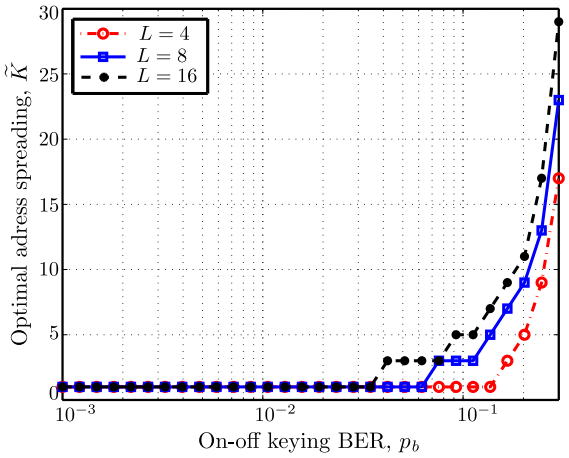


(b)

**Figure 5.4:** (a) Optimal preamble length vs. on-off keying raw BER, (b) Optimal address spreading vs. on-off keying raw BER, for address-spaces of size 4, 8, and 16 bits.

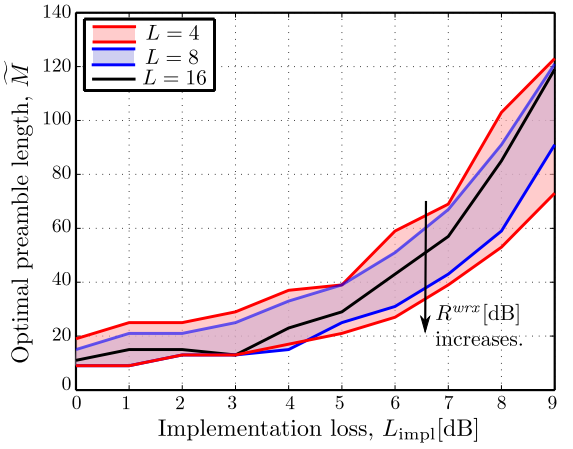


(a)

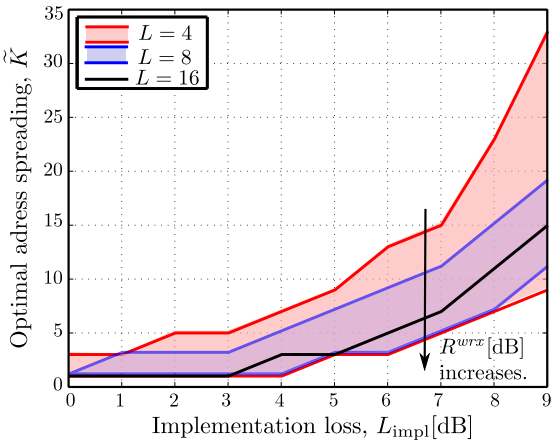


(b)

**Figure 5.5:** Optimal (a) preamble length and (b) address spreading vs. WRx implementation, for address-spaces of size 4,8, and 16 bits. Shaded regions show variations when relative WRx power consumption varies from -30dB (higher values) to 0dB (lower values). For the largest address space, $L = 16$, there are no such variations.

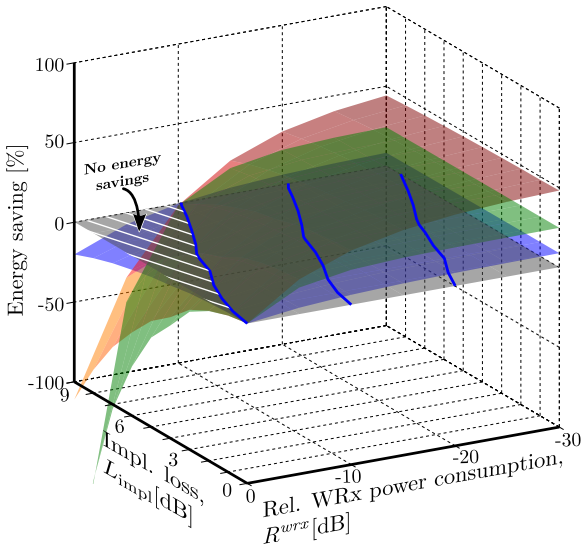
100
50
0
-50
-100
Energy saving [%]
No energy savings
9
6
3
0
Impl. loss, $L_{impl}$[dB]
0
-10
-20
-30
Rel. WRx power consumption, $R^{wrx}$[dB]

(a)

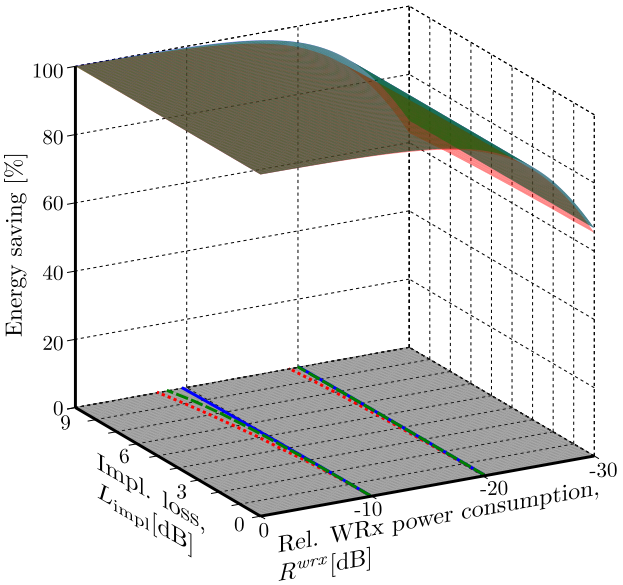
100
80
60
40
20
0
Energy saving [%]
9
6
3
0
Impl. loss, $L_{impl}$[dB]
0
-10
-20
-30
Rel. WRx power consumption, $R^{wrx}$[dB]

(b)

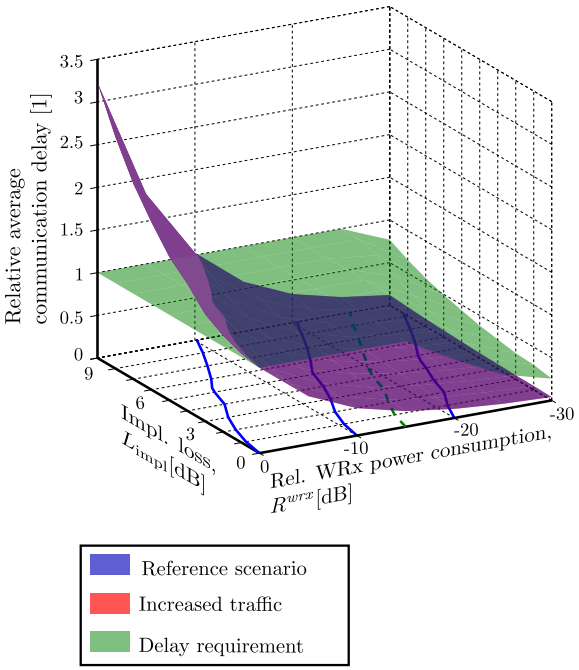


(c)

**Figure 5.6:** 3D illustration of DCW-MAC (a) energy savings relative to X-MAC, (b) energy savings relative to Always-On WRx-MAC, and (c) average communication delay, together with their corresponding level curves, for three different scenarios. The reference scenario has a 1000 sec. $1/\lambda$ and no delay requirement. Based on the reference scenario, the other two scenarios have traffic increased to a 10 sec. $1/\lambda$ and a 0.1% relative delay requirement, respectively. Results are shown for an 8-bit address space.

# Chapter 6

# Contributions and Discussion

This chapter presents a summary of my contributions to the research field and provides concluding remarks and comments on future work. The five papers which constitute the core of this thesis are summarized and the contributions are highlighted. For all these papers, I am the main contributor, and took part in all steps in scientific process including implementing the algorithms, performing simulations, evaluating the results, and writing the papers. The circuit layout of the WRx in Paper IV is done by one of the co-authors.

## 6.1 Research Contributions

### 6.1.1 Paper I: DCW-MAC: An energy efficient medium access scheme using duty-cycled low-power wake-up receivers

In the first paper we introduce the DCW-MAC scheme, and present a "limited" analysis and performance evaluation of the proposed scheme. The DCW-MAC combines the energy saving mechanisms of duty-cycled channel listening and ultra-low power WRxs and the objective in this paper is to investigate if we can benefit from using it. The main contributions are:

- We derive an energy expression for the analysis of the energy consumption of the DCW-MAC for the studied network type. The ultra low-power WRx allows for low-power channel listening, but their low-power design

may lead to performance degradation as compared to the main receiver A key feature of the energy analysis is that we take into account the influence of the WRx performance loss on total energy consumption.

- We then use the energy expression to find WRx optimal sleep time for the lowest possible energy consumption of an entire network. The energy optimization is performed both for applications with and without delay requirements. The energy minimization based on closed-form expressions leads to explicit formulas for optimal sleep interval. This allows us to study how hardware parameters, network size, and traffic influence the optimal sleep intervals and possible energy savings.

- Our energy analysis framework is flexible and can be easily modified for our reference scenarios, i.e., i) the Always-On WRx-MAC where nodes do not perform duty-cycling and the WRxs are always on and continuously monitor the channel, and ii) X-MAC where no extra WRx is used and the main receivers duty-cycles for channel listening. We compare the performance of the DCW-MAC against that of these two schemes.

The results show that while wake-up performance loss limits the DCW-MAC performance for high-traffic scenarios, it outperforms the other two MAC schemes in low-traffic scenarios encountered in many low-power sensor networks. The DCW-MAC has the largest gain over X-MAC when we introduce a maximum-delay requirement where the sleep mechanism gives less energy savings. These results motivate further investigation of DCW-MAC.

### 6.1.2 Paper II: Performance analysis and energy optimization of wake-up receiver schemes for wireless low-power applications

In this paper, we take the analysis of the DCW-MAC one step further and study the influence of the WRx properties on WB parameters and the resulting WB detection performance. The goal of this study is to provide an analysis framework that can be used to find optimal WB design parameters for a system using low-power WRxs with a certain implementation loss. The contributions are:

- We assume a WRx architecture consisting of an analog front-end and a digital base-band. We express characteristics of the analog front-end for the resulting BER in terms of SNR.

- We propose a WB structure with flexible design parameter so that we can compensate for the high BER of the analog front-end. The selected WB

structure also leads us to an architecture for the WRx digital base-band.

- We develop analytical expressions for WB detection performance, in terms of WB miss and false-alarm probabilities, based on the proposed WB structure and the digital base-band processing. Using these expressions we analyze the impact of design parameters.
- Using the above expressions, we minimize WB transmit energy cost.

The WRx operating characteristics in terms of WB detection and false alarm probabilities are verifies by simulations. The results show that by adjusting WB packet structure parameters we compensate for WRx performance loss, improve on its practical sensitivity, and achieve sufficient levels of WB detection.

### 6.1.3 Paper III: Duty-cycled wake-up receivers and single-hop wireless sensor network energy optimization

This paper provides a complete system analysis and parameter optimization of the DCW-MAC scheme, including protocol parameters, WRx design characteristics, and WB structure parameters. Here we complete the analysis of the DCW-MAC scheme by merging our previous results to a complete analytical framework allowing us to optimize energy consumption of an entire network. The contributions are:

- We develop analytical expressions for energy consumption and the resulting communication delays in a single-hop network.
- Analytical expressions are also developed, based on the same principle, for our two reference MAC schemes:i) the Always-On WRx-MAC where nodes do not perform duty-cycling and the WRxs are always on and continuously monitor the channel, and ii) X-MAC where no extra WRx is used and the main receivers duty-cycles for channel listening.
- The expressions allow for a cross-layer optimization where we find optimal wake-up beacon and protocol parameters, sleep and listen intervals, for different WRx design characteristics, that minimize total network energy consumption per data packet. Optimization is performed both for scenarios with and without requirements on average delay.
- We evaluate DCW-MAC performance by comparing its energy consumption to that of the reference MAC schemes and study resulting communication delays. In the evaluation process we discuss the importance of both using dedicated WRxs and performing duty-cycle channel listening.

- We derive simple approximations of key results, energy consumption and communication delay, for wide parameter ranges. The approximation can be used as a simple design tool to evaluate the influence of WRx characteristics.

The optimization results show that the DCW-MAC always outperforms the always-on MAC scheme in terms of energy consumption, even for scenarios with requirements on average delay, unless the delay requirement is so tight that it prevents sleeping. When comparing to X-MAC, the optimization results show that the energy saving largely depends on the characteristics of the low-power WRxs used. The importance of the optimization is that it provides information on how much we can save in an entire network by selecting a WRx with certain properties.

### 6.1.4 Paper IV: Improving practical sensitivity of energy optimized wake-up receivers: proof of concept in 65 nm CMOS

This paper presents a digital base-band circuit design for a duty-cycled WRx scheme. The objective of this paper is to show that the implementation loss of the WRx analog front-end, resulting from a very limited power budget, can be compensated by digital base-band processing at a negligible power consumption and area. The contributions are:

- We propose an architecture for the WRx digital base-band based on analysis and optimization results from Paper II.
- We use binary input matched filters as the main building block, which are optimized for ultra-low voltage operation.
- The digital base-band is fabricated in 65 nm CMOS technology. We evaluate the energy performance of the design by measurement, for different operating frequencies and a wide range of supply voltages.

Measurement down to sub-threshold region shows that the digital base-band is fully functional at a minimum supply voltage $V_{\mathrm{DD}}$ of 0.23 V. With adequate detection and false-alarm probabilities the digital base-band consumes 0.9 $\mu$W at the targeted 250 kbps, showing that the WRx front-end (50 $\mu$W) implementation loss can be efficiently compensated at a negligible cost. This implies an improvement in practical sensitivity of the analog front-end, compared to what is traditionally reported. The digital base-band design has the advantage of high address-space scalability, at a negligible hardware cost, and makes the design an attractive candidate both for small and large networks. The flexibility

of the proposed digital base-band also allows us to adjust the design without significant changes in hardware architecture and power consumption. Taking advantage of this characteristic, we can connect the proposed digital base-band to a wide range of optimized analog front-ends and improve on their practical sensitivity.

### 6.1.5 Paper V: Comparing analog front-ends for duty-cycled wake-up receivers in wireless sensor networks

This paper presents a systematic analysis, evaluation and performance comparison of WRx analog front-ends with different characteristics. Energy-saving predicted in low-power WRx schemes is possible only if WRxs can be realized in hardware. A large part of total power budget is consumed in the analog front-end of the WRx and many analog front-end architectures have been proposed to meet strict low-power requirements. In literature WRx front-ends are typically evaluated and compared by their sensitivity, related to BER of $10^{-3}$, and their power consumption, both these at some data rate and operating frequency. While these measures are important for individual analog front-ends, they do not reflect their impact on total energy consumption in a network. The objective in this paper is to find a tool for comparing WRx analog front-ends when operating in a network. In our analysis we assume WRxs are used in a network where nodes communicate using the DCW-MAC principles. The contributions of this work are as follows:

- We derive a simple expression for comparing analog front-ends, in terms of total energy required in a network to perform a wake-up.
- We discuss overall behavior of the wake-up energy cost by studying the characteristics of its corresponding level curves. We also discuss how the characteristics of the level curves can be used as a graphical tool for comparing the relative merit of different analog front-ends, without going through complete energy calculation of each individual node.
- The characteristics of the level curves also allows us to find the set of best performing analog front-ends. The set includes all the analog front-end designs that, for at least some scenario, result in the lowest wake-up energy among all studied designs. By evaluating the range of scenarios for which each analog front-end is the best performing one, we rank the best-performing analog front-ends against each other. Having access to such a set provide a simple means to decide whether a new design is among the best-performing ones.

## 6.2 Discussion and Future Work

One of the primary purposes of this study is to show the potential energy savings in a single-hop network when introducing duty-cycled low-power WRxs. Since WRx design characteristics strongly influence WB parameters, WB error probabilities and the choice of protocol parameters, i.e., sleep and listen interval, we have included all these low-level parameters in our analysis and find minimum energy consumption through a cross-layer optimization. The results are important as they can be used in the early stage of a network design, either to predict how much energy is saved when introducing a duty-cycled WRx or to determine which WRxs can deliver a targeted energy saving. They can also be used in the first step of a more advanced cross-layer design. The analysis and optimization are based on simplifying assumptions, making it possible to perform analytical optimization and approximation. In this section we discuss some of these assumptions and also present some interesting points on further extensions and improvements of the analysis.

In the entire analysis we assume an Additive White Gaussian Noise (AWGN) channel. As we mention in Paper II, an interesting extension of the analysis framework is to include more realistic channel models and interference scenarios. The analysis can be adapted as long as the relationship between WRx and main receiver SNR and raw BER is known. More generic interference types can also be included by either modifying the noise level in the bit-error expressions to imitate interference or providing a more detailed analysis where interference scenarios are more realistic.

We also assume a symmetric single-hop network where all nodes are equal. A possible extension to this is to modify the energy expressions to also address networks with different node types. Depending on energy resources available for each node, a suitable multi-hop algorithm can be applied to transmit the data packet from source node to destination node. With a multi-hop approach it is, however, very unlikely to find a tractable analytical solution, making it necessary to optimize energy through simulations.

In the entire analysis we assume a Poisson traffic distribution. Even though we use Poisson traffic notation, the analysis framework is general since the energy analysis only depend on the average packet inter-arrival interval. A possible future extension is, however, to allow inhomogeneous average traffic conditions. This can be done by forming a state diagram including all possible traffic variations and the corresponding probability of occurrence.

When deciding on WB or WACK/DACK packet structure, we choose a simple structure consisting of a preamble, source and destination nodes addresses. For future extension of the analysis, as we mention in Paper II, additional fields can be attached to the WB or to the WACK packet such as maximum number

of WBs or the next wake-up time of the nodes. This information can be used after two nodes communicate to reduce energy cost resulting from periodic WB transmission.

# Bibliography


[1] C.-Y. Chong and S. Kumar, "Sensor networks: evolution, opportunities, and challenges," *Proceedings of the IEEE*, vol. 91, pp. 1247–1256, Aug 2003.

[2] J. M. Rabaey, J. Ammer, T. Karalar, S. Li, B. Otis, M. Sheets, and T. Tuan, "Picoradios for wireless sensor networks: the next challenge in ultra-low power design," in *IEEE International Solid-State Circuits Conference*, vol. 1, 2002, pp. 200–201.

[3] I. F. Akyildiz and M. C. Vuran, *Wireless sensor networks*. John Wiley & Sons, 2010, vol. 4.

[4] A. J. Goldsmith and S. B. Wicker, "Design challenges for energy-constrained ad hoc wireless networks," *IEEE Wireless Communications*, vol. 9, no. 4, pp. 8–27, 2002.

[5] C. Guo, L. C. Zhong, and J. Rabaey, "Low power distributed MAC for ad hoc sensor radio networks," in *IEEE Global Telecomm. Conf.*, vol. 5, 2001, pp. 2944–2948.

[6] C. C. Enz, N. Scolari, and U. Yodprasit, "Ultra low-power radio design for wireless sensor networks," in *IEEE Proceedings International Workshop on Radio-Frequency Integration Technology: Integrated Circuits for Wideband Communication and Wireless Sensor Networks.*, 2005, pp. 1–17.

[7] J. Ammer and J. M. Rabaey, "The energy-per-useful-bit metric for evaluating and optimizing sensor network physical layers," in *3rd Annual IEEE Communications Society on Sensor and Ad Hoc Communications and Networks*, vol. 2, 2006, pp. 695–700.

[8] A. Wang, S. Cho, C. Sodini, and A. Chandrakasan, "Energy efficient modulation and MAC for asymmetric RF microsensor systems," in *Proceedings*

*of the 2001 international symposium on Low power electronics and design*, 2001, pp. 106–111.

[9] Y. Wei, J. Heidemann, and D. Estrin, "An energy-efficient MAC protocol for wireless sensor networks," in *Proc. 21st Ann. Joint Conf. IEEE Comput. and Commun. Soc.*, vol. 3, November 2002, pp. 1567–1576.

[10] Z. A. Eu, H.-P. Tan, and W. K. Seah, "Design and performance analysis of MAC schemes for wireless sensor networks powered by ambient energy harvesting," *Ad Hoc Networks*, vol. 9, no. 3, pp. 300–323, 2011.

[11] X. Fafoutis and N. Dragoni, "Analytical comparison of MAC schemes for energy harvestingwireless sensor networks," in *Ninth International Conference on Networked Sensing Systems (INSS)*. IEEE, 2012, pp. 1–6.

[12] H. Yoo, M. Shim, and D. Kim, "Dynamic duty-cycle scheduling schemes for energy-harvesting wireless sensor networks," *IEEE Communications Letters*, vol. 16, no. 2, pp. 202–204, 2012.

[13] Y. Sun, S. Du, O. Gurewitz, and D. B. Johnson, "DW-MAC: a low latency, energy efficient demand-wakeup MAC protocol for wireless sensor networks," in *Proceedings of the 9th ACM international symposium on Mobile ad hoc networking and computing*, 2008, pp. 53–62.

[14] Y. Sun, O. Gurewitz, S. Du, L. Tang, and D. B. Johnson, "ADB: an efficient multihop broadcast protocol based on asynchronous duty-cycling in wireless sensor networks," in *Proc. 7th Int. Conf. Embedded Networked Sensor Syst.*, 2009, pp. 43–56.

[15] M. S. Hefeida, T. Canli, and A. Khokhar, "CL-MAC: A cross-layer mac protocol for heterogeneous wireless sensor networks," *Ad Hoc Networks*, vol. 11, no. 1, pp. 213–225, 2013.

[16] M. C. Vuran and I. F. Akyildiz, "XLP: A cross-layer protocol for efficient communication in wireless sensor networks," *IEEE Transactions on Mobile Computing*, vol. 9, no. 11, pp. 1578–1591, 2010.

[17] J. Ayers, K. Mayaram, and T. S. Fiez, "An ultralow-power receiver for wireless sensor networks," *IEEE Journal of Solid-State Circuits*, vol. 45, no. 9, pp. 1759–1769, 2010.

[18] M. Vidojkovic, X. Huang, P. Harpe, S. Rampu, C. Zhou, L. Huang, J. van de Molengraft, K. Imamura, B. Busze, F. Bouwens *et al.*, "A 2.4 GHz ULP OOK single-chip transceiver for healthcare applications," *IEEE*

*Transactions on Biomedical Circuits and Systems,*, vol. 5, no. 6, pp. 523–534, 2011.

[19] P. D. Bradley, "Wireless medical implant technologyrecent advances and future developments," in *Proceedings of the ESSCIRC*, 2011.

[20] M. Mark, Y. Chen, C. Sutardja, C. Tang, S. Gowda, M. Wagner, D. Werthimer, and J. Rabaey, "A 1mm$^3$ 2mbps 330fj/b transponder for implanted neural sensors," in *Symposium on VLSI Circuits-Digest of Technical Papers*, 2011.

[21] C. C. Enz, A. El-Hoiydi, J.-D. Decotignie, and V. Peiris, "WiseNET: an ultralow-power wireless sensor network solution," *Computer*, vol. 37, no. 8, pp. 62–70, 2004.

[22] J. M. Rabaey, M. J. Ammer, J. L. da Silva, D. Patel, and S. Roundy, "PicoRadio supports ad hoc ultra-low power wireless networking," *Computer*, vol. 33, no. 7, pp. 42–48, 2000.

[23] W. Ye, J. Heidemann, and D. Estrin, "Medium access control with coordinated adaptive sleeping for wireless sensor networks," *IEEE/ACM Transactions on Networking*, vol. 12, no. 3, pp. 493–506, 2004.

[24] T. van Dam and K. Langendoen, "An adaptive energy-efficient MAC protocol for wireless sensor networks," in *Proc. 1st Int. Conf. Embedded Networked Sensor Syst.*, 2003, pp. 171–180.

[25] W. Ye, F. Silva, and J. Heidemann, "Ultra-low duty cycle MAC with scheduled channel polling," in *Proc. 4th International Conference Embedded Ntworked Sensor Syst.*, 2006, pp. 321–334.

[26] S. Du, A. K. Saha, and D. B. Johnson, "RMAC: A routing-enhanced duty-cycle MAC protocol for wireless sensor networks," in *26th IEEE International Conference on Computer Communications*. IEEE, 2007, pp. 1478–1486.

[27] I. Rhee, A. Warrier, M. Aia, J. Min, and M. L. Sichitiu, "Z-MAC: a hybrid MAC for wireless sensor networks," *IEEE/ACM Transactions on Networking (TON)*, vol. 16, no. 3, pp. 511–524, 2008.

[28] A. El-Hoiydi, "Aloha with preamble sampling for sporadic traffic in ad hoc wireless sensor networks," in *IEEE Int. Conf. Commun.*, vol. 5, April 2002, pp. 3418–3423.

[29] C. Schurgers, V. Tsiatsis, and M. B. Srivastava, "STEM: Topology management for energy efficient sensor networks," in *IEEE Aerospace Conference Proceedings*, vol. 3, 2002, pp. 3–1099.

[30] A. El-Hoiydi and J.-D. Decotignie, "WiseMAC: An ultra low power mac protocol for multi-hop wireless sensor networks," in *Proc. 4th Int. Conf. Embedded Networked Sensor Syst.*, 2004.

[31] J. Polastre, J. Hill, and D. Culler, "Versatile low power media access for wireless sensor networks," in *Proc. 2th International Conference Embedded Networked Sensor Syst.*, 2004, pp. 95–107.

[32] X. Shi, G. Stromberg, Y. Gsottberger, and T. Sturm, "Wake-up-frame scheme for ultra low power wireless transceivers," in *IEEE Global Telecommunications Conference*, vol. 6, 2004, pp. 3619–3623.

[33] X. Shi and G. Stromberg, "SyncWUF: An ultra low-power MAC protocol for wireless sensor networks," *IEEE Transactions on Mobile Computing*, vol. 6, no. 1, pp. 115–125, 2007.

[34] S. Mahlknecht and M. Bock, "CSMA-MPS: a minimum preamble sampling MAC protocol for low power wireless sensor networks," in *Proc. IEEE Int. Workshop on Factory Commun. Syst.*, 2004, pp. 73–80.

[35] M. Buettner *et al.*, "X-MAC: a short preamble MAC protocol for duty-cycled wireless sensor networks," in *Proc. 4th Int. conf. Embedded networked sensor syst.*, 2006, pp. 307–320.

[36] E.-Y. Lin, J. Rabaey, and A. Wolisz, "Power-efficient rendez-vous schemes for dense wireless sensor networks," in *IEEE Int. Conf. Commun.*, vol. 7, June 2004, pp. 3769–3776.

[37] H. Wang, X. Zhang, F. Naït-Abdesselam, and A. Khokhar, "DPS-MAC: An asynchronous MAC protocol for wireless sensor networks," in *Proceedings of the 14th International Conference on High Performance Computing*, 2007, pp. 393–404.

[38] J. Kim, X. Lin, N. B. Shroff, and P. Sinha, "Minimizing delay and maximizing lifetime for wireless sensor networks with anycast," *IEEE/ACM Transactions on Networking (TON)*, vol. 18, no. 2, pp. 515–528, 2010.

[39] A. Sfairopoulou, C. Cano, E. Bonada, and B. Bellalta, "Evaluating the LWT-MAC performance in query-driven WSNs using data-centric routing," in *Multiple Access Communications*. Springer, 2011, pp. 156–167.

[40] Y. Sun, O. Gurewitz, and D. B. Johnson, "RI-MAC: a receiver-initiated asynchronous duty cycle MAC protocol for dynamic traffic loads in wireless sensor networks," *Proc. 6th Int. Conf. Embedded Ntworked Sensor Syst.*, pp. 1–14, 2008.

[41] H. Lee, J. Hong, S. Yang, I. Jang, and H. Yoon, "A pseudo-random asynchronous duty cycle MAC protocol in wireless sensor networks," *IEEE Communications Letters*, vol. 14, no. 2, pp. 136–138, 2010.

[42] L. Tang, Y. Sun, O. Gurewitz, and D. B. Johnson, "PW-MAC: An energy-efficient predictive-wakeup MAC protocol for wireless sensor networks," in *Proceedings IEEE INFOCOM*, 2011, pp. 1305–1313.

[43] ——, "EM-MAC: a dynamic multichannel energy-efficient MAC protocol for wireless sensor networks," in *Proceedings of the Twelfth ACM International Symposium on Mobile Ad Hoc Networking and Computing*, 2011, p. 23.

[44] S. Henna, "SA-RI-MAC: sender-assisted receiver-initiated asynchronous duty cycle MAC protocol for dynamic traffic loads in wireless sensor networks," in *Mobile Lightweight Wireless Systems*, 2012, pp. 120–135.

[45] N. Pletcher, S. Gambini, and J. Rabaey, "A 65$\mu$W, 1.9GHz RF to digital baseband wakeup receiver for wireless sensor nodes," in *IEEE Custom Integrated Circuits Conf. (CICC)*, 2007.

[46] N. M. Pletcher, S. Gambini, and J. Rabaey, "A 52$\mu$W wake-up receiver with $-$72dBm sensitivity using an uncertain-IF architecture," *IEEE J. Solid-State Circuits*, vol. 44, pp. 269–280, January 2009.

[47] M. S. Durante and S. Mahlknecht, "An ultra low power wakeup receiver for wireless sensor nodes," in *Proc. 3rd Int. Conf. Sensor Technologies and Applicat.*, June 2009, pp. 167–170.

[48] K.-W. Cheng, X. Liu, and M. Je, "A 2.4/5.8GHz 10$\mu$W wake-up receiver with -65/-50dBm sensitivity using direct active RF detection," *IEEE Asian Solid-State Circuits Conf. (A-SSCC)*, pp. 337–340, 2012.

[49] J. Choi, K. Lee, S.-O. Yun, S.-G. Lee, and J. Ko, "An interference-aware 5.8GHz wake-up radio for ETCS," in *IEEE Int. Solid-State Circuits Conf. Dig. of Tech. Papers (ISSCC)*, 2012, pp. 446–448.

[50] E. Nilsson and C. Svensson, "Ultra low power wake-up radio using envelope detector and transmission line voltage transformer," *IEEE Journal*

*on Emerging and Selected Topics in Circuits and Systems*, vol. 3, no. 1, pp. 5–12, 2013.

[51] S. Oh, N. E. Roberts, and D. D. Wentzloff, "A 116nW multi-band wake-up receiver with 31-bit correlator and interference rejection," in *IEEE Custom Integrated Circuits Conf.*, 2013, pp. 1–4.

[52] K. Takahagi, H. Matsushita, T. Iida, M. Ikebe, Y. Amemiya, and E. Sano, "Low-power wake-up receiver with subthreshold CMOS circuits for wireless sensor networks," *Analog Integrated Circuits and Signal Process.*, vol. 75, no. 2, pp. 199–205, 2013.

[53] T. Wada, M. Ikebe, and E. Sano, "60GHz, 9$\mu$W wake-up receiver for short-range wireless communications," in *Proc. of the Eur. Solid State Circuits Conf.*, 2013, pp. 383–386.

[54] J. Lee, I. Lee, J. Park, J. Moon, S. Kim, and J. Lee, "A sub-GHz low-power wireless sensor node with remote power-up receiver," in *IEEE Radio Frequency Integrated Circuits Symp.*, 2013, pp. 79–82.

[55] M. Lont, D. Milosevic, A. van Roermund, and G. Dolmans, "Ultra-low power FSK wake-up receiver front-end for body area networks," in *RFIC*, 2011, pp. 1–4.

[56] J. Bae and H.-J. Yoo, "A 45$\mu$W injection-locked FSK wake-up receiver for crystal-less wireless body-area-network," in *IEEE Asian Solid State Circuits Conf.*, 2012, pp. 333–336.

[57] T. Abe, T. Morie, K. Satou, D. Nomasaki, S. Nakamura, Y. Horiuchi, and K. Imamura, "An ultra-low-power 2-step wake-up receiver for IEEE 802.15.4g wireless sensor networks," in *Symp. on VLSI Circuits Dig. of Tech. Papers*, 2014, pp. 1–2.

[58] C. Salazar, A. Kaiser, A. Cathelin, and J. Rabaey, "A -97dBm sensitivity interferer-resilient 2.4GHz wake-up receiver using dual-IF multi-N-path architecture in 65nm CMOS," in *IEEE Int. Solid-State Circuits Conf.*, 2015, pp. 1–3.

[59] C. Bryant and H. Sjöland, "A 2.45GHz, 50$\mu$W wake-up receiver front-end with -88dBm sensitivity and 250kbps data rate," in *European Solid State Circuits Conf. (ESSCIRC)*, September 2014, pp. 235–238.

[60] X. Huang, P. Harpe, G. Dolmans, H. de Groot, and J. R. Long, "A 780–950MHz, 64–146$\mu$W power-scalable synchronized-switching OOK receiver

for wireless event-driven applications," *IEEE J. of Solid-State Circuits*, 2014.

[61] H. Milosiu, F. Oehler, M. Eppel, D. Fruhsorger, S. Lensing, G. Popken, and T. Thones, "A 3$\mu$W 868MHz wake-up receiver with -83dBm sensitivity and scalable data rate," in *Proc. of the ESSCIRC*, 2013, pp. 387–390.

[62] T. Copani, S. Min, S. Shashidharan, S. Chakraborty, M. Stevens, S. Kiaei, and B. Bakkaloglu, "A CMOS low-power transceiver with reconfigurable antenna interface for medical implant applications," *IEEE Trans. Microwave Theory and Techniques*, vol. 59, pp. 1369–1378, 2011.

[63] S. J. Marinkovic and E. M. Popovici, "Nano-power wireless wake-up receiver with serial peripheral interface," *IEEE J. on Select. Areas in Commun.*, vol. 29, no. 8, pp. 1641–1647, 2011.

[64] S. Drago, D. Leenaerts, F. Sebastiano, L. J. Breems, K. A. Makinwa, and B. Nauta, "A 2.4GHz 830pJ/bit duty-cycled wake-up receiver with $-82$dBm sensitivity for crystal-less wireless sensor nodes," in *IEEE Int. Solid-State Circuits Conf. Digest Tech. Papers (ISSCC)*, 2010, pp. 224–225.

[65] P. Le-Huy and S. Roy, "Low-power wake-up radio for wireless sensor networks," *Mobile Networks and Appl.*, vol. 15, no. 2, pp. 226–236, 2010.

[66] C. Hambeck, S. Mahlknecht, and T. Herndl, "A 2.4$\mu$W wake-up receiver for wireless sensor nodes with -71dBm sensitivity," in *IEEE Proc. Int. Symp. Circuits and Syst. (ISCAS)*, 2011, pp. 534–537.

[67] M. Lont *et al.*, "Analytical models for the wake-up receiver power budget for wireless sensor networks," in *Proc. 28th IEEE conf. Global Telecomm.*, 2009, pp. 1146–1151.

[68] Y. Zhang, L. Huang, G. Dolmans, and H. de Groot, "An analytical model for energy efficiency analysis of different wakeup radio schemes," in *IEEE 20th Int. Symp. Personal, Indoor and Mobile Radio Commun.*, 2009, pp. 1148–1152.

[69] O. Yang and W. B. Heinzelman, "Modeling and performance analysis for duty-cycled MAC protocols with applications to S-MAC and X-MAC," *IEEE Transactions on Mobile Computing*, vol. 11, no. 6, pp. 905–921, 2012.

[70] M. Zimmerling, F. Ferrari, L. Mottola, T. Voigt, and L. Thiele, "pTunes: Runtime parameter adaptation for low-power MAC protocols," in *Proc. 11th Int. Conf. Inform. Process. in Sensor Networks*, 2012, pp. 173–184.

[71] C. Fischione, P. Park, and S. C. Ergen, "Analysis and optimization of duty-cycle in preamble-based random access networks," *Wireless networks*, vol. 19, no. 7, pp. 1691–1707, 2013.

[72] R. Jurdak, A. G. Ruzzelli, and G. M. O'Hare, "Radio sleep mode optimization in wireless sensor networks," *IEEE Transactions on Mobile Computing*, vol. 9, no. 7, pp. 955–968, 2010.

[73] K.-T. Cho and S. Bahk, "Duty cycle optimization for a multi hop transmission method in wireless sensor networks," *IEEE Communications Letters*, vol. 14, no. 3, pp. 269–271, 2010.

[74] R. H. Walden, "Analog-to-digital converter survey and analysis," *IEEE Journal on Selected Areas in Communications*, vol. 17, no. 4, pp. 539–550, 1999.

[75] N. F. Kiyani, P. Harpe, and G. Dolmans, "Performance analysis of OOK modulated signals in the presence of ADC quantization noise," in *IEEE 75th Vehicular Technology Conference (VTC Spring)*. IEEE, 2012, pp. 1–5.

[76] Y. Zhang *et al.*, "A 3.72 $\mu$W ultra-low power digital baseband for wake-up radios," in *Int. Symp. VLSI Design, Automation and Test (VLSI-DAT)*, April 2011, pp. 1–4.

[77] J. Nocedal and S. Wright, *Numerical optimization*. Springer Science & Business Media, 2006.

[78] R. Hooke and T. A. Jeeves, "Direct search solution of numerical and statistical problems," *Journal of the ACM (JACM)*, vol. 8, no. 2, pp. 212–229, 1961.

[79] R. M. Lewis, V. Torczon, and M. W. Trosset, "Direct search methods: then and now," *Journal of computational and Applied Mathematics*, vol. 124, no. 1, pp. 191–207, 2000.

# Part II

# Included Papers

# *Paper I*

# DCW-MAC: An Energy Efficient Medium Access Scheme Using Duty-cycled Low-power Wake-up Receivers

**In this work we present a new low-power medium access scheme for sensor-type networks specifically with low traffic intensity. We call the proposed scheme DCW-MAC where ultra-low-power wake-up receivers are combined with optimal duty-cycled listening. First we introduce a framework for the analysis of energy consumption of the studied network type, then we use it to optimize the MAC scheme to achieve very low total energy consumption per transmitted data packet. It is shown that even with large sacrifices in terms of wake-up receiver detection performance, required to achieve ultra-low-power consumption with a limited form factor, we can achieve very competitive total energy consumption and outperform other MAC schemes for scenarios with low traffic.**

---


Nafiseh Seyed Mazloum and Ove Edfors,
"DCW-MAC: An Energy Efficient Medium Access Scheme Using Duty-cycled Low-power Wake-up Receivers,"
in *Proc. IEEE Vehicular Technology Conference (VTC Fall))*, San Francisco, CA, United States, pp. 1–5, September 2011.

# 1 Introduction

Energy efficiency is a key design issue for wireless sensor network (WSN) applications. In these applications energy resources are severely limited, both due to node sizes and possible placements in locations where batteries cannot easily be replaced. To design a long lifetime network, it is important both to design low-power transceivers and to use energy efficient protocols to control the communication. In general, the dominant sources of energy waste in a communication system include, but are not limited to, *idle listening*, *collisions*, *data overhead* and *overhearing* [1]. These energy costs are reduced to a large extent by designing an energy efficient medium access control (MAC) protocol.

In this paper we focus on the principle of duty-cycled MAC protocols, which is a very common approach to reduce energy cost in the design of low power communication systems [1–3]. In this approach the idle listening, which is the dominant factor for energy consumption, is reduced by only listening for transmissions at certain time instants and turning off the transceiver at other time instants. Several different communication strategies for duty-cycled sensor networks have been proposed [1, 2, 4, 5]. These solutions are often categorized into synchronous and asynchronous schemes. In the synchronous communication schemes [6, 7], all nodes wake up and sleep periodically according to a predefined common schedule. The disadvantage of this approach is that the data overhead due to pre-synchronization and overhearing may consume significant energy [4,5]. In the asynchronous communication schemes, the nodes also wake up periodically, but not based on a common synchronized schedule [4, 8, 9]. A wake-up preamble, at least equal in length to one sleep-listen period of the receiver, is sent ahead of data. An important benefit is that the asynchronous schemes avoid the energy cost required to synchronize nodes. A drawback, however, is that the lack of synchronization between nodes and the periodic listening requires longer (higher energy) wake-up preambles. The latter issue is avoided by an approach proposed by the authors of [5], known as the X-MAC protocol. In this approach the transmitter replaces the long preamble with periodic short wake-up preambles. The X-MAC reduces the redundant energy consumption due to idle listening, overhearing and data overhead. However, the energy consumption of the nodes for periodic channel listening is still a substantial issue of WSNs. It is therefore of interest to study WSNs where nodes are equipped with low-power wake-up receivers (WRxs).

Low-power WRxs for WSNs have been discussed for about a decade [10,11]. Early WRxs [11] were assumed to be always on and continuously listen to the channel, while the main receiver and transmitter are switched off. When a wake-up preamble is detected, the main radio is switched on for data reception. Low-power WRxs can be combined with periodic listening to achieve even lower

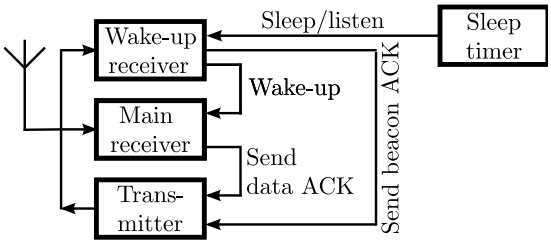


**Figure 1:** Node architecture block diagram, with signaling in listen/receive mode shown.

energy consumption.

In this work we develop and analyze a duty-cycled medium access scheme for low-power WRxs, the DCW-MAC. We define a generic system where the nodes use low-power WRxs, for which we derive closed form expressions for total energy consumption per packet. These expressions are then used to optimize protocol parameters for lowest possible energy consumption, given certain hardware parameters. The main differences between this work and [10] are that we *i) take into account that ultra-low-power WRxs may come with a significant performance degradation* and *ii) analyze the total power consumption of an entire network with duty-cycled WRxs.* The model is provided for two different WRx scenarios: a) with receiver duty cycling, listening to the channel periodically, and b) when the WRx is always on and continuously monitors the channel, like in [11]. We compare these energy models with the energy models of a system where no low-power WRx is available and the main receiver is used for listening to the channel.

First we give a description of the overall operation of the addressed systems in Section 2. The different states of the nodes (sleep, active, standby, off, etc.) and the interaction between them are described in detail. In Section 3 we present the analytical models of the average energy consumption per packet for different MAC schemes and for nodes with different hardware architectures. The analytical expressions are then used to determine the optimal protocol parameters (sleep-listen periods) in Section 4. Next, we evaluate the performance of the WRx-MAC protocols[1] and compare them for different traffic conditions in Section 5. Finally, conclusions and remarks are given in Section 6.

# 2 System Description

A generic block diagram of the reference node architecture is shown in Fig. 1, where the node consists of a transmitter, a main receiver and a duty-cycled WRx. The WRx is switched on periodically by the sleep/listen timer and listens to the channel for any potential communication. The main receiver is switched on only when there is data to receive. Whenever the node has a packet to transmit, the transmitter is set up to send out periodic wake-up beacons (WBs) to the target receiver, similar to the X-MAC scheme. When the listen period of the WRx coincide with a WB transmission carrying its ID, it detects the beacon and transmits a beacon acknowledgment (BACK) message back. The transmitter node therefore has to change to the receive mode after each WB to investigate if a BACK is available. If a BACK is received, the node starts transmitting data, which is then acknowledged by the receiver (DACK). As long as no BACK is received, a node with data continuously repeats WB transmission.

In the always-on WRx MAC protocol, which we use as a reference, the WRx listens continuously to the channel and no listen/sleep timer is required. In this scenario, only one WB carrying the address of the target receiver need to be transmitted. After the target receiver detects the WB with its ID, similar to the DCW-MAC, it sends back a BACK message. In these scenarios, both the WB and the BACK carry the source and destination addresses. However, the WB is detected by a low performance (low-power) WRx, while BACK is received by the main radio of its counterpart. We take this performance loss into account as a WRx loss. Assuming that the WRx has a $k$[dB] higher noise figure than the main receiver, the WB needs to have $k$[dB] more energy than the BACK for equal detection performance. This is achieved in principally two different ways; *i) keeping WB time duration (same data rate) and increase the transmit power* or *ii) keeping the WB transmit power and making the duration longer (lower data rate)*. The first approach requires a large dynamic range of the transmitter, while the second increases the delay before a WB is detected. We have chosen to follow the second approach in this analysis.

## 2.1 Reference traffic scenario and assumptions

We consider a system of $N$ nodes where all nodes have equal functionality and are able to directly communicate with each other. Furthermore, we assume that data packets to transmit, arrive according to an exponential distribution with parameter $\lambda$ where each data packet transmission takes $T_d$ seconds. This implies that the mean interval time between two packets is $1/\lambda$ seconds on

[1] In this paper WRx-MAC refers to both the DCW-MAC and the always-on WRx-MAC.

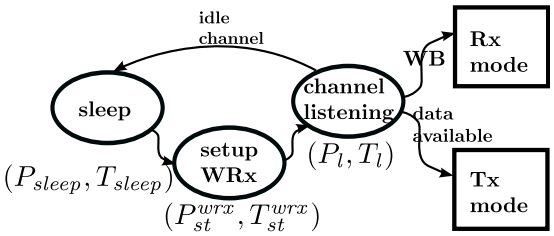


(a) DCW-MAC scheme.

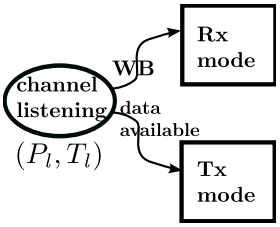


(b) Always-on WRx MAC scheme.

**Figure 2:** State-transition diagram of overall operation of a node for WRx-MAC schemes.

average. Since we are interested in ultra-low power scenario, we also assume that packets are rare in the sense that $1/\lambda \gg T_d$. Under these assumptions we ignore any energy consumption resulting from side-effects of collisions in the transmission, allowing us to make tractable analytical derivations of optimal sleep and listen times for the analyzed protocols. We will also assume perfect detection of signals, whenever the targeted receiver is listening in the correct time interval.

## 2.2 State-space model

The overall operation of a single node accessing the medium for two different MAC scenarios is illustrated in Fig. 2. The sleep state in the DCW in Fig. 2(a) represents the node status when both the WRx and the main radio are switched off. The power consumption in this state is determined by the sleep/listen timer and the radio static power. In the channel-listening state the low power WRx is turned on to examine the channel. The parameters $(P_{state}^{part}, T_{state}^{part})$, shown below each state represent the power consumption of, and the time interval

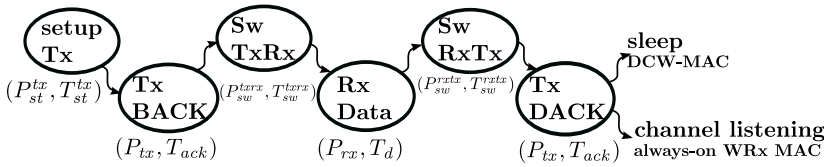


**Figure 3:** Receiver state-space model.

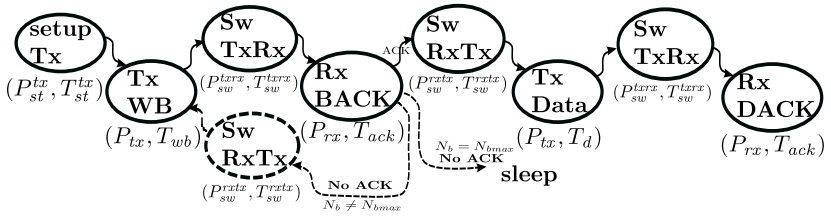


**Figure 4:** Transmitter state-space model.

spent in, the corresponding state. With this notation, the energy consumed in a certain *part* of the receiver when in a certain *state* is $E_{state}^{part} = P_{state}^{part} T_{state}^{part}$.

The behavior of a node when acting as a transmitter or receiver is described in more detail by the state-space diagrams in Fig. 3 and Fig. 4. Switching between transmitting and receiving modes comes at a cost in both time delay and energy consumption, which are represented by the switching states **Sw TxRx** and **Sw RxTx**. Correspondingly, the transition to setup the main radio is modeled by the state **Setup Tx**. The node has the same behavior for the two MAC schemes in receiving mode, see Fig. 3. However, the node operates differently in the transmitter mode. When using the always-on WRx protocol, the transmitter needs to send only one WB to wake the target receiver. When using the duty-cycled WRx protocol the nodes communicate asynchronously and the transmitter sends the WB periodically until a BACK is received from the target node. This difference in the behavior of a node in Tx mode is depicted by the dashed lines in Fig. 4. The parameter $N_{bmax}$ denotes the maximum number of periodic WB transmissions/BACK listening for a guaranteed success (given the perfect detection assumption).

# 3 Energy Analysis

Based on the above, we present analytical models of the energy consumption for the addressed MAC schemes. For reference, we also compare these models to MAC protocols where nodes only consist of the main radio. The measure

of energy consumption that we will use is the average energy consumption per packet, for an entire network of $N$ nodes. In its simplest form, it is the sum of the transmitter, target receiver, and non-target receivers energy consumptions per transmitted packet. Denoting these $E_{tx}$, $E_{rx}$, and $E_{nrx}$, respectively, the average energy consumption per packet for $N$ network nodes becomes

$$E = E_{tx} + E_{rx} + (N-2)E_{nrx}. \tag{1}$$

For notational convenience we assume that all nodes have a base-level power consumption, the sleep power $P_{sleep}$ below which they cannot go. All other energy figures are in addition to this base-level. The base-level energy per received packet becomes $P_{sleep}/\lambda$, where $P_{sleep}$ is the power consumption of the node in its sleep state. Furthermore, the switching energies as well as the switching times are all considered equal, *i.e.*, $E_{sw}^{txrx} = E_{sw}^{rxtx}$ and $T_{sw}^{txrx} = T_{sw}^{rxtx}$.

## 3.1 DCW-MAC

In the proposed DCW-MAC scheme, nodes always duty cycle unless data is available for transmission or the WRx has detected a WB. The communication between nodes is illustrated schematically for one packet arrival interval in Fig. 5, where **Node1** is the transmitter, **Node2** is the target receiver, and the other $N-2$ nodes are non-target receivers. Average energy consumption of the transmitter and receiver nodes, per packet, is given by

$$E_{tx} = \frac{P_{sleep}}{\lambda} + E_l^{tx} + E_{data}^{tx}, \text{and} \tag{2}$$

$$E_{rx} = \frac{P_{sleep}}{\lambda} + E_l^{rx} + E_{data}^{rx}, \tag{3}$$

respectively. The first term in these expressions is the base-level energy and the second term is the additional energy required for duty cycling, while the third term expresses the additional energy in Tx and Rx modes for the transmitter and receiver, respectively. The average energy consumption per packet for a non-target receiver is determined by the base-level energy consumption and the additional energy required for duty-cycling during one packet arrival interval, as

$$E_{nrx} = \frac{P_{sleep}}{\lambda} + E_l^{nrx}. \tag{4}$$

The transmitter and WRx communicate asynchronously, therefore the WRx needs to listen to the channel for at least a time-period $2\,T_{wb} + 2\,T_{sw}^{txrx} + T_{ack}$ to guarantee detection of a WB. Furthermore, when data is available for transmission, the transmitter sends the WB periodically and waits to receive a BACK

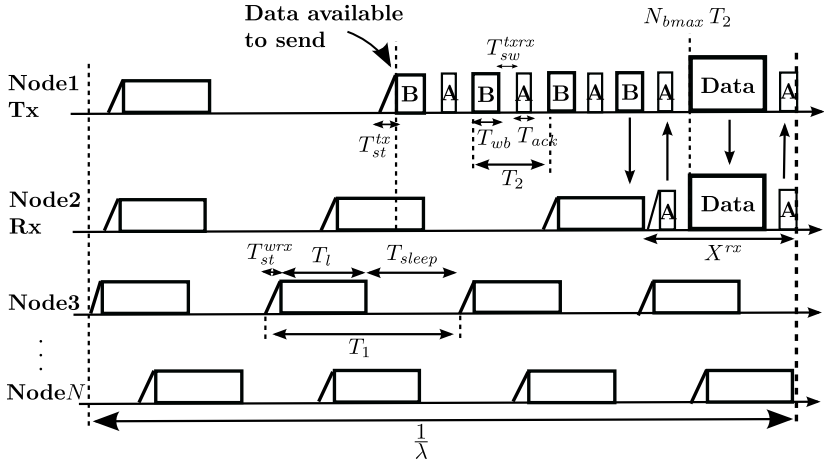


**Figure 5:** DCW-MAC scheme.

after each one. At least one WB need to be transmitted to initiate communication and in the worst case, depicted in Fig. 5, the first WB is incompletely received by the target WRx and consequently WBs need to be transmitted until the next WRx listening period. This maximum number of WB transmissions is given by

$$N_{bmax} = \frac{T_1 + T_2}{T_2} = 1 + \frac{T_{sleep} + T_{st}^{wrx} + T_l}{T_l - T_{wb}}.$$

With asynchronous nodes, no number of transmitted WBs is more likely than any other and the average number of periodic WB-BACK periods per packet is

$$\bar{N}_b = \frac{N_{bmax} + 1}{2} = \frac{T_{sleep} + T_{st}^{wrx} + T_l}{2\,(T_l - T_{wb})} + 1.$$

The consumed energy in Tx mode, $E_{data}^{tx}$ in (2), is the contribution of the energy of periodic WB-BACK as well as the energy of data transmission and is given by

$$E_{data}^{tx} = E_{st}^{tx} + \bar{N}_b\,E_{wb} + E_d, \tag{5}$$

where

$$E_{wb} = P_{tx}\,T_{wb} + P_{mrx}\,T_{ack} + 2\,E_{sw}^{txrx}, \text{and}$$
$$E_d = P_{tx}\,T_d + E_{sw}^{txrx} + P_{mrx}\,T_{ack}.$$

Using the state-space model, the average energy consumption in Rx mode, $E_{data}^{rx}$ in (3), becomes

$$E_{data}^{rx} = E_{st}^{tx} + P_{tx}\,T_{ack} + P_{mrx}\,T_d + P_{tx}\,T_{ack} + 2\,E_{sw}^{txrx}. \tag{6}$$

Moreover, the channel listening energy, consumed by the transmitter, receiver, and non-target receiver, becomes

$$E_l^{part} = \bar{N}_l^{part}\,\left(E_{st}^{wrx} + P_{wrx}\,T_l\right), \tag{7}$$

where

$$\bar{N}_l^{part} = \frac{1/\lambda - X^{part}}{(T_{sleep} + T_{st}^{wrx} + T_l)}$$

denotes the average number of WRx duty-cycles in the interval where nodes are in idle mode. Above, *part* is either *tx*, *rx*, or *nrx*, and for notational convenience we introduced

$$\begin{aligned} X^{tx} &= T_{st}^{tx} + \bar{N}_b\,T_2 + T_d + T_{sw}^{txrx} + T_{ack}, \\ X^{rx} &= T_{st}^{tx} + 2\,T_{ack} + 2\,T_{sw}^{txrx} + T_d, \text{and} \\ X^{nrx} &= 0. \end{aligned}$$

Replacing (6) and (7) back in (2)-(4) and (1) gives the energy consumption per packet.

## 3.2 Always-on WRx-MAC

The communication between nodes in the always-on WRx-MAC protocol, for one packet arrival interval, is illustrated in Fig. 6. As for the DCW, the average energy consumption of the transmitter, receiver and non-target receivers is modeled by (2)-(4), respectively. The two fundamental differences, as compared to the DCW case, are i) that the WRx now continuously monitors the channel, which changes (7) to

$$E_l^{part} = \frac{P_{wrx}}{\lambda}, \tag{8}$$

and ii) the transmitter only needs to send one WB to initiate communication, which changes (5) to

$$E_{data}^{tx} = E_{st}^{tx} + E_{wb} + E_d. \tag{9}$$

With these changes, the same procedure as for the DCW-MAC is used to calculate the energy per packet.

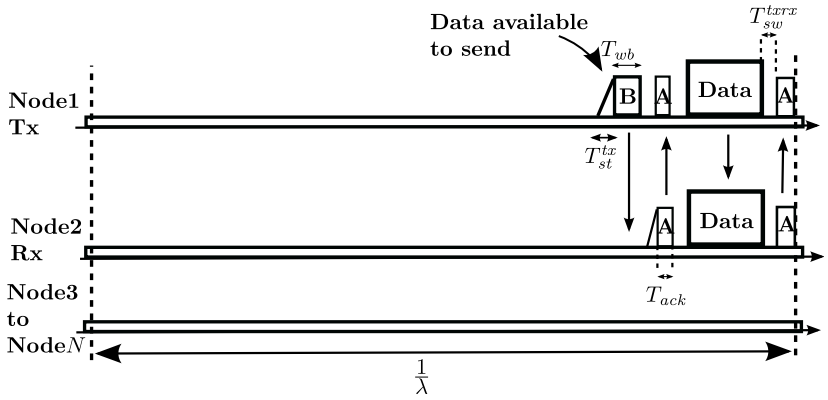


**Figure 6:** Always on WRx-MAC scheme.

### 3.3 X-MAC

In the X-MAC, nodes consist of only the main radio, which duty-cycles and listens to the channel periodically [5]. The energy models of the transmitter, receiver and non-target receivers presented in Section 3.1 apply to this algorithm as well. In the energy models, however, the WRx power consumption, $P_{wrx}$, setup time, $T_{st}^{wrx}$, and setup energy, $E_{st}^{wrx}$, are replaced by $P_{mrx}$, $T_{st}^{mrx}$ and $E_{st}^{mrx}$, respectively.

Furthermore, in this scenario both the ACK and WB are received by the full performance main receiver and therefore no increase in transmit energy for the WB is needed to compensate for the low performance of the WRx. This does not change the energy expressions, but the required transmission time $T_{wb}$ for the WB will be reduced, as compared to the other cases.

## 4 Optimal Sleep Intervals

To complete the design of the DCW-MAC protocol, we need to select the sleep-listen time intervals for given power consumptions in the different states, energies required for state transitions, and specific traffic conditions. The first step in this process is the observation that the WRx needs to listen during a time interval

$$T_l \geq 2\,T_{wb} + 2\,T_{sw}^{txrx} + T_{ack} \tag{10}$$

to guarantee that entire incoming WB will be caught. The second step is to select, for a given listen time $T_l$, a sleep time $T_{sleep}$ which minimizes the total power consumption of the network. By differentiating (1) w.r.t. $T_{sleep}$ and

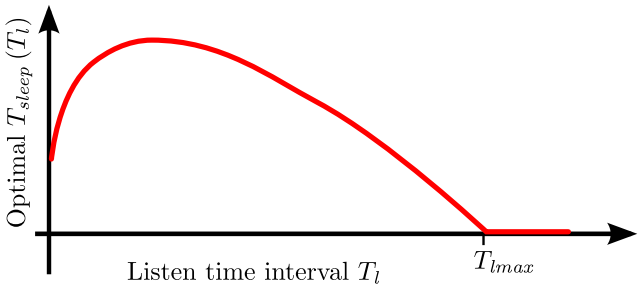


**Figure 7:** Illustration of the optimal relationship between sleep and listen interval.

taking into account that the sleep time has to be non-negative, we obtain an optimal value of

$$T_{sleep}(T_l) = \max\left(\sqrt{\Gamma} - T_l - T_{st}^{wrx}, 0\right), \tag{11}$$

where

$$\Gamma = \frac{2\,(P_{wrx}\,T_l + E_{st}^{wrx})}{(k\,P_{tx} + P_{mrx})\,T_l + (2\,k+1)\,E_{sw}^{rxtx}} \cdot \left(\frac{N}{\lambda} - 2\,T_d - T_{st}^{tx} - 5\,T_{sw}^{txrx} + \frac{k+4}{2\,k+1}\,T_l\right) \cdot \left((k+1)\,T_l + (2\,k+1)\,T_{sw}^{rxtx}\right).$$

Fig. 7 illustrates the relationship between listen and optimal sleep time intervals. We observe that for long listen times the best choice for the nodes is not to sleep at all, since $T_{sleep}(T_l) = 0$ for $T_l$s larger than some $T_{lmax}$.

The sleep time interval increases with power or energies related to the WRx and decreases with higher beacon transmit power. Furthermore, both the maximum listen time interval and the sleep time interval increase with higher average intervals between packets (lower packet arrival rate). The latter will introduce a long delay before initiating any data transmission since the transmitter must send periodic WB-ACKs until the target receiver wakes up and detects a WB. Moreover, an extra delay is introduced due to the poor performance of the WRx and transmission of the long WBs. In the worst case, the longest delay occurs when the first WB is incompletely received by the target WRx and WBs have to be transmitted until the next WRx listening period and is given by

$$D = T_{sleep} + \alpha\,T_l + A, \tag{12}$$

**Table 1:** System parameters.

(a) Radio characteristics.

| Parameter | Value |
|---|---|
| $P_{sleep}$ | 0.5 $\mu$W |
| $P_{tx}$ | 1 mW |
| $P_{mrx}$ | 1 mW |
| $P_{wrx}$ | 0.01 mW |
| $P_{st}^{tx} = P_{st}^{mrx}$ | 0.5 mW |
| $P_{st}^{wrx}$ | 0.01 mW |
| $P_{sw}^{txrx} = P_{sw}^{rxtx}$ | 1 mW |
| $T_{st}^{tx} = T_{st}^{mrx}$ | 1 ms |
| $T_{st}^{wrx}$ | negligible |
| $T_{sw}^{txrx} = T_{sw}^{rxtx}$ | 5 $\mu$s |

(b) Protocol parameters.

| Parameter | Value |
|---|---|
| $T_{ack}$ | 0.08 ms |
| $T_{wb}$ | $k$ (0.08) ms |
| $T_d$ | 2 ms |
| $R_b$ | 250 kbps |

where $\alpha = (\frac{3}{2} + \frac{1}{2\,(2\,k+1)})$ and $A = T_{sw}^{txrx} + T_{st}^{tx} + T_{st}^{wrx}$.

If a receiver node is required to respond in a limited time period $D < D_{max}$, then from (12) the receiver sleep time is restricted to

$$T_{sleep}(D_{max}, T_l) < D_{max} - \alpha\, T_l - A \tag{13}$$

to meet the requirement of the system. However, to minimize the total energy consumption of the system the optimal value of $T_{sleep}$ is selected by (11). Therefore, to fulfill the system requirement and to minimize the network total energy consumption for a given listen time $T_l$, the sleep time is selected as

$$T_{sleep} = max(0, min(T_{sleep}^{opt}, T_{sleep}^{dreq})), \tag{14}$$

where $T_{sleep}^{opt}$ and $T_{sleep}^{dreq}$ denote the optimal sleep time and the required sleep time to meet the delay requirement, respectively.

# 5 Results

In this section we evaluate the energy performance of the WRx-MAC schemes and compare it with the X-MAC. The radio characteristics and protocol parameters used to obtain the numerical results are listed in Table 1. The parameters are based on initial estimates from the *Ultra-portable devices* project at the Department of Electrical and Information Technology, Lund University.

The lengths of the WB and ACK are chosen to be 20 bits. We also assume that the WRx has a 20 dB worse noise figure (NF) than the main radio. This

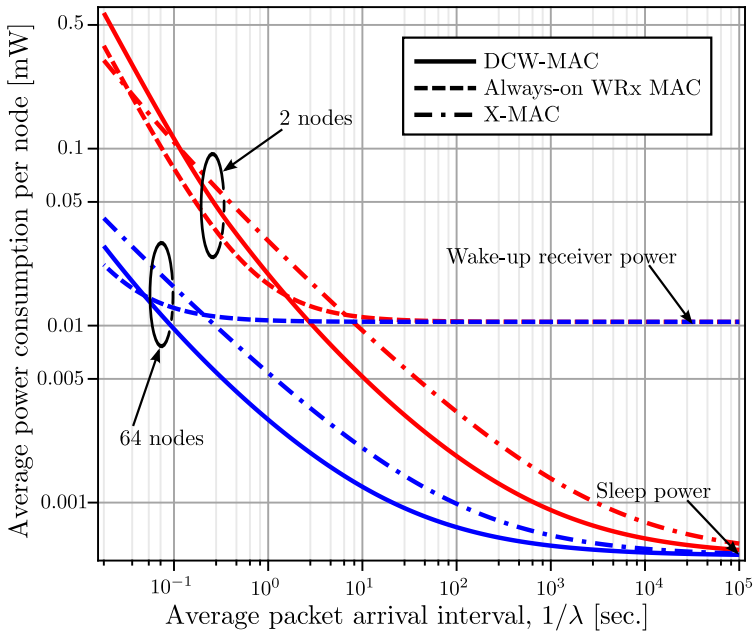


**Figure 8:** Average power consumption per node vs. average packet arrival interval.

is compensated by a WB which is $k = 100$ times longer in the WRx-MAC scenarios. For the X-MAC scenario, where the main receiver is used for receiving the WB, we set $k = 1$. Considering equality in (10), the listen intervals for the WRx-MAC and the X-MAC become 16.08 ms and 0.25 ms, respectively.

Let us start without delay requirements. Fig. 8 shows the node mean power consumption[2] of the DCW-MAC, always-on WRx-MAC and X-MAC, as a function of average packet-arrival intervals for two different network sizes and with optimal sleep intervals chosen according to (11). Two principal things are observed: i) for long average packet-arrival intervals (low traffic), the optimal sleep intervals of the DCW-MAC and the X-MAC increase and they result in the lowest power consumption; ii) for short average packet-arrival intervals (high traffic), the sleep mechanism gives less energy savings and the MAC schemes using the low-performance WRxs start to suffer from the high-energy WBs needed. The proposed DCW-MAC has the largest gain over the other schemes in the "mid-range" of packet-arrival intervals.

[2]Calculated as energy per packet per node per packet arrival time.

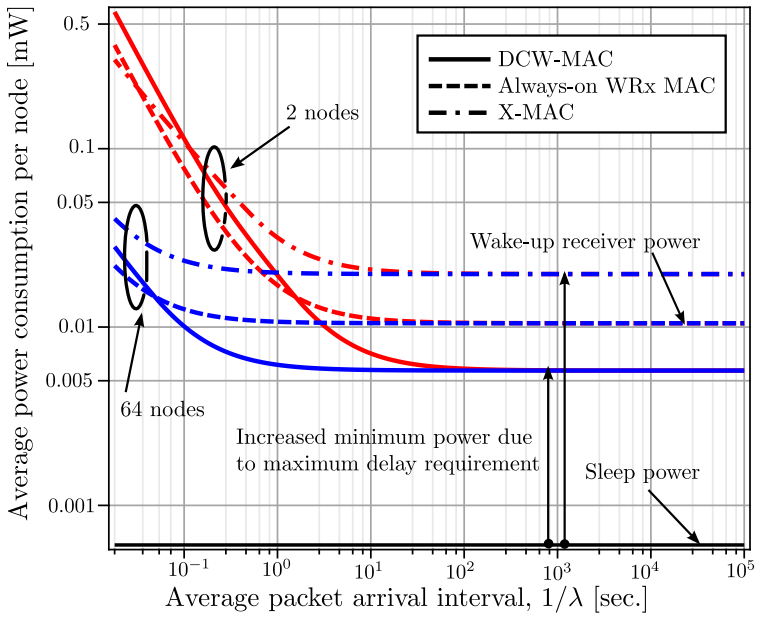


**Figure 9:** Average power consumption per node vs. average packet arrival interval.

Now, we consider the case where we have a maximum-delay requirement. Both the DCW-MAC and the X-MAC consume more power at long average packet-arrival intervals (low traffic), since their sleep periods now get restricted. This in contrast to the always-on WRx-MAC, where the nodes continuously monitor the channel. We illustrate the resulting power consumption, for a maximum delay requirement of 40 msec, in Fig. 9. The power performance of the DCW-MAC, always-on WRx-MAC and X-MAC are again compared for two different network sizes – this time with the sleep interval selected according to (14). The minimum power consumption of the X-MAC increases beyond the WRx power consumption and becomes inferior to the always-on WRx-MAC scheme. With increasing demands on maximum delay, the DCW-MAC minimum power consumption converges to the WRx power consumption, while the X-MAC minimum power consumption converges to the (much higher) main receiver power. The proposed DCW-MAC now has clear gains over the other two MAC schemes, for all "long" packet-arrival intervals.

## 6 Conclusions and Remarks

This paper presents a new medium access control scheme for WSNs, the DCW-MAC, which combines the energy saving mechanisms of duty-cycled medium access [5] and low-power wake-up radios [10]. An important part of the energy analysis is that we take the reduced detection performance of low-power WRxs into account in the analysis. The DCW-MAC is analyzed, energy optimized and compared with other MAC schemes. While the low performance of the WRx limits the performance of the DCW-MAC for high-traffic scenarios, it significantly outperforms other MAC schemes in low-traffic scenarios encountered in many low-power sensor networks.

# Bibliography


[1] Y. Wei, J. Heidemann, and D. Estrin, "An energy-efficient MAC protocol for wireless sensor networks," in *Proc. 21st Ann. Joint Conf. IEEE Comput. and Commun. Soc.*, vol. 3, November 2002, pp. 1567–1576.

[2] A. El-Hoiydi, "Aloha with preamble sampling for sporadic traffic in ad hoc wireless sensor networks," in *IEEE Int. Conf. Commun.*, vol. 5, April 2002, pp. 3418–3423.

[3] J. Polastre, J. Hill, and D. Culler, "Versatile low power media access for wireless sensor networks," in *Proc. 2th International Conference Embedded Ntworked Sensor Syst.*, 2004, pp. 95–107.

[4] A. El-Hoiydi and J.-D. Decotignie, "WiseMAC: An ultra low power mac protocol for multi-hop wireless sensor networks," in *Proc. 4th Int. Conf. Embedded Ntworked Sensor Syst.*, 2004.

[5] M. Buettner *et al.*, "X-MAC: a short preamble MAC protocol for duty-cycled wireless sensor networks," in *Proc. 4th Int. conf. Embedded networked sensor syst.*, 2006, pp. 307–320.

[6] W. Ye, F. Silva, and J. Heidemann, "Ultra-low duty cycle MAC with scheduled channel polling," in *Proc. 4th International Conference Embedded Ntworked Sensor Syst.*, 2006, pp. 321–334.

[7] T. van Dam and K. Langendoen, "An adaptive energy-efficient mac protocol for wireless sensor networks," in *Proc. 1st Int. Conf. Embedded Ntworked Sensor Syst.*, 2003, pp. 171–180.

[8] S. Mahlknecht and M. Bock, "CSMA-MPS: a minimum preamble sampling MAC protocol for low power wireless sensor networks," in *Proc. IEEE Int. Workshop on Factory Commun. Syst.*, 2004, pp. 73–80.

[9] M. S. Durante and S. Mahlknecht, "An ultra low power wakeup receiver for wireless sensor nodes," in *Proc. 3rd Int. Conf. Sensor Technologies and Applicat.*, June 2009, pp. 167–170.

[10] M. Lont *et al.*, "Analytical models for the wake-up receiver power budget for wireless sensor networks," in *Proc. 28th IEEE conf. Global Telecomm.*, 2009, pp. 1146–1151.

[11] C. Guo, L. C. Zhong, and J. Rabaey, "Low power distributed mac for ad hoc sensor radio networks," in *IEEE, Global Telecomm. Conf.*, vol. 5, 2002, pp. 2944–2948.

# *Paper II*

# Performance Analysis and Energy Optimization of Wake-up Receiver Schemes for Wireless Low-power Applications

**The use of duty-cycled ultra-low power wake-up receivers (WRxs) can significantly extend a node life time in low-power sensor network applications. In the WRx design, both low-power operation of the WRx and wake-up beacon (WB) detection performance are of importance. We present a system-level of a duty-cycled WRx design, including analog front-end, digital base-band, WB structure, and the resulting WB detection and false alarm probabilities. We select a low-power WRx design, with about two orders of magnitude lower power consumption than the main receiver. The associated cost is an increase in raw bit-error rate (BER), as compared to the main receiver, at the same received power level. To compensate, we use a WB structure that employs spreading. The WB structure leads us to an architecture for the digital base-band with a high address-space scalability. We calculate closed form expressions for detection and false alarm probabilities. Using these we analyze the impact of design parameters. The analytical framework is exemplified by minimization of WB transmit energy. For this particular optimization, we also show that the obtained results are valid for all transmission schemes with an exponential relationship between signal-to-noise ratio and bit-error rate, *e.g.*, the binary orthogonal schemes with non-coherent detection used in many low-power applications.**

---


Nafiseh Seyed Mazloum, Ove Edfors,
"Performance Analysis and Energy Optimization of Wake-up Receiver Schemes for Wireless Low-power Applications,"
in *IEEE Transaction on Wireless Communications*, Vol. 13, No. 12, pp. 7050-7061, 2014.

# 1 Introduction

A long life-time network where the nodes can operate over an extended time period is a main requirement in many sensor network applications. With limited source of energy, both due to node sizes and/or difficult battery replacements, it can be very challenging to fulfill demanding life-time requirements. To optimize the network life-time it is crucial to design an ultra low power communication system [1–3]. The use of ultra-low power wake-up receivers (WRxs) can significantly reduce the overall power consumption of the system. Previous studies on WRx schemes mainly address scenarios where delay is the main design requirement and therefore the WRxs monitor the channel continuously [4–7]. The energy consumption of the WRx due to continuous channel monitoring, however, becomes dominant in scenarios with rare data packets. Thus, to further lower the system power consumption, we combine the ultra-low power WRxs and duty-cycled channel listening [8,9]. For this class of WRx schemes, periodic wake-up beacons (WBs) are transmitted ahead of data packets for synchronization of the communicating nodes. The WRx is switched on periodically for a certain time interval to observe the channel, listening for the WB. The WB consists of a preamble and an address part. The main receiver is only powered up when the WRx detects a WB with the correct address. We have shown in [8] that by optimizing the sleep time of a duty-cycled WRx we can minimize energy consumption while meeting delay requirements. It is therefore of interests to further pursue this type of WRx schemes. As no previous study on duty-cycled WRx is available in the literature, we have no direct reference system to compare against. We can either choose a duty-cycled main receiver scheme or an always-on WRx scheme as reference. In this work, we compare power consumption to the always-on WRx schemes, since the focus is on low-power WRxs and in principle an always-on WRx scheme can be duty-cycled.

A WRx is designed for low power operation, typically two orders of magnitude lower than the power consumption of a main transceiver, e.g. in the order of $10\mu W$ under realistic assumptions [7]. To meet strict power consumption requirements, early attempts avoided power-hungry components such as mixers and synthesizers and simple modulation schemes were often selected. One early such design is given in [16], where a competitive power consumption of 65 $\mu$W is achieved, at the cost of a -50 dBm WRx sensitivity. Later designs [10–15][3] have refined the design concepts to improve sensitivity and, in several cases,

[3]The design presented in [12] is intended for a duty-cycled WRx scheme, but this is not explicitly analyzed.

**Table 1:** Comparison of Wake-up Receiver Designs

| Parameter | [10] | [11] | [12] | [13] | [14] | [15] |
|---|---|---|---|---|---|---|
| Operating frequency [GHz] | 2.4 | 2 | 2.4 | 0.915 | 2.4 | 0.4 |
| Modulation | OOK | OOK | PPM | FSK | OOK | OOK |
| Sensitivity [dBm] @ BER $10^{-3}$ | $-75$ | $-70$ | $-87$ | $-65$ | $-64$ | $-80$ |
| Data rate [kbps] | 100 | 200 | 250 | 50 | 100 | 50 |
| Noise figure [dB] | - | - | - | 23 | - | - |
| Power consumption [$\mu$W] | 56 | 52 | 415 | 126 | 51 | 280 |
| Technology [nm] | 180 | 90 | 65 | 90 | 90 | 90 |
| Supply voltage | 1.8 | 0.5 | 1.2 | 0.75 | 0.5 | 1.5 |

different low-power mixing strategies have been introduced [11–13]. Today we see power consumption levels at around 50 $\mu$W and corresponding sensitivity levels at about -70 dBm, in the 2.4GHz frequency range used in this paper. These sensitivity levels are typically related to raw bit-error rates (BERs) in the order of $10^{-3}$, *cf.* Table 1. While the improvements are impressive, the sensitivity levels reached are significantly worse than the ones for main receiver designs, where we allow orders of magnitude higher power consumption. This also means that orders of magnitude higher transmit power is needed when waking up a node, as compared to normal data transmission. Using a single transmitter structure, such large variations in transmit power will make the design more complicated and also less power efficient [17]. We therefore aim for a simple and power efficient solution with a single transmitter, using the same transmit power both for data and wake-up. With a low-power WRx front-end, and the corresponding loss in sensitivity, the raw BER will be higher than the $10^{-3}$ level normally used for receiver benchmarking. We show that, by applying proper WB structures and digital base-band processing, the processing gain can compensate for the high raw BER, even for very aggressive power savings in the WRx analog front-end. The costs to pay are longer WBs and longer wake-up delays, which may cause congestion in situations with high enough data traffic. However, in extreme low-power networks with rare data transmission and low demands on delay, these costs can be quite tolerable.

If our goal is to optimize an entire wake-up scheme, to achieve as low power consumption as possible, we need to look beyond sensitivity levels and in a more elaborate way take into account mechanisms that influence power consumption. A missed WB leads to additional WB transmissions by the source node and a

falsely detected WB leads to an unnecessary power-up of the main transceiver by the WRx. Hence, we should focus our attention on the WB detection performance, and its connection to power consumption. A few studies [18] [19] address WB detection performance and digital base-band processing, and there are also studies addressing the entire WRx chain, e.g. [20]. However, none of these attempt to make a complete analysis where system parameters can be optimized.

Our approach is to analyze the complete system-level design of a duty-cycled WRx, including the analog front-end and digital base-band architectures, the WB packet structure, and the resulting WB detection and false alarm probabilities. First we express the characteristics of the analog front-end for the resulting BER in terms of signal to noise ratio. We then select a WB packet structure that allows for high flexibility in the size of the address-space and makes the design an attractive candidate both for small networks as well as massive ones. The choice of the WB structure leads us to an architecture for the digital base-band, where we improve the design as compared to [21]. We show that by adjusting the WB packet parameters we can compensate for increased raw BERs from the analog front-end and achieve adequate levels of WB detection performance, at the same received power levels as the main receiver sensitivity. Finally, given the raw BER characteristics of the analog front-end, the WB structure, and the digital base-band architecture, we perform analytical calculations of WB detection and false alarm probabilities. These probabilities are defined per listening interval which, without loss of generality, simplifies calculations and make them independent of the length of the sleep interval. Having this analytical framework, we have the prerequisites for a complete analysis of energy/power consumption of the entire system, along the lines of what is introduced in [8], where the influence of the length of the sleep interval is included in the energy models rather than in the detection and false-alarm probabilities. Performing such a complete energy analysis is however beyond the scope of this paper and, as an example, we perform a simplified analysis where we focus on the energy required to transmit the WBs. Using this simplified energy model we illustrate how to optimize WB design parameters for different address-space sizes.

This paper is organized as follows. In Section 2 we give a description of the overall operation of the addressed system. We present a design choice for the WRx analog front-end and propose a basic structure for the WB packet in Section 3. In Section 4 we further detail a structure for the digital base-band of the WRx and then present analytical expressions for the detection performance of the proposed design configuration. In Section 5 simulations are performed to validate the analytical expressions and to evaluate the performance of the proposed structure. These expressions are further used in Section 6 to deter-

mine the optimal design parameters of WRx schemes. Conclusions and final remarks are given in Section 7.

# 2 Duty-cycled Medium Access

When targeting wireless sensor network applications with low traffic intensity, idle channel listening becomes a dominant source of power consumption. One of the solutions to this problem is duty-cycled channel listening, where the receiver only periodically wakes-up. This can be done using the main receiver, which is also used for data communication, but we can reduce power consumption even more if a dedicated low-power WRx is employed. This concept, Duty-Cycled Wake-up receiver based Medium ACcess (DCW-MAC), was outlined and partly analyzed in [8]. As the medium access is the center of the analysis in this study, we describe the DCW-MAC scheme in some more detail below.

## 2.1 DCW-MAC

In the DCW-MAC scheme, as shown in Fig. 1(a), a node consists of a transmitter, a high performance main receiver, and a low-power/high-BER WRx. All these components are switched off when they are not in use, and thereby we can save energy at the receiver side. The transmitter is used both for data and WB transissions. In data-transmission mode it may use any suitable modulation technique, while in WB transmission mode it resorts to OOK to allow simple low-power detection at the destination node. All nodes in a network share the same radio resource and transmissions are time duplexed. Figure 1(b) shows the timing diagram of the DCW-MAC for one packet arrival and a network of $N$ nodes. The node that has data available for transmission is called the source node (SN), while the intended receiving node is called the destination node (DN). The remaining $N-2$ nodes are what we call non-destination nodes (NDNs), which are the ones that suffer from the false alarms mentioned in the introduction. Periodic WBs are transmitted by the SN ahead of the data packet to synchronize communication between the SN and the DN. The WRxs of all nodes are switched on periodically, in an asynchronous way, and listen to the channel for WBs. The WBs carry both the SN and DN addresses/identities and this way we can avoid overhearing [1] by the NDNs in the network. If the WRx listening interval coincides with a WB transmission with the correct address and the WB is detected, the receiving node switches on its transmitter to reply with a WB acknowledgment (WACK). Between the transmitted WBs the SN is listening to the channel with its main receiver and, when a WACK is received, data transmission is initiated.

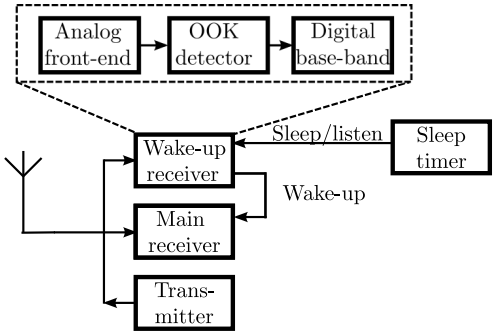


(a) Simplified node architecture block diagram, with control signaling shown. The wake-up receiver is broken down in slightly finer structure.

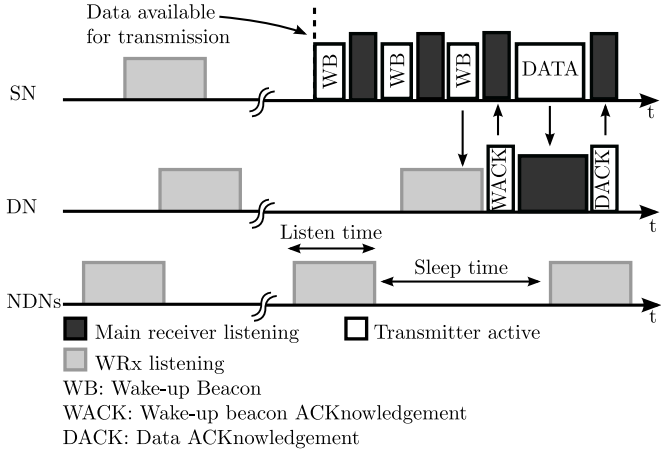


(b) Timing diagram of the DCW-MAC scheme for one packet arrival and a network of $N$ nodes, with one source node (SN), one destination node (DN), and $N-2$ non-destination nodes (NDNs).

**Figure 1:** Sensor node architecture and timing diagram used for the DCW-MAC scheme.

One thing that we need to guarantee is that the listening interval of the WRx can cover a complete WB, despite lack of synchronization. In other words, the WRx needs to listen to the channel long enough so that if it barely misses one WB it still has a chance to capture the next one in the same listen interval. This means that the listening interval has to be longer than twice

the time-extent of the WB plus the time between the WBs. The time between the WBs is assumed to be long enough to contain a WACK packet. Ideally no error is involved in the detection of the WB, but in reality the transmitted WB is corrupted by noise and possibly interference. This leads to imperfections in terms of detection errors and associated energy costs. While we include the above effects in our analysis, we assume that the data packets are rare and far between, so that effects of collisions can be ignored.

## 2.2 Event probabilities and energy costs

As a preparation for the coming analysis of detection errors, let us discuss them in general terms and introduce some of the notation we will use. When we have noise and interference, there is a certain probability that the transmitted WB is missed by the WRx or the WRx accidentally detects a WB that is not there. The latter can happen both when only noise is received or, more likely, when a WB addressed to another node is present on the channel. We will call these events a miss (M) and a false alarm (FA), respectively. The miss event occurs with some probability $P_{\mathrm{M}}^{\mathrm{WB}}$ and generates extra energy consumption in the SN, since additional WBs need to be transmitted before the DN WRx listening time and the SN WB transmission coincide again. The false alarm event happens with a probability $P_{\mathrm{FA}}^{\mathrm{WB}}$ and generates additional energy consumption on the receiver side, since the main transceiver is switched on by the WRx without receiving any data.

The choice of the WB structure as well as the design of the WRx, and the resulting raw BER, highly influence the miss and false alarm probabilities, and consequently the total power consumption of the entire network. For instance, transmission of a long WB may, on the one hand, reduce the miss and false alarm probabilities, and consequently lowers the total energy cost due to WB retransmissions. A long WB, on the other hand, may also increase the consumed power at both SN and WRx DN. The SN needs to transmit longer WBs and the WRx has to both listen for longer periods and be able to process longer sequences. While this type of mechanisms lead to a complex energy analysis, it also allows us to optimize the total energy consumption in a structured way. Our focus in this paper is on deriving the performance of our wake-up scheme, in terms of $P_{\mathrm{M}}^{\mathrm{WB}}$ and $P_{\mathrm{FA}}^{\mathrm{WB}}$, while we illustrate the principle of energy optimization using a simplified energy model.

To be able to analyze the performance of the wake-up scheme we need to find characterizations of the different parts of the WRx, as shown in Fig. 1(a), and provide a more detailed description of the chosen WB structure.

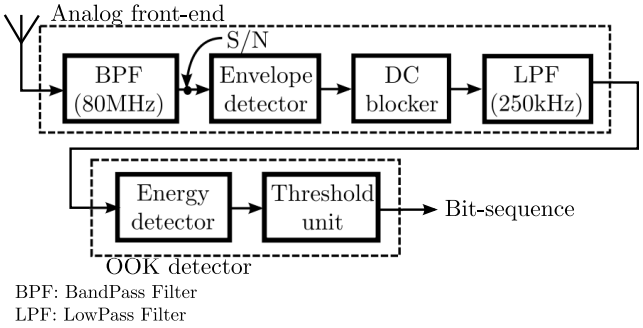


**Figure 2:** Simplified block diagram of the low-power/low-complexity WRx analog front-end (AFE) and On-Off Keying (OOK) detector.

# 3 Front-end and Wake-up Beacon Structure

As we saw in Table 1, different structures are available for design of the analog front-end (AFE) with different characteristics in terms of operating frequency and receiver sensitivity. In these works, different modulation techniques such as OOK, Pulse Position Modulation (PPM), and Frequency Shift Keying (FSK) are used to keep the power consumption of the WRx at a low level. For the analysis in this paper, details like the source of the noise or the choice of the modulation technique is not of prime interest. From a conceptual point of view, as long as the relationship between BER and SNR is known for a certain configuration, the analysis framework of this paper can be applied. Nevertheless, we will use a WRx reference design and characterize its BER vs. S/N performance using simulations.

We have chosen a simple non-coherent OOK modulation for the WB transmission and thereby avoid the use of power-hungry components such as frequency-synthesizer and mixer at the AFE. Figure 2 presents a simplified block diagram of the AFE and OOK detector of the WRx. The RF signal is down-converted to the base-band by an envelope detector. A DC blocker and a low-pass filter follow the envelope detector to filter out the DC component and components at the multiples of carrier frequency, generated by the nonlinear characteristics of the envelope detector. The OOK detector measures the energy content of the incoming signal during one symbol interval and converts the base-band signals to a bit-sequence. As mentioned, the drawback of such a design is a generally poor receiver sensitivity. However, our entire WRx design is based on relaxing the requirements on raw BER and thereby allowing it to operate at the same received power level as the main receiver, in our case -90 dBm [9], thus allowing the same transmit power for WB transmission and

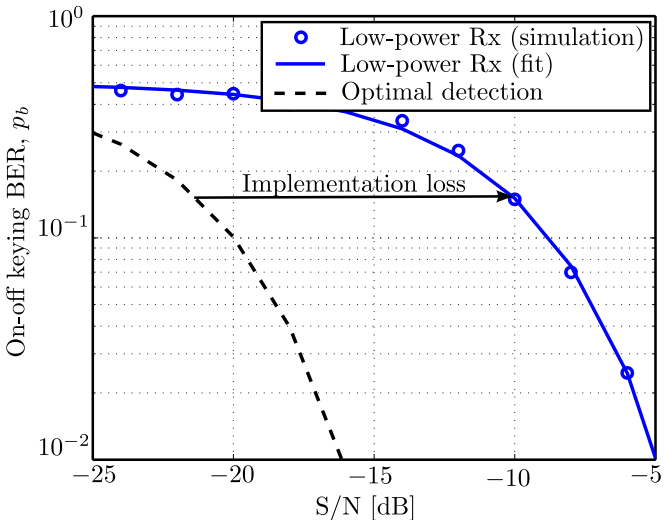


**Figure 3:** BER performance of the WRx analog front-end and OOK detector shown in Fig. 2, for an Additive White Gaussian Noise (AWGN) channel. The S/N is measured directly after the 80 MHz wide band-pass filter, at the input of the envelope detector. As reference, we show the BER performance of an optimal OOK detector, operating on the same signal. This shows that our low-power design has about 11 dB implementation loss.

data. In the following we analyze, by simulation, the performance of the OOK detector and adopt a fitted exponential expression for the BER that later allows us to analytically optimize energy consumption.

## 3.1 OOK detector performance simulation

Figure 3 shows the simulated BER performance for an AFE and OOK detector consisting of the above components and in an Additive White Gaussian Noise (AWGN) channel. The design is tailored to the 80MHz wide 2.4GHz ISM band [9] and, to allow for on-chip integration and ultra-low power consumption, the bandwidth of the first filter (bandpass filter) is chosen as the full 80MHz. We further model the envelope detector by a component that outputs the squared input signal. The bandwidth of the low-pass filter is 250kHz to fit the 250kbps data rate [9]. After simulation we find an analytical expression for the raw

BER $p_b$, by curve fitting,

$$p_b = 0.5\,\mathrm{e}^{-12\,\mathrm{S/N}}, \tag{1}$$

where S/N is the SNR at the input of the envelope detector. At this point it is worth noting that the BER resulting from our AFE and OOK detector follows that of other non-coherent detection schemes in that it is an exponential function of the S/N, while the low SNRs are a result of the 80 MHz wide band-pass filter on the input. Comparing to an optimal OOK detector, operating on the same signal, the implementation loss is about 11 dB. This is the price we pay to reduce the power consumption of the WRx in the range of 20 dB compared to the main receiver [7]. Further, the exponential relationship between BER and S/N in (1) will carry through to our energy analysis and optimization in Section 6, making the results more general and valid for all non-coherent detection schemes with the same type of BER relationship.

Since we have deliberately chosen to operate our WRx at the same received power level as the main receiver sensitivity, we will have to operate at very low SNRs on the input. In our numerical examples we use a nominal raw BER of $p_b = 0.15$, operating at S/N $= -10$ dB. To compensate for these high raw BERs, it is essential to find a WB structure that allows for low-complex/low-power compensation in a digital base-band (DBB) processing.

## 3.2 Wake-up beacon structure

A basic WB, as depicted in Fig. 4, should consist of a *preamble*, a *destination address*, and a *source address*. The $M$-bit preamble sequence, used to detect the presence of a WB and for time synchronization, is selected to be the same for all WBs. The preamble is followed by the $L$-bit destination and source node addresses. The destination address is needed to prevent power-up of other nodes, while the source address is used in the destination address field of the WACK message.

As we mentioned previously, the WB is received by a high BER front-end and nodes are not synchronized. Therefore, to find an accurate starting-point of the WB and to achieve low probabilities of miss and false alarm, the preamble needs to provide both a processing gain and should be selected from sequences with good auto-correlation properties. We have chosen to generate the preamble using maximum-length shift-register sequences ($m$-sequences). An important characteristic of an $m$-sequence is the high peak auto-correlation function while the off-peak values of the auto-correlation function relative to the peak value are small. For the address bits we do not need good auto-correlation properties, but still need a processing gain to compensate for the high BER. Each bit in both the source and destination address fields is therefore

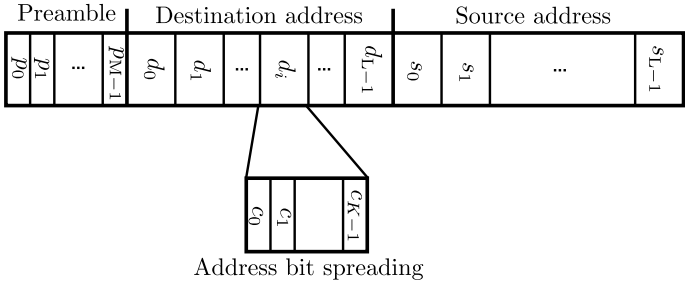


**Figure 4:** Wake-up beacon structure consisting of a length $M$ preamble, and length $L$ destination/source addresses. The address bits are, in turn, spread by a $K$ bit sequence.

spread by an arbitrary $K$-bit code[4]. The total number of bits of both source and destination addresses, when spreading is applied, is $KL$. In this work we select the same spreading, $K$, for both the destination and source addresses. In principle, however, the spreading can be different.

Additional fields can be attached to the WB to carry information such as maximum number of WBs or the next listen interval of the SN WRx [19, 22]. To keep the analysis tractable, we disregard any such fields and focus on how WRx performance is related to the WB parameters $M$, $K$, and $L$.

# 4 Digital Base-band

During the listen interval, the front-end of the WRx delivers its received signal in the form of a bit sequence, with a high raw BER since we operate at lower received power than the sensitivity level. The task of the digital base-band (DBB) is to detect the presence of a WB in this bit sequence. We propose a design, based on the WB structure given above, and develop analytical expressions for the detection performance in terms of the WB detection and false alarm probabilities *per listen interval*.[5] The analytical expressions are later used to analyze the WRx operating characteristic for different design parameters.


**Figure 5:** Block diagram of a detector consisting of a matched filter (MF) and a threshold unit.

## 4.1 Digital base-band design

We use matched filters (MFs) as the main building blocks in our DBB. This is a very common approach to detect known deterministic sequences in noise and binary-input matched-filters can be implemented with very high energy efficiency [21]. The overall operation of a detector unit is illustrated in Fig. 5. The incoming signal is correlated with the known sequence and whenever the output of the MF exceeds a certain threshold, the sequence is declared to be present by the threshold device.

Figure 6(a) illustrates the proposed DBB design consisting of two detector units and an address decoder. The detector units contain a preamble matched filter (PMF) and an address-spreading matched filter (AMF), respectively. Initially the DBB can power up only the PMF and search for the preamble to obtain synchronization, since detecting address bits only makes sense after synchronization is obtained. A WB/preamble may arrive at any random time in the listening interval, which is twice the time-extent of the WB $M + 2\,KL$ plus the time-extent of the WACK message $\delta$. The PMF can catch a complete WB only if the WB arrives at a position $i \in [0 \;\; M + 2\,KL + \delta]$, as shown in Fig. 6(b). Note that, since the WACK is received by the main receiver of the SN, no spreading needs to be applied and therefore the WACK window is short compared to the WB length. To simplify the analysis, we therefore set $\delta = 0$ in the remainder of this paper. With the unknown arrival time $i$ of the WB, the PMF may need to correlate the incoming bit-sequence with all the possible arrival times of the preamble, $i \in [0 \;\; M + 2\,KL]$. The MF stops the correlation whenever the PMF output exceeds the decision threshold and announces that a preamble is detected. After the preamble detection, the AMF and the address decoder are activated and the remainder of the input sequence is fed to the AMF, where the individual address bits are detected by correlating the bit-sequence with the address-spreading. Knowing the position of the preamble,

[4]Even if the choice of spreading code is less critical for the address bits, some sort of pseudo-random code would be used in a real system to avoid a DC level. In our simulations we use m-sequences.

[5]Here we change from using the probability of miss, $P_{\mathrm{M}}^{\mathrm{WB}}$, to using the probability of detection, $P_{\mathrm{D}}^{\mathrm{WB}} = 1 - P_{\mathrm{M}}^{\mathrm{WB}}$, since it will simplify the coming mathematical expressions.

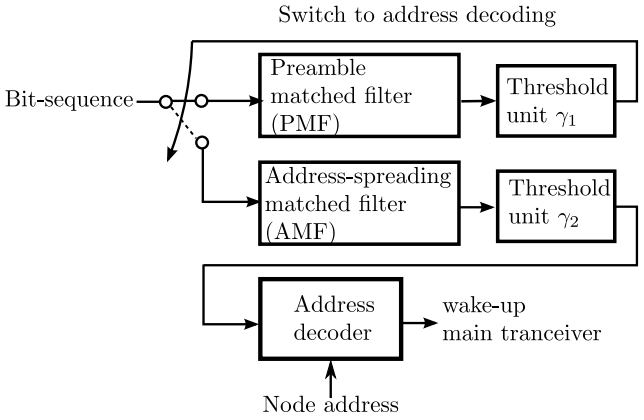


(a) Digital base-band (DBB) block-diagram with a detector for the preamble, a detector for the address bits, and an address decoder.

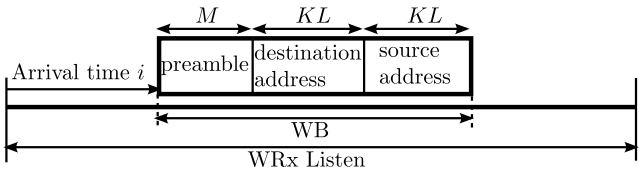


WB length $= M + 2\,KL$
WRx Listen time $= 2\,(M + 2\,KL) + \delta$

(b) Illustration of a wake-up beacon (WB) arriving at time instant $i$ during a WRx listen interval.

**Figure 6:** Block diagram of the proposed WRx digital base-band and an illustration of the arrival of a wake-up beacon during a WRx listening interval.

the positions of the address bits in the sequence are also known. Therefore, the AMF correlation only needs to be performed once per address bit. Finally, the detected bits are collected by an address decoder and compared against the node address. If the detected address bits match the node address, the main transceiver is powered up. With the proposed architecture, the PMF and AMF are identical in all nodes in the network. Only the address decoders need to be programmed with the respective node addresses. This leads to a very flexible WRx design, where the node address-space is easily scaled without any major change of the DBB. For instance, to change a network of 256 nodes

to a network of 8192 nodes, only the size of the address decoder needs to be increased by 5 bits, while the PMF and AMF can remain unchanged.

## 4.2 Detection Performance Analysis

After discussing the overall operation of the DBB, we move on to characterization of the DBB in terms of WB detection and false alarm probabilities. More precisely, the detection probability $P_{\mathrm{D}}^{\mathrm{WB}}$ is defined as the probability of successful WB detection during one channel listening interval, when a WB is indeed transmitted to the DN. The WB false alarm probability $P_{\mathrm{FA}}^{\mathrm{WB}}$ is the probability of detecting either a WB with an incorrect address or a non-existing WB, during a WRx listening interval.

The outline of our analysis is as follows. Our DBB consists of two MF-threshold units with slightly different parameters. Therefore, we first express the detection performance of a generic MF-threshold unit and then use these generic expressions to derive closed form expressions for the WB detection and false alarm probabilities.

Let us assume a binary symmetric channel, where the bit errors at the OOK detector occur independently and with probability $p_b$, for instance given by (1). When the known sequence is present on the channel, the probability $P(n, W)$ that $n$ bits in the sequence of length $W$ are detected correctly, is

$$P(n, W) = \binom{W}{n} (1 - p_b)^n \, p_b^{W-n}. \tag{2}$$

Assuming that the arrival time of the sequence at the MF is known, an MF detects the known sequence correctly with probability

$$\rho^{\mathrm{seq}}(\gamma) = \sum_{n=\gamma}^{W} P(n, W) = \sum_{n=\gamma}^{W} \binom{W}{n} (1 - p_b)^n \, p_b^{W-n}, \tag{3}$$

if the number of correct bits $n$ in the length $W$ sequence is above the threshold $\gamma \in [0, W-1]$. When only noise is present on the channel, the OOK detector generates random bits with equal probability. Using (3), the probability that the MF erroneously detects a non-existing sequence therefore becomes

$$\nu^{\mathrm{seq}}(\gamma) = (\frac{1}{2})^W \sum_{n=\gamma}^{W} \binom{W}{n}. \tag{4}$$

Now, lets continue with the detection performance of the DBB, using the above generic expressions. A WB is declared to be detected only if both the

preamble and the node address are correctly detected. The PMF and AMF outputs used for detection are calculated using different parts of the bit sequence and are therefore independent. Hence, the probability $P_{\mathrm{D}}^{\mathrm{WB}}$ of detecting a WB when it is present on the channel is equal to the product of the respective detection probabilities of the preamble and the address,

$$P_{\mathrm{D}}^{\mathrm{WB}} = P_{\mathrm{D}}^{\mathrm{pre}} P_{\mathrm{D}}^{\mathrm{addr}}, \tag{5}$$

where $P_{\mathrm{D}}^{\mathrm{pre}}$ is the probability that the PMF detects the preamble correctly and $P_{\mathrm{D}}^{\mathrm{addr}}$ is the probability that the address decoder correctly detects the node address. The DBB falsely detects a WB if i) both the preamble and the address code are falsely detected or ii) the preamble is correctly detected, but the address decoder falsely detects an address which belongs to another node. We define the WB interference level, $\alpha$, as the probability that a WB with an incorrect address is present during the WRx listening. The probability $P_{\mathrm{FA}}^{\mathrm{WB}}$ that a WB is falsely detected can therefore be calculated as

$$P_{\mathrm{FA}}^{\mathrm{WB}} = P_{\mathrm{FA}}^{\mathrm{pre}} P_{\mathrm{FA}}^{\mathrm{addr}} + \alpha\, P_{\mathrm{D}}^{\mathrm{pre}} \widetilde{P}_{\mathrm{FA}}^{\mathrm{addr}}, \tag{6}$$

where $P_{\mathrm{FA}}^{\mathrm{pre}}$ is the probability that the PMF falsely detects a non-existing preamble, $P_{\mathrm{FA}}^{\mathrm{addr}}$ is the probability that a non-existing address is erroneously detected as the correct one by the address decoder, and $\widetilde{P}_{\mathrm{FA}}^{\mathrm{addr}}$ is the probability that the address decoder falsely detects an address, which belongs to another node, as its own.

Below we first detail how to calculate the preamble detection performance $P_{\mathrm{D}}^{\mathrm{pre}}$ and $P_{\mathrm{FA}}^{\mathrm{pre}}$ and then turn our attention to the calculation of the node address detection performance in terms of $P_{\mathrm{D}}^{\mathrm{addr}}$, $P_{\mathrm{FA}}^{\mathrm{addr}}$, and $\widetilde{P}_{\mathrm{FA}}^{\mathrm{addr}}$.

When a WB is present on the channel during the WRx listening interval, the preamble detection probability $P_{\mathrm{D}}^{\mathrm{pre}}$ is determined by three factors: i) the probability $f(i)$ that the WB arrives at time $i$, ii) the probability $\rho^{\mathrm{pre}}(\gamma_1)$ of detecting the preamble at the correct arrival time $i$, and iii) the probability $\Omega^{\mathrm{pre}}(\gamma_1, i)$ of no erroneous detection of the preamble before time $i$, where $i \in [0 \;\; M + 2\,KL]$ and $\gamma_1$ is the PMF threshold level. Considering all the possible arrival times of the WB, we get

$$P_{\mathrm{D}}^{\mathrm{pre}}(\gamma_1) = \sum_{i=1}^{M+2\,KL} \left[ f(i)\, \rho^{\mathrm{pre}}(\gamma_1)\, \Omega^{\mathrm{pre}}(\gamma_1, i) \right]. \tag{7}$$

Since the nodes are un-synchronized, the arrival time $i$ of the WB is unknown and it is reasonable to assume that all arrival times are equally likely, *i.e.*,

$$f(i) = \frac{1}{M + 2\,K\,L}, \qquad 0 \le i \le M + 2\,KL. \tag{8}$$

To calculate $\rho^{\mathrm{pre}}(\gamma_1)$, we use (3) and substitute the preamble length $M$ and the threshold $\gamma_1$ for $W$ and $\gamma$. Assuming ideal correlation properties and denoting the probability of a preamble detection at an incorrect time instant by $\nu^{\mathrm{pre}}(\gamma_1)$, the probability $\Omega^{\mathrm{pre}}(\gamma_1, i)$ becomes

$$\Omega^{\mathrm{pre}}(\gamma_1, i) = (1 - \nu^{\mathrm{pre}}(\gamma_1))^{i-1}. \tag{9}$$

To calculate $\nu^{\mathrm{pre}}(\gamma_1)$, we assume that detecting a preamble at incorrect timing is equivalent to detecting a preamble when no data is available on the channel, since we assume ideal auto-correlation properties. Using (4), we substitute the preamble length $M$ and the threshold level $\gamma_1$ for $W$ and $\gamma$. Replacing (8) and (9) back in (7) the preamble detection probability becomes

$$P_{\mathrm{D}}^{\mathrm{pre}}(\gamma_1) = \frac{1}{M + 2\,K\,L}\,\rho^{\mathrm{pre}}(\gamma_1) \sum_{i=1}^{M+2\,KL} (1 - \nu^{\mathrm{pre}}(\gamma_1))^{i-1}. \tag{10}$$

The probability $P_{\mathrm{FA}}^{\mathrm{pre}}$, that the PMF erroneously detects a preamble when no data is available in the listening interval, is equivalent to the probability that the number of random bits that matches the preamble sequence goes above the threshold $\gamma_1$ at least once in the observation interval, *i.e.*,

$$P_{\mathrm{FA}}^{\mathrm{pre}}(\gamma_1) = 1 - (1 - \nu^{\mathrm{pre}}(\gamma_1))^{M+2\,KL-1}. \tag{11}$$

As shown in (6), to calculate the detection performance of the node address, we consider the operation of the AMF together with the address decoder. The probability $P_{\mathrm{D}}^{\mathrm{addr}}$ of detecting an address correctly in the address decoder is equal to the probability that the AMF detects all individual address bits correctly. Since the outputs of the AMF are uncorrelated, being based on different parts of the bit sequence,

$$P_{\mathrm{D}}^{\mathrm{addr}}(\gamma_2) = (\rho^{\mathrm{spcode}}(\gamma_2))^{L}, \tag{12}$$

where $\rho^{\mathrm{spcode}}$ denotes the detection probability of an address bit and is calculated by substituting the spreading code length $K$ and the AMF threshold level $\gamma_2$ for $W$ and $\gamma$ in (3).

When there is no data available on the channel, the AMF generates random address bits. Therefore the probability $P_{\mathrm{FA}}^{\mathrm{addr}}$ that the address decoder falsely announces that the correct address is detected becomes

$$P_{\mathrm{FA}}^{\mathrm{addr}} = (\frac{1}{2})^{L}. \tag{13}$$

Finally, it is likely that a WB which refers to another node is falsely detected. To derive the expression for the probability $\widetilde{P}_{\mathrm{FA}}^{\mathrm{addr}}$, we introduce $q$ which

refers to the number of bits that the nodes own address differs from the address that belongs to another node. Given $q$, the probability $\widetilde{P}_{\mathrm{FA}}^{\mathrm{addr}}$ is expressed as

$$\begin{aligned}\widetilde{P}_{\mathrm{FA}}^{\mathrm{addr}}(\gamma_2) &= \sum_{q=1}^{L}\left[\binom{L}{q}/2^L\ \left(\rho^{\mathrm{spcode}}(\gamma_2)\right)^{L-q}\right. \\ &\quad \left.\left(1-\rho^{\mathrm{spcode}}(\gamma_2)\right)^{q}\right], \end{aligned} \tag{14}$$

where $\binom{L}{q}/2^L$ is the probability that $q$ bits are different in randomly chosen $L$-bit addresses. The second factor is the probability that the AMF detects the $L-q$ matching address bits correctly. The third factor represents the probability that the $q$ non-matching address bits are erroneously detected. We approximate (14) using the fact that errors caused by a single address bit error ($q=1$) are the most likely,

$$\widetilde{P}_{\mathrm{FA}}^{\mathrm{addr}}(\gamma_2) \approx \frac{L}{2^L}\ \left(\rho^{\mathrm{spcode}}(\gamma_2)\right)^{L-1}\ \left(1-\rho^{\mathrm{spcode}}(\gamma_2)\right). \tag{15}$$

The analysis below has been performed using both the exact expressions (14) and the approximation (15), without noticeable differences in the results. For the sake of brevity, we only present expressions based on the approximation.

Substituting (7) and (12) in (5) and (11), (13), (7), and (15) in (6) we can calculate the WB detection and false alarm probabilities. The calculation is a relatively straightforward, but tedious, operation that results in

$$\begin{aligned} P_{\mathrm{D}}^{\mathrm{WB}} &= P_{\mathrm{D}}^{\mathrm{pre}} P_{\mathrm{D}}^{\mathrm{addr}} \\ &= \left(\frac{1}{M+2KL}\rho^{\mathrm{pre}}(\gamma_1)\ \sum_{i=1}^{M+2KL}\left(1-\nu^{\mathrm{pre}}(\gamma_1)\right)^{i-1}\right) \\ &\quad \left(\rho^{\mathrm{spcode}}(\gamma_2)\right)^{L} \\ &= \left[\frac{1}{M+2\,KL}\left(\sum_{n=\gamma_1}^{M}\binom{M}{n}(1-p_b)^n\,p_b^{M-n}\right)\right. \\ &\quad \left.\left(\sum_{i=1}^{M+2\,KL}\left(1-(\frac{1}{2})^M\sum_{n=\gamma_1}^{M}\binom{M}{n}\right)^{i-1}\right)\right] \\ &\quad \left(\sum_{n=\gamma_2}^{K}\binom{K}{n}(1-p_b)^n\,p_b^{K-n}\right)^{L}, \end{aligned} \tag{16}$$

and

$$
\begin{aligned}
P_{\mathrm{FA}}^{\mathrm{WB}} &= P_{\mathrm{FA}}^{\mathrm{pre}} P_{\mathrm{FA}}^{\mathrm{addr}} + \alpha P_{\mathrm{D}}^{\mathrm{pre}} \widetilde{P}_{\mathrm{FA}}^{\mathrm{addr}} \\
&= \left(1 - (1 - \nu^{\mathrm{pre}}(\gamma_1))^{M+2KL-1}\right) (\frac{1}{2})^L + \\
&\quad \alpha \left( \frac{1}{M+2KL} \rho^{\mathrm{pre}}(\gamma_1) \sum_{i=1}^{M+2KL} (1 - \nu^{\mathrm{pre}}(\gamma_1))^{i-1} \right) \\
&\quad \left( \frac{L}{2^L} \left(\rho^{\mathrm{spcode}}(\gamma_2)\right)^{L-1} \left(1 - \rho^{\mathrm{spcode}}(\gamma_2)\right) \right) \\
&= \left[ 1 - \left( 1 - (\frac{1}{2})^M \sum_{n=\gamma_1}^{M} \binom{M}{n} \right)^{M+2KL-1} \right] (\frac{1}{2})^L + \\
&\quad \alpha \left[ \frac{1}{M+2KL} \left( \sum_{n=\gamma_1}^{M} \binom{M}{n} (1-p_b)^n p_b^{M-n} \right) \right. \\
&\quad \left. \sum_{i=1}^{M+2KL} \left( 1 - \sum_{n=\gamma_1}^{M} \binom{M}{n} (1-p_b)^n p_b^{M-n} \right)^{i-1} \right] \\
&\quad \left[ \frac{L}{2^L} \left( \sum_{n=\gamma_2}^{K} \binom{K}{n} (1-p_b)^n p_b^{K-n} \right)^{L-1} \right. \\
&\quad \left. \left( 1 - \sum_{n=\gamma_2}^{K} \binom{K}{n} (1-p_b)^n p_b^{K-n} \right) \right]. \qquad (17)
\end{aligned}
$$

With the above derivations, we have closed form expressions for the WB detection performance. The rest of the paper will focus on verifying the expressions and illustrating how they can be used to analyze and optimize wake-up receiver schemes.

# 5 Receiver Operating Characteristics

The analytical expressions for WRx detection performance were derived for ideal correlation properties, while realistic WBs will have a certain amount of auto-correlation. By performing Monte Carlo simulations in MATLAB, using $m$-sequences both for WB preamble and address spreading we obtain realistic values on WRx performance. By comparing simulated and calculated receiver operating characteristics (ROCs), we both verify the correctness of the analytical derivations and the validity of the ideal-correlation assumptions made. To

enhance understanding of the analytical results, we also discuss the overall influence from parameters such as raw BER, preamble length, address spreading length, and network size.

We simulate the behavior of the entire WRx signal chain, detecting WBs, as specified in sections 3 and 4, for an Additive White Gaussian Noise (AWGN) channel. In the simulation we set the nominal raw BER $p_b$ to 0.15, based on a front-end operating at S/N $= -10$ dB, *cf.* Fig. 3. The length of the preamble $M$ determines the sharpness of the peak at the PMF output and thereby the preamble detection performance, while the address spreading $K$ determines the performance of the address decoding by the AMF. We change the threshold level $\gamma_1 \in [0, M-1]$ of the PMF, both in the simulations and in the analytical expressions, to evaluate the behavior of the WRx for different choices. As the outputs of the AMF are symmetric, the address bit threshold level is set to the midpoint of the range of possible outcomes, $\gamma_2 = \lceil K/2 \rceil$. Figure 7 shows two example ROCs for a WB with a preamble length $M = 63$, address spreading length $K = 15$, and a network of 256 nodes ($L = 8$). The ROCs are for two levels of WB interference, $\alpha = 1$ and $\alpha = 0.1$. The analytical ROCs match the simulated ones well, but there is a small difference that can be seen in the upper right part of the curve with full WB interference $\alpha = 1$. The analytical expressions over-estimate the false alarm probability somewhat in this region of low to medium threshold levels. The best detection probability $P_{\mathrm{D}}^{\mathrm{WB}}$ of 0.97 is achieved for both cases at a decision threshold $\gamma_1$ of 0.76 with a resulting false alarm probability $P_{\mathrm{FA}}^{\mathrm{WB}}$ in the order of $10^{-4} - 10^{-5}$. For lower or higher thresholds $\gamma_1$, the most significant effect on the ROC is the reduced detection probability. For low thresholds we find the incorrect preamble position and for high thresholds we miss the preamble entirely. That the false alarm probability stays below a certain value, less than $10^{-2}$ in this example, for all thresholds is a result of using the destination address to decrease overhearing.

In Fig. 7 we can see clear asymptotic behavior of the analytic ROC for small and large threshold levels. By quantifying these, we simplify the interpretation of how different parameters influence the overall WRx detection performance. For high thresholds $\gamma_1$, the relationship between $P_{\mathrm{D}}^{\mathrm{WB}}$ and $P_{\mathrm{FA}}^{\mathrm{WB}}$ can be approximated as

$$P_{\mathrm{D}}^{\mathrm{WB}} \approx \frac{1}{\alpha} \frac{\rho^{\mathrm{spcode}}}{L(1-\rho^{\mathrm{spcode}})} \, 2^L \, P_{\mathrm{FA}}^{\mathrm{WB}}. \tag{18}$$

The rationale behind the approximation is that at high thresholds $\gamma_1$, we may miss preambles on the channel, but if they are detected it is most likely in the correct position. Further, at high thresholds, it is also very unlikely that we make a false-alarm if there is no preamble on the channel. Therefore (10) collapses to $P_{\mathrm{D}}^{\mathrm{pre}}(\gamma_1) \approx \rho^{\mathrm{pre}}(\gamma_1)$ and (11) to $P_{\mathrm{FA}}^{\mathrm{pre}}(\gamma_1) \approx 0$, which through (5)

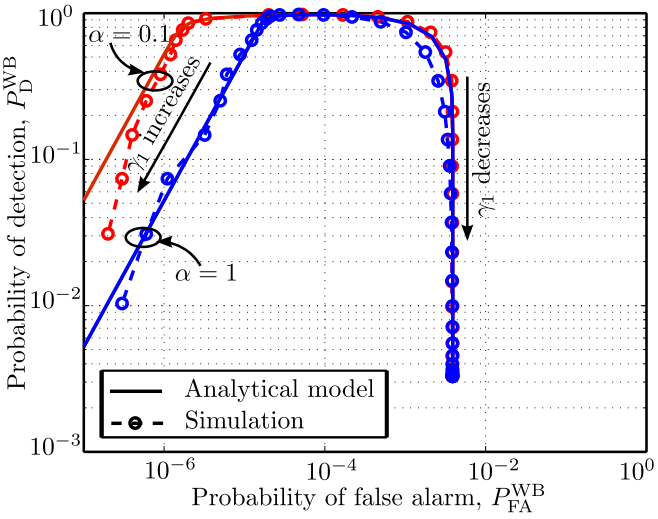


**Figure 7:** Simulated and calculated receiver operating characteristics, ROCs, for a wake-up beacon (WB) with a preamble of length $M = 63$, $L = 8$ bit addresses and address spreading $K = 15$, for two different levels of WB interference, $\alpha = 1$ and $\alpha = 0.1$.

and (6) leads to (18). The scaling factor in (18) depends indirectly on the raw BER and the address spreading length, through $\rho^{\mathrm{spcode}}$, while the size of the node address-space $L$ and the WB interference level $\alpha$ have direct influence.

For low thresholds $\gamma_1$, the false alarm probability is, as we mentioned, upper limited by the use of a destination address in the WB. At very low thresholds the probability $P_{\mathrm{FA}}^{\mathrm{pre}}$ of erroneously detecting a preamble is close to one and the probability of detecting a preamble at its correct position is very low. This essentially leads to entirely random detection of address bits and the probability that the obtained address matches the node address depends only on the size of the address-space – the more address bits, the smaller the probability. In more detail, at low thresholds, (11) collapses to $P_{\mathrm{FA}}^{\mathrm{pre}}(\gamma_1) \approx 1$ and the WB false alarm probability $P_{\mathrm{FA}}^{\mathrm{WB}}$ in (6) can be approximated

$$P_{\mathrm{FA}}^{\mathrm{WB}} \approx (\frac{1}{2})^L. \tag{19}$$

In Fig. 8 we illustrate the principal detection behavior, using the asymptotes (18) and (19), together with corresponding theoretical ROCs. For performance

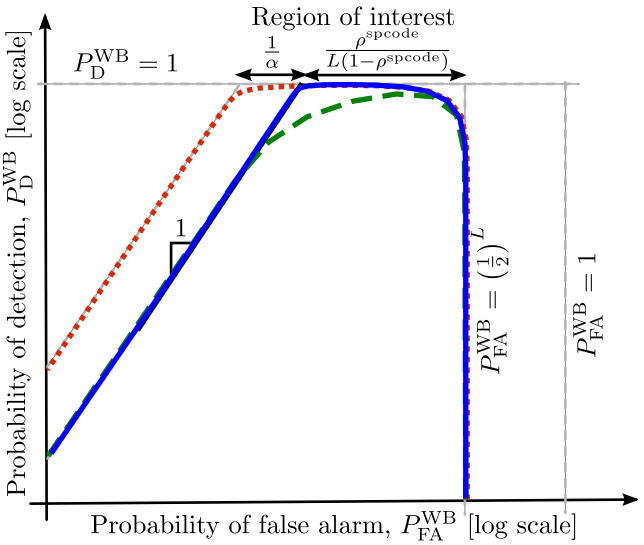


**Figure 8:** Illustration of the general properties of the receiver operating characteristic, ROC, for different design parameters, together with the asymptotes in (18) and (19).

reasons the primary region of interest is where we have high detection probabilities, as indicated in the figure. The nominal design, with full WB interference $\alpha = 1$, is shown as a solid blue line. If, on the one hand, the WB interference level is decreased, $\alpha < 1$, the number of false alarms for high thresholds reduces and the left asymptote is shifted accordingly. As a result, the dotted red ROC curve is obtained and the region of interest increases. If, on the other hand, the detection probability of address bits $\rho^{spcode}$ decreases, we can see in (18) that the false alarm probability for high thresholds increases. As a result, the left asymptote is shifted to the right and the region of interest becomes smaller. Note that a lower $\rho^{spcode}$ is obtained through shorter address spreading $K$ and/or higher raw BER $p_b$, according to (3) with $W = K$. Reducing the number of bits $L$ in the address-space results in higher number of false alarms for both low thresholds and high thresholds and therefore both asymptotes are shifted accordingly. The region of interest, however, increases as compared to the nominal design. If we reduce the preamble length $M$ the asymptotes stay in place, but the detection probability decreases in the region of interest and the dashed green curve is obtained. The detection probability in the region of

interest is also decreased if the raw BER increases[6].

Above we provided a qualitative and quantitative understanding of how different parameters influence the detection performance of the proposed WRx. We have done it by discussing both the full ROC as well as the locations of high- and low-threshold asymptotes.

# 6 Optimal Design Parameters

By combining our detailed understanding of how detection performance of the proposed WRx depends on different system parameters with a cost function we can make optimal system designs. Such a cost function will, for sensor networks, typically reflect energy consumption of individual nodes or of the entire network. Assuming that the cost function $J(\boldsymbol{\theta})$ depends on a number of parameters collected in $\boldsymbol{\theta}$ and the permissible range of parameters is $\mathcal{D}$, the optimal system design is given by

$$\boldsymbol{\theta}_{\text{opt}} = \underset{\boldsymbol{\theta}\in\mathcal{D}}{\text{argmin}} J(\boldsymbol{\theta}). \tag{20}$$

Most relevant cost functions related to energy will indirectly depend on the ROC of the WRx, as derived above, since detection performance has a fundamental impact on energy consumption. Some of these mechanisms were briefly discussed in Section 2.

A comprehensive optimization for an entire network is a very complex task and therefore a topic that needs to be covered separately. Therefore, to illustrate how the ROC expressions can be used for WRx system optimization, we have chosen a simplified case where we are only interested in minimizing the energy used by the source node, SN, to wake up the destination node, DN. When doing this, we also assume that the total energy required at the SN to transmit a WB is proportional to the received WB energy at the DN. The proportionality factor includes transmitter efficiency, propagation losses, etc. These assumptions result in a tractable optimization where we find the optimal WB parameters, preamble length $M$ and address spreading $K$, for different number of address bits $L$ and raw BERs $p_b$.

Our cost function can be expressed in terms of the energy required to transmit a single WB, $E_{\text{WB}}$, and the average number of WBs, $\bar{\eta}$, needed to activate the DN, according to

$$J(\boldsymbol{\theta}) = E_{\text{WB}}(\boldsymbol{\theta})\,\bar{\eta}(\boldsymbol{\theta}), \tag{21}$$

[6]Note: A change in BER also affects the location of the left asymptote, as described above.

where $\boldsymbol{\theta}$ contains WB parameters we optimize, $M$ and $K$. In the sequel we will suppress $\boldsymbol{\theta}$ in our expressions.

With the front-end characteristic from (1) the transmitted/received energy per bit is proportional to $-\ln(2\,p_b)$. As we already indicated in Section 3, this expression will be the same for all non-coherent schemes where the raw BER is an exponential function of the S/N at the receiver input and the following optimization is therefore valid for all schemes in that class. With this proportionality, the total energy needed to transmit a single WB with a length $M$ preamble and two $L$ bit addresses spread by a factor $K$ is

$$E_{\mathrm{WB}} \propto -\ln(2\,p_b)\,(M + 2\,KL). \tag{22}$$

We will not optimize the sleep time of the WRx, as was done in [8], and simply assume a constant activity factor where the listen period is a constant fraction of the entire sleep-listen cycle. Through this, there will always be a fixed number of WBs per sleep-listen cycle, independent of WB length. Therefore, the average number of WBs transmitted before a successful wake-up, $\bar{\eta}$, is proportional to the average number of sleep-listen cycles, i.e.

$$\begin{aligned}\bar{\eta} &\propto 0.5 + P_{\mathrm{D}}^{\mathrm{WB}} \sum_{k=0}^{\infty} k\,(1 - P_{\mathrm{D}}^{\mathrm{WB}})^k \\ &= \frac{1}{P_{\mathrm{D}}^{\mathrm{WB}}} - 0.5,\end{aligned} \tag{23}$$

which is a result of random starting times, due to asynchronous communication, and a probability $P_{\mathrm{D}}^{\mathrm{WB}}$ of detecting the WB during the listen interval. The proportionality factor is the, in our case fixed, number of WBs per sleep-listen cycle.

Replacing (22) and (23) back in (21), the total energy cost becomes

$$J \propto -\ln(2\,p_b)\,(M + 2\,KL)\,\left(\frac{1}{P_{\mathrm{D}}^{\mathrm{WB}}} - 0.5\right). \tag{24}$$

The optimization parameters $M$ and $K$ influence the total energy through two contradicting mechanisms. Increasing $M$ and $K$ will increase the energy required per transmitted WB, while, at the same time, it decreases the number of WB required to activate the DN. The balance between these two mechanisms is what our analytical framework provides, in this case, through (16).

Let us move on to numerical optimization of the preamble length $M$ and address spreading $K$ to minimize the energy cost (24) for different raw BERs $p_b$, for three different sizes of the address-space, namely 4, 8 and 16 address bits. To cover both the reported BERs of the WRx designs in Table 1 and our choice

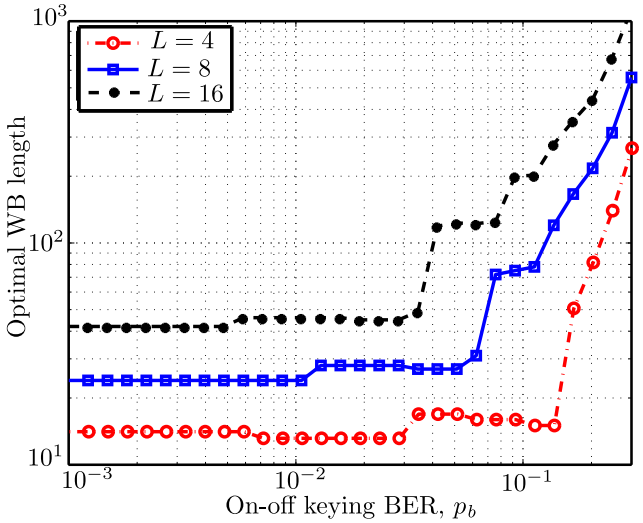


**Figure 9:** Optimal wake-up beacon (WB) length vs. OOK raw BER, for address-spaces of size 4, 8 and 16 bits.

to use low-power/low-performance front-ends, we perform the optimization for BERs from 0.001 to 0.3. For these parameter ranges, with discrete parameter values, we resort to a quite tractable exhaustive search for 30 values on BER between 0.001 and 0.3. Figure 9 shows the optimal WB length, resulting from the optimal choices of $M$ and $K$. At low BERs, there is no address spreading ($K = 1$) and only a short preamble is used to obtain synchronization. When the BER increases beyond a certain point, the WB length increases sharply, since additional WB transmissions due to misses are more costly than increasing the WB length. Both preamble length and address spreading are increasing rapidly, but the influence from increases in address spreading changes are more visible, since its influence on the WB length is magnified by the number of address bits.

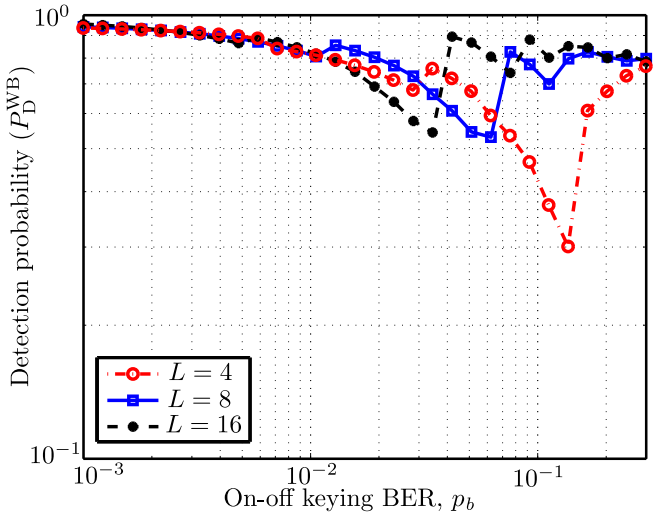


(a) Probability of detection ($P_{\mathrm{D}}^{\mathrm{WB}}$) vs. OOK raw BER.

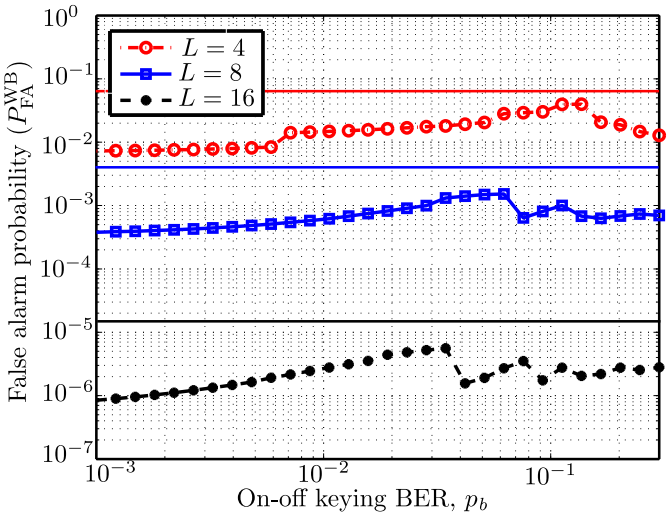


(b) Probability of false alarm ($P_{\mathrm{FA}}^{\mathrm{WB}}$) vs. OOK raw BER. The solid line above each curve is the corresponding upper asymptote (19).

**Figure 10:** Optimal probability of detection and the corresponding probability of false alarm, resulting from the optimization, vs. OOK raw BER, for address-spaces of size 4, 8 and 16 bits.

It is quite natural that increasing BERs lead to longer WBs, in general terms, since detection of them becomes increasingly difficult. However, the relationship between BER and optimal WB length is more intricate than that. Perhaps somewhat counter-intuitively, there are also examples of increasing BERs leading to shorter optimal WB-length. Several examples of this can be seen in Fig. 9, especially for the 4-bit address case where the shorter WB lengths make them more visible. In these cases, even if shorter WBs mean lower detection probability and a higher average number of WBs need to be transmitted, the total cost becomes smaller for a shorter WB since it requires less transmission energy.

The cost function we are using in this paper measures the required transmit energy and, as such, it only depends on the detection probability part of the ROC. The detection probabilities resulting from the optimization are shown in Fig. 10(a). The detection probability has a tendency to decrease with increasing BERs, but adjustments of WB length in the optimization brings it back up again when this is favorable from a transmission energy point of view. The largest variations can be seen in the transition regions of BERs where the WB length starts to increase rapidly, as we observed in Fig. 9. The generally shorter WBs for smaller address spaces also lead to the fact that transmission of additional WB due to a miss in the WRx is less costly. Hence, we see that lower detection probabilities can be optimal, from a transmit energy point of view, for smaller address spaces.

False alarm probabilities do not influence our cost function, but the ROC relation implicitly gives us certain false alarm values. These are related to other energy costs in the network, due to unnecessary wake-ups. It is therefore of interest to study these probabilities as well. The false alarm probabilities resulting from the optimization are shown in Fig. 10(b). We can see that they are about 5-10 times lower than the upper asymptote (19) we derived for the ROC (solid line above each curve). For reasonably large address-spaces, the false alarm rates are at very low levels and unnecessary wake-ups should not have a large impact on the total energy consumption of the network. A detailed analysis of these influences is both non-trivial and requires more detailed and complete information about how energy consumption relates to the optimization parameters. While important, this analysis is beyond the scope of this paper.

Finally, let us study the optimal transmission energy cost, per wake-up, as a function of raw BER. Since we only know the energy cost up to proportionality, as detailed in (24), we present the normalized optimal WB transmit energies in Fig. 11, for the three investigated address-space sizes. The normalization is with respect to the minimal energy cost for the smallest, 4-bit, address space. For all three address-spaces, we can see that the $10^{-3}$ BER used as a reference

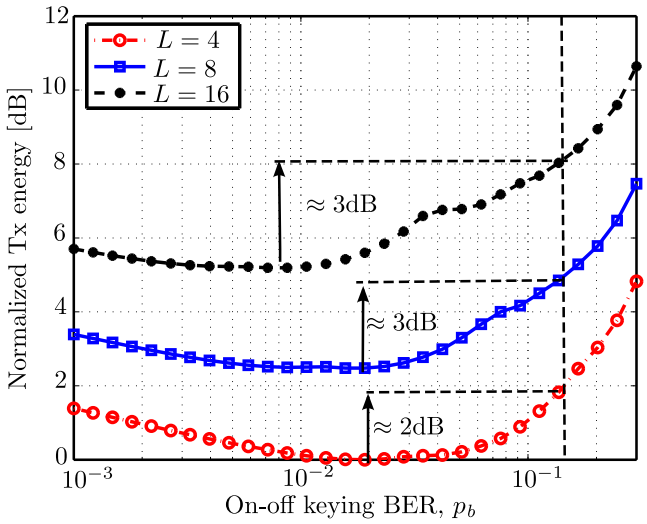


**Figure 11:** Optimal wake-up beacon (WB) transmit energies, per wake-up, for different raw BERs and address-spaces of size 4, 8 and 16 bits. Energies are normalized to the minimal energy for the smallest 4-bit address space.

level in previous studies, *cf.* Table 1, is not the optimal point of operation when using the duty-cycled wake-up scheme studied in this paper. The optimal BER is closer to $10^{-2}$ for all three address-spaces and larger address-spaces tend to have a slightly lower optimal BER. When raw BER is lower than the optimal one, the increased transmit power required to lower the BER is larger than the corresponding shortening of the WB, resulting in a higher total energy cost. The differences are, however, quite small.

Since we aim at using the same transmitter and the same transmit power both for data and wake-up, our low-complexity/low-power WRx will operate at high raw BERs, and in this context the most interesting part of the energy curves is at high BERs. The nominal BER in our WRx design is therefore set to 0.15 , as discussed in Section 3, and the additional Tx energy cost as shown in Fig. 11 is only around 2-3 dB. This relatively small additional cost in transmit energy for the SN should be compared to the roughly two orders of magnitude power savings estimated on the WRx side for all nodes in the network.

# 7 Conclusions and Remarks

The goal of this paper has been to provide an analysis framework for duty-cycled low-complexity/low-power wake-up receiver schemes, which can be used for design optimization. We perform a complete system-level analysis based on a proposed wake-up beacon structure and the corresponding WRx architecture. The analysis first leads to closed form expressions for detection and false alarm probabilities, as well as qualitative and quantitative understanding of how detection performance relates to changes in design parameters. This understanding of detection performance is fundamental to system-level analysis and optimization of energy consumption. Such an optimization can be done in many different ways, depending on what the ultimate goal is. For instance, it is quite possible to minimize the total power consumption of an entire network, given that we have access to detailed enough information about how energy consumption is related to different design parameters. With limited space we chose to focus on how the detection performance expressions can be used for an optimization of wake-up beacon transmit energy. This means that the presented optimizations are only related to the transmit energy of the source node. While somewhat limited in its scope, the optimization led to several important observations regarding the transmit energy required to successfully activate a destination node. The trade-off between increasing transmit power and the use of longer beacons becomes evident and a combination of both is required to minimize transmit power. Based on a specific analog front-end and OOK detection scheme, we also showed that the obtained optimization results are more general and valid for all schemes with an exponential relationship between signal-to-noise ratio and bit-error rate.

In more detail, our analysis shows that it is quite possible to use duty-cycled low-complexity/low-power wake-up receivers, with roughly two orders of magnitude less power consumption in the WRx of all nodes in the network, while allowing the transmitter to use the same transmit power for both wake-up beacons and data. To achieve this, at our chosen nominal raw BER of 0.15, we need to transmit longer beacons than those that give minimal transmit energy. The increase in transmit energy per wake-up is, however, quite moderate at a level of about 2-3 dB for the studied address-space sizes and only applies to the source node.

While analysis and optimization of wake-up beacon transmit energy is performed in detail in this paper, the true value of the analysis framework is that it can be used as a basis for detailed studies and optimization of the energy consumption of entire networks, where other energy models are used. The nature, level of detail, and the particular energy costs taken into account in these depend on the intended application. The analysis framework should also be

used to extend the optimization beyond parameters used in this paper. One such example is finding the optimal sleep/listen cycle, along the lines of [8].

Other interesting extensions of the analysis framework is to include more realistic channel models and interference scenarios. As long as we know the relation between SNR and the raw BER on our channel, we can apply the analysis performed in this paper. The only modification needed is to replace (1) with the particular relationship applying to the analyzed channel. While self-interference from the own network is included in the presented analysis, more generic interference types can be included by either adjusting the noise level in the BER expressions or providing a more detailed interference analysis where the properties of the interference signals are more realistic.

# Bibliography


[1] Y. Wei, J. Heidemann, and D. Estrin, "An energy-efficient MAC protocol for wireless sensor networks," in *Proceedings IEEE INFOCOM.*, 2002, pp. 1567–1576 vol.3.

[2] M. Buettner, G. V. Yee, E. Anderson, and R. Han, "X-MAC: a short preamble MAC protocol for duty-cycled wireless sensor networks," in *ACM SenSys.*, 2006, pp. 307–320.

[3] S. Mahlknecht and M. Bock, "CSMA-MPS: A minimum preamble sampling MAC protocol for low power wireless sensor networks," in *Proceedings IEEE International Workshop on Factory Communication Systems.*, 2004, pp. 73–80.

[4] M. Lont *et al.*, "Analytical models for the wake-up receiver power budget for wireless sensor networks," in *IEEE GLOBECOM*, 2009, pp. 1146–1151.

[5] C. Guo, L. C. Zhong, and J. Rabaey, "Low power distributed MAC for ad hoc sensor radio networks," in *IEEE GLOBECOM*, vol. 5, 2001, pp. 2944–2948.

[6] Y. Zhang, L. Huang, G. Dolmans, and H. de Groot, "An analytical model for energy efficiency analysis of different wakeup radio schemes," in *IEEE PMIRC*, 2009, pp. 1148–1152.

[7] E.-Y. Lin, J. Rabaey, and A. Wolisz, "Power-efficient rendez-vous schemes for dense wireless sensor networks," in *IEEE International Conference on Communications*, vol. 7, 2004, pp. 3769–3776.

[8] N. S. Mazloum and O. Edfors, "DCW-MAC: An energy efficient medium access scheme using duty-cycled low-power wake-up receivers," in *IEEE VTC Fall*, 2011, pp. 1–5.

[9] H. Sjöland *et al.*, "A receiver architecture for devices in wireless body area networks," *JETCAS*, vol. 2, pp. 82–95, 2012.

[10] X. Yu, J.-S. Lee, C. Shu, and S.-G. Lee, "A 53$\mu$W super-regenerative receiver for 2.4 GHz wake-up application," in *IEEE APMC*, 2008, pp. 1–4.

[11] N. M. Pletcher, S. Gambini, and J. Rabaey, "A 52$\mu$W wake-up receiver with $-$72dBm sensitivity using an uncertain-IF architecture," *IEEE J. Solid-State Circuits*, vol. 59, pp. 269–280, 2009.

[12] S. Drago, D. Leenaerts, F. Sebastiano, L. J. Breems, K. A. Makinwa, and B. Nauta, "A 2.4GHz 830pJ/bit duty-cycled wake-up receiver with $-$82dBm sensitivity for crystal-less wireless sensor nodes," in *IEEE ISSCC*, 2010, pp. 224–225.

[13] M. Lont, D. Milosevic, A. van Roermund, and G. Dolmans, "Ultra-low power FSK wake-up receiver front-end for body area networks," in *RFIC*, 2011, pp. 1–4.

[14] X. Huang, S. Rampu, W. X., G. Dolmans, and H. de Groot, "A 2.4GHz/915MHz 51$\mu$W wake-up receiver with offset and noise suppression," in *ISSCC*, 2010, pp. 222–223.

[15] T. Copani, S. Min, S. Shashidharan, S. Chakraborty, M. Stevens, S. Kiaei, and B. Bakkaloglu, "A CMOS low-power transceiver with reconfigurable antenna interface for medical implant applications," *IEEE Transactions on Microwave Theory and Techniques*, vol. 59, pp. 1369–1378, 2011.

[16] N. Pletcher, S. Gambini, and J. Rabaey, "A 65$\mu$W, 1.9GHz RF to digital baseband wakeup receiver for wireless sensor nodes," in *IEEE CICC*, 2007.

[17] F. Raab, P. Asbeck, S. Cripps, P. Kenington, Z. Popovic, N. Pothecary, J. Sevic, and N. Sokal, "Power amplifiers and transmitters for RF and microwave," *IEEE Transactions on Microwave Theory and Techniques*, vol. 50, no. 3, pp. 814–826, 2002.

[18] R. de Francisco and Y. Zhang, "An interference robust multi-carrier wake-up radio," in *IEEE WCNC*, 2011, pp. 1265–1270.

[19] Y. Zhang, S. Chen, N. F. Kiyani, G. Dolmans, J. Huisken, B. Busze, P. Harpe, N. van der Meijs, and H. de Groot, "A 3.72$\mu$W ultra-low power digital baseband for wake-up radios," in *IEEE VLSI-DAT*, 2011, pp. 1–4.

[20] C. Hambeck, S. Mahlknecht, and T. Herndl, "A 2.4$\mu$W wake-up receiver for wireless sensor nodes with -71dbm sensitivity," in *IEEE International Symposium on Circuits and Systems (ISCAS)*, 2011, pp. 534–537.

[21] N. S. Mazloum, J. N. Rodrigues, and O. Edfors, "Sub-Vt design of a wake-up receiver back-end in 65nm CMOS," in *IEEE SubVT*, 2012, pp. 1–3.

[22] F. Herrmann, A. Manjeshwar, and J. Hill, "Protocol for reliable, self-organizing, low-power wireless network for security and building automation system," 2003, WO Patent 2,003,061,176.

# *Paper III*

# Duty-cycled Wake-up Receivers and Single-hop Wireless Sensor Network Energy optimization

**In sensor network applications with low traffic intensity, idle channel listening is one of the main sources of energy waste. The use of a dedicated low-power wake-up receiver (WRx) which utilizes duty-cycled channel listening can significantly reduce idle listening energy cost. We present a system analysis and parameter optimization for a Duty-Cycled Wake-up receiver Medium Access Control (DCW-MAC) scheme. First we introduce a framework for analysis of energy consumption of an entire single-hop network. The analysis framework is used to find optimal wake-up beacon and protocol parameters for different WRx performance characteristics to minimize total network energy consumption per data packet. Optimization is performed for scenarios with and without requirements on average delay and optimal parameters are further used to evaluate DCW-MAC energy consumption and resulting communication delays. The importance of the optimization is that it provides information on how much we can save in terms of energy in an entire network by choosing a WRx with a certain reduction in power consumption and associated loss of performance, compared to the main receiver. We also present accurate and easy to calculate approximations of both optimal energy savings and resulting delays.**

---

Nafiseh Seyed Mazloum and Ove Edfors,
"Duty-cycled Wake-up Receivers and Single-hop Wireless Sensor Network Energy optimization,"
under review for possible publication in *IEEE Transactions on Wireless Communications*.

# 1 Introduction

Energy optimization of wireless sensor networks (WSNs) is becoming increasingly important with more connected devices, as envisioned for the Internet of Things. In this work we optimize single-hop WSNs with low traffic intensity, where idle channel listening is a major source of energy waste. Several communication strategies to reduce the cost of idle listening have been proposed, e.g., [1–12]. One approach is to introduce an ultra low-power wake-up receiver (WRx) dedicated for continuous channel monitoring, as in [8], which we refer to as an Always-On WRx scheme. This reduces the energy cost of idle listening, since the main receiver only has to be powered on when data is available on the channel. Another important approach is to employ asynchronous duty-cycled listening, e.g., X-MAC [3], CSMA-MPS [9], and TICER [11], where nodes wake up periodically, without using energy consuming time-synchronization. By adding duty-cycling to low-power WRx schemes, we can potentially save even more energy. First steps in this direction were taken in [13], a more complete concept was introduced as duty-cycled wake-up receiver medium access control (DCW-MAC) in [14], and followed up by an analysis of DCW-MAC detection-error performance in [15]. In this work we substantially extend [14] and [15] by performing a complete energy analysis and parameter optimization, under simplified network and traffic conditions, to find the achievable energy savings when using DCW-MAC. Our main contribution is a structured energy optimization of a new MAC scheme, through which we provide analytical expressions for, and approximations of, optimal energy performance.

Our approach is different from most other attempts at analyzing energy consumption in sensor networks, in the sense that we perform optimization for entire ranges of parameter choices and therefore obtain more general results. Most analytical studies and optimization of duty-cycled MAC schemes address scenarios where no dedicated WRx is used [3,16,17]. Analytical studies addressing Always-On WRx schemes mostly focus on comparing performance of these schemes to duty-cycled ones, for certain hardware parameters [18, 19]. None of these studies address a combined solution where both protocol parameters and WRx design characteristics are analyzed and optimized together.

In Section 2 we prepare for the energy analysis by introducing the inner workings of DCW-MAC, calculating basic error events influencing energy consumption, and establishing a simple model capturing low-power WRx characteristics. Calculation of energy consumption and average communication delay is detailed in Section 3, where we develop an analysis framework for DCW-MAC. We also describe how two reference schemes, X-MAC [3] and Always-On WRx-MAC [8], which we later compare against, can be analyzed in the same framework. Resulting energy and delay expressions depend on MAC protocol

properties, WRx design characteristics, network size and traffic intensity. In Section 4 we specify a wake-up beacon (WB) structure, based on [20], connecting WB parameters and WRx characteristics to energy consumption through analytical expressions for detection-error events. This enables joint optimization of MAC protocol parameters, minimizing energy consumption in a given scenario. The resulting non-linear mixed-integer optimization problem is stated and a simple strategy for finding the global optimum, both with and without requirement on delay, is described. An evaluation of energy-optimal DCW-MAC designs is done in Section 5. Using numerical examples we show how optimal duty-cycling and resulting energy savings, compared to optimized reference schemes, depend on network size, traffic conditions and WRx characteristics. Performing the analysis for ranges of WRx characteristics, we establish requirements on their design when used in DCW-MAC schemes. Observations made this far allow us to derive simple approximations of optimal results, in Section 6, making it possible to evaluate and perform parts of an optimal DCW-MAC design without time-consuming numerical optimizations. Final conclusions and remarks are provided in Section 7.

## 2 System and Protocol Description

The DCW-MAC is developed with a particular node reference design in mind, described in [14,15] and shown in Fig. 1(a). This design consists of a sleep timer, a wake-up receiver/WRx, a transmitter, and a main receiver. To save power, the WRx typically needs to operate at a power level two orders of magnitude below the main receiver [8], which typically means sacrificing performance [10, 21–28]. To model this in more detail, we assume that the WRx characteristics can be reduced to two parameters: its power consumption and performance loss, relative to the main receiver. Relative WRx power consumption is defined as

$$R^{wrx} = \frac{P^{wrx}}{P^{mrx}}, \tag{1}$$

where $P^{wrx}$ and $P^{mrx}$ are the WRx and main receiver power consumptions, respectively. Relative performance can be characterized in different ways. Here we assume that both receivers follow the same type of BER expression, which depends on the modulation type, and associate any performance difference to a shift in signal-to-noise ratio (SNR) that we call implementation loss of the WRx. Bit-error probabilities of the two receivers, at equal SNR after the receiving antenna, become

$$p_b^{mrx} = \mathrm{BER}(\mathrm{SNR}), \text{ and } \quad p_b^{wrx} = \mathrm{BER}(\mathrm{SNR}/L_{impl}), \tag{2}$$

where BER(·) is the bit-error characteristics of the main receiver for the chosen modulation scheme, SNR the signal-to-noise ratio on the receiver input, and $L_{impl}$ the implicitly defined implementation loss of the WRx. While both $R^{wrx}$ and $L_{impl}$ are defined in linear scale, we often use dB scale in our text. This condensed WRx performance characterization is an important corner-stone of the analysis performed later in this paper.

The high-level operation of a sensor node is shown as a state diagram in Fig. 1(b). Both transmitter and main receiver are switched off when not engaged in active communication. A node only periodically switches on its low-power WRx to listen for a WB in the duty-cycling (DC) mode. The high-performance main receiver and the transmitter are only switched on when data packets are expected to be received, in receive (RX) mode, or when data is available for transmission, in transmit (TX) mode. Compensation for the WRx implementation loss can, in principle, be done by increasing power when WBs are transmitted. However, since we are addressing low-power nodes, where simplicity is important, we assume that a single transmitter chain is used with the same transmit power for both data and WBs[7]. Before we move on, let us define some important naming conventions and describe DCW-MAC protocol details.

In a network of $N$ nodes, the one that has data available for transmission is called the source node (SN) and the intended receiving one the destination node (DN). The remaining $N-2$ nodes are called non-destination nodes (NDNs). When analyzing energy consumption, we need to analyze all three types of nodes. We assume a symmetric single-hop network where all nodes are equal and communication takes place directly between pairs of nodes. More advanced schemes, including e.g. multi-hop, may be used but are not considered in this work. Data packet arrivals follow a Poisson process with exponentially distributed inter-arrival times with an average of $1/\lambda$ seconds. Data packet transmission takes $T_{data}$ seconds and, in our ultra-low power scenario, we assume rare packets in the sense that average inter-arrival time is much longer than packet length ($1/\lambda \gg T_{data}$). Under these assumptions we ignore any energy consumption resulting from collisions in the transmission, allowing us to make tractable analytical derivations of optimal sleep and listen times for the analyzed protocols.

Fig. 2 shows a communication timing diagram of the DCW-MAC for one average packet inter-arrival time and a network of $N$ nodes. For detailed specification of variables in the figure, see Table 1. The principle of data transmission between SN and DN is as follows. Whenever the SN has data to transmit, the transmitter is set up and transmits periodic WBs to the DN, similar to the

[7]By using separate variables for data and WB transmit powers the analytical framework in this paper also covers the general case. This is, however, beyond the scope of the paper.

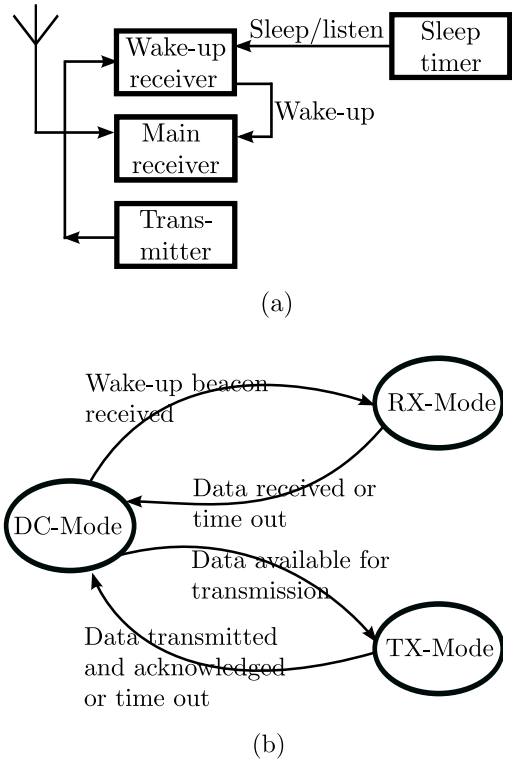


**Figure 1:** (a) Simplified node architecture block diagram, with signaling in listen/receive mode shown. (b) State-transition diagram of overall operation of a node for the DCW-MAC scheme.

X-MAC scheme. These WBs carry both SN and DN addresses to avoid overhearing by NDNs [1]. Ideally, if transmission of a WB coincides with a DN listen interval, the DN WRx detects the WB and switches on its transmitter to reply with a wake-up acknowledgment (WACK). After transmitting a WB, the SN switches to receive mode to listen for the WACK. If a WACK is received, the SN initiates data transmission, whose reception is then acknowledged by the DN in a data acknowledgment (DACK). The number of WBs that need to be transmitted before the DN switches on its WRx depends on the relative timing of data available for transmission at the SN and the DN listen time intervals. We need to guarantee that the WRx listen interval can cover one full WB. In other words, the WRx needs to listen long enough so that barely

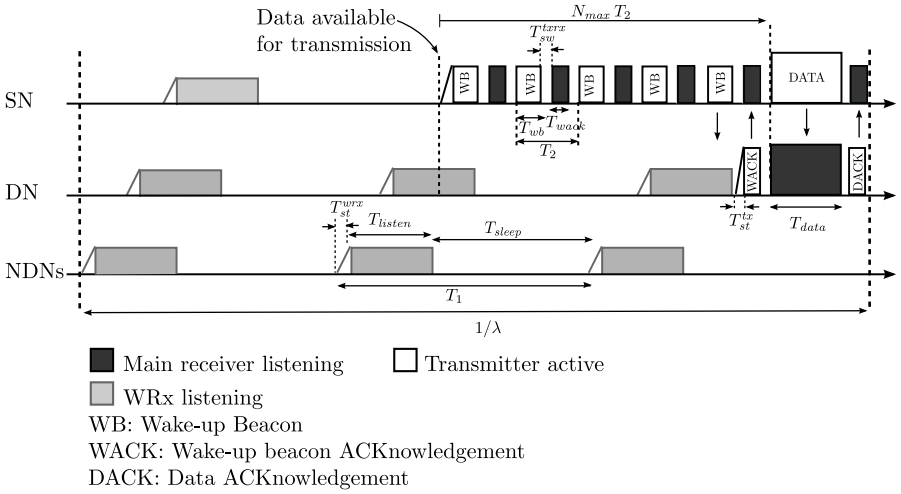


**Figure 2:** Timing diagram of DCW-MAC for one average packet inter-arrival time and a network of $N$ nodes, with one source node (SN), one destination node (DN), and $N-2$ non-destination nodes (NDNs).

missing one WB still allows the next one to be heard in the same listen interval. Through this the WB length impacts listen interval length and total power consumption.

An ideal behavior assumes that there are no errors involved in reception of WBs, data packets, or acknowledgments. In a realistic scenario, however, there will be certain probabilities that transmitted packets are missed by the receiver or non-existing packets are erroneously detected. We call these events miss (M) and false-alarm (FA), respectively. Both incur additional energy consumption, but in different ways depending on the packet type affected. Severity of the energy cost also depends on the energy/power consumption of the parts of the circuits affected. Below we prepare for our calculation and minimization of energy consumption by providing basic calculations of error event probabilities. Some error events are fundamental in the sense that they do not depend on other error events. To begin with, we assume they are known.

## 2.1 DC mode error events

In the DC-mode, two types of error may occur: i) the WRx may miss a WB transmitted to it or ii) it may falsely detect a non-existing WB. The latter can happen both when only noise is received or, more likely, when a WB addressed

to another node is present on the channel. Both WB miss and false-alarm are fundamental and occur with probabilities $p_M^{wb}$ and $p_{FA}^{wb}$, respectively.

## 2.2 TX and RX mode error events

In the TX- and RX-Modes, all error events are combinations of other types of events and of the *miss* type, quantifying misses in a packet/acknowledgment exchange. A miss occurs if the acknowledgment is not received, which happens if the packet itself is missed, or if the packet is received, but the acknowledgment is missed. Its probability is calculated

$$p_M^{pkt,ack} = p_M^{pkt} + (1 - p_M^{pkt})\, p_M^{ack}, \tag{3}$$

where $p_M^{pkt}$ and $p_M^{ack}$ are the probabilities of missing a transmitted packet, and a transmitted acknowledgment, respectively.

In the TX-Mode we have one error event where a WB is transmitted, but a WACK is not received (under the assumption that the WB is transmitted during a listening period of the DN), and another where a data packet is transmitted but a DACK is not received. Using (3), the probabilities of these two become

$$p_M^{wb,wack} = p_M^{wb} + (1 - p_M^{wb})\, p_M^{wack}, \text{and} \tag{4}$$

$$p_M^{data,dack} = p_M^{data} + (1 - p_M^{data})\, p_M^{dack}, \tag{5}$$

where the fundamental error event probabilities involved are $p_M^{wb}$, the probability of missing a transmitted WB during a channel listen interval, $p_M^{wack}$, $p_M^{data}$ and $p_M^{dack}$, the probabilities of missing a transmitted WACK, a transmitted data and a transmitted DACK, respectively.

In the RX-Mode we only have one such error event, that a WACK is transmitted (as an acknowledgment of a received WB), but no data is received[8]. The probability of this miss is, again using (3), calculated as

$$p_M^{wack,data} = p_M^{wack} + (1 - p_M^{wack})\, p_M^{data}, \tag{6}$$

where the fundamental error event probabilities are $p_M^{wack}$ and $p_M^{data}$, the probabilities of missing a transmitted WACK and a transmitted data packet, respectively.

The ultimate energy consumption of the nodes depends heavily on the probabilities of these error events.

[8]The packet/acknowledgment terminology is somewhat reversed here, but the mechanism is exactly the same.

# 3 Energy and Delay Analysis

We now present analytical models of energy consumption and average communication delays, for the DCW-MAC scheme addressed above. For reference, we use the same analytical framework to compare DCW-MAC to two other low-power MAC protocols: i) the Always-On WRx-MAC, where the WRxs monitor the medium continuously and ii) X-MAC, where the main receiver acts as a duty-cycled WRx. The DCW-MAC energy models are then used to find the jointly optimal sleep times and WB parameters, for different WRx characteristics and communication scenarios. The measure we use is average energy consumption per packet for an entire network of $N$ nodes[9]. The total SN, DN, and NDN energy consumption becomes

$$E = E^{SN} + E^{DN} + (N-2)E^{NDN}. \tag{7}$$

For notational convenience we assume that there is a base-level power consumption for all the nodes, the sleep power $P^{sleep}$, below which the node power consumption cannot go. The base-level energy per packet then becomes $P^{sleep}/\lambda$ and all other energy figures are added to this base level. The additional power consumption, when a node is not sleeping, depends on the state of operation and part of the node being active. The energy consumed in a certain *part* of the node when in a certain *state* can be written $E^{part}_{state} = P^{part}_{state} T^{part}_{state}$, where $P^{part}_{state}$ and $T^{part}_{state}$ are the corresponding power consumption and time spent in that state. When both the *state* of operation and the active *part* are the same, we simplify notation to $P^{part}$ and $T_{state}$. Power consumption and time interval parameters, needed in the energy analysis, are listed and briefly explained in Table 1. Nominal values are based on measurement results and assumptions from the *Ultra-portable devices* project [29,30] at the Department of Electrical and Information Technology, Lund University, and will be used in the numerical optimizations in Section 4.2. For simplicity, we assume that switching powers and times are equal, making switching energies equal. The upcoming results depend mainly on relative power consumptions, we therefore introduce two more variables for relative power consumptions, $R^{sleep}$ and $R^{tx}$, in the table. Let us start detailing the calculations of energy and delay for the DCW-MAC scheme and later reformulate them for the X-MAC and Always-On WRx, as special cases.

[9] Energy consumption per packet per node is easily calculated by dividing the total energy consumption by $N$.

**Table 1:** System parameters

| **Radio parameter** | **Variable** | **Nominal values** |
|---|---|---|
| Main receiver power (reference) | $P^{mrx}$ | 1 mW |
| Sleep power | $P^{sleep} = R^{sleep} P^{mrx}$ | 0.5 $\mu$W |
| Transmit power | $P^{tx} = R^{tx} P^{mrx}$ | 1 mW |
| Wake-up receiver power | $P^{wrx} = R^{wrx} P^{mrx}$ | 0.05 mW |
| Transmitter/main receiver set-up power | $P_{st}^{tx} = P_{st}^{mrx}$ | 0.5 mW |
| Wake-up receiver set-up power | $P_{st}^{wrx}$ | 0.01 mW |
| Switch power | $P_{sw}^{txrx} = P_{sw}^{rxtx}$ | 1 mW |
| Wake-up receiver implementation loss | $L_{impl}$ | 7 dB |
| Transmitter/main receiver set-up time | $T_{st}^{tx} = T_{st}^{mrx}$ | 1 ms |
| Wake-up receiver set-up time | $T_{st}^{wrx}$ | negligible |
| Switch time | $T_{sw}^{txrx} = T_{sw}^{rxtx}$ | 5 $\mu$s |

| **Protocol parameter** | **Variable** | **Nominal values** |
|---|---|---|
| No. of address bits | $L$ | 4, 8, 16 |
| Raw channel bit time | $T_b$ | 4 $\mu$sec. |
| WACK/DACK time | $T_{wack} = T_{dack}$ | $(9 + 2L)\, T_b$ [10] |
| Data transmission time | $T_{data}$ | 4 ms |
| Wake-up receiver listen interval | $T_{listen}$ | (opt. param.) |
| Node sleep time | $T_{sleep}$ | (opt. param.) |
| Wake-up beacon duration | $T_{wb}$ | (opt. param.) |
| **Transmission** | **Modulation** | |
| Data/acknowledgment | FSK | |
| Wake-up beacon | OOK | |

## 3.1 DCW-MAC

In the DCW-MAC scheme, Fig. 1(b), the node always duty cycles unless the WRx detects a WB or a data packet is available for transmission. To assist derivation of energy expressions, we use the communication timing diagram in Fig. 2 and the notation in Table 1. In (7) the average energy consumption of the SN and the DN, per packet, are

$$E^{SN} = \frac{P^{sleep}}{\lambda} + E_l^{SN} + E_{TXMode}^{SN}, \text{ and} \tag{8}$$

$$E^{DN} = \frac{P^{sleep}}{\lambda} + E_l^{DN} + E_{RXMode}^{DN}, \tag{9}$$

[10] Nine synchronization bits plus source and destination address fields.

respectively. In both expressions, the first term represents the base-level energy, the second the additional energy required for listening during duty-cycling, and the third the additional SN and DN energy in TX-Mode and RX-Mode, respectively. Average energy consumption per packet for an NDN, in (7), is determined by the base-level energy consumption and the additional energy required for duty-cycling, as

$$E^{NDN} = \frac{P^{sleep}}{\lambda} + E_l^{NDN}. \tag{10}$$

Energy terms appearing in (8), (9), and (10), are accumulated energies resulting from different events during the initiation of a packet transmission. For this we need to calculate how many times different events occur, on average, and combine these with their associated energy costs.

When a data packet is available for transmission, the SN transmits the WBs periodically and listen for a WACK after each. At least one WB needs to be transmitted to initiate communication. In the worst case, the first WB is incompletely received by the DN WRx and, consequently, WBs need to be transmitted until the next WRx listen period. The number of WB-WACK cycles between listen intervals is

$$N_{cycle} = \frac{T_1 + T_2}{T_2} = 1 + \frac{T_{sleep} + T_{st}^{wrx} + T_{listen}}{T_{listen} - T_{wb}}, \tag{11}$$

where $T_1$ and $T_2$ are defined indirectly in Fig. 2. Assuming no packet arrival time more likely than any other, we can use (11) to calculate the average number of periodically transmitted WBs before a WB falls within the listen interval of the DN as

$$\bar{N}_{sync} = \frac{N_{cycle} + 1}{2} = \frac{T_{sleep} + T_{st}^{wrx} + T_{listen}}{2\,(T_{listen} - T_{wb})} + 1. \tag{12}$$

If the WB transmission coincides with the DN listen interval, but a miss occurs in the WB/WACK exchange, the SN has to transmit extra WBs for at least one more listen-sleep period of the WRx to get the chance to wake the DN again. The probability that $k$ consecutive misses occur in the WB/WACK exchange is $(p_M^{wb,wack})^k$, where $p_M^{wb,wack}$ is given by (4). Thus, the average number of times per packet the WB and listen intervals coincide, without successful wake-up is

$$\bar{L} = (1 - p_M^{wb,wack}) \sum_{k=0}^{\infty} k\,(p_M^{wb,wack})^k = \frac{p_M^{wb,wack}}{1 - p_M^{wb,wack}}, \tag{13}$$

and the average number of periodic WB/WACK, per packet, becomes

$$\bar{N}_{wb,wack} = N_{cycle}\,\bar{L}. \tag{14}$$

Whenever the WACK message is received, the SN starts to transmit the data packet. However, if a miss occurs in the data/DACK exchange the SN initiates data transmission from start, returning to periodic WB transmissions. Similar to the WB/WACK the probability of $k$ consecutive unsuccessful attempts due to misses in data/DACK exchange is $(p_M^{data,dack})^k$, where $(p_M^{data,dack})$ is given by (5). Using this, the average number of times the SN enters TX-Mode, per packet, without achieving successful data transmissions becomes

$$\bar{N}_{data,dack} = (1 - p_M^{data,dack}) \sum_{k=0}^{\infty} k \left(p_M^{data,dack}\right)^k = \frac{p_M^{data,dack}}{1 - p_M^{data,dack}}. \quad (15)$$

With expressions for average number of events occurrences, we can calculate the energy terms in (8), (9), and (10). The TX-Mode energy in (8) becomes

$$E_{TXMode}^{SN} = (\bar{N}_{data,dack} + 1)\, E_{DATA}^{SN}, \text{ where} \quad (16)$$

$$E_{DATA}^{SN} = E_{WTXMode}^{SN} + E_{DTXMode}^{SN} \quad (17)$$

is the consumed energy per time the SN is in the TX-Mode. The term $E_{WTXMode}^{SN}$ is the energy of periodic WB transmissions until a WACK is received and $E_{DTXMode}^{SN}$ the energy of data transmission. The first of these, $E_{WTXMode}^{SN}$, can be further specified as

$$E_{WTXMode}^{SN} = E_{SWB}^{SN} + E_{WB}^{SN}, \text{ where} \quad (18)$$

$$E_{SWB}^{SN} = E_{st}^{tx} + \bar{N}_{sync}\,(P^{tx}\,T_{wb} + P^{mrx}\,T_{wack} + 2\,E_{sw}^{txrx}) \quad (19)$$

denotes the average SN energy cost before a WB coincide with the DN listen time and

$$E_{WB}^{SN} = \bar{N}_{wb,wack}\,(P^{tx}\,T_{wb} + P^{mrx}\,T_{wack} + 2\,E_{sw}^{txrx}) \quad (20)$$

the additional SN energy cost from misses in the WB/WACK exchange. The terms $\bar{N}_{sync}$ and $\bar{N}_{wb,wack}$ are given by (12) and (14), respectively, and all other parameters are energies, powers or times related to a specific state. Similarly, the energy cost of data transmission is

$$E_{DTXMode}^{SN} = P^{tx}\,T_{data} + 2\,E_{sw}^{txrx} + P^{mrx}\,T_{dack}. \quad (21)$$

Substituting (17)–(21) back in (16) completes the calculation of $E_{TXMode}^{SN}$ in (8).

A miss in the data/DACK exchange also leads to an extra cost in RX-Mode, since data transmission has to be performed all over again. RX-Mode energy in (9) becomes

$$E_{RXMode}^{DN} = (\bar{N}_{data,dack} + 1)\,(1 - p_M^{wb})\,E_{DATA}^{DN}, \quad (22)$$

where $\bar{N}_{data,dack}$ is given by (15), $(1-p_M^{wb})$ accounts for that RX-Mode is only entered if the WB is detected, and

$$E_{DATA}^{DN} = E_{DRXMode}^{DN} + E_{DARXMode}^{DN}, \tag{23}$$

is the energy consumed per time the DN visits the RX-Mode. The first term, $E_{DRXMode}^{DN}$, is the energy of both WACK transmission and data reception, while $E_{DARXMode}^{DN}$ is the energy of DACK transmission. These are calculated as follows. If the DN WRx misses the WB during channel listening there is no associated energy cost at the DN. However, an extra cost is introduced if the WRx detects the WB, but the SN fails to detect the corresponding WACK. The DN does not receive data and returns to duty-cycled channel listening after a certain time limit. We calculate

$$E_{DRXMode}^{DN} = (\bar{L}+1)\,(E_{st}^{tx} + P^{tx}\,T_{wack} + E_{sw}^{txrx} + P^{mrx}\,T_{data}), \tag{24}$$

in (23) as the energy necessary to successfully receive the data packet and the extra energy cost from misses in the WB/WACK exchange. The average number of unsuccessful wake-ups, $\bar{L}$, is given by (13). When calculating

$$E_{DARXMode}^{DN} = (1-p_M^{wack,data})\,(E_{sw}^{rxtx} + P^{tx}\,T_{dack}) \tag{25}$$

in (23), $(1-p_M^{wack,data})$ takes into account that DACKs are only transmitted if there is no error in the WACK/data exchange. Substituting (23)–(25) in (22) completes the calculation of $E_{RXMode}^{DN}$ in (9).

The last energy term we need to calculate is the contribution from idle channel listening. This includes energy consumed in DC-Mode and the additional cost of false WB detections. In the latter case the node enters the RX-Mode, transmits a WACK, and waits for non-existing data. The average costs of channel listening, $E_l^{SN}$, $E_l^{DN}$ and $E_l^{NDN}$, in (8), (9), and (10), therefore become

$$E_l^{type} = \bar{N}_l^{type}\,(E_{st}^{wrx} + P^{wrx}\,T_{listen} + p_{FA}^{wb}\,E_{FA}), \tag{26}$$

where *type* is the node type,

$$\bar{N}_l^{type} = \frac{1/\lambda - X^{type}}{(T_{sleep} + T_{st}^{wrx} + T_{listen})} \tag{27}$$

the average number of times the node duty-cycles per packet, $p_{FA}^{wb}$ the probability of false WB detection, and $E_{FA}$ the associated energy cost. In (27) $X^{type}$ denotes the average time, per packet, that nodes are not sleeping

$$X^{SN} = (\bar{N}_{data,dack}+1)\,T_{DATA}^{SN} + p_{FA}^{wb}\,\bar{N}_l^{SN}\,T_{FA}, \tag{28}$$

$$X^{DN} = (\bar{N}_{data,dack} + 1)\, T^{DN}_{DATA} + p^{wb}_{FA}\, \bar{N}^{DN}_{l}\, T_{FA}, \text{ or} \tag{29}$$

$$X^{NDN} = p^{wb}_{FA}\, \bar{N}^{NDN}_{l}\, T_{FA}, \tag{30}$$

where

$$T^{SN}_{DATA} = T^{tx}_{st} + \bar{N}_{sync}\, T_2 + \bar{N}_{wb,wack}\, T_2 + T_{data} + T^{txrx}_{sw} + T_{dack}, \tag{31}$$

is the time interval required to transmit a data packet. This includes both the average time needed for a WB to first coincide with a listen interval and the average time consumed by misses in the WB/WACK exchange. Similarly,

$$\begin{aligned} T^{DN}_{DATA} \;=\; & (1 - p^{wb}_{M})\, \big[(\bar{L} + 1)\, (T^{tx}_{st} + T_{wack} + T^{txrx}_{sw} + T_{data}) + \\ & (1 - p^{wack,data}_{M})\, (T^{txrx}_{sw} + T_{dack})\big]. \end{aligned} \tag{32}$$

is the average time spent on receiving data. The energy and time consumed if a node falsely detects a WB are given by

$$E_{FA} = E^{tx}_{st} + P^{tx}\, T_{wack} + E^{txrx}_{sw} + P^{mrx}\, T_{data}, \tag{33}$$

and

$$T_{FA} = T^{tx}_{st} + T_{wack} + T^{txrx}_{sw} + T_{data}, \tag{34}$$

respectively. By substituting (27)–(34) in (26), we can calculate the idle listening energy costs in (8), (9), and (10). We have now completed calculation of all components needed in (7). Performing substitutions leads to the full energy expression which is given in the Appendix.

Average communication delay is also of prime interest, since many applications are delay sensitive. By taking into account contributing events, average communication delay before data is successfully received becomes

$$\bar{D} = (\bar{N}_{data,dack} + 1)\, T^{SN}_{DATA} - (T_{data} + T^{txrx}_{sw} + T_{dack}), \tag{35}$$

where $\bar{N}_{data,dack}$ and $T^{SN}_{DATA}$ are given by (15) and (31), respectively. Performing substitution gives

$$\bar{D} = \frac{A}{B}\, (T_{sleep} + T^{wrx}_{st}) + \frac{1/2 + A}{B}\, T_{listen} + C, \tag{36}$$

where

$$\begin{aligned} A =& \frac{(1 + p^{wb}_{M} + p^{wack}_{M} - p^{wb}_{M}\, p^{wack}_{M})}{2}, \\ B =& \left(1 - p^{wb}_{M}\right)\, \left(1 - p^{wack}_{M}\right)\, \left(1 - p^{dack}_{M}\right)\, \left(1 - p^{data}_{M}\right), \\ C =& F\, T^{tx}_{st} + (\frac{1}{B} + G)\, T^{txrx}_{sw} + (\frac{1}{2\,B} + G)\, T_{data}, \end{aligned} \tag{37}$$

and

$$F = \frac{1}{(1-p_M^{data})(1-p_M^{dack})}, \quad G = \frac{p_M^{data} + p_M^{dack} - p_M^{data} p_M^{dack}}{(1-p_M^{data})(1-p_M^{dack})}. \tag{38}$$

After establishing analytical expressions for DCW-MAC energy consumption and average communication delay, we now address X-MAC and Always-On WRx-MAC as special cases.

## 3.2 X-MAC

In the X-MAC scheme the node's behavior is the same as in DCW-MAC, with the difference that nodes only consist of a main receiver which also duty-cycles and listens to the channel [3]. The energy models of the SN, DN and NDNs, as well as the average delay calculation, presented in Section 3.1 also apply to this scheme. In both energy and delay expressions, however, the WRx power consumption, $P^{wrx}$, setup time, $T_{st}^{wrx}$, and setup energy, $E_{st}^{wrx}$, are replaced by the main radio power consumption, $P^{mrx}$, setup time, $T_{st}^{mrx}$ and setup energy $E_{st}^{mrx}$, respectively. Moreover, the WB miss $p_M^{wb}$ and false alarm $p_{FA}^{wb}$ probabilities are related to the main receiver detection performance. The full expression does not give any direct additional insight and is therefore not explicitly stated in the text.

## 3.3 Always-On WRx-MAC

In the Always-On WRx-MAC a single WB, carrying the address of the DN, is often enough to initiate communication. After the DN receives the WB, a WACK is transmitted to acknowledge the wake-up. As for the DCW-MAC, the average energy consumption of the SN, DN and NDN is modeled by (8)-(10), respectively. However, there are also fundamental differences, as compared to the DCW-MAC case. Since, in the ideal case, the SN needs to send only one WB to initiate communication, there is no periodic WB transmission needed before a WB coincides with a listen interval and $\bar{N}_{sync} = 1$ in (19). This also means that communication delays are typically much shorter than with DCW-MAC and X-MAC. Additionally, if a miss occurs in the WB/WACK exchange, there is no sleep period before the DN listens to the channel again. An additional WB transmitted by the SN can therefore be detected directly by the DN, which means that $N_{cycle} = 1$ in (14). The continuous monitoring of the channel also means that there is no listen interval to relate to and we calculate miss and false alarms per bit time $T_b$ instead. For this reason we change notation of WB miss and false alarm probabilities to $\rho^{wrx}$ and $\nu^{wrx}$,

respectively. This changes $p_M^{wb,wack}$ in (14) to

$$p_M^{wb,wack} = \rho^{wrx} + (1 - \rho^{wrx}\, p_M^{wack}) \tag{39}$$

and the expression corresponding to (26) becomes

$$E_l^{aon,type} = P^{wrx} \left( \frac{1}{\lambda} - X^{aon,type} \right) + \bar{N}_l^{aon,type}\, \nu^{wrx}\, E_{FA}, \tag{40}$$

where the first term is the consumed energy of continuous channel listening and the second the extra cost of falsely detected WBs. Superscript *aon* indicates that these variables are calculated specifically for the Always-On case. Replacing the denominator in (27) by the bit time gives us an approximation of $\bar{N}_l^{aon,type}$. With these changes, the same procedure as for the DCW-MAC is used to calculate energy per packet.

# 4 System parameters and Optimization Strategy

By minimizing total energy consumption when using the DCW-MAC scheme, we show how much energy can be saved by applying low-power WRxs in combination with optimized WB parameters and optimized duty-cycling. The analysis also shows how good our WRx designs have to be, in terms of relative power consumption and implementation loss, to significantly contribute to energy savings in different scenarios.

We re-use the WB structure and analysis of error events for different WRx designs from [15]. This completes the current analysis in the sense that we can replace WB error probabilities needed in (7) by their explicit expressions, depending on WB parameters, WRx design characteristics and other system settings.

## 4.1 Wake-up beacon structure

The WB structure is shown in Fig. 3, consisting of an $M$-bit preamble and $L$-bit destination and source addresses. The preamble sequence, used for WBs detection and time synchronization, is identical for all nodes. The destination address is needed to avoid overhearing, i.e., preventing activation of the NDNs, while the source address is used in the destination address field of WACK packet. The number of nodes in the network, $N$, may be any number below the size of the address space $2^L$. We will, however, assume the worst case $N = 2^L$.

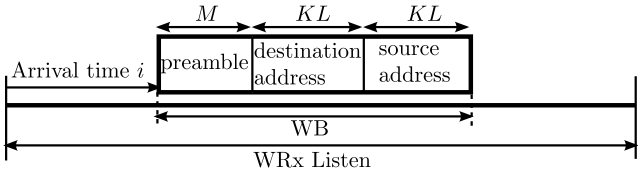


**Figure 3:** Illustration of the wake-up beacon (WB) structure and its arrival at an unknown time instant $i$ during a listen interval. All lengths are given in multiples of bit-times.

Assuming a low-power low-performance WRx, the WB preamble is chosen as a sequence with good autocorrelation properties, providing necessary processing gain and accurate time synchronization. For the destination and source address bits we only need processing gain, since synchronization is already provided by the preamble, and each address bit can be spread by an arbitrary $K$-bit code. This gives a total of $KL$-bits per address field.

Analysis of this WB structure in [15] provides analytical expressions for the receiver operating characteristics (ROC), where we assume worst-case interference,

$$\begin{aligned} p_D^{wb} &= \frac{1}{M+2KL}\sum_{n=\gamma}^{M}\binom{M}{n}(1-p_b^{wrx})^n\,(p_b^{wrx})^{M-n}\times \\ &\quad \sum_{i=1}^{M+2KL}\left(1-(\frac{1}{2})^M\sum_{n=\gamma}^{M}\binom{M}{n}\right)^{i-1}\times \\ &\quad \left(\sum_{n=\lceil K/2\rceil}^{K}\binom{K}{n}(1-p_b^{wrx})^n\,(p_b^{wrx})^{K-n}\right)^{L}, \text{and} \end{aligned} \tag{41}$$

$$\begin{aligned} p_{FA}^{wb} &= \left[1-\left(1-(\frac{1}{2})^M\sum_{n=\gamma}^{M}\binom{M}{n}\right)^{M+2KL-1}\right](\frac{1}{2})^L+\frac{1}{M+2KL}\times \\ &\quad \left(\sum_{n=\gamma}^{M}\binom{M}{n}(1-p_b^{wrx})^n(p_b^{wrx})^{M-n}\right)\times \\ &\quad \sum_{i=1}^{M+2KL}\left(1-\sum_{n=\gamma}^{M}\binom{M}{n}(1-p_b^{wrx})^n(p_b^{wrx})^{M-n}\right)^{i-1}\times \end{aligned}$$

$$\frac{L}{2^L}\left(\sum_{n=\lceil K/2\rceil}^{K}\binom{K}{n}(1-p_b^{wrx})^n(p_b^{wrx})^{K-n}\right)^{L-1}\times$$
$$\left(1-\sum_{n=\lceil K/2\rceil}^{K}\binom{K}{n}(1-p_b^{wrx})^n(p_b^{wrx})^{K-n}\right), \quad (42)$$

using matched filter detection of the preamble with threshold value $\gamma \in [0, M-1]$, under the assumption of ideal preamble correlation properties. The corresponding WB miss probability becomes $p_M^{wb} = 1 - p_D^{wb}$.

## 4.2 Energy optimization

When minimizing energy consumption we can only influence certain parameters in the system, while the remaining ones are defined by the scenario. Parameters typically given as input are those related to hardware properties, propagation environment, traffic, and network size. We consider five free parameters used to optimize energy consumption. These are WRx duty-cycle sleep/listen times, WB preamble length and address spreading, and WB preamble matched-filter threshold. Making these explicit in (7), assigning them to a parameter vector $\boldsymbol{\theta} = (T_{listen}, T_{sleep}, M, K, \gamma)$, the jointly optimal parameters become[11]

$$\widetilde{\boldsymbol{\theta}} = \underset{\boldsymbol{\theta}\in\mathcal{D}}{\operatorname{argmin}} E(\boldsymbol{\theta}), \quad (43)$$

where $\mathcal{D}$ is the permissible parameter range.

Considering that we have two continuous non-negative real parameters, $T_{sleep}$ and $T_{listen}$, two discrete positive integer parameters, $M$ and $K$, and one discrete constrained integer parameter $\gamma \in [0, M-1]$, this is a potentially very difficult mixed integer optimization problem. Fortunately, this particular optimization problem can be solved in two relatively simple steps:

- First, optimal values on the continuous parameters can be found analytically, for given values on the discrete parameters.
- Second, with analytical expressions for the optimal continuous parameters, we can perform a structured search over the three discrete parameters, of which one is constrained.

These two steps are detailed below.

[11] From now on, we use *tilde* to indicate optimal parameter values.

**Continuous parameters $T_{listen}$ and $T_{sleep}$**

With asynchronous communication, listen time has to fulfill $T_{listen} \geq 2\,T_{wb} + 2\,T_{sw}^{txrx} + T_{wack}$, as discussed in Section 2. To save listen energy we choose the smallest possible value. With a WB structure of length

$$T_{wb} = (M + 2\,KL)\,T_b, \tag{44}$$

we obtain the energy-minimizing listen time as a function

$$\widetilde{T}_{listen}(M, K) = 2\,(M + 2\,KL)\,T_b + 2\,T_{sw}^{txrx} + T_{wack} \tag{45}$$

of the free parameters $M$ and $K$. Optimizing sleep time is a bit more involved, but conceptually straight-forward. All we need to do is differentiate (7), whose explicit dependence on $T_{sleep}$ can be found in the Appendix, and solve $\partial E/\partial T_{sleep} = 0$ to find local optima. There are two such optima, of which one is always negative and therefore not valid. The optimal non-negative sleep time becomes

$$\widetilde{T}_{sleep}(M, K, \gamma) = \max\left(\sqrt{\Gamma_E\,\Gamma_{WB}\,\Gamma_X} - \Delta_{listen} - \Delta_{FA}, 0\right), \tag{46}$$

where the dependence on $M$, $K$, and $\gamma$, is implicit through $\Gamma_E$, $\Gamma_{WB}$, $\Gamma_X$, $\Delta_{listen}$, and $\Delta_{FA}$, explained below. An important property of the energy consumption is that it decreases monotonically with sleep times in the interval $[0, \widetilde{T}_{sleep}(M, K, \gamma)]$, showing that (46) corresponds to a minimum. The first factor

$$\begin{aligned} \Gamma_E &= \frac{E_{st}^{wrx} + P^{wrx}\,T_{listen} + H}{P^{tx}\,T_{wb} + P^{mrx}\,T_{wack} + 2\,E_{sw}^{rxtx}}, \\ H &= p_{FA}^{wb}\left(P^{tx}\,T_{st}^{tx} + P^{mrx}\,T_{data} + E_{sw}^{txrx} + P^{tx}\,T_{wack}\right), \end{aligned} \tag{47}$$

under the square root in (46) is the ratio of channel listening energy (including falsely detected WBs) and energy needed to transmit one WB (including receiving a WACK). This shows that optimal sleep time increases with channel listening energy, and decreases with WB transmission energy. The second factor

$$\Gamma_{WB} = \frac{T_{wb} + T_{wack} + 2\,T_{sw}^{rxtx}}{1 + p_M^{wb} + p_M^{wack} - p_M^{wack}\,p_M^{wb}}, \tag{48}$$

is time spent on WB transmissions (including waiting time to receive a WACK), compensated for WB and WACK misses by the denominator. This shows that optimal sleep time increases with longer WB transmission time. Finally,

$$\Gamma_X = 2\,B\,N\,\frac{1}{\lambda} + T_{listen} - S\,(T_{data} + T_{setup}^{tx}) - (8+Q)\,T_{sw}^{txrx} + (7+Q)\,T_{wack}, \tag{49}$$

is a sum of several terms, where $B$ is from (37) and

$$\begin{aligned} S &= 2\left(2-p_M^{wack}\right)\left(1-p_M^{wb}\right)-p_{FA}^{wb}\left(1+p_M^{wb}+p_M^{wack}-p_M^{wack}\,p_M^{wb}\right), \text{and} \\ Q &= p_{FA}^{wb}\left(1+p_M^{wack}+p_M^{wb}-p_M^{wack}\,p_M^{wb}\right)-2\,p_M^{wack}\left(3-2\,p_M^{data}\right)+ \\ &\quad 2\,p_M^{wack}\,p_M^{wb}\left(5+-4\,p_M^{data}\right)+2\left(1-p_M^{data}\right)\Big[\left(p_M^{wb}\right)^2+\left(p_M^{wack}\right)^2+ \\ &\quad \left(p_M^{wb}\,p_M^{wack}\right)^2\Big]-4\,p_M^{wb}\,p_M^{wack}\left(1+-p_M^{data}\right)\left(p_M^{wb}+p_M^{wack}\right)+ \\ &\quad 2\,p_M^{data}\left(2\,p_M^{wb}-1\right)-8\,p_M^{wb}. \end{aligned}$$

The first term in (49) is the effective packet inter-arrival time, the second the listen interval, the third the data packet transmission time and the last two the time used to switch role and to transmit/receive WACKs or DACKs, respectively. We see that the optimal sleep time increases with network size and decreases with traffic and packet lengths. Furthermore, (47)-(49) show that both switching time and WACK/DACK packet length have minor impact on the length of the sleep time interval. The second term

$$\Delta_{listen} = T_{st}^{wrx} + T_{listen} \tag{50}$$

in (46) is the time the WRx is active and the third term

$$\Delta_{FA} = p_{FA}^{wb}\,T_{FA} \tag{51}$$

is the average time spent on WB false-alarm recovery and $T_{FA}$ is defined in (34).

So far, we have not taken any average delay requirement into account. Using (36) we now introduce the restriction $\bar{D} \leq D^{req}$, which implies that the sleep time has to fulfill

$$T_{sleep} \leq T_{sleep}^{*}(M,K,\gamma) = \frac{B}{A}\left(D^{req}-C\right) - \frac{1/2+A}{A}\,T_{listen} - T_{st}^{wrx}. \tag{52}$$

Above we observed that energy consumption is monotonically decreasing with sleep time all the way up to the unrestricted minima in (46). The optimal sleep time with a delay requirement is therefore obtained as the largest non-negative value below $\widetilde{T}_{sleep}(M,K,\gamma)$ satisfying (52), i.e.

$$\widetilde{T}_{sleep}^{dreq}(M,K,\gamma) = \max(0, \min(\widetilde{T}_{sleep}(M,K,\gamma), T_{sleep}^{*}(M,K,\gamma))). \tag{53}$$

**Discrete parameters $M$, $K$ and $\gamma$**

After finding analytical expressions for the optimal continuous parameters, we need to find the optimal discrete parameters. An exhaustive search for the

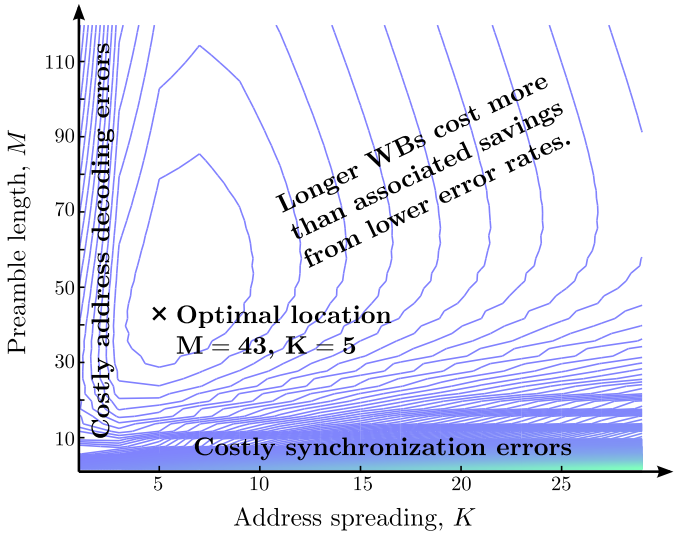


**Figure 4:** Illustration of energy consumption as a function of WB parameters $M$ and $K$. Energy contours used are for an 8-bit address space, 1000 sec. average packet inter-arrival time, 7 dB implementation loss, and -10 dB relative power consumption.

optimal $\gamma$, when $M$ and $K$ are given, can be done by calculating the energy consumption for each of the $M$ possible values. What remains is to find the optimal values on $M$ and $K$.

We have not been able to fully characterize the minimization problem in terms of $M$ and $K$, since it contains highly non-linear relations. However, by studying extreme cases and contour plots of the energy consumption for different system parameter settings, like those shown in Fig. 4, we conjecture that there is a single energy minimum[12] in terms of $M$ and $K$. At short preambles and short address spreading, energy costs are high due to synchronization and address decoding errors, respectively. Increasing preamble and address spreading reduces costs related to these errors, but beyond a certain point the extra costs for longer WBs outweigh these gains. These observations support our conjecture and we use a simple search, increasing $M$ and $K$ from low values, and as soon as a local minimum is found, we assume it is the global one.

[12]Except possibly for neighboring points in the grid giving the same minimal value.

# 5 System Performance Evaluation

As a reference case for our numerical optimization we use radio characteristics and protocol parameters listed in Table 1. We also use non-coherent BFSK for data transmission and non-coherent OOK modulation for WB transmission, in an additive white Gaussian noise (AWGN) channel, where both follow the same type of bit-error expression

$$\mathrm{BER}(\mathrm{SNR}) = 0.5\,\mathrm{e}^{-0.5\,\mathrm{SNR}} \tag{54}$$

which applied in (2) gives the bit-error probabilities of both receivers. Further, we assume that all error events related to the main receiver, with better decoding and processing capabilities, are negligible compared to those related to the WRx. Hence, we assume $p_M^{wack} = p_M^{data} = p_M^{dack} = 0$.

Numerical optimization is performed, as outlined in Section 4.2, for a range of WRx implementation losses, $L_{impl} \in [0, 9]$ dB, and levels of relative WRx power consumption, $R^{wrx} \in [-30, 0]$ dB. The implementation losses correspond to WRx BERs $p_b^{wrx} \in [0.001, 0.23]$, assuming that it operates at a received power level equal to the main receiver sensitivity. Three different address-space sizes $L$, namely 4, 8, and 16 bits, and three average packet inter-arrival times $1/\lambda$, 100000 sec. (about a day), 1000 sec. (about 15 min.), and 10 seconds, are used in the examples. Initially we assume that transmitter power consumption is equal to the receiver power consumption, i.e. $R^{tx} = 0$ dB, but extend this to the range $R^{tx} \in [-10, 10]$ dB to allow a wider range of application of derived approximations.

Before addressing the question of how much energy we can save, let us discuss how optimal sleep times and WB lengths depend on different system parameters.

## 5.1 Optimal sleep time and WB length

The relationship between optimal sleep time and WB length is studied both with and without requirements on average delay.

### Without requirement on average delay

Fig. 5(a)-(c) shows the relationship between optimal sleep interval and WB lengths, for different relative WRx power consumptions and implementation losses, when there are no requirements on average delay. The relationship is shown for all three average packet inter-arrival times in each sub-figure and there is one sub-figure for each of the three address-space sizes. As indicated, $L_{impl}$ is fixed along dashed lines while $R^{wrx}$ is fixed along solid lines.

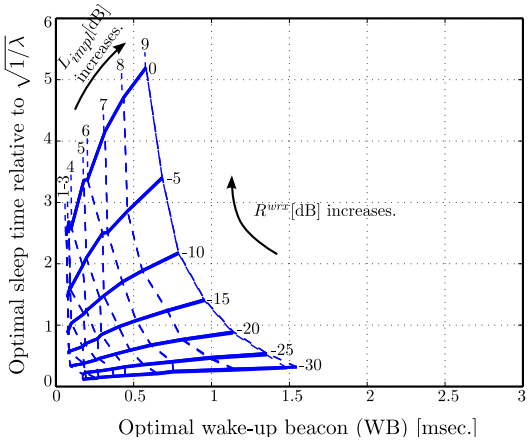


(a)

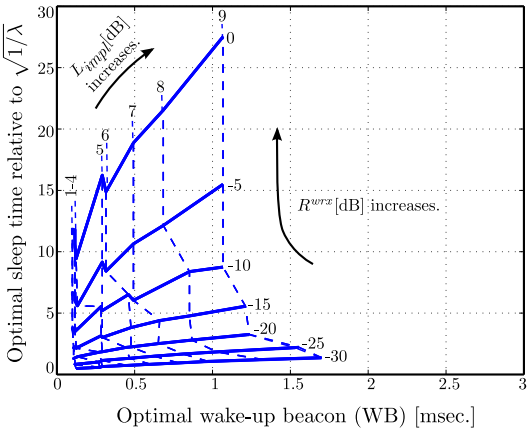


(b)

By presenting optimal sleep interval lengths relative to the square root of their respective average inter-packet intervals, $\sqrt{1/\lambda}$, all three sets of curves in each sub figure essentially fall on top of each other. The reason behind this behavior is that the optimization results in values on $T_{wb}$ and $p_{\text{FA}}^{wb}$ that make $\Delta_{listen}$ and $\Delta_{FA}$ small compared to the square root term in (46), which in turn is nearly proportional to $\sqrt{1/\lambda}$ through $\Gamma_X$ in (49).

Studying these three sub figures we make several observations regarding optimal values:

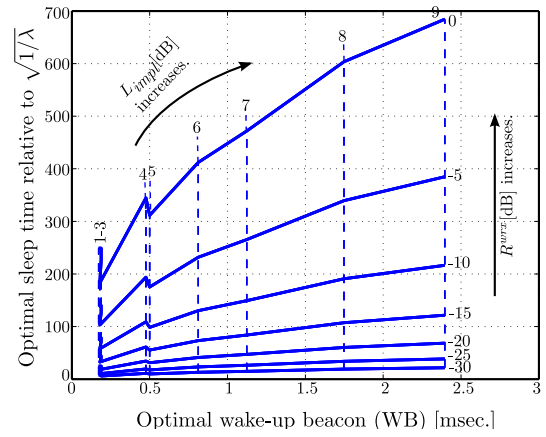


(c)

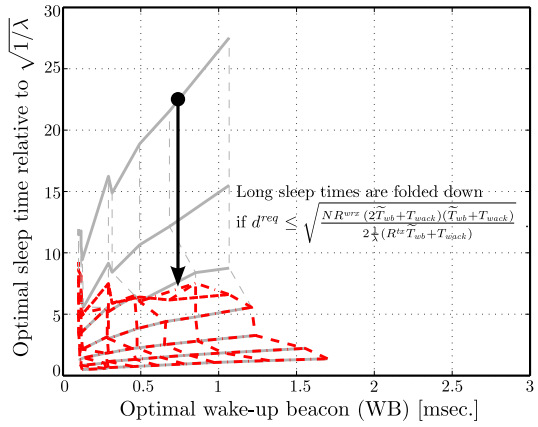


(d)

**Figure 5:** Optimal sleep time vs. optimal WB length, for different relative WRx power consumptions $R^{wrx}$ and implementation losses $L_{impl}$. The first three sub-figures each show the relationship for three packet inter-arrival times $1/\lambda$: 100000 sec., 1000 sec., and 10 seconds. The address space sizes are (a) 4 bits, (b) 8 bits, and (c) 16 bits. In (d) the influence from a requirement on average delay is illustrated, using an 8-bit address space, a 1000 sec. $1/\lambda$, and a relative average delay $d^{req}$ of 0.5%.

- Sleep interval length, relative to the average inter-packet arrival time, grows with network size. This is a result of energy costs associated with listening being multiplied by more nodes in larger networks, which is compensated by longer sleep times.

- Sleep interval length also increases with higher relative WRx power consumption. More power consumption in the WRx needs to be compensated by longer sleep intervals.

- Sleep interval and WB lengths both increase with higher implementation losses, except for some small artifacts resulting from optimizing in an integer-valued parameter space[13]. Longer WBs, and thereby more transmit energy per WB, are needed to compensate for lower WRx performance. This, in turn, results in longer sleep times.

- WB length increases with network size, but much less than we may expect. There are at least two mechanisms behind this behavior. The listening cost increases both with WB length and the number of nodes. It is therefore more costly to use long WBs in large networks. Another cost that increases with network size is the one related to false alarms, which should push the WB length up. Fortunately, with increasing network size, $p_{FA}^{wb}$ reduces without making WBs longer, since address decoding bounds it below $2^{-L}$ [15].

**With requirement on average delay**

To illustrate what happens to optimal sleep interval and WB lengths when we introduce a requirement on average delay, we show optimization results for the 8-bit address space in Fig. 5(d), for an average packet inter-arrival time of 1000 sec. and a relative average delay requirement $d^{req} = D^{req}\lambda = 0.5\%$[14]. The optimization result is shown in red and, for comparison, the unrestricted result from Fig. 5(b) is included in light gray.

While we only show optimization results for one case when we have delay requirements, to save space, we draw the following general conclusions, based on the complete set of optimization results:

- WB lengths (and their general relations to other parameters) are largely maintained from the case without delay requirements. This is a result of

[13]The jumps in optimal sleep time, more visible for larger address spaces, are a result of integer-valued optimization parameters. The influence on the resulting energy cost are small, since the optima are relatively shallow.

[14]To make the influence of a delay requirement more visible in the figure, we use a less tight one than in the rest of the analysis.

only a weak dependence between WB length and delay near the optimum reached without the delay requirement.

- The permissible sleep interval lengths are limited by the average delay requirement and long sleep intervals are no longer allowed as a means of compensating for poor WRx characteristics. In Section 6 we discuss this behavior in more detail and derive the approximation shown in the figure.

## 5.2 Performance of energy optimized DCW-MAC schemes

Two important performance indicators are how much energy we can save by introducing energy optimized DCW-MAC schemes and what communication delays the optimization results in. For the purpose of measuring energy savings, we define the relative measure

$$S_E = \frac{E_{ref} - E_{DCW\text{-}MAC}}{E_{ref}}, \tag{55}$$

where $E_{ref}$ and $E_{DCW\text{-}MAC}$ are the optimized energy consumptions of the reference scheme (X-MAC or Always-On WRx-MAC) and the DCW-MAC scheme, respectively, under the same system parameters and traffic conditions. When studying delay, we choose to directly use the average communication delay as introduced in (36).

The general behavior of energy savings and communication delays do not change significantly with address size and we therefore focus on address size $L = 8$ bits. Generalizations to other address sizes are done later. What remains to show is influence from changes in traffic intensity and delay requirement. We do this using three scenarios. The reference scenario has $1/\lambda = 1000$ sec. inter-packet arrival and no requirement on delay, while the other two scenarios correspond to a hundred-fold increase in traffic, $1/\lambda = 10$ sec., and introduction of a tight delay requirement, $d^{req} = 0.1\%$, respectively.

We base our discussion below on Fig. 6 which shows DCW-MAC energy savings over both X-MAC and Always-On WRx-MAC, as well as resulting average communication delays. Results are shown as level curves, starting at every 10 dB reduction in relative WRx power consumption, for zero implementation loss.

### Importance of dedicated wake-up receivers

When studying duty-cycling schemes we use full relative WRx power consumption and no implementation loss ($R^{wrx} = 0$ dB and $L_{impl} = 0$ dB) as our

reference, which implies that we compare to the case when the main receiver is used for wake-up, as in X-MAC. The amount of energy saving from using a low-power WRx depends on its characteristics in relation to other system parameters. Fig. 6(a) shows achieved relative energy saving as a function of WRx relative power consumption $R^{wrx}$ and WRx implementation loss $L_{impl}$. The obtained energy saving percentages along the level curves are shown as triplets, one for each scenario. Interestingly, all curves follow roughly the same trend. They are almost linear and essentially parallel to each other, in the dB-dB plot. This is an important observation that we use later to derive simple approximations of optimal energy saving. For this purpose, we denote their slope by $\Omega_E$. The 0% energy saving level curves indicate the break-even WRx characteristics for which we do not save any energy and in the gray area above them, DCW-MAC does not improve on X-MAC. Energy savings increase both with increasing traffic and when introducing a delay requirement. Both these imply that nodes wake up more often, in the first case to optimize energy saving and in the second case to fulfill the delay requirement. With nodes waking up more often, the savings related to having a low-power WRx become more pronounced.

**Importance of duty-cycling**

To illustrate the importance of duty-cycling we show relative energy savings between DCW-MAC and Always-On WRx-MAC in Fig. 6(b), when both use dedicated WRxs with the same characteristics $R^{wrx}$ and $L_{impl}$. The level curves have a significantly different shape than in Fig. 6(a) and, as we can see, energy savings are almost 100% for all three scenarios. Using WRxs with the same characteristics in both schemes, energy savings are associated with increased communication delays. The great advantage of DCW-MAC is that we can use a delay requirement to trade between energy savings and resulting delays.

**Average communication delay**

In Fig. 6(c) we show the resulting communication delays in seconds. Like in Fig. 6(a), the level curves are almost linear and parallel to each other. Using a separate low-power WRx allows shorter communication delays, since channel listening becomes less costly. Using a 0.1% relative delay requirement limits the average communication delay to 1 sec. The limit applies to the upper part of the figure, where the WRx is relatively power hungry and energy optimization relies on long sleep times. Despite level curve slopes very similar to those in Fig. 6(a) we use a separate variable, $\Omega_D$. Later we will see that there are cases where $\Omega_D$ is different from $\Omega_E$. The level curves starting at $L_{impl} = 0$ dB

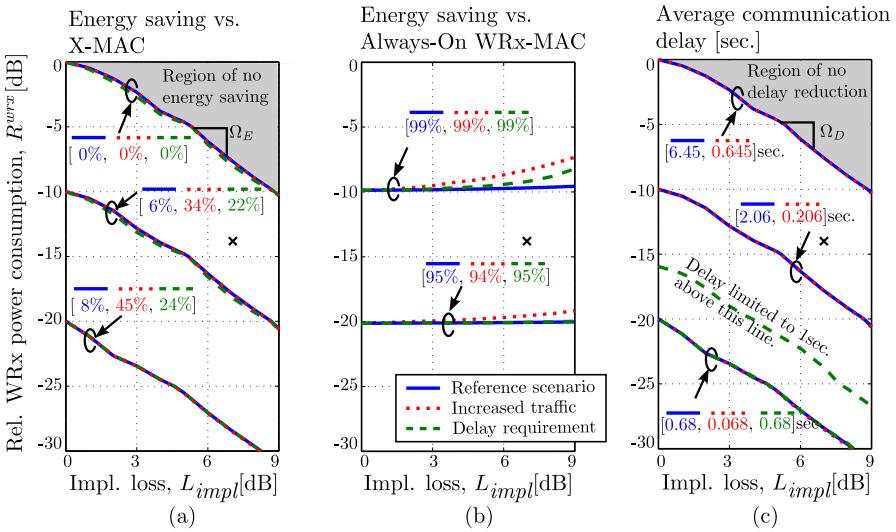


**Figure 6:** DCW-MAC (a) energy savings relative to X-MAC, (b) energy savings relative to Always-On WRx-MAC, and (c) average communication delay, shown as level curves, for three different scenarios. The reference scenario has a 1000 sec. $1/\lambda$ and no delay requirement. Based on the reference scenario, the other two scenarios have traffic increased to a 10 sec. $1/\lambda$ and a 0.1% relative delay requirement, respectively. Results are shown for an 8-bit address space. Energy savings, in (a) and (b), and average communication delay, in (c), for the three scenarios are shown as triplets next to each set of level curves. The 'x' shows the characteristics of the example WRx in Table 1.

and $R^{wrx} = 0$ dB show the break-even WRx characteristics for which DCW-MAC and X-MAC result in equal delays. In the gray area above these curves DCW-MAC result in equal or longer delays than X-MAC.

*A simple design comparison:* To put optimal relative energy savings into context we perform a simple design comparison. Assume that we are interested in using the example WRx in Table 1 in a network of 256 nodes. The average packet inter-arrival interval is 1000 sec. and a tight 0.01% relative delay is required. We use a Panasonic CG-320 battery [31] with nominal capacity and voltage of 13mAh and 3.75V, respectively, as our node energy source. When applying optimal DCW-MAC, the resulting average energy consumption per node leads to 6.8 years of battery life-time. This node battery life-time is around 2.5 and 40 times longer than with X-MAC and Always-On WRx MAC,

respectively. Using a high performance main receiver, with no energy saving strategy, the battery life-time is only around 2 days.

# 6 Approximations of Optimal Energy Savings and Resulting Delays

Performing numerical optimization to analyze achievable energy savings when using DCW-MAC is tractable, but somewhat tedious and time consuming. The same is true for finding the resulting communication delays. We therefore derive closed form approximations of these, using observations from the numerical optimization in the previous section. These approximations can be used without going through the entire optimization procedure and they also provide deeper insights into the properties of DCW-MAC. We concentrate on energy savings relative to X-MAC and the resulting communication delays.

In the previous section we observed that level curves for both energy savings and average communication delay are almost linear and parallel, *cf.* Fig. 6(a) and 6(c), and we express them as a simple relationship between $R^{wrx}$ and $L_{impl}$,

$$R^{wrx} \approx \Omega_* \, L_{impl} - \Delta \text{ [dB]}, \tag{56}$$

where $\Omega_*$ is either $\Omega_E$ or $\Omega_D$, depending on if we address energy savings or delay, while $\Delta$ is the associated reduction of WRx power consumption beyond break-even (0% energy saving or no delay reduction). Optimization results for a larger set of scenarios (address sizes, delay requirements, ratios between transmit and receive power consumption, and ratios between sleep and receive power consumption) show essentially the same linear and parallel level curves. The only significant influence is on slopes $\Omega_E$ and $\Omega_D$, which change in opposite direction with i) the ratio $R^{tx} = P^{tx}/P^{mrx}$, and in the same direction with ii) the network size/address bits $L$. We show these variations in Fig.7(a). Imposing a strict enough delay requirement, energy slopes $\Omega_E$ become essentially independent of parameter settings and settles at -1.2, while delay slopes $\Omega_D$ are not influenced by delay requirements.

To complete our approximation we need to characterize how parameter settings influence energy savings at different $\Delta$. Since both energy savings and delays are parallel-shifted with slope $\Omega_E$ and $\Omega_D$, respectively, we can perform the approximation at $L_{impl} = 0$ dB, where the WRx has the same good error-performance as the main receiver, and $R^{wrx} = -\Delta$. Given this, we assume that $p_{FA}^{wb} = p_M^{wb} = p_M^{wack} = p_M^{dack} = p_M^{data} = 0$ and, with rare packets, we use that $1/\lambda \gg T_{data}$. Consequently, the second and third terms in (46) are negligible and (47), (48) and (49), for the optimal parameter selection, become

$\frac{R^{wrx}\,(2\widetilde{T}_{wb}+T_{wack})}{R^{tx}\widetilde{T}_{wb}+T_{wack}}$, $\widetilde{T}_{wb}+T_{wack}$, and $2\,N\,(1/\lambda)$, respectively. We arrive at an approximation

$$\widetilde{T}_{sleep} \approx \sqrt{\frac{2N\frac{1}{\lambda}R^{wrx}\,(2\widetilde{T}_{wb}+T_{wack})(\widetilde{T}_{wb}+T_{wack})}{R^{tx}\widetilde{T}_{wb}+T_{wack}}} \tag{57}$$

of (46), when there is no requirement on average delay. The WB length in the expression, $\widetilde{T}_{wb}$, is the optimal one at $R^{wrx}=0$ dB and $L_{impl}=0$ dB.

When there is a strict requirement on average delay, i.e., when $d^{req}=D^{req}\lambda$ is small, following (53) and the above assumptions, we approximate the optimal sleep time as

$$\widetilde{T}^{dreq}_{sleep} \approx 2\,d^{req}\,\frac{1}{\lambda} - 4\,\widetilde{T}_{wb} - 2\,T_{wack}. \tag{58}$$

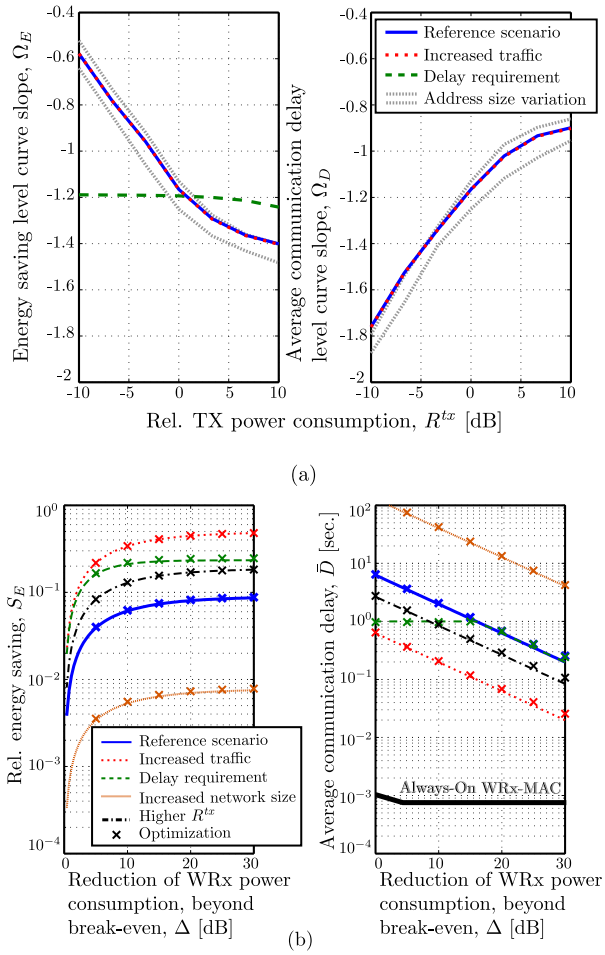


**Figure 7:** (a) Level curve slopes $\Omega_E$ and $\Omega_D$ for different relative transmit power consumptions. (b) Comparison of optimal values (crosses) and corresponding approximations (lines) of energy savings and average communication delays, for different WRx power reductions beyond break-even ($\Delta$) without implementation loss.

For the investigated parameter ranges, $\widetilde{T}_{wb}$ depends mainly on the number of address bits $L$, as optimal WB parameters show preamble lengths $M$ close to 10 and no address spreading, i.e. $K = 1$, when $R^{wrx} = L_{impl} = 0$ dB.

Hence, we can use $\widetilde{T}_{wb} \approx (10 + 2L)T_b$ for the entire range of network sizes studied. Depending on our requirement on average delay, optimal sleep time is approximated either by (57) or (58), according to (53). We can use this to find the relative delay requirement

$$d^{req} \lesssim \sqrt{\frac{NR^{wrx}\,(2\widetilde{T}_{wb} + T_{wack})(\widetilde{T}_{wb} + T_{wack})}{2\frac{1}{\lambda}(R^{tx}\widetilde{T}_{wb} + T_{wack})}}, \tag{59}$$

for which optimal sleep time becomes restricted and full power savings cannot be achieved. The effect of this is clearly seen in Fig. 5(d).

With approximations of sleep time available, we approximate $S_E$ in (55) as a function of $\Delta$, writing it as $S_E(\Delta)$, where the dependence on other system parameters is implicit. Using approximations (57) and (58) for the sleep interval and replacing them back in (7) and (55) we obtain

$$S_E(\Delta) \approx \begin{cases} \dfrac{\sqrt{\frac{2\,N\,\frac{1}{\lambda}\,(2\widetilde{T}_{wb}+T_{wack})(R^{tx}\widetilde{T}_{wb}+T_{wack})}{\widetilde{T}_{wb}+T_{wack}}}(1-\sqrt{1/\Delta})}{N\frac{1}{\lambda}R^{sleep}+\sqrt{\frac{2\,N\,\frac{1}{\lambda}\,(2\widetilde{T}_{wb}+T_{wack})(R^{tx}\widetilde{T}_{wb}+T_{wack})}{\widetilde{T}_{wb}+T_{wack}}}}, & \text{No delay req.} \\ \dfrac{(2\widetilde{T}_{wb}+T_{wack})\,(\frac{N}{2\,d^{req}}-1)(1-1/\Delta)}{N\frac{1}{\lambda}R^{sleep}+\frac{d^{req}\,\frac{1}{\lambda}(R^{tx}\widetilde{T}_{wb}+T_{wack})}{\widetilde{T}_{wb}+T_{wack}}+(2\widetilde{T}_{wb}+T_{wack})\,(\frac{N}{2\,d^{req}}-1)}, & \text{Delay req.} \end{cases} \tag{60}$$

and substituting $\Delta = \Omega_E L_{impl} - R^{wrx}$ [dB] gives the full approximation for different values on $R^{wrx}$ and $L_{impl}$. An attractive feature of (60) is that it depends on relative power consumptions, rather than their absolute values.

To verify (60), we compare to exact optimization results for different $\Delta$s. Fig. 7(b) shows optimal and approximated energy savings for the same three scenarios as in Fig. 6(a), plus two additional ones to show how the approximation works for a larger network size and for a higher transmit power. The energy-savings approximation matches the optimization results well. Evaluated for all studied scenarios and optimization grid points $R^{wrx}$ and $L_{impl}$ in Fig. 6(a), excluding the gray area, the maximal relative deviation is less than 10% and the average is below 2.5%.

Using sleep time approximations, (57) and (58), together with other assumptions introduced above, (36) is approximated

$$\bar{D}(\Delta) \approx \begin{cases} \sqrt{\frac{N\frac{1}{\lambda}(2\widetilde{T}_{wb}+T_{wack})(\widetilde{T}_{wb}+T_{wack})}{2\,\Delta(R^{tx}\widetilde{T}_{wb}+T_{wack})}}, & \text{No delay req.} \\ \min\left(d^{req}\frac{1}{\lambda} - 2\widetilde{T}_{wb} - T_{wack}, \sqrt{\frac{N\frac{1}{\lambda}(2\widetilde{T}_{wb}+T_{wack})(\widetilde{T}_{wb}+T_{wack})}{2\Delta(R^{tx}\widetilde{T}_{wb}+T_{wack})}}\right). & \text{Delay req.} \end{cases} \tag{61}$$

Substituting $\Delta = \Omega_D L_{impl} - R^{wrx}$ [dB] gives the full approximation for different values on $R^{wrx}$ and $L_{impl}$. Again, the approximation has the attractive

feature to only depend on relative power consumptions, rather than absolute values.

Similar to the energy savings, and for the same scenarios, we compare the communication delay exact values from numerical optimization with the derived approximation. The result is shown in Fig. 7(b), where the approximation matches optimization results well for all cases. Evaluated for all studied scenarios and optimization grid points $R^{wrx}$ and $L_{impl}$ in Fig. 6(c), excluding the gray area, the maximal relative deviation is less than 25% and the average is below 9%. The much shorter Always-On WRx-MAC delays are shown as an additional reference. Using the approximation we can also quantify that DCW-MAC delays are roughly $\sqrt{\Delta}$ times shorter than those for X-MAC (which is at $\Delta = 0$ dB), as long as a delay requirement does not restrict sleep times. Further, with the $d_{req} = 0.1\%$ delays become limited, as expected, to 1 sec.

# 7 Conclusions and Remarks

We present a complete system-level analysis and optimization of energy consumption for DCW-MAC, a duty-cycled wake-up receiver medium access scheme. We perform energy and communication delay analysis of an entire single-hop network where all nodes are equal and use an extra WRx for wake-up. The analysis includes a break-down of total node functionality into basic operations, analyzed separately and combined into a complete energy expression. The closed form expression give a good understanding how energy consumption relates to changes in system parameters. Scenarios with and without requirement on average delay are addressed and DCW-MAC energy consumption is related to both X-MAC and Always-On WRx-MAC. Optimization results show that while low-power requirements on the WRx limits its performance, as compared to the main receiver, a substantial amount of energy can be saved in the entire network for many system parameter settings. Approximations of key results, optimal energy savings and resulting delays, have been derived and verified. These can, e.g., be used to perform simple design evaluations before realizing a WRx in hardware, to see that any goals on energy savings and delay can be reached.

# Appendix: Energy Expressions

To obtain the full per packet energy expression for DCW-MAC, we substitute (16), (22) and (26) back in (8)-(10) and (7). The form, where the dependency on $T_{sleep}$ is shown explicitly, is helpful when performing the analytical optimization

of sleep time in Section 4.2:

$$E = C_1 + C_2\,T_{sleep} + C_3\left(C_4\frac{1}{T_{sleep}+C_6} - C_5\frac{T_{sleep}}{T_{sleep}+C_6}\right), \quad (62)$$

where

$$\begin{aligned}
C_1 &= \frac{N\,P^{sleep}}{\lambda} + (\bar{N}_{data,dack}+1)\,\Big[(E^{tx}_{st} + P^{tx}\,T_{data} + 2\,E^{txrx}_{sw} + P^{mrx}\,T_{dack}) + \\
&\quad \frac{(1+2\,\bar{L})(T^{wrx}_{st} - T_{wb}) + (3+4\,\bar{L})T_{listen}}{2\,(T_{listen} - T_{wb})}(P^{tx}\,T_{wb} + P^{mrx}\,T_{wack} + 2\,E^{txrx}_{sw})\Big] + \\
&\quad (\bar{N}_{data,dack}+1)\,(1-p^{wb}_{M})\,\Big[(\bar{L}+1)\,(E^{tx}_{st} + P^{tx}\,T_{wack} + E^{txrx}_{sw} + P^{mrx}\,T_{data}) + \\
&\quad (1-p^{wack,data}_{M})\,(E^{rxtx}_{sw} + P^{tx}\,T_{dack})\Big], \\
C_2 &= \frac{(\bar{N}_{data,dack}+1)\,(1+2\,\bar{L})}{2\,(T_{listen} - T_{wb})}(P^{tx}\,T_{wb} + P^{mrx}\,T_{wack} + 2\,E^{txrx}_{sw}), \\
C_3 &= E^{wrx}_{st} + P^{wrx}\,T_{listen} + p^{wb}_{FA}\,(E^{tx}_{st} + P^{tx}\,T_{wack} + E^{txrx}_{sw} + P^{mrx}\,T_{data}), \\
C_4 &= N\frac{1}{\lambda} - (\bar{N}_{data,dack}+1)\,\Big[(T^{tx}_{st} + T_{data} + 2\,T^{txrx}_{sw} + T_{dack}) - \\
&\quad \frac{(1+2\,\bar{L})(T^{wrx}_{st} - T_{wb}) + (3+4\,\bar{L})T_{listen}}{2\,(T_{listen} - T_{wb})}(T_{wb} + T_{wack} + 2\,T^{txrx}_{sw}) - \\
&\quad (1-p^{wb}_{M})\,\Big[(\bar{L}+1)\,(T^{tx}_{st} + T_{wack} + T^{txrx}_{sw} + T_{data}) + \\
&\quad (1-p^{wack,data}_{M})\,(T^{rxtx}_{sw} + T_{dack})\Big]\Big], \\
C_5 &= \frac{(\bar{N}_{data,dack}+1)\,(1+2\,\bar{L})}{2\,(T_{listen} - T_{wb})}(T_{wb} + T_{wack} + 2\,T^{txrx}_{sw}), \text{and} \\
C_6 &= T^{wrx}_{st} + T_{listen} + p^{wb}_{FA}\,(T^{tx}_{st} + T_{wack} + T^{txrx}_{sw} + T_{data}).
\end{aligned}$$

# Bibliography


[1] Y. Wei, J. Heidemann, and D. Estrin, "An energy-efficient MAC protocol for wireless sensor networks," in *Proc. 21st Ann. Joint Conf. IEEE Comput. and Commun. Soc.*, vol. 3, November 2002, pp. 1567–1576.

[2] A. El-Hoiydi and J.-D. Decotignie, "WiseMAC: An ultra low power mac protocol for multi-hop wireless sensor networks," in *Proc. 4th Int. Conf. Embedded Ntworked Sensor Syst.*, 2004.

[3] M. Buettner *et al.*, "X-MAC: a short preamble MAC protocol for duty-cycled wireless sensor networks," in *Proc. 4th Int. conf. Embedded networked sensor syst.*, 2006, pp. 307–320.

[4] W. Ye, F. Silva, and J. Heidemann, "Ultra-low duty cycle MAC with scheduled channel polling," in *Proc. 4th Int. Conf. Embedded Ntworked Sensor Syst.*, 2006, pp. 321–334.

[5] T. van Dam and K. Langendoen, "An adaptive energy-efficient mac protocol for wireless sensor networks," in *Proc. 1st Int. Conf. Embedded Ntworked Sensor Syst.*, 2003, pp. 171–180.

[6] J. Polastre, J. Hill, and D. Culler, "Versatile low power media access for wireless sensor networks," in *Proc. 2th Int. Conf. Embedded Ntworked Sensor Syst.*, 2004, pp. 95–107.

[7] A. El-Hoiydi, "Aloha with preamble sampling for sporadic traffic in ad hoc wireless sensor networks," in *IEEE Int. Conf. Commun.*, vol. 5, April 2002, pp. 3418–3423.

[8] C. Guo, L. C. Zhong, and J. Rabaey, "Low power distributed mac for ad hoc sensor radio networks," in *IEEE, Global Telecomm. Conf.*, vol. 5, 2002, pp. 2944–2948.

[9] S. Mahlknecht and M. Bock, "CSMA-MPS: a minimum preamble sampling MAC protocol for low power wireless sensor networks," in *Proc. IEEE Int. Workshop on Factory Commun. Syst.*, 2004, pp. 73–80.

[10] M. S. Durante and S. Mahlknecht, "An ultra low power wakeup receiver for wireless sensor nodes," in *Proc. 3rd Int. Conf. Sensor Technologies and Applicat.*, 2009, pp. 167–170.

[11] E.-Y. Lin, J. Rabaey, and A. Wolisz, "Power-efficient rendez-vous schemes for dense wireless sensor networks," in *IEEE Int. Conf. Commun.*, vol. 7, June 2004, pp. 3769–3776.

[12] Y. Sun, O. Gurewitz, and D. B. Johnson, "RI-MAC: a receiver-initiated asynchronous duty cycle mac protocol for dynamic traffic loads in wireless sensor networks," *Proc. 6th Int. Conf. Embedded Ntworked Sensor Syst.*, pp. 1–14, 2008.

[13] E.-Y. Lin, "A comprehensive study of power-efficient rendezvous schemes for wireless sensor networks," Ph.D. dissertation, University of California, Berkeley, 2005.

[14] N. S. Mazloum and O. Edfors, "DCW-MAC: An energy efficient medium access scheme using duty-cycled low-power wake-up receivers," in *IEEE Vehicular Technology Conf.*, September 2011, pp. 1–5.

[15] ——, "Performance analysis and energy optimization of wake-up receiver schemes for low-power applications," *IEEE Trans. Wireless Commun.*, vol. 13, pp. 7050–7061, 2014.

[16] M. Zimmerling, F. Ferrari, L. Mottola, T. Voigt, and L. Thiele, "pTunes: Runtime parameter adaptation for low-power MAC protocols," in *Proc. 11th Int. Conf. Inform. Process. in Sensor Networks*, 2012, pp. 173–184.

[17] C. Fischione, P. Park, and S. C. Ergen, "Analysis and optimization of duty-cycle in preamble-based random access networks," *Wireless networks*, vol. 19, pp. 1691–1707, 2013.

[18] M. Lont *et al.*, "Analytical models for the wake-up receiver power budget for wireless sensor networks," in *Proc. 28th IEEE conf. Global Telecomm.*, 2009, pp. 1146–1151.

[19] Y. Zhang, L. Huang, G. Dolmans, and H. de Groot, "An analytical model for energy efficiency analysis of different wakeup radio schemes," in *IEEE 20th Int. Symp. Personal, Indoor and Mobile Radio Commun.*, 2009, pp. 1148–1152.

[20] N. S. Mazloum, J. N. Rodrigues, and O. Edfors, "Sub-$V_T$ design of a wake-up receiver back-end in 65nm CMOS," in *IEEE Subthreshold Microelectronics Conf.*, October 2012, pp. 1–3.

[21] N. Pletcher, S. Gambini, and J. Rabaey, "A 65$\mu$W, 1.9GHz RF to digital baseband wakeup receiver for wireless sensor nodes," in *IEEE Custom Integrated Circuits Conf. (CICC)*, 2007.

[22] X. Huang *et al.*, "A 2.4GHz/915MHz 51$\mu$W wake-up receiver with offset and noise suppression," in *IEEE Int. Solid-State Circuits Conf. Digest Tech. Papers (ISSCC)*, February 2010, pp. 222–223.

[23] T. Copani, S. Min, S. Shashidharan, S. Chakraborty, M. Stevens, S. Kiaei, and B. Bakkaloglu, "A CMOS low-power transceiver with reconfigurable antenna interface for medical implant applications," *IEEE Trans. Microwave Theory and Techniques*, vol. 59, pp. 1369–1378, 2011.

[24] C. Hambeck, S. Mahlknecht, and T. Herndl, "A 2.4$\mu$W wake-up receiver for wireless sensor nodes with -71dBm sensitivity," in *IEEE Proc. Int. Symp. Circuits and Syst. (ISCAS)*, 2011, pp. 534–537.

[25] K.-W. Cheng, X. Liu, and M. Je, "A 2.4/5.8GHz 10$\mu$W wake-up receiver with -65/-50dBm sensitivity using direct active RF detection," *IEEE Asian Solid-State Circuits Conf. (A-SSCC)*, pp. 337–340, 2012.

[26] N. M. Pletcher, S. Gambini, and J. Rabaey, "A 52$\mu$W wake-up receiver with $-72$dBm sensitivity using an uncertain-IF architecture," *IEEE J. Solid-State Circuits*, vol. 44, pp. 269–280, January 2009.

[27] S. Drago, D. Leenaerts, F. Sebastiano, L. J. Breems, K. A. Makinwa, and B. Nauta, "A 2.4GHz 830pJ/bit duty-cycled wake-up receiver with $-82$dBm sensitivity for crystal-less wireless sensor nodes," in *IEEE Int. Solid-State Circuits Conf. Digest Tech. Papers (ISSCC)*, 2010, pp. 224–225.

[28] C. Bryant and H. Sjöland, "A 2.45GHz, 50$\mu$W wake-up receiver front-end with -88dBm sensitivity and 250kbps data rate," in *European Solid State Circuits Conf. (ESSCIRC)*, September 2014, pp. 235–238.

[29] H. Sjöland *et al.*, "A receiver architecture for devices in wireless body area networks," *IEEE J. Emerg. Sel. Topic Circuits Syst.*, vol. 2, pp. 82–95, March 2012.

[30] ——, "Ultra low power transceivers for wireless sensors and body area networks," in *8th Int. Symp. Medical Inform. and Commun. Technology (ISMICT)*, April 2014, pp. 1–5.

[31] "Panasonic commercializes the industry's smallest pin shaped lithium ion battery." [Online]. Available: http://news.panasonic.com/global/topics/2014/29437.html

# *Paper IV*

# Improving Practical Sensitivity of Energy Optimized Wake-up Receivers: Proof of Concept in 65nm CMOS

**We present a high performance low-power digital base-band architecture, specially designed for an energy optimized duty-cycled wake-up receiver scheme. Based on a careful wake-up beacon design, a structured wake-up beacon detection technique leads to an architecture that compensates for the implementation loss of a low-power wake-up receiver front-end at low energy and area costs. Design parameters are selected by energy optimization and the architecture is easily scalable to support various network sizes. Fabricated in 65nm CMOS, the digital base-band consumes 0.9$\mu$W ($V_{\mathrm{DD}}$ = 0.37V) in sub-threshold operation at 250kbps, with appropriate 97% wake-up beacon detection and 0.04% false alarm probabilities. The circuit is fully functional at a minimum $V_{\mathrm{DD}}$ of 0.23V at $f_{\mathrm{max}}$ = 5kHz and 0.018$\mu$W power consumption. Based on these results we show that our digital base-band can be used as a companion to compensate for front-end implementation losses resulting from the limited wake-up receiver power budget at a negligible cost. This implies an improvement of the practical sensitivity of the wake-up receiver, compared to what is traditionally reported.**

---

Nafiseh Seyed Mazloum, Joachim Neves Rodrigues, Oskar Andersson, Anders Nejdel, and Ove Edfors,
"Improving Practical Sensitivity of Energy Optimized Wake-up Receivers: Proof of Concept in 65nm CMOS,"
under review for possible publication in *IEEE Sensors Journal*.

# 1 Introduction

Today, the success of Internet of Things has led to increasing demands on wireless sensor network (WSN) applications, through which more devices intelligently communicate with each other. In most of the WSN applications energy resources are severely limited both due to node sizes and the possible placement where energy resources cannot easily be replaced. To design a long life network it is, therefore, necessary to avoid unnecessary energy cost in the network. In general, in the WSNs idle channel listening is a dominant factor for energy consumption, due to their relatively low traffic intensity. Using an extra ultra-low power receiver, typically referred to as a wake-up receiver (WRx), dedicated for channel monitoring can significantly reduce this cost [1–4]. There are two main approaches for how a WRx is used. In one, the WRx is always on, continuously listening to the channel, while in the other the WRx is duty-cycled, and only turned on periodically to listen to the channel. Such a WRx has limited functionality and is only used to look for potential communication, a wake-up beacon (WB), on the channel. When a WB is detected, the main receiver is powered up. A generic block diagram of an entire sensor node of this type is shown in Fig. 1, where a sleep timer is used only if we employ duty-cycling. The choice of WB structure and WB detection algorithm are important in WRx schemes as they directly/indirectly influence system energy consumption. We have proposed and analyzed detection performance of a particular WB structure in [5, 6]. In this paper we present the design and implementation of a WRx digital base-band (DBB) for the proposed WB. We show that the proposed DBB design delivers predicted performance enhancements at an energy cost low enough to make it a suitable companion to all WRx analog front-ends found in literature [7–28].

Under realistic assumptions, a WRx typically has two orders of magnitude lower power budget than the main receiver, e.g., in the order of $10\mu$W [1, 2]. Since the majority of power is consumed by the WRx analog front-end, most studies focus on its design and try to minimize power consumption of this part of the circuitry [7–28]. Simple non-coherent modulation schemes, such as on-off keying (OOK) [7–13, 15, 16, 20–25, 28], binary frequency shift keying (BFSK) [17–19], pulse position modulation (PPM) [26], and pulse width modulation (PWM) [14, 27], are often used for WB transmission since they allow low-power low-complex front-end architectures. Extreme low-power design of such receivers, however, leads to higher noise figure and degraded sensitivity compared to a main receiver. The implementation/performance loss has to be compensated by increasing WB transmit energy. This can in principle be done by transmitting WBs with higher transmit power without extending the WB duration, or keeping the WB transmit power and making the WBs longer, e.g.,

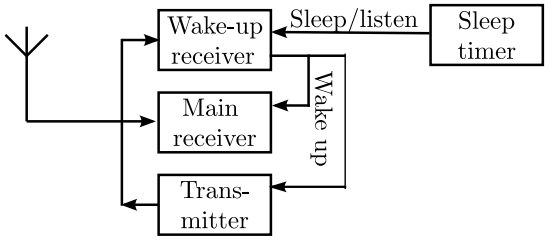


**Figure 1:** Simplified node block diagram. The transmitter is used both for data and wake-up beacon (WB) transmission, while the main receiver and wake-up receiver (WRx) are used for data and WB reception, respectively. The sleep timer is used when we have duty-cycled WRx scheme.

by lowering data rate or applying spreading. The first approach requires drastic increase in transmit power making it more suitable for applications where a master node without severe restricted energy source is available for WB transmission. In this work we are aiming for applications where all nodes have equal functionality with equal energy resources. To allow using energy resources as distributed as possible among nodes, we make the WBs longer by applying spreading. A correlator based on analogue processing [10, 11] is a low-power approach commonly chosen to examine energy level of the received signal for WB detection. Using this approach, however, makes it difficult to distinguish between different patterns and avoid overhearing. Digital processing, on the other hand, allows for more flexible WB signal processing and detection algorithms. To prevent overhearing, identity of a node is included in the WB in the form of i) a completely unique sequence for each node [13, 23, 28] or ii) a more structured arrangement [4, 19, 29] consisting of, e.g., a preamble and an address part. In such an arrangement the preamble is used for synchronization purposes and identification related to individual nodes is carried in the address part. Correlation is performed in digital domain to detect these sequences. Our approach is based on the second WB structure and a corresponding digital base-band processing as it gives more flexibility to save energy by adjusting the WB to hardware characteristics and traffic requirements. The structured WB approach also allows for shorter correlators compared to using entirely unique sequences as WB, making the signal processing more efficient both in terms of power consumption and hardware architecture flexibility. A more detailed study of how WRx front-end characteristics influence detection performance and WB design is presented in [6], where optimization is used to adjust the WB structure to minimize the energy cost of WB transmissions.

What remains is to show, by implementation and characterization of the required base-band processing, that these schemes can deliver the performance enhancements predicted by theory without significantly increasing WRx energy consumption. This is what we do in this paper.

As mentioned above, we present a DBB circuit design for a duty-cycled WRx scheme, where we show that the implementation loss of the WRx front-end, resulting from a very limited power budget, can be compensated by digital base-band processing at a negligible power consumption and area cost. We compare our design with those presented by others in [19], [28] (analog/mixed signal correlator) and [29] (pure digital). The two main differences are: i) their work assume continuous channel monitoring, while we have chosen duty-cycled operation to reduce idle listening [4], and ii) our WB structure [5] is more flexible and allows minimization of energy cost for a wider range of node address spaces, traffic conditions, and different characteristics of the WRx analog front-end, without major changes to the DBB implementation. This design also has the advantage of high address-space scalability, at negligible hardware cost, making the design attractive both for small and large sensor networks. An application specific integrated circuit (ASIC) is optimized for ultra-low voltage (ULV) operation and is characterized by measurements for different operating frequencies and a wide range of supply voltages. While the DBB is primarily designed and implemented for a WB with certain design parameters, chosen to compensate for the implementation loss of the WRx front-end in [21], we show that the DBB can be used as a companion to a wide range of WRx front-end design presented in literature and improve on practical sensitivities at a negligible cost in terms of power consumption.

The paper is organized as follows. In Section 2 we give a description of the overall system operation. We present a hardware architecture of a WRx DBB in Section 3. In Section 4 we provide details of parameter selection for prototype implementation. Simulations are performed to evaluate receiver operating characteristics for the selected parameters. Measurement results from the prototype implementation are presented in Section 5. The performance of state-of-the-art analog front-ends is compared and discussed in Section 6. Conclusions and final remarks are given in Section 7.

## 2 System Description

We design a DBB integrated circuit for a low-power duty-cycled WRx, used to search for a WB with a certain pattern, in a given time-interval. While low power, area efficiency and sufficient WB detection performance are essential for the DBB design itself, its integration into a larger system also has to be

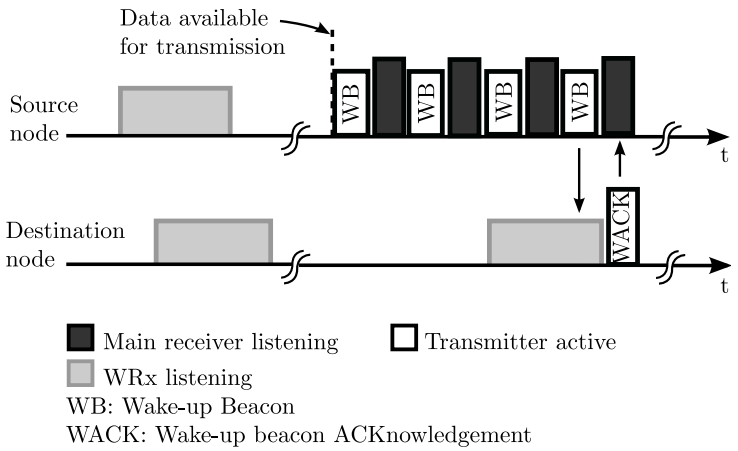


**Figure 2:** Simplified timing diagram of periodic wake-up beacons (WBs) and WRx duty-cycled channel listening.

considered. In our reference system, nodes communicate according to the Duty-Cycled Wake-up receiver Medium Access Control (DCW-MAC) scheme. In the following we highlight some important system properties that influence our design, but for details we refer to [4].

In the DCW-MAC, combining a low-power WRx with asynchronous duty-cycled channel listening can significantly reduce idle channel listening. With a low-power WRx, and the corresponding loss in performance/sensitivity, as discussed in Section 1, the WRx needs to operate at a raw bit error rate (BER) higher than the $10^{-3}$ normally used to evaluate receiver performance. Since WRxs asynchronously listen to the channel, strobed WBs are transmitted, as shown in Fig. 2, whenever data is ready for transmission. Using spreading and transmitting long WBs, processing gain can compensate for high BERs, improving on the practical sensitivity of the WRx. The WBs also carry the address of the destination node and overhearing by non-destination nodes is thereby largely avoided [30]. To guarantee that the WRx can hear one complete such WB, the listen interval needs to be selected long enough so that if the WRx barely misses one WB it still has the chance to capture the next one in the same listen time. Consequently, the listen interval is chosen to be at least twice the time extent of the WB, plus the time between the WBs. The time between the WBs needs to be long enough to contain a WACK packet[15].

[15]Whenever the WRx detects a WB, carrying its own address, the node's transmitter replies with a WB acknowledgment (WACK).

Ideally no errors occur during WB detection, but in a real system we have both noise and interference. Therefore, there is a certain probability that a transmitted WB is missed, or the WRx erroneously detects a non-existing WB. The miss event occurs with some probability $P_{\mathrm{M}}^{\mathrm{WB}}$ and the false alarm event occurs with some probability $P_{\mathrm{FA}}^{\mathrm{WB}}$. Both detection errors lead to unnecessary power-up of energy expensive parts of circuity, and thereby result in extra energy costs.

All the above shows that the WRx design has an important influence on both the WB structure and the total power consumption. For details on this we refer the reader to [6]. In short, the use of low-power WRxs with high BER, listening to the channel asynchronously makes it important to structure the WB so that:

- synchronization can be achieved,
- the probabilities of missing or falsely detecting a WB are kept low, and
- unnecessary wake-ups due to overhearing are avoided.

Here we use the WB structure from [5], which fulfills the above requirements.

## 2.1 Wake-up Beacon Structure

The WB consist of an $M$-bit preamble and $L$-bit destination and source addresses. The preamble is needed to detect the presence of a WB and for time-synchronization, as the arrival time of the WB in the WRx listen interval is unknown. For simplicity, the preamble is selected to be identical for all nodes since uniqueness is provided by the address part. The destination address is used to avoid activating non-destination nodes, while the source address is used in the destination address field of the WACK.

For accurate time-synchronization, the preamble should have good autocorrelation properties and it should be long enough to compensate for the high BER of the front-end. For the destination and source address fields, we do not need the autocorrelation properties, but the high BER still has to be compensated. We do this by $K$-bit spreading of each address bit, using an arbitrary code, resulting in a total of $2KL$ bits for both addresses. This leads to a $M + 2KL$ bit WB where energy optimization can be done over $M$ and $K$. The optimal $M$ and $K$ depend on system parameters like traffic conditions, delay requirements and network size. It is therefore of interest to make a DBB implementation, as done below, that can be easily adjusted to different $M$, $K$ and $L$. Typical ranges, when energy optimizing networks with up to $L = 16$ address bits and front-end BERs as high as 0.15, are $M \lesssim 60$ and $K \lesssim 10$, with $M$ roughly ten times larger than $K$ for individual optima [6].

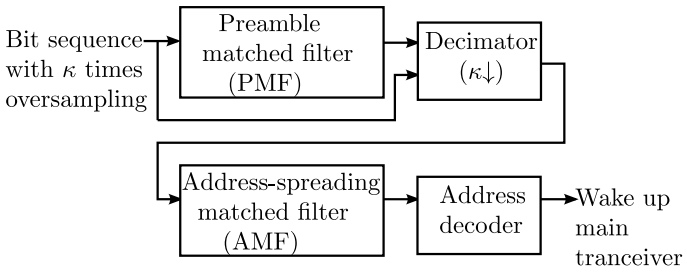


**Figure 3:** Digital base-band (DBB) block diagram.

# 3 Digital Base-band Hardware Architecture

After establishing our WB structure, we propose a hardware architecture for the DBB processing. There is, however, a point that we deliberately avoided in the above discussions that need to be addressed. We implicitly assumed that there was a bit-synchronization between transmitter and receiver, which of course is not the case. We handle this by assuming an oversampling factor, where the analog front-end of the WRx delivers bit-decisions at $\kappa$ times the actual bit rate. The DBB therefore has to perform its processing at $\kappa$ times the channel bit rate. Given this, the task of the DBB is to search for the presence of a WB in this bit sequence.

We have chosen the block diagram shown in Fig. 3, consisting of a preamble matched filter (PMF), a decimator, an address-spreading matched filter (AMF), and an address decoder. All MFs in our design are finite impulse response (FIR) filters with the transfer function $F(z) = \sum_{i=0}^{J-1} f_i\, z^{-i}$ where $J$ is the number of filter taps, and the values of the filter impulse response $f_i$s are the reversed known sequence, i.e., the preamble, the address spreading, and the node address, we are looking for. All these MFs are also followed by a comparator acting as decision device and, for simplicity, we include this component when using the term MF. Feeding the input $x[n]$ in the form of a bit stream to the MF, the filter output $y[n]$ becomes

$$y[n] = \sum_{k=0}^{J-1} f_k\, x[n-k], \tag{1}$$

and when $y[n]$ is larger than a predefined threshold $\gamma$, we assume a detection. The DBB searches the received bit sequence for the WB, based on above principle, in the following steps. First the PMF is used to search for the preamble, at a $\kappa$ times oversampling, since it is the part of the WB designed for synchronization. Whenever the output of the PMF exceeds a certain threshold a

preamble is detected. The maximum peak, indicating the correct clock phase, is found among $\kappa$ successive samples for improved time synchronization. After preamble detection, the input sequence is passed to a decimator ($\kappa\downarrow$), and the rest of the processing is performed at channel bit rate. The remainder of the bit-sequence is fed to the address-spreading matched filter (AMF), where the individual address bits are detected by correlating the sequence with the address spreading sequence. At this stage the DBB knows the synchronization and performs correlation only once per address bit. Finally, the detected address bits are collected by the address decoder and compared against the node address. If there is a match, the main transceiver is powered up.

With the proposed architecture, the PMF and the AMF are identical in all nodes of a network. Only the address decoder needs to be programmed with the respective node addresses. The advantages of our WB structure, and DBB design, over the structures proposed in [28] and [29] are that the selection of WB pattern and address code is not limited to a certain code-book, and the programmable address decoder enables a large address-space scalability. For instance, to scale a network size from 256 to 1024 nodes, we only need to increase the address decoder length (from 8 to 10 bits), while the PMF and the AMF can remain unchanged. Moreover, accurate time-synchronization provided by oversampling and using preambles with sharp peaks allows us to process the address part of the WB without oversampling, leading to shorter correlators for address detection. Furthermore, the DBB design is improved, over a previous design [4], by detecting the address bits using the AMF and the address decoder, instead of using one MF for the entire address field. The new design, realized in hardware as binary-input MFs, leads to both a shorter critical path and smaller area and, consequently, less leakage energy. Latency is the same for both structures since the number of clock-cycles before the DBB decides if a WB is present remains the same.

What now remains is to specify in more detail the implementation of the MFs and the decimator.

## 3.1 Matched filters

We describe a generic hardware mapping of a binary-input MF used to compute (1), since MFs are the main building blocks of our DBB design. The differences in the deployment of the MF for the PMF, AMF, and address decoder are further explained.

As depicted in Fig. 4 the binary-input MF is implemented using two shift registers, one for storing the filter impulse response (SRF) and one acting as a delay line for the incoming bits (SRI). During the initialization phase, the clock enable ClkEn is set to one and the reversed known sequence, i.e., the preamble,

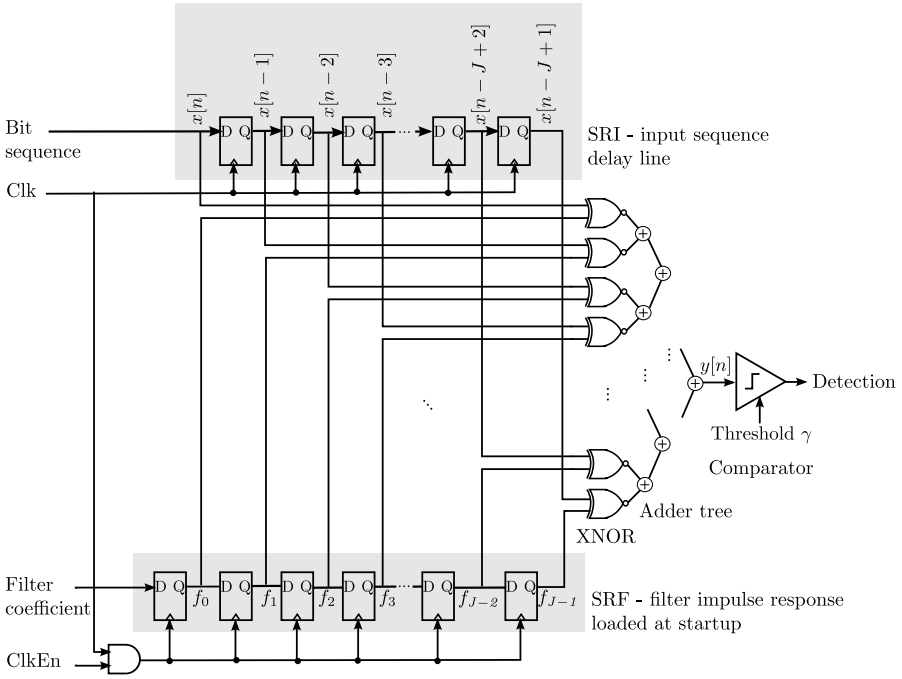


**Figure 4:** Hardware mapping of a generic binary-input matched filter, consisting of two shift registers (SRI and SRF), XNORs, an adder tree, and a comparator.

the address spreading or the node address, is fed to the SRF. All values of the filter impulse response, $f_0 ... f_{J-1}$, are stored in the SRF after $J$ clock cycles. All bits in the sequence $x[n]...x[n-J+1]$ necessary to calculate the output are available by feeding the incoming bits to the SRD, which is shifted one bit at each clock cycle. Correlation of the input signals ($x[n]...x[n-J+1]$) with the values of the filter impulse response ($f_0 ... f_{J-1}$) is performed at bit-level, where XNORs are the first stage to create filter tap outputs. Summation of these outputs is then realized by a fully balanced adder tree. Thus, *idle time* of the gates is kept low and, consequently, energy dissipation due to leakage reduces. The adder tree is composed of half-adders (mirror architecture), taken form the standard-cell library.

Using the above MF hardware mapping, the differences between PMF, AMF and address decoder are in clock rate, length of SRs, number of filter taps, and comparator threshold level. Both the number of SRs and filter taps for the PMF

are $\kappa$ times the preamble length $M$, since the PMF receives the oversampled bit sequence. The PMF is clocked at $\kappa$ times the bit rate. The AMF and the address decoder are placed after the decimator and receive the bit sequence at a normal channel bit rate. This means that the number of SRs and filter taps for the AMF and the address decoder are equivalent to the length of the address-spreading $K$ and the number of address bits $L$, respectively. The decision level in the PMF can vary in the range $[0 \;\; (4M-1)]$ and depends on performance requirements and front-end BER. In the AMF, responsible for address-bit detection, we set the threshold level to the midpoint $\lceil K/2 \rceil$. Since we require all address bits to match the node address, the address decoder threshold is set to $L$.

**Sub-$V_{\mathrm{T}}$ characterization of the MFs**

Sub-$V_{\mathrm{T}}$ characterization of a single MF in [5] shows that maximum operational frequency varies only slightly with filter length. This agrees with the fact that the critical path primarily depends on the depth of balanced adder tree, growing only logarithmically with filter length. Energy per clock cycle and area, on the other hand, are highly dependent on the filter length and scale roughly linearly. Given the experience discussed in Section 2, with $M \approx 10K$, DBB characteristics will be dominated by the large PMF of length $\kappa M$.

## 3.2 Decimator

After preamble detection and bit-synchronization, we do not need to continue at the oversampled rate and can operate at normal bit rate when de-spreading and detecting node address. This, as previously mentioned, saves energy and reduce area compared to operating directly on the oversampled sequence. The decimator in Fig. 3 is, therefore, used to perform the down-sampling. Using the position of bit-timing/clock-phase from the PMF output, the decimator down-samples the sequence by adding $\kappa$ oversampled bits at a time. The result of this is thresholded to decide whether the down-sampled bit is a zero or one. Figure 5 shows the hardware implementation of a decimator, consisting of a $(2\kappa-1)$-bit SR, indicated by SRD, a $(\kappa-1)$-bit $\kappa$ to 1 multiplexer, an adder and a comparator. With $\kappa$ times oversampling, there are $\kappa$ possible correct bit-timing/clock-phase for the decimator to perform the summation of the incoming oversampled bits. To have access to all $x[n]...x[n-(2\kappa+2)]$ samples needed to calculate the output for any of the clock phases, the $(2\kappa-1)$-bit SRD is used. The input $x[n]$ is directly connected to the oversampled bit sequence and the SRD stores all above samples by shifting the incoming bits every clock cycle. The multiplexer inputs are then fed with $\kappa$ choices of

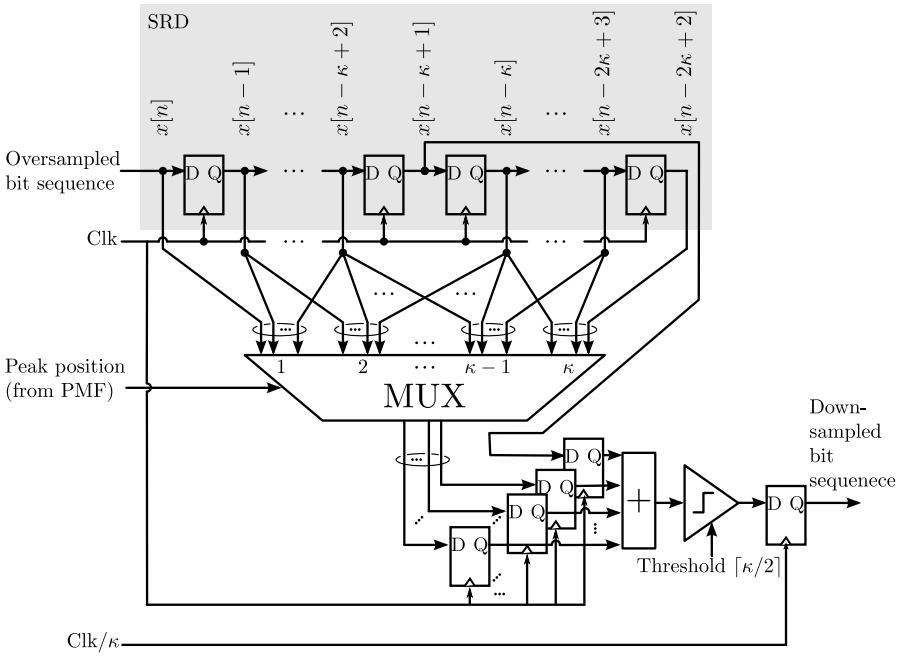


**Figure 5:** Hardware-mapping of a decimator consisting of a shift register (SRD), a multiplexer, an adder, and a comparator.

incoming sample sequences, grouped based on the possible clock phase. The peak position of the PMF output is fed to the multiplexer control input. The control output in return feeds through the correct $(\kappa - 1)$ samples to the adder for further processing. Since input sample $x[n - \kappa + 1]$ is present in all sums, independent of the peak position, it is fed directly to the adder instead of through the multiplexer. This allows us to use a multiplexer with a smaller size, saving both on energy and area. The comparator output is set to zero if the output of the adder is smaller than $\kappa/2$ while it is set to one for the other values.

Due to its small size, contributions from the decimator on total DBB sub-$V_{\mathrm{T}}$ characteristics will be negligible for reasonable parameter choices.

# 4 Parameter Selection

Both WB detection performance and power consumption of the DBB implementation are of importance to the overall evaluation of the proposed architecture. In this section we select implementation parameters to obtain sufficient detection performance, while power consumption is discussed in the next section.

The WB detection performance has been extensively studied from theoretical point of view in [6], where WB parameters are optimized for different front-end characteristics and network sizes. Ranges of resulting parameters were discussed briefly in Section 2. As a proof of concept we implement the DBB with realistic design parameters from the *Ultra-Portable Devices* project at the Department of Electrical and Information Technology, Lund University [31], [32] and a particular low-power analog front-end [21] in mind. The analog front-end is designed for operation at 2.4GHz and 250kbps on-off keying carrying Manchester coded bits. Using a passive mixer together with a ring oscillator, the analog front-end down-converts the received RF signal to IF. The envelope of the IF signal is detected and filtered by a band-pass filter that reduces noise and interference outside the expected range, including DC from constant envelope signals. Using a simple non-coherent signal energy detector, channel bits are detected at $\kappa = 4$ times oversampling and fed to the DBB. The combination of passive mixer with three-phase mixing and complementary IF amplifiers improves efficiency resulting in $-88$dBm sensitivity at $10^{-3}$ BER and 50 $\mu$W power consumption. For more details and a block diagram of this particular analog front-end see [21]. We consider a network with maximum 256 nodes ($L = 8$) and a channel BER of 0.15. The high BER can be traced back to operating the analog front-end at a practical sensitivity level equal to that of the main receiver, $-94$dBm. This corresponds to a need to improve the practical sensitivity by 6dB. Along the lines described in Section 2.1, energy optimized WB parameters fall in the range of $M = 31$ and $K = 7$, for this scenario. The particular value $M = 31$ is related to lengths of $m$-sequences with good autocorrelation properties [33]. Applying the factor-four oversampling, Manchester coding of bits, and rounding up to the nearest power of two, gives PMF and AMF lengths of 256 and 16 bits, respectively.

While thresholds for the AMF and address decoder are fixed, the DBB performance, in terms of detection $P_D^{\mathrm{WB}} = 1 - P_M^{\mathrm{WB}}$ and false alarm $P_{\mathrm{FA}}^{\mathrm{WB}}$ probabilities, changes with the PMF threshold level. Using the analytical framework from [6] with parameters as specified above, we show the receiver operational characteristics (ROC) of the DBB in Fig. 6. The analytical curve shows the ROC for ideal correlation properties, while simulations are performed for the non-ideal Manchester-coded 31-bit m-sequence used in the implementation. As

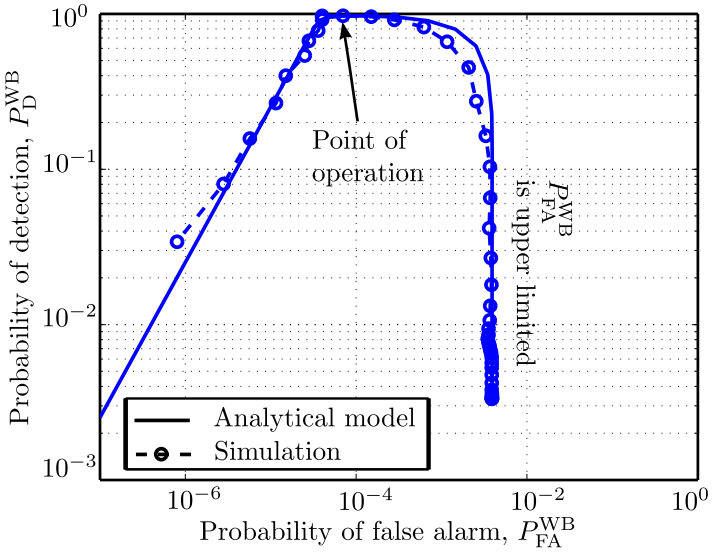


**Figure 6:** Simulated and calculated receiver operating characteristics, ROCs, for a Manchester-coded wake-up beacon (WB) with a preamble of length $M = 62$, $L = 8$ bit addresses and address spreading $K = 14$. $P_{\mathrm{FA}}^{\mathrm{WB}}$ is calculated assuming that an interfering WB is always present during channel listening.

can be seen, the simplified analysis and realistic simulations agree well. The chosen point of operation for our implementation is a PMF threshold at 92% of the maximum filter output, which provides 97% WB detection probability and a low WB false alarm probability, in the order of $10^{-4}$. Both probabilities are given per listen interval, which is set to the minimal value of twice the WB length.

## 5 Measurement Results

The DBB is fabricated in a 65nm CMOS technology. Figure 7 shows the chip micro-photograph. The area of the integrated circuit, including peripheral access, is 0.062mm$^2$. The functionality of the fabricated chip has been verified by connecting the output of an analog front-end [21], from the *Ultra-Portable Devices* project, to the DBB input.

Fig. 8 shows the result of our measurements. The dashed vertical line at

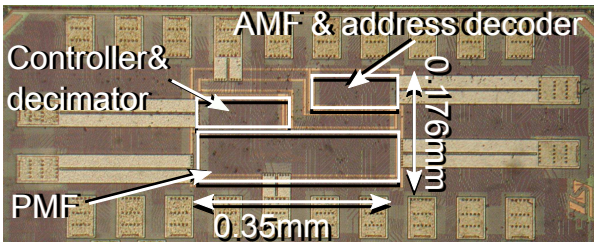


**Figure 7:** Chip micro-photograph.

$V_{\mathrm{DD}} = 0.37$V indicates the lowest supply voltage at which the 250kbps ($f = 1$MHz with $\kappa = 4$ oversampling) can be maintained. At 250kbps operation, we see that leakage is negligible at 30× below dynamic energy dissipation, even if the circuit is not operated at maximum operating frequency ($f_{\mathrm{max}}$). Dissipating 0.9pJ/operation at 1MHz gives a power consumption of 0.9$\mu$W. This shows that the presented DBB design compensates for the implementation loss of the low-power analog front-end (50$\mu$W) [21] at negligible power consumption.

Measurements in the sub-$V_{\mathrm{T}}$ region, at $f_{\mathrm{max}}$, show an energy minimum of $E_{\mathrm{min}} = 0.7$pJ/operation at $\mathrm{V_{DD}} = 0.31$V ($f_{\mathrm{max}} = 200$kHz), giving a power consumption of 140nW. The DBB is fully functional down to lowest supply voltage $V_{\mathrm{DDmin}} = 0.23$V ($f_{\mathrm{max}} = 5$kHz) which, to the authors best knowledge, is lower than any number published in literature. While Fig. 8 shows measurement results at room temperature, measurements at body temperature show that minimal energy per operation, $V_{\mathrm{DD}}$ at minimal energy, and lowest operational $V_{\mathrm{DD}}$, all increase by less than 20%. This shows that despite the 20% increase, the DBB power consumption is still negligible compared to the analog front-end power consumption. Fig. 9 displays the oscilloscope measurements of the circuit at $\mathrm{V_{DDmin}}$ at room temperature. The power consumption at this point is 18nW.

Comparison with previous DBB designs[16] is shown in Table 1. Our WB structure is more flexible than previous designs, allowing arbitrary WB pattern and address spreading. The selected WB structure and DBB processing results in two to three orders of magnitude lower $P_{\mathrm{FA}}^{\mathrm{WB}}$ than in [19], [28] and [29], while $P_{\mathrm{D}}^{\mathrm{WB}}$ remains on the same level. Moreover, this work outperforms [29] both in terms of power consumption and lowest supply voltage at which it is fully functional. The power consumption of this work and the efficient analog hybrid solution [28], not characterized for low supply voltage, are comparable at their

[16] Among the solutions found in literature [10,11,13,19,23,28,29] we have chosen to directly compare to those where WB detection performance has been reported, namely [19], [28] and [29].

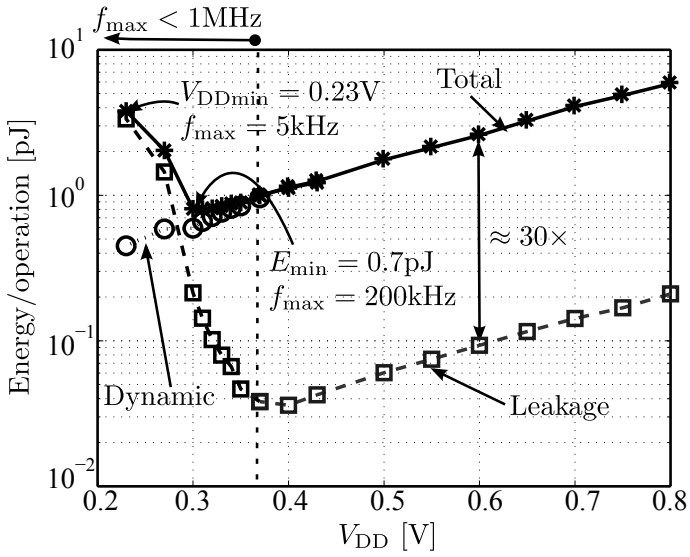


**Figure 8:** Measured energy vs. $V_{DD}$ at room temperature. The dashed vertical line indicates the lowest $V_{DD}$ at which the target 250kbps can be sustained.

normal $V_{DD}$s when taking the difference in data rates into consideration. By using the WRx for address detection, we also avoid the energy consuming process of waking up the power-hungry main receiver to check the address [19] of each WB. Moreover, our DBB is optimized for duty-cycled WRxs and by optimizing sleep time of our WRx the average power consumption can go down drastically and ideally approach the WRx sleep power, which for our design is 0.5nW. Previous studies on the DBB are optimized for always-on processing and do not use a sleep mode to reduce average power consumption.

# 6 Discussion

We have shown, in the previous section, that our proposed DBB outperforms the existing DBB solutions in terms of power consumption and detection performance. We have also shown that the flexibility of the proposed DBB allows adjusting the design without significant changes in hardware architecture or power consumption. In this section we show that, without significantly increasing power consumption of the WRx, the proposed DBB can be connected to a wide range of optimized WRx analog front-ends and improve on their

**Table 1:** Comparison to previous work.

| **Parameter** | [19] [17] | [28] | [29] | This work |
|---|---|---|---|---|
| WB type | EDP + ADP | Unique sequence | Preamble+Sync.+ Codebook addr. | Preamble + Spread address |
| $P_D^{WB}$, $P_{FA}^{WB}$ (per wake-up beacon) | 0.999, 1E-3 Always-ON | 0.99, 1E-3 Always-ON | 0.98, 2.8E-2 Always-ON | 0.97, 4E-5 Duty-cycled |
| Power cons. [$\mu$W] and | 44.2 | 0.4 | 3.72 | 0.9 |
| Data rate [kbps] | 50 | 100 | 200 | 250 |
| @ $V_{DD}$ [V] | 0.7 | 1.0 | 1.2 | 0.37 |
| Power cons. [$\mu$W] | NA | NA | 0.9 | 0.018 |
| @ $V_{DDmin}$ [V] | | | 0.6 | 0.23 |
| Technology [nm] | 65 | 130 | 90 | 65 |
| Area [mm$^2$] | ~0.42 | ~0.12 | 0.1 | 0.062 |

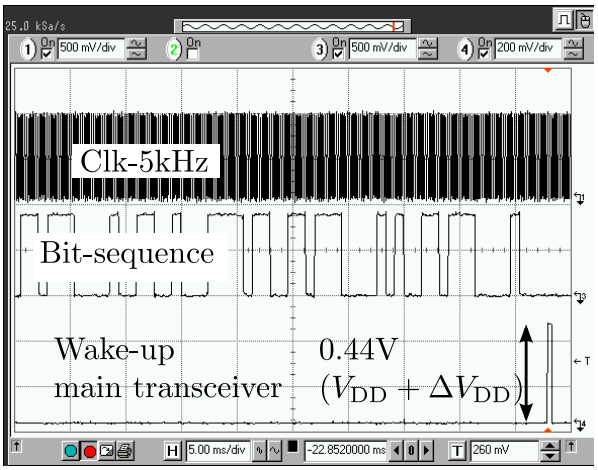


**Figure 9:** Oscilloscope measurement at min. $V_{DD}$ of 0.23V@5kHz at room temperature. A $\Delta V_{DD}$ higher supply voltage is needed to drive the pads.

performance.

[17] When Energy Detection Packet (EDP) is detected by a low-power receiver, a more power hungry receiver is powered up to detect Address Detection Packet (ADP). Presented power consumption is only for low-power wake-up receiver.

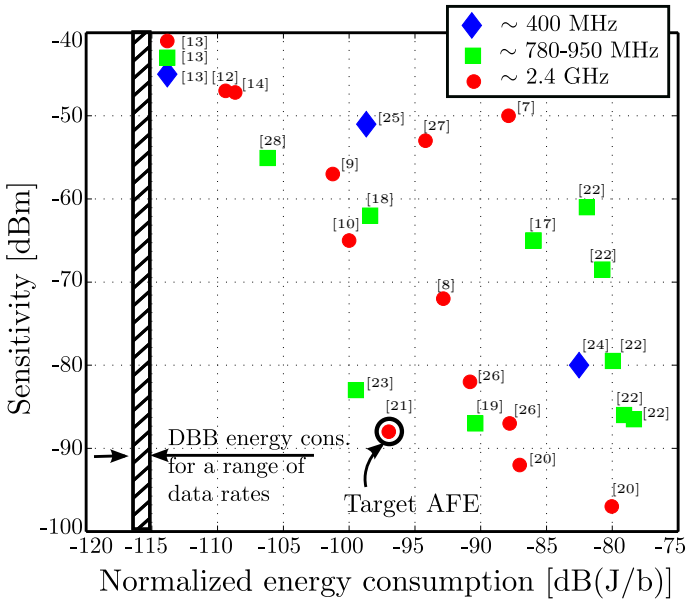


**Figure 10:** Performance comparison of WRx analog front-ends found in literature, in terms of energy consumption and sensitivity. The measured range of energy consumption of the proposed DBB, for 10 to 250 kbps, is shown as a hatched region.

Low-power analog front-end WRx design, as mentioned in Section 1, has been a popular and active research area for more than a decade [7–28]. Depending on the target applications and parameter choices, these designs are optimized to operate at different data rates and operating frequencies making a trade-off between sensitivity, power consumption and resulting wake-up delay. The performance, sensitivity vs. energy consumption, of existing analog front-ends (including the targeted AFE from the *Ultra-Portable Devices* project) is presented in Fig. 10. To be able to compare these designs reasonably fair we normalize power consumptions to their corresponding data rates. The hatched region to the left is the range of energy consumption measured for our DBB, for data rates between 10 and 250 kbps. This covers most data rates at which the analog front-ends are operable. The DBB in itself does not have an associated sensitivity and the region therefore extends across all sensitivity levels. We can see that our DBB will essentially not increase the total WRx power consumption, since its energy consumption is significantly lower, often orders of

magnitude, than that of the analog front-ends. This shows that our proposed DBB can compensate for implementation losses and improve the practical sensitivity of the target analog front-end, for which it was designed, at a negligible energy cost and it can do the same for a wide range of analog front-ends found the literature. The improvement in terms of practical sensitivity for our target analog front-end, as shown in Section 4, is 6dB and for the same requirement on detection performance the same improvement can be achieved for the other analog front-ends as well.

# 7 Conclusions

A digital base-band design for a duty-cycled WRx in 65nm CMOS is presented. With adequate level of detection performance, the total power consumption of the digital base-band ($0.9\mu$W) is negligible in comparison with our analog front-end power consumption ($50\mu$W) [21]. This shows that implementation loss resulting from aggressive power savings in the analog front-end can be efficiently compensated with digital base-band processing.

# Bibliography


[1] C. Guo, L. C. Zhong, and J. Rabaey, "Low power distributed MAC for ad hoc sensor radio networks," in *IEEE Global Telecommun. Conf.*, 2001, pp. 2944–2948.

[2] E.-Y. Lin, J. Rabaey, and A. Wolisz, "Power-efficient rendez-vous schemes for dense wireless sensor networks," in *IEEE Int. Conf. Commun.*, vol. 7, June 2004, pp. 3769–3776.

[3] M. Lont *et al.*, "Analytical models for the wake-up receiver power budget for wireless sensor networks," in *Proc. 28th IEEE Global Telecommun. Conf.*, 2009, pp. 1146–1151.

[4] N. S. Mazloum and O. Edfors, "DCW-MAC: An energy efficient medium access scheme using duty-cycled low-power wake-up receivers," in *IEEE Vehicular Technol. Conf.*, September 2011, pp. 1–5.

[5] N. S. Mazloum, J. N. Rodrigues, and O. Edfors, "Sub-$V_{\mathrm{T}}$ design of a wake-up receiver back-end in 65nm CMOS," in *IEEE Subthreshold Microelectronics Conf.*, October 2012, pp. 1–3.

[6] N. S. Mazloum and O. Edfors, "Performance analysis and energy optimization of wake-up receiver schemes for low-power applications," *IEEE Trans. Wireless Commun.*, vol. 13, pp. 7050–7061, 2014.

[7] N. Pletcher, S. Gambini, and J. Rabaey, "A 65$\mu$W, 1.9GHz RF to digital baseband wakeup receiver for wireless sensor nodes," in *IEEE Custom Integrated Circuits Conf. CICC*, 2007.

[8] N. M. Pletcher, S. Gambini, and J. Rabaey, "A 52$\mu$W wake-up receiver with -72dBm sensitivity using an uncertain-IF architecture," *IEEE J. Solid-State Circuits*, vol. 44, pp. 269–280, January 2009.

[9] M. S. Durante and S. Mahlknecht, "An ultra low power wakeup receiver for wireless sensor nodes," in *Proc. 3rd Int. Conf. Sensor Technol. and Applicat.*, June 2009, pp. 167–170.

[10] K.-W. Cheng, X. Liu, and M. Je, "A 2.4/5.8GHz 10$\mu$W wake-up receiver with -65/-50dBm sensitivity using direct active RF detection," *IEEE Asian Solid-State Circuits Conf. (A-SSCC)*, pp. 337–340, 2012.

[11] J. Choi, K. Lee, S.-O. Yun, S.-G. Lee, and J. Ko, "An interference-aware 5.8GHz wake-up radio for ETCS," in *IEEE Int. Solid-State Circuits Conf. Dig. of Tech. Papers (ISSCC)*, 2012, pp. 446–448.

[12] E. Nilsson and C. Svensson, "Ultra low power wake-up radio using envelope detector and transmission line voltage transformer," *IEEE J. on Emerging and Select. Topics in Circuits and Syst.*, vol. 3, no. 1, pp. 5–12, 2013.

[13] S. Oh, N. E. Roberts, and D. D. Wentzloff, "A 116nW multi-band wake-up receiver with 31-bit correlator and interference rejection," in *IEEE Custom Integrated Circuits Conf. (CICC)*, 2013, pp. 1–4.

[14] K. Takahagi, H. Matsushita, T. Iida, M. Ikebe, Y. Amemiya, and E. Sano, "Low-power wake-up receiver with subthreshold CMOS circuits for wireless sensor networks," *Analog Integrated Circuits and Signal Process.*, vol. 75, no. 2, pp. 199–205, 2013.

[15] T. Wada, M. Ikebe, and E. Sano, "60GHz, 9$\mu$W wake-up receiver for short-range wireless communications," in *Proc. of the ESSCIRC (ESSCIRC)*, 2013, pp. 383–386.

[16] J. Lee, I. Lee, J. Park, J. Moon, S. Kim, and J. Lee, "A sub-GHz low-power wireless sensor node with remote power-up receiver," in *IEEE Radio Frequency Integrated Circuits Symp. (RFIC)*, 2013, pp. 79–82.

[17] M. Lont, D. Milosevic, A. van Roermund, and G. Dolmans, "Ultra-low power FSK wake-up receiver front-end for body area networks," in *IEEE Radio Frequency Integrated Circuits Symposium (RFIC)*, 2011, pp. 1–4.

[18] J. Bae and H.-J. Yoo, "A 45$\mu$W injection-locked FSK wake-up receiver for crystal-less wireless body-area-network," in *IEEE Asian Solid State Circuits Conf. (A-SSCC)*, 2012, pp. 333–336.

[19] T. Abe, T. Morie, K. Satou, D. Nomasaki, S. Nakamura, Y. Horiuchi, and K. Imamura, "An ultra-low-power 2-step wake-up receiver for IEEE 802.15.4g wireless sensor networks," in *Symp. on VLSI Circuits Dig. of Tech. Papers*, 2014, pp. 1–2.

[20] C. Salazar, A. Kaiser, A. Cathelin, and J. Rabaey, "A -97dBm sensitivity interferer-resilient 2.4GHz wake-up receiver using dual-IF multi-n-path architecture in 65nm CMOS," in *IEEE Int. Solid-State Circuits Conf. (ISSCC)*, 2015, pp. 1–3.

[21] C. Bryant and H. Sjöland, "A 2.45GHz, 50$\mu$W wake-up receiver front-end with -88dBm sensitivity and 250kbps data rate," in *Eur. Solid State Circuits Conf. (ESSCIRC)*, September 2014, pp. 235–238.

[22] X. Huang, P. Harpe, G. Dolmans, H. de Groot, and J. R. Long, "A 780–950MHz, 64–146$\mu$W power-scalable synchronized-switching OOK receiver for wireless event-driven applications," *IEEE J. of Solid-State Circuits*, 2014.

[23] H. Milosiu, F. Oehler, M. Eppel, D. Fruhsorger, S. Lensing, G. Popken, and T. Thones, "A 3$\mu$W 868MHz wake-up receiver with -83dBm sensitivity and scalable data rate," in *Proc. of the ESSCIRC (ESSCIRC)*, 2013, pp. 387–390.

[24] T. Copani, S. Min, S. Shashidharan, S. Chakraborty, M. Stevens, S. Kiaei, and B. Bakkaloglu, "A CMOS low-power transceiver with reconfigurable antenna interface for medical implant applications," *IEEE Trans. on Microwave Theory and Techn.*, vol. 59, no. 5, pp. 1369–1378, 2011.

[25] S. J. Marinkovic and E. M. Popovici, "Nano-power wireless wake-up receiver with serial peripheral interface," *IEEE J. on Select. Areas in Commun.*, vol. 29, no. 8, pp. 1641–1647, 2011.

[26] S. Drago, D. Leenaerts, F. Sebastiano, L. J. Breems, K. A. Makinwa, and B. Nauta, "A 2.4GHz 830pJ/bit duty-cycled wake-up receiver with -82dBm sensitivity for crystal-less wireless sensor nodes," in *IEEE Int. Solid-State Circuits Conf. Digest Tech. Papers (ISSCC)*, 2010, pp. 224–225.

[27] P. Le-Huy and S. Roy, "Low-power wake-up radio for wireless sensor networks," *Mobile Networks and Appl.*, vol. 15, no. 2, pp. 226–236, 2010.

[28] C. Hambeck, S. Mahlknecht, and T. Herndl, "A 2.4$\mu$W wake-up receiver for wireless sensor nodes with -71dBm sensitivity," in *IEEE Proc. Int. Symp. Circuits and Syst. (ISCAS)*, 2011, pp. 534–537.

[29] Y. Zhang *et al.*, "A 3.72 $\mu$W ultra-low power digital baseband for wake-up radios," in *Int. Symp. VLSI Design, Automation and Test (VLSI-DAT)*, April 2011, pp. 1–4.

[30] Y. Wei, J. Heidemann, and D. Estrin, "An energy-efficient MAC protocol for wireless sensor networks," in *Proc. 21st Ann. Joint Conf. IEEE Comput. and Commun. Soc.*, vol. 3, 2002, pp. 1567–1576.

[31] H. Sjöland *et al.*, "A receiver architecture for devices in wireless body area networks," *IEEE J. Emerg. Sel. Topic Circuits Syst.*, vol. 2, pp. 82–95, March 2012.

[32] ——, "Ultra low power transceivers for wireless sensors and body area networks," in *8th Int. Symp. Medical Inform. and Commun. Technology (ISMICT)*, April 2014, pp. 1–5.

[33] M. Cohn and A. Lempel, "On fast M-sequence transforms," *IEEE Trans. Inf. Theory*, vol. 23, pp. 135–137, January 1977.

# *Paper V*

# Comparing Analog Front-ends for Duty-cycled Wake-up Receivers in Wireless Sensor Networks

**Wake-up receivers (WRxs) for wireless sensor networks have a large impact on total network energy consumption. This has led to many WRx analog front-end (AFE) designs presented in literature, with a large variety of trade-offs between sensitivity, data rate, and power consumption. We present an analysis of duty-cycled WRx schemes which provides a simple tool for comparing different WRx AFEs, based on the energy consumed in an entire single-hop network during a wake-up. The simplicity is largely due to the fact that all network and communication parameter settings can be condensed into a single scenario constant. This tool allows us to both compare AFEs for specific scenarios and draw more general conclusions about AFE performance across all scenarios.**

---

Nafiseh Seyed Mazloum and Ove Edfors,
"Comparing Analog Front-ends for Duty-cycled Wake-up Receivers in Wireless Sensor Networks,"
under review for possible publication in *IEEE Sensors Journal*.

# 1 Introduction

The use of an extra ultra-low power receiver, typically referred to as a wake-up receiver (WRx), is accounted as a practical solution to reduce idle channel monitoring energy cost in wireless sensor network applications with low traffic intensity [1]. An ultra-low power WRx monitors the wireless channel while the nodes high power main receiver is switched off. The WRx powers up the main receiver only when a wake-up beacon (WB) is detected. There are two main approaches for how a WRx monitors the channel. A WRx can be always on [1,2] or it can be duty-cycled [3,4]. While the always-on approach allows for short wake-up delays, the system average power consumption is relatively high as it cannot go below the (always-on) WRx power consumption. The duty-cycling approach, on the other hand, is more energy efficient as WRxs sleep most of the time. The associated draw-back is, of course, longer wake-up delays. By introducing a requirement on average delay [4] we can, however, optimize sleep intervals to also meet requirements for delay sensitive applications. With this work we assume that nodes operate according to duty-cycled WRx scheme principles and compare WRx analog front-end (AFE) performances for this type of WRx schemes.

To save power a WRx needs to operate at a very limited power consumption, typically two orders of magnitude lower than the main receiver, e.g., in the order of 10$\mu$W [1,5]. A large fraction of total power is consumed in the AFE of a WRx and many front-end architectures have been proposed to meet strict low-power requirements [6–27][18]. Simple non-coherent modulation schemes, e.g., on-off keying (OOK) [6–12,14,15,19–24,27], binary frequency shift-keying (BFSK) [16–18], pulse position modulation (PPM) [25], and pulse width modulation (PWM) [13,26], are often chosen for WB transmission, since they allow low-power low-complex AFE designs. In literature WRx AFEs are typically evaluated by their sensitivity, related to a BER of $10^{-3}$, and their corresponding power consumption. Both these at some operating frequency and data rate suitable for the scenario at hand. The ones listed above are no exception to this. In [21] a figure-of-merit also based on sensitivity, power consumption, and data rate, is introduced. While these measures are important for the individual AFE designs, they are not sufficient if we want to compare how WRx AFEs influence total wake-up energy consumption in a network. Extreme low-power design of an AFE typically leads to a high noise figure and degraded sensitivity, compared to the main receiver. High WB transmit power required to compensate for the reduced sensitivity can lead to an energy cost substantially higher

[18] WRxs are proposed for different data communication channels such as radio frequency (RF), infrared, ultrasound, and body coupled communication (for WBAN). This study includes only RF based WRx designs.

than the energy saving obtained from using a low-power WRx. Therefore, a comparison needs to include both transmit and receive energy costs. By calculating the total energy required in a network to perform a wake-up, we enable such a comparison. Our measure takes both channel listening and WB transmission costs into account and makes WRx AFE design comparisons dependent on scenario parameters like network size, coverage needed, and limitations on average wake-up delays.

In Section 2, we describe the overall operation of a duty-cycled WRx scheme. A simple expression is developed for the energy analysis of the addressed system in Section 3. By studying the energy model in Section 4 we obtain insight into how changes in WRx AFE characteristics and system parameters relate to energy consumption attributed to wake-ups. Using this simple energy model we illustrate how to compare the wake-up energy performance of WRx AFEs for different network settings and channel conditions and single out the best performing ones. Conclusions and final remarks are presented in Section 5.

## 2 System Overview

In our reference system all nodes are equal and communicate in a single-hop fashion according to the addressed duty-cycled WRx scheme. With all nodes in the network being equal, limitation of energy costs for WB transmission and reception are of equal importance. Each node consists of a transmitter, a main receiver, and a duty-cycled WRx. The principle of communication in a single-hop network of $N$ nodes with packet inter-arrival interval $1/\lambda$ is as follows. The WRxs of all nodes listen periodically and asynchronously to the channel for a WB. Both the transmitter and the main receiver are switched off. A node with data available for transmission, called the source node, turns on its transmitter and initiates communication by transmitting strobed WBs ahead of data. These WBs carry both source and destination node addresses to avoid overhearing by non-destination nodes [28]. When a WB transmission coincides with the WRx listen interval of the destination node, the WRx detects the WB and turns on the transmitter to reply with a wake-up acknowledgment (WACK). It also prepares for data reception by turning on the main receiver.

Ideally no error occurs when detecting a WB, but in a real system there exist both noise and interference. Therefore, there is a certain probability that the transmitted WB is missed by the WRx or the WRx erroneously detects a WB. The latter can occur both when only noise/external interference is received or, when a WB addressed to another node is present on the channel. Subsequently, not only does the chosen duty cycle of the WRx determine the energy cost of channel listening, together with WB error probabilities it also influences

transmission cost through the number of WBs that needs to be transmitted to perform a wake-up. Through these mechanisms WRx characteristics, in terms of sensitivity and power consumption, have direct impact on transmit and receive energy consumption and thereby on total wake-up energy cost.

# 3 Wake-up Energy Analysis

With a direct relation, as discussed above, between WRx characteristics and total energy required for a wake-up, we calculate this energy and use it as basis for comparing WRx AFE designs. With limited battery resources, we can see it as a ranking of WRx AFEs according to resulting battery life times. The comparison relies on everything but AFEs being equal.

Independent of the WRx front-end used, the WB length (counted in bits) has to be the same to achieve the same WB detection performance when operating at the same channel BER. This can be used to simplify our calculations by focusing on the energy required to receive one bit in the WB waking up our receiver. We also assume that node power consumption in sleep mode is insignificant compared to that in other modes. The rationale behind this is found in, e.g., [29] where sleep power consumption is five and seven orders of magnitude lower than the WRx and transmitter/main receiver power consumptions. WB detection performance, in terms of WB miss and false-alarm probabilities, has been extensively studied in [30] for a WB consisting of a preamble and an address part. The preamble is used to provide synchronization and the address part is necessary to avoid overhearing. Additionally, to limit WB miss and false alarm error probabilities, we select the preamble from sequences with good auto-correlation properties and apply spreading on the address bits. This also provides protection against external interference. WB parameters have been optimized for a wide range of channel BERs in [30], but WRx front-end sensitivity figures in literature are often measured at $10^{-3}$ BER, making it an attractive reference point[19] in the analysis. This low BER also results in very rare WB detection errors, making it possible to ignore their influence on energy consumption and thereby further simplify the analysis.

Given the above, total wake-up energy per data packet is calculated as the sum of periodic WB transmissions by the source node and duty-cycled channel listening, by all $N$ nodes, during an average packet arrival interval. Calculated

[19]Since WRxs AFEs typically have the same type of exponential BER characteristic, a change of BER reference point or any applied coding changes the WRxs absolute energy levels but has no effect on their relative ranking, as long as we can assume rare WB detection errors.

per received WB bit, it becomes

$$E_{tot} = W\,P^{tx}\,T_b + K\,N\,P^{wrx}\,T_b, \tag{1}$$

where $W$ is the average number of WB transmissions needed for a wake-up, $P^{tx}$ the transmitter power consumption, $T_b$ the bit time, $K$ the number of WRx duty-cycles per average packet-arrival interval, and $P^{wrx}$ the WRx power consumption.

We can calculate $W$ in (1) as half the number of WBs that fit in one WRx duty cycle of length $(1/\lambda)/K$, since nodes are asynchronous and no data packet arrival time is more likely than any other. With $Z_{wb}$ bits in a WB, each has a length of $Z_{wb}T_b$ and we get

$$W = \frac{1/\lambda}{2KZ_{wb}T_b}. \tag{2}$$

As expected, $K$ and $W$ are inversely related. The more frequently the WRx duty cycles, the fewer WBs need to be transmitted before a wake-up. By changing $K$ we can control the resulting average wake-up delay. To meet an average wake-up delay requirement of $D^{req}$, we set

$$K = \frac{1/\lambda}{2D^{req}}. \tag{3}$$

Next we relate transmitter power consumption $P^{tx}$ in (1) to WRx AFE sensitivity $P_s^{wrx}$ through the largest expected propagation loss $L_{p,\max}$ and transmitter efficiency $\eta$ as[20]

$$P^{tx} = \frac{P_s^{wrx}\,L_{p,\max}}{\eta}, \tag{4}$$

where $\eta$ refers to the ratio of actual transmitted power and transmitter power consumption. Substituting (2), (3), and (4) back in (1), and defining the WRx energy consumption per bit time

$$E^{wrx} = P^{wrx}\,T_b, \tag{5}$$

we get

$$E_{tot} = \frac{D^{req}L_{p,\max}}{\eta Z_{wb}}\,P_s^{wrx} + N\frac{1/\lambda}{2D^{req}}\,E^{wrx}, \tag{6}$$

showing that wake-up energy consumption depends on more parameters than AFE sensitivity and energy consumption per bit. The additional parameters,

[20]Propagation loss $L_{p,\max}$ is a number larger than one and transmitter efficiency $\eta$ is a number smaller than one.

constituting the scenario, are delay requirement, maximum propagation loss, transmitter efficiency, WB length, network size, and traffic. An important feature of (6) is that it does not depend on data rate, or bandwidth, making it possible to compare WRx designs with quite different design specifications when operated in the same scenario.

# 4 Wake-up Receiver Front-end Comparisons

In this section we show how to use (6) to compare and evaluate energy performance of WRx AFEs. Let us first study the overall behavior of (6) for two example scenarios. Comparing front-ends across vastly different bands is not favorable as their propagation loss will be different. We therefore compare AFEs designed for the same frequency band. Our scenarios are:
*Scenario 1*: 2.4 GHz wireless body area network (WBAN) applications with a worst case path loss of 88 dB[21] corresponding to ear-to-ear communication [29,31]. We assume a network size $N$ of 64 nodes, packet inter-arrival interval $1/\lambda$ of 1000 sec., and a 10 msec. average delay requirement $D^{req}$.
*Scenario 2*: 900 MHz short range wireless communication applications with a worst case path loss set to 55 dB [32]. For this scenario, we assume a larger network size $N$ of 512 nodes, a lower traffic with packet inter-arrival interval $1/\lambda$ of 100000 sec., and an average delay requirement $D^{req}$ of 0.25 second.
We set the WB length $Z_{wb}$ to 21 and 25 bits in Scenario 1 and Scenario 2, respectively, based on optimization results in [30]. In both scenarios, we assume transmitter efficiency $\eta$ of 50%. Replacing the values specified above in (6) we calculate the total energy consumption for wake-up per received WB bit. Results are shown as level curves in Fig. 1(a) with axes AFE sensitivity $P_s^{wrx}$ and corresponding AFE energy consumption per bit $E^{wrx}$ in dB scale[22]. Almost straight level curves stemming either from $P_s^{wrx}$ or from $E^{wrx}$ show that total energy consumption in most cases is dominated either by WB transmission or AFE channel listening. To illustrate for which values on $P_s^{wrx}$ and $E^{wrx}$ the two energy costs are balanced, we calculate what we call *balance lines* by making the two terms in (6) equal. This gives

$$P_s^{wrx} = E^{wrx} + \Gamma \ \text{[dB]}, \tag{7}$$

where all scenario parameters have been condensed into a single scenario constant

$$\Gamma = N + \eta + Z_{wb} + (1/\lambda) - 2D^{req} - 3 - L_{p,\max} \ \text{[dB]}. \tag{8}$$

[21] Variables are defined in linear scale, but we often assume dB scale in the text – which one should be clear from the context.

[22] Presenting $P_s^{wrx}$ and $E^{wrx}$ in non-dB, the level curves are straight lines, but large dynamic ranges in $P_s^{wrx}$ and $E^{wrx}$ make a dB scale more convenient.

Using (7) and (8), replacing scenario parameters with values specified above, we calculate balance lines for the two scenarios, shown as diagonal lines in Fig. 1(a). Studying $E_{tot}$ level curves, together with their corresponding balance lines, we make several observations regarding energy consumption characteristics:

- All level curves have the same shape, are symmetric around the balance line, and shifted along it with changes in energy level.
- The total energy, as indicated in the figure, increases with increasing $P_s^{wrx}$ and $E^{wrx}$.
- Changes in scenario parameters will change $\Gamma$ and accordingly shift both the balance line and the corresponding level curves.

These characteristics can be used as a tool for comparing the relative merits of different WRx AFE designs, without going though complete energy calculation for the individual designs. In the following we first compare AFE performances for systems with certain parameter settings, and then provide a mechanism through which we find the set of best-performing WRx AFEs across all scenarios.

## 4.1 Best performance in a specific scenario

In Fig. 1(b) we show characteristics of the AFEs listed in Table 1. We replace $E^{wrx}$ in (6) by the front-end energy consumption per bit, assuming that energy consumption of the WRx digital base-band is negligible [34], compared to that of the AFE. We are interested to find a WRx AFE among the existing solutions that is the best in terms of wake-up energy performance in a certain scenario. Graphically, this can be done in two steps.
*Step 1*: Calculate the scenario constant $\Gamma$, using (8), for the given scenario parameters and plot the corresponding balance line (7).
*Step 2*: Slide a level curve, with the same shape as in Fig. 1(a), along the balance line, starting from the lower left corner, until it hits the first AFE design. This AFE provides the lowest wake-up energy consumption for that particular scenario.

Let us illustrate the above for our two example scenarios, finding the respective best-performing WRx AFEs among those listed in Table 1. First we add the balance line that corresponds to each scenario (red solid and blue dashed), to Fig. 1(b). For Scenario 1, we search among the WRx AFEs designed to operate at 2.4 GHz (red dots), while for Scenario 2, we search among the ones operating at $780 - 950$ MHz (blue squares). As indicated in the figure, the lowest energy consumption is obtained for the WRx AFE designs in [20] and [27]

**Table 1:** Wake-up receiver (WRx) designs.

| **Reference**[23] | Sensitivity[24] [dBm] | Power cons. [$\mu$W] | Data rate [kbps] | $E^{wrx}$ [dB(J/b)] |
|---|---|---|---|---|
| Pletcher ('07) [6] | -50* | 65 | 40 | -87.9 |
| Pletcher ('09) [7] | -72* | 52 | 100 | -92.8 |
| Durante ('09) [8] | -57* | 7.5 | 100 | -101.2 |
| Lont ('09) [33] | -65 | 126 | 50 | -86 |
| Drago ('10) [25] | -87/-82* | 415 | 250/500 | -87.8/-90.8 |
| Le ('10) [26] | -53* | 19 | 50 | -94 |
| Hambeck ('11) [27] | -71 | 2.4 | 100 | -106 |
| Cheng ('12) [9] | -65* | 10 | 100 | -100 |
| Bae ('12) [17] | -62 | 45 | 312 | -98.4 |
| Nilsson ('13) [11] | -47* | 2.3 | 200 | -109 |
| Oh ('13) [12] | -45 | 0.116 | 12.5 | -110.3 |
| | -43* | | | |
| Takahagi ('13) [13] | -47.2* | 6.8 | 500 | -108.6 |
| Milosiu ('13) [22] | -83 | 7.2 | 64 | -99.5 |
| Abe ('14) [18] | -87 | 45.5 | 50 | -90.4 |
| Bryant ('14) [20] | -88* | 50 | 250 | -97 |
| Huang ('14) [21] | -86.5 | 146 | 10 | -78.3 |
| | -86 | 123 | | -79.1 |
| | -79.5 | 101 | | -80 |
| | -68.5 | 84 | | -80.7 |
| | -61 | 64 | | -81.9 |
| Salazar ('15) [19] | -97/-92* | 99 | 10/50 | -80/-87 |

for Scenario 1 and Scenario 2, respectively.

## 4.2 Best-performing front-ends across all scenarios

Characteristics of energy level curves and balance lines can also be used to find the set of AFE designs that, for at least some scenario constant $\Gamma$, results in the lowest energy consumption compared to the other designs. Having

[23]The sensitivity and power consumption in [12], [18] and [27] are reported for the entire WRx design. We have excluded their processing gains from sensitivity and their correlator power consumptions from the total power consumption in Fig.1(a) and Fig.3(a).

[24]Sensitivities marked by '*' are for 2.4 GHz operating frequency, all others for 780 – 950 MHz.

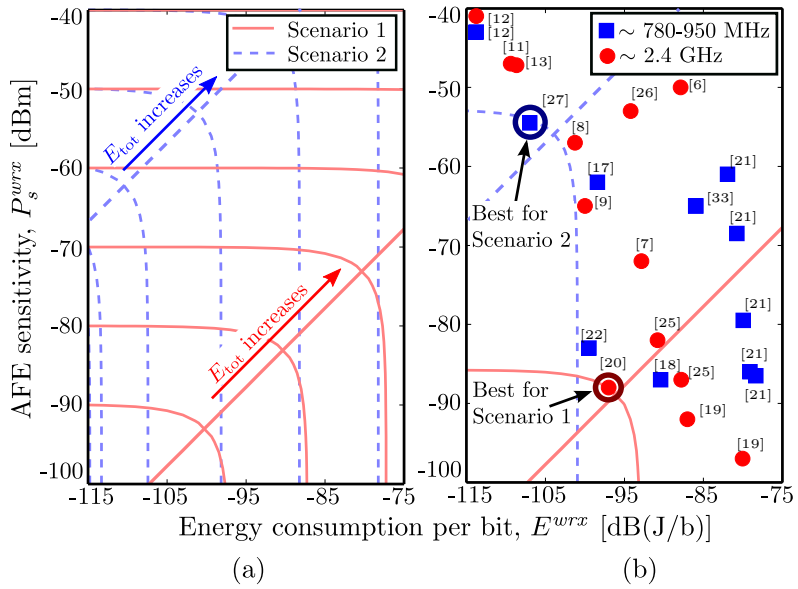


**Figure 1:** (a) Total energy consumption per wake-up level curves as functions of wake-up receiver (WRx) sensitivity and energy consumption per bit for two examples scenarios. (b) Performance comparison of WRx analog front-ends listed in Table 1.

access to such a set provides a quick and simple evaluation approach when adding/designing a new WRx AFE as we only need to compare to a smaller set of designs.

We find WRx AFEs with such characteristics by varying $\Gamma$ throughout its entire range, $(-\infty, \infty)$ dB, finding the best performing AFE design for each $\Gamma$. Let us illustrate this graphically, using the two-step approach in the previous section for a large number of $\Gamma$s. First, we study only one WRx front-end design, as in Fig. 2(a). This single AFE will, trivially, be the best-performing one for all scenarios. The main point of the illustration is that the collection of level curves (gray) going through the reference AFE location create four regions, or quadrants, around it. With total energy consumption $E_{tot}$ increasing when $P_s^{wrx}$ and $E^{wrx}$ increase, any AFE design in the lower left quadrant always have a lower $E_{tot}$ than the reference AFE. Correspondingly, all AFE designs in the upper right quadrant always have a higher $E_{tot}$ than the reference AFE. The energy performance of AFE designs ending up in the other two quadrants,

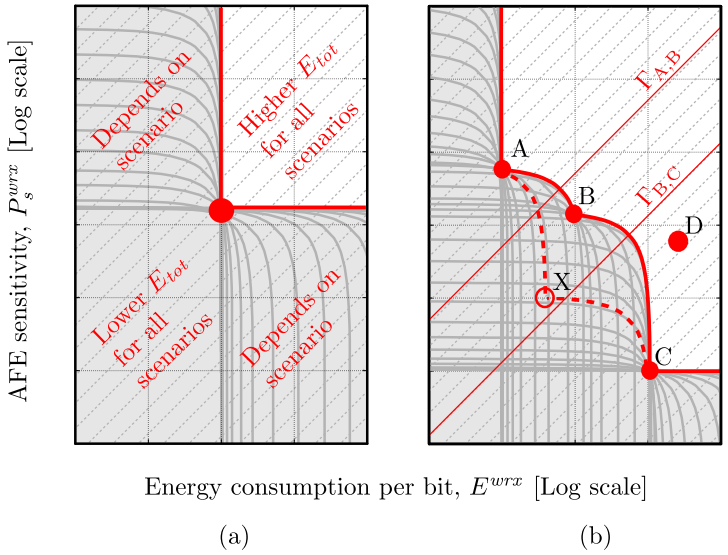


**Figure 2:** Graphical illustration of finding best performing WRx AFE designs across scenarios. The trivial single-AFE case (a) and multiple AFEs (b).

however, can be both better or worse in terms of energy performance, depending on scenario.

When we have more than one WRx AFE to compare we apply the same principle, sweeping over scenario constants $\Gamma$ to find the best performing AFE for each scenario. The result of a simplified case with four AFEs is shown in Fig. 2(b), where AFE A is the best performing one for $\Gamma > \Gamma_{A,B}$, AFE B for $\Gamma_{A,B} > \Gamma > \Gamma_{B,C}$, and AFE C for $\Gamma < \Gamma_{B,C}$. At the boundary scenarios $\Gamma = \Gamma_{A,B}$ and $\Gamma = \Gamma_{B,C}$, two AFEs have equal energy performance – A and B in the first case and B and C in the second case. AFE D is not best performing in any scenario. A new AFE in the gray region will be added to the set of best-performing AFEs. This may also imply that other AFEs are removed from the set, as indicated in Fig. 2(b) where the new hypothetical design AFE X replaces AFE B. This changes the corresponding scenario constants ($\Gamma$s at boundary scenarios) for which AFE A, AFE X, and AFE C perform the best[25]. As we show in the following, knowing the AFEs sensitivity and energy consumption per bit we can calculate $\Gamma$s for boundary scenarios. While we explicitly perform the calculation for AFE A and AFE B in Fig. 2(b), the same calculation can

[25]The new boundary $\Gamma$s are not shown to avoid overcrowding the figure.

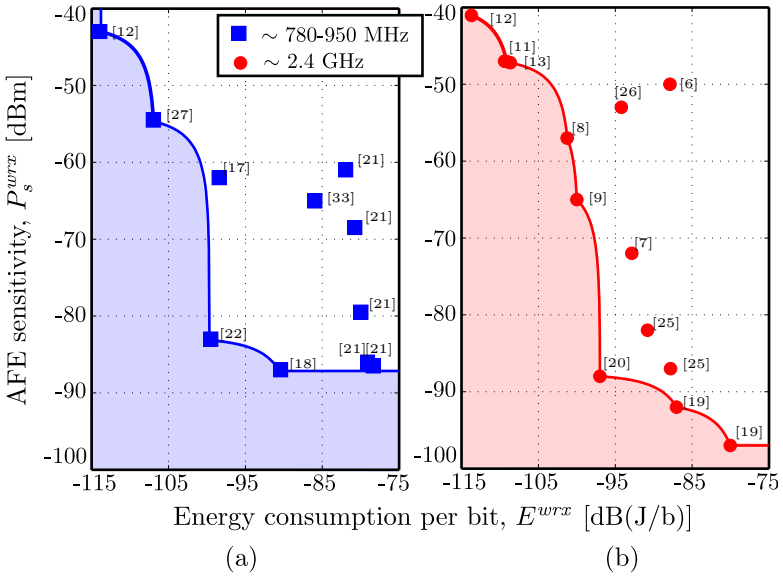


**Figure 3:** Best-performing analog front-ends for WRxs operating at (a) $780 - 950$ MHz and (b) 2.4 GHz.

be applied to any pair of AFE designs. Let $P_{s,\mathrm{A}}^{wrx}$, $P_{s,\mathrm{B}}^{wrx}$, $E_{\mathrm{A}}^{wrx}$, and $E_{\mathrm{B}}^{wrx}$ be the sensitivities and energy consumptions per bit for AFEs A and B, respectively. Substituting these in (6) and setting the two obtained energy levels equal we identify the resulting boundary scenario constant

$$\Gamma_{\mathrm{A,B}} = -\frac{P_{s,\mathrm{A}}^{wrx} - P_{s,\mathrm{B}}^{wrx}}{E_{\mathrm{A}}^{wrx} - E_{\mathrm{B}}^{wrx}}. \tag{9}$$

This uniquely defines the scenario constant for which AFEs A and B preform equally in terms of total wake-up energy. Since the scenario constant, per definition, is a non-negative real number the ratio $(P_{s,\mathrm{A}}^{wrx} - P_{s,\mathrm{B}}^{wrx})/(E_{\mathrm{A}}^{wrx} - E_{\mathrm{B}}^{wrx})$ has to be negative. This shows that two AFEs cannot have equal performance in any scenario if one is better both in terms of sensitivity and energy consumption per bit. It also explains the lower-left and upper-right quadrants in Fig. 2(a).

We now apply above mechanism separately to the two WRx categories in Table 1, operating at $780 - 950$ MHz and 2.4 GHz. The results are shown in Fig. 3. In both sub-figures, all WRx AFE designs on the solid curve belong to the set of best performing AFEs. In the white area we see AFE designs

**Table 2:** Scenario constant range for AFEs belonging to the set of best-performing AFE, (a) for 780-950 MHz operating frequency, (b) for 2.4 GHz operating frequency.

(a)

| **Reference** | Range of scenario constant (dB) |
|---|---|
| Oh ('13) [12] | N.A. (lowest $E^{wrx}$) |
| Hambeck ('11) [27] | 33.6 |
| Milosiu ('13) [22] | 23.5 |
| Abe ('14) [18] | N.A. (lowest $P_s^{wrx}$) |

(b)

| **Reference** | Range of scenario constant (dB) |
|---|---|
| Oh ('13) [12] | N.A. (lowest $E^{wrx}$) |
| Nilsson ('13) [11] | 11 |
| Takahagi ('13) [13] | 4.3 |
| Durante ('09) [8] | 6 |
| Cheng ('12) [9] | 13.4 |
| Bryant ('14) [20] | 37.7 |
| Salazar ('15) [19] | 10 |
| Salazar ('15) [19] | N.A. (lowest $P_s^{wrx}$) |

that are not best-performing in any scenario[26] . To rank the best-performing AFEs against each other we measure the range of scenarios for which each AFE is the best-performing one. For AFE B in Fig. 2(b), this range is between boundary scenarios $\Gamma_{A,B}$ and $\Gamma_{B,C}$. By merit of being the best-performing AFE for more scenarios, a larger range is considered better. Using (9) we calculate the boundary scenario constants for all AFEs in the two sets of best performing ones AFEs shown in Fig. 3. The obtained ranges are listed in Table 2. The calculation is, however, not applicable to the two designs having either the best sensitivity or the lowest energy consumption per bit. They are best for extreme scenarios, where scenario constants are either very low or very high. Among AFEs operating at 780-950 MHz [27] has the widest range and among those at 2.4 GHz [20].

# 5 Conclusions and Remarks

This paper presents a system-level analysis of low-power WRx which can be used to evaluate and compare WRx AFEs with different design characteristics. We calculate wake-up energy consumption for an entire network where nodes only wake up periodically using a duty-cycled WRx. The closed form energy expressions give us a good understanding how energy consumption is related

[26]It should be noted that we only compare total wake-up energy consumption. AFE designs not being among the best-performing ones in this measure may have other merits that do not come through in this analysis.

to WRx front-end design characteristics and scenario parameters. By studying energy consumption level curves, we propose a simple and intuitive tool for comparing existing WRx AFE designs found in literature. The tool allows us to find the best-performing AFE design for a specific scenario and draw conclusions about overall best-performing AFEs. For any given set of AFE designs, the latter analysis provides a simple mean to decide whether a new design will be among the best-performing ones or not. This is particularly valuable when setting design targets for new WRx AFE designs, if low total wake-up energy consumption in a network is the objective.

# Bibliography


[1] C. Guo, L. C. Zhong, and J. Rabaey, "Low power distributed MAC for ad hoc sensor radio networks," in *IEEE Global Telecommun. Conf.*, 2002, pp. 2944–2948.

[2] Y. Zhang *et al.*, "A 3.72 $\mu$W ultra-low power digital baseband for wake-up radios," in *Int. Symp. VLSI Design, Automation and Test*, April 2011, pp. 1–4.

[3] E.-Y. Lin, "A comprehensive study of power-efficient rendezvous schemes for wireless sensor networks," Ph.D. dissertation, University of California, Berkeley, 2005.

[4] N. S. Mazloum and O. Edfors, "DCW-MAC: An energy efficient medium access scheme using duty-cycled low-power wake-up receivers," in *IEEE Vehicular Technol. Conf.*, September 2011, pp. 1–5.

[5] E.-Y. Lin, J. Rabaey, and A. Wolisz, "Power-efficient rendez-vous schemes for dense wireless sensor networks," in *IEEE Int. Conf. Commun.*, vol. 7, June 2004, pp. 3769–3776.

[6] N. Pletcher, S. Gambini, and J. Rabaey, "A 65$\mu$W, 1.9GHz RF to digital baseband wakeup receiver for wireless sensor nodes," in *IEEE Custom Integrated Circuits Conf.*, 2007.

[7] N. M. Pletcher, S. Gambini, and J. Rabaey, "A 52$\mu$W wake-up receiver with -72dBm sensitivity using an uncertain-IF architecture," *IEEE J. Solid-State Circuits*, vol. 44, pp. 269–280, January 2009.

[8] M. S. Durante and S. Mahlknecht, "An ultra low power wakeup receiver for wireless sensor nodes," in *Proc. 3rd Int. Conf. Sensor Technol. and Applicat.*, June 2009, pp. 167–170.

[9] K.-W. Cheng, X. Liu, and M. Je, "A 2.4/5.8GHz 10$\mu$W wake-up receiver with -65/-50dBm sensitivity using direct active RF detection," *IEEE Asian Solid-State Circuits Conf.*, pp. 337–340, 2012.

[10] J. Choi, K. Lee, S.-O. Yun, S.-G. Lee, and J. Ko, "An interference-aware 5.8GHz wake-up radio for ETCS," in *IEEE Int. Solid-State Circuits Conf. Dig. of Tech. Papers*, 2012, pp. 446–448.

[11] E. Nilsson and C. Svensson, "Ultra low power wake-up radio using envelope detector and transmission line voltage transformer," *IEEE J. on Emerging and Select. Topics in Circuits and Syst.*, vol. 3, no. 1, pp. 5–12, 2013.

[12] S. Oh, N. E. Roberts, and D. D. Wentzloff, "A 116nW multi-band wake-up receiver with 31-bit correlator and interference rejection," in *IEEE Custom Integrated Circuits Conf.*, 2013, pp. 1–4.

[13] K. Takahagi, H. Matsushita, T. Iida, M. Ikebe, Y. Amemiya, and E. Sano, "Low-power wake-up receiver with subthreshold CMOS circuits for wireless sensor networks," *Analog Integrated Circuits and Signal Process.*, vol. 75, no. 2, pp. 199–205, 2013.

[14] T. Wada, M. Ikebe, and E. Sano, "60GHz, 9$\mu$W wake-up receiver for short-range wireless communications," in *Proc. of the Eur. Solid State Circuits Conf.*, 2013, pp. 383–386.

[15] J. Lee, I. Lee, J. Park, J. Moon, S. Kim, and J. Lee, "A sub-GHz low-power wireless sensor node with remote power-up receiver," in *IEEE Radio Frequency Integrated Circuits Symp.*, 2013, pp. 79–82.

[16] M. Lont, D. Milosevic, A. van Roermund, and G. Dolmans, "Ultra-low power FSK wake-up receiver front-end for body area networks," in *IEEE Radio Frequency Integrated Circuits Symp.*, 2011, pp. 1–4.

[17] J. Bae and H.-J. Yoo, "A 45$\mu$W injection-locked FSK wake-up receiver for crystal-less wireless body-area-network," in *IEEE Asian Solid State Circuits Conf.*, 2012, pp. 333–336.

[18] T. Abe, T. Morie, K. Satou, D. Nomasaki, S. Nakamura, Y. Horiuchi, and K. Imamura, "An ultra-low-power 2-step wake-up receiver for IEEE 802.15.4g wireless sensor networks," in *Symp. on VLSI Circuits Dig. of Tech. Papers*, 2014, pp. 1–2.

[19] C. Salazar, A. Kaiser, A. Cathelin, and J. Rabaey, "A -97dBm sensitivity interferer-resilient 2.4GHz wake-up receiver using dual-IF multi-n-path architecture in 65nm CMOS," in *IEEE Int. Solid-State Circuits Conf.*, 2015, pp. 1–3.

[20] C. Bryant and H. Sjöland, "A 2.45GHz, 50$\mu$W wake-up receiver front-end with -88dBm sensitivity and 250kbps data rate," in *Eur. Solid State Circuits Conf.*, September 2014, pp. 235–238.

[21] X. Huang, P. Harpe, G. Dolmans, H. de Groot, and J. R. Long, "A 780–950MHz, 64–146$\mu$W power-scalable synchronized-switching OOK receiver for wireless event-driven applications," *IEEE J. of Solid-State Circuits*, 2014.

[22] H. Milosiu, F. Oehler, M. Eppel, D. Fruhsorger, S. Lensing, G. Popken, and T. Thones, "A 3$\mu$W 868MHz wake-up receiver with -83dBm sensitivity and scalable data rate," in *Proc. of the Eur. Solid State Circuits Conf.*, 2013, pp. 387–390.

[23] T. Copani, S. Min, S. Shashidharan, S. Chakraborty, M. Stevens, S. Kiaei, and B. Bakkaloglu, "A CMOS low-power transceiver with reconfigurable antenna interface for medical implant applications," *IEEE Trans. on Microwave Theory and Techn.*, vol. 59, no. 5, pp. 1369–1378, 2011.

[24] S. J. Marinkovic and E. M. Popovici, "Nano-power wireless wake-up receiver with serial peripheral interface," *IEEE J. on Select. Areas in Commun.*, vol. 29, no. 8, pp. 1641–1647, 2011.

[25] S. Drago, D. Leenaerts, F. Sebastiano, L. J. Breems, K. A. Makinwa, and B. Nauta, "A 2.4GHz 830pJ/bit duty-cycled wake-up receiver with -82dBm sensitivity for crystal-less wireless sensor nodes," in *IEEE Int. Solid-State Circuits Conf. Dig. Tech. Papers*, 2010, pp. 224–225.

[26] P. Le-Huy and S. Roy, "Low-power wake-up radio for wireless sensor networks," *Mobile Networks and Appl.*, vol. 15, no. 2, pp. 226–236, 2010.

[27] C. Hambeck, S. Mahlknecht, and T. Herndl, "A 2.4$\mu$W wake-up receiver for wireless sensor nodes with -71dBm sensitivity," in *IEEE Proc. Int. Symp. Circuits and Syst.*, 2011, pp. 534–537.

[28] Y. Wei, J. Heidemann, and D. Estrin, "An energy-efficient MAC protocol for wireless sensor networks," in *Proc. 21st Ann. Joint Conf. IEEE Comput. and Commun. Soc.*, vol. 3, 2002, pp. 1567–1576.

[29] H. Sjöland *et al.*, "Ultra low power transceivers for wireless sensors and body area networks," in *8th Int. Symp. Medical Inform. and Commun. Technology*, April 2014, pp. 1–5.

[30] N. S. Mazloum and O. Edfors, "Performance analysis and energy optimization of wake-up receiver schemes for low-power applications," *IEEE Trans. Wireless Commun.*, vol. 13, pp. 7050–7061, 2014.

[31] H. Sjöland *et al.*, "A receiver architecture for devices in wireless body area networks," *IEEE J. Emerg. Sel. Topic Circuits Syst.*, vol. 2, pp. 82–95, March 2012.

[32] S. Y. Seidel and T. S. Rappaport, "914 MHz path loss prediction models for indoor wireless communications in multifloored buildings," *IEEE Trans. on Antennas and Propagation*, vol. 40, no. 2, pp. 207–217, 1992.

[33] M. Lont *et al.*, "Analytical models for the wake-up receiver power budget for wireless sensor networks," in *Proc. 28th IEEE Global Telecommun. Conf.*, 2009, pp. 1146–1151.

[34] N. S. Mazloum, J. N. Rodrigues, O. Andersson, A. Nejdel, and O. Edfors, "Improving practical sensitivity of energy optimized wake-up receivers: proof of concept in 65nm CMOS," *Under review for publication in IEEE Sensors Journal. (Manuscript available on arXiv.org)*, 2016.